DOCTORAL THESIS

Study of Heavy Baryons Phenomenology

Author:
Ailier RIVERO ACOSTA

Supervisors:
Dr. Elena SANTOPINTO (INFN, Sezione di Genova)
Dr. Carlos Alberto VAQUERA ARAUJO (UGto-CONAHCyT)

A thesis submitted in fulfillment of the requirements
for the degrees of
Doctor in Physics
in the
División de Ciencias e Ingenierías, Campus León
UNIVERSIDAD DE GUANAJUATO

and
Doctor in Physics and Nanosciences
in the
Dipartimento di Fisica
Scuola di Scienze Matematiche, Fisiche e Naturali
UNIVERSITÀ DEGLI STUDI DI GENOVA

May 7, 2025

"The scientist finds his rewards in what Henri Poincaré calls the joy of comprehension, and not in the possibilities of application to which any discovery may lead."

Albert Einstein

Abstract

The objective of this research is to investigate the properties of singly heavy baryons within the framework of the constituent quark model. This study focuses on calculating the mass spectra and the strong and electromagnetic decay widths for singly bottom baryons, as well as the electromagnetic decay widths for singly charmed baryons. The mass spectra are computed using a quark model, while the $^3P_0$ model is employed to analyze the open-flavor strong decay channels of singly bottom baryons. The electromagnetic decay widths for singly bottom baryons are calculated up to the second shell states using the Hamiltonian of electromagnetic interactions in the nonrelativistic approximation. For singly charmed baryons, the electromagnetic decay widths are specifically determined for the Ξ_c P-wave states. A novel method is introduced for the calculation of electromagnetic decay widths. This innovative approach enables the completely analytical evaluation of transition amplitudes without introducing any additional approximations used in previous articles in the heavy baryon sector. Notably, this work represents the first theoretical study of the electromagnetic decays of D_ρ-wave states, $\rho\lambda$ mixed states, and radially excited ρ and λ states.

Resumen

El objetivo de esta investigación es estudiar las propiedades de los bariones con un solo quark pesado dentro del marco del modelo de quarks constituyentes. Este estudio se centra en el cálculo de los espectros de masa y de las anchuras de decaimiento fuerte y electromagnético para los bariones con un quark bottom, así como en las anchuras de decaimiento electromagnético para los bariones con un quark charm. Los espectros de masa se calculan utilizando un modelo de quarks, mientras que para analizar los canales de sabor abierto en la desintegración fuerte de los bariones con un quark bottom se emplea el modelo $^3P_0$. Las anchuras de decaimiento electromagnético para los bariones con un quark bottom se calculan desde los estados bases hasta los estados de la segunda banda de energía utilizando el Hamiltoniano de las interacciones electromagnéticas en la aproximación no relativista. Para los bariones con un quark charm, las anchuras de decaimiento electromagnético se determinan específicamente para los estados P-wave del Ξ_c.

Se introduce un método novedoso para el cálculo de las anchuras de decaimiento electromagnético. Este innovador enfoque permite la evaluación completamente analítica de las amplitudes de transición sin necesidad de introducir aproximaciones adicionales como las utilizadas en artículos previos en el sector de los bariones pesados. En particular, este trabajo representa el primer estudio teórico de los decaimientos electromagnéticos de los estados D_ρ-wave, los estados mixtos $\rho\lambda$ y los estados excitados radialmente en ρ y λ.

Riassunto

L'obiettivo di questa ricerca è investigare le proprietà dei barioni con un singolo quark pesante nel contesto del modello a quark costituenti. Questo studio si concentra sul calcolo degli spettri di massa e delle larghezze di decadimento forte ed elettromagnetico per i barioni con un singolo quark bottom , nonché delle larghezze di decadimento elettromagnetico per i barioni con un singolo quark charm. Gli spettri di massa sono calcolati utilizzando un modello a quark, mentre per analizzare i canali di sapore aperti per il decadimento forte dei barioni con un singolo quark bottom viene impiegato il modello $^3P_0$. Le larghezze di decadimento elettromagnetico per i barioni bottom con un singolo quark pesante sono calcolate fino agli stati della seconda shell utilizzando l'Hamiltoniana delle interazioni elettromagnetiche nell'approssimazione non relativistica. Per i barioni charmati con un singolo quark pesante, le larghezze di decadimento elettromagnetico sono determinate specificamente per gli stati P-wave della Ξ_c.

Viene introdotto un metodo innovativo per il calcolo delle larghezze di decadimento elettromagnetico. Questo approccio innovativo consente la valutazione completamente analitica delle ampiezze di transizione senza introdurre alcuna ulteriore approssimazione rispetto a quelle utilizzate nei precedenti articoli sul settore dei barioni pesanti. In particolare, questo lavoro rappresenta il primo studio teorico dei decadimenti elettromagnetici degli stati D_ρ-wave, degli stati misti $\rho\lambda$ e degli stati eccitati radialmente ρ e λ.

Acknowledgements

"When you drink water,
remember the source."
Chinese Proverb

I would like to express my deepest gratitude to those who have supported me throughout this journey.

First and foremost, I am profoundly thankful to my wife, Amanda, my parents, my sister, and my entire family, as well as my wife's family, for their unconditional support and encouragement.

I extend my most sincere thanks to my supervisors, Dr. Elena Santopinto and Dr. Carlos Vaquera, for their invaluable guidance, support, and significant contributions to the preparation of this thesis over these long years of hard work.

I am also grateful to the members of my Thesis Committee for their insightful discussions and constructive suggestions, which have greatly improved this dissertation.

Special thanks go to the members of our research group, Dr. Hugo García Tecocoatzi, Dr. Andrés Morales, and Dr. Alessandro Giachino, for their stimulating discussions and for all that they have taught me.

To my friends Claudia, Paul, Maria, José Alberto, and Sebastian, thank you for making my time in Mexico and Italy more pleasant.

Finally, I would like to acknowledge the University of Guanajuato, the CONAHCyT, the Università degli Studi di Genova, and the Istituto Nazionale di Fisica Nucleare (INFN) for their invaluable support and the opportunities they have provided.

Contents

Chapter 1

Introduction

Particle physics, which investigates the fundamental constituents of matter and their interactions, is built upon the framework of the Standard Model (SM). This theory describes three of the four fundamental interactions of the universe: electromagnetic, weak and strong interactions. The strong interaction, responsible for binding quarks and gluons, is governed by Quantum Chromodynamics (QCD) [1, 2].

The strength of the strong interaction is characterized by a coupling constant that, at low energies, is significantly larger than those associated with the electromagnetic and weak interactions. QCD displays interesting behaviors across different energy scales. At high energies, asymptotic freedom causes the coupling between quarks and gluons to weaken, enabling the use of perturbative techniques for theoretical calculations. Conversely, at low energies, where the interaction becomes strongly coupled, perturbative methods break down. In this nonperturbative regime, confinement emerges, giving rise to the formation of hadrons.

To study systems in the nonperturbative regime, theoretical approaches relying on nonperturbative models have been developed. In this work, a constituent quark model (CQM) is employed to explore the properties and phenomenology of hadronic systems.

Hadron physics [3] is the study of subatomic particles known as hadrons, which are composed of quarks and gluons bound together by the strong force. The behavior of hadrons is fundamentally governed by the strong interaction. Within the Quark Model (QM), hadrons are classified based on their constituent quark content [4].

According to the QM [5, 6], conventional hadrons are categorized as either mesons, which consist of quark-antiquark pairs ($q\bar{q}$), or baryons, made up of three constituent quarks (qqq). In the same work, Gell-Mann also postulated the existence of unconventional configurations, such as mesons composed of the combination ($qq\bar{q}\bar{q}$), etc., or baryons containing the configuration ($qqqq\bar{q}$), etc. These configurations, now referred to as exotic hadrons, include states like tetraquarks ($qq\bar{q}\bar{q}$) and pentaquarks ($qqqq\bar{q}$). Some of these exotic states have been experimentally observed by the LHCb Collaboration [7–10].

The internal structure of hadrons is highly complex. At low energies, their properties can be effectively described using effective degrees of freedom such as spin, isospin, flavor, and spatial

degrees of freedom. These effective parameters provide valuable insight into the nonperturbative dynamics of the strong interaction.

The goal of the present work is to study the phenomenology of singly heavy baryons. These baryons consist of two light quarks and a single heavy quark, which can be either charm or bottom (qqc and qqc with $q = u, d$ors). The experimental search for singly heavy baryon states poses significant challenges, as their production requires accelerators capable of reaching higher energies. As a result, only a limited number of these states have been discovered, with many remaining to be observed in the future.

Some of the states discovered to date have been observed by experiments such as the CERN-ISR experiment (R415) [11], the CDF Collaboration [12–16], the D0 Collaboration [17, 18], the CMS Collaboration [19, 20], the LHCb Collaboration [21–30], and the Belle Collaboration [31, 32], among others.

The study of the mass spectra and decay properties of singly heavy baryons is essential for advancing our understanding of hadron physics. In this work, the focus is on calculating the mass spectra as well as the strong and electromagnetic decay widths of singly bottom baryons. In the charm sector, only the electromagnetic decay widths of singly charmed baryons are analyzed, as their mass spectra and strong decays were previously studied in reference [33].

From a theoretical perspective, numerous studies have investigated the mass spectra and decay properties of singly heavy baryons using various models [34–82]. The mass spectra and decay properties are among the main magnitudes that are useful for making consistent assignments of hadronic states. A reliable approach for identifying these states involves matching the experimental data with theoretical predictions for mass spectra and decay widths. This matching process is a key focus of the present study.

This thesis focuses on the spectroscopy of heavy baryons and their strong and electromagnetic decays. The work presented here is the result of a study conducted in collaboration with the members of our Research Group, with my primary contributions centered on the calculations of the electromagnetic decays of singly heavy baryons (Chapters 3, 4, 5).

The thesis begins with an **Introduction 1** that provides a brief review of the subject and outlines the main objectives of the study. The rest of this document is organized as follows:

Chapter 2 discusses theoretical aspects of hadron physics that are essential for a better understanding of the rest of the thesis. It also presents the mass spectra and strong decays of singly bottom baryons. The masses are calculated using the model introduced in reference [83], which incorporates a three-dimensional harmonic oscillator Hamiltonian supplemented by a perturbation term that includes spin, spin-orbit, isospin, and flavor-dependent contributions. The strong decays are computed by means of the $^3P_0$ model [33, 84–88]. The calculated masses and strong decay widths are compared with results from other theoretical works and experimental values from the Particle Data Group (PDG) [89]. The discussions and results regarding singly bottom baryons reported in this chapter have been published in *Physical Review D* [90].

Chapter 3 is devoted to the calculation of the electromagnetic decay widths of singly bottom baryons, specifically transitions from ground and P-wave states to ground states. These decay widths are computed using the electromagnetic interaction Hamiltonian within the nonrelativistic approximation. The analytical expressions of the transition amplitudes evaluation in the spatial space are also given. To calculate these expressions a novel method for evaluating transition amplitudes analytically and exactly is employed. This method, introduced in reference [90], is presented in detail in Appendix A. Electromagnetic decays are particularly significant in scenarios where strong decays are forbidden. The discussions and results presented in this Chapter have been published in *Physical Review D* [90].

Chapter 4 presents a study of the electromagnetic decay widths of singly bottom baryons, focusing on transitions from second-shell states to ground and P-wave states. These calculations follow the procedure used in Chapter 3 to evaluate the transition amplitudes. Notably, this work marks the first study of the electromagnetic decays of D_ρ-wave states, $\rho\lambda$ mixed states, and ρ and λ radially excited states. The discussions and results reported in this Chapter are being prepared for publication in two separated articles: one for the Λ_b and Ξ_b baryons, belonging to the flavor anti-triplet ($\bar{\mathbf{3}}_\mathrm{F}$) [91], and another one for the Σ_b, Ξ_b' and Ω_b baryons, belonging to the flavor sextet ($\mathbf{6}_\mathrm{F}$) [92].

Chapter 5 exposes the study of the electromagnetic decay widths of the Ξ_c baryons, focusing on transitions from P-wave states to ground states. These calculations are also based on the procedure used in Chapter 3 for the evaluation of the transition amplitudes. The theoretical results obtained for the $\Xi_c(2790)^{+/0}$ and $\Xi_c(2815)^{+/0}$ states are in good agreement with the recent data reported by the Belle Collaboration [93]. This agreement highlights the accuracy of the methodology used to evaluate the transition amplitudes, which avoids introducing additional approximations and provides more precise decay width predictions. The discussions and results reported in this Chapter have been submitted to *Physics Letters B* and are available on arXiv [94].

The **Conclusions 6** summarize the key findings and general results obtained from this research. **Appendix A** provides detailed calculations of the matrix elements in the flavor, spin, and spatial spaces for the electromagnetic decay widths.

Chapter 2

Singly bottom baryons spectroscopy and strong decays

This Chapter provides a brief review of some key topics relevant in the field of Hadron Physics, with a particular focus on heavy baryons. It introduces the theoretical foundations necessary for understanding the subsequent chapters of this thesis, aiming to make the document more self-contained. Additionally, the calculations of the mass spectra and strong decay widths for singly bottom baryons within the framework of the Quark Model are presented.

Singly bottom baryons consist of two light quarks and a single bottom quark (qqb, where $q = u, d$, or s). The experimental search for these baryons is challenging due to the high energies required to produce them, necessitating advanced particle accelerators. As a result, only a limited number of singly bottom baryon states have been discovered and most of them have yet to be observed in the future. According to the PDG [89], only 23 singly bottom baryons are currently listed (27 when accounting for different charge states). Furthermore, the lack of precise information about their quantum numbers makes it difficult to distinguish between three-quark structures and quark-diquark configurations.

The Λ_b^0 baryon was first observed in 1981 by the CERN-ISR experiment (R415) [11], with a statistical significance of 6σ. This initial observation was later confirmed in 1991 by the R422 experiment [95] and the UA1 Collaboration [96], which reported the state with statistical significances of approximately 4σ and 5σ, respectively. Subsequent confirmations came from several other experiments, including the ALEPH Collaboration in 1996 [97] with 3.3σ, the DELPHI Collaboration [98], the CDF Collaboration in 2014 [16], and the LHCb Collaboration in both 2014 [22] and 2017 [24]. The Ξ_b^- baryon was first observed in 2007 by the D0 Collaboration [17] and the CDF Collaboration [12]. In the same year, the CDF Collaboration also reported the discovery of the $\Sigma_b^{\pm}$ and $\Sigma_b^{*,\pm}$ baryons with a statistical significance exceeding 5.2σ [13], later confirming these findings in 2012 [15]. The ground state Ω_b^- baryon was discovered in 2008 by the D0 Collaboration [18] with 5.4σ and subsequently confirmed by the CDF Collaboration [99]. The ground state of the Ξ_b^0 baryon was observed by the CDF Collaboration in 2011 [14]. In 2012, the CMS Collaboration discovered an excited state, most likely corresponding to the partner of the Ξ_b' with $J^P = 3/2^+$, which is denoted as Ξ_b^*, with a statistical significance exceeding 5σ [19]. In the same year, the LHCb Collaboration [21] reported the discovery of two

narrow P-wave Λ_b^0 baryons, identified as $\Lambda_b(5912)^0$ and $\Lambda_b(5920)^0$, with significances of 5.2σ and 10.2σ, respectively. These findings were confirmed one year later by the CDF Collaboration [100]. The $\Xi_b^{'-}$ baryon was discovered, and the observation of the Ξ_b^{*-} state was confirmed in 2015 by the LHCb Collaboration [23]. The LHCb Collaboration reported in 2018 the discovery of an excited Ξ_b state, denoted as $\Xi_b(6227)^-$ [25], along with two excited Σ_b states, identified as $\Sigma_b(6097)^\pm$ [26]. Two D-wave Λ_b^0 candidates, $\Lambda_b(6146)^0$ and $\Lambda_b(6152)^0$, were discovered by the LHCb in 2020 [101]. In the same year, the LHCb collaboration [27] observed four narrow peaks in the $\Xi_b^0 K^-$ invariant mass spectrum, corresponding to the $\Omega_b(6316)$, $\Omega_b(6330)$, $\Omega_b(6340)$, and $\Omega_b(6350)$ states. Also in 2020, the CMS Collaboration [20] reported the first evidence for the $\Lambda_b(6070)$ baryon, a result later confirmed by the LHCb Collaboration [28] with a significance exceeding 7σ. In 2021, the $\Xi_b(6100)^-$ baryon was discovered by the CMS Collaboration [102]. Additionally, in the same year, the LHCb Collaboration [29] announced the discovery of two new Ξ_b states, identified as $\Xi_b(6327)^0$ and $\Xi_b(6333)^0$. More recently, in 2023, the LHCb Collaboration [30] discovered two additional states, $\Xi_b(6087)^0$ and $\Xi_b(6095)^0$.

From a theoretical perspective, numerous studies have explored the mass spectra and strong decays of singly bottom baryons. The pioneering work of Capstick and Isgur in 1986 [34, 35] was the first published study to use quark model predictions to compute the mass spectra of Λ_b and Σ_b baryons in the bottom sector. In 1992, E. Bagan *et al.* [36] conducted the first QCD spectral sum rule calculations, also focusing on the Σ_b and Λ_b baryons. In 1995, R. Roncaglia *et al.* [37] estimated the masses of ground-state singly bottom baryons using the Feynman-Hellmann theorem. A year later, in 1996, B. Silvestre-Brac [38] computed the mass spectra of Λ_b, Σ_b, Ξ_b, $\Xi' b$, and Ω_b baryons using a nonrelativistic quark model. In the same year, K. C. Bowler *et al.* [39] provided lattice QCD-based estimates for the masses of ground state singly bottom baryons. That same year, E. Jenkins [40] studied the masses of ground state bottom baryons by applying a combined expansion in $1/mQ$, $1/N_c$, and $SU(3)$ flavor symmetry breaking within the heavy quark effective theory. In 2002, N. Mathur *et al.* [41] employed quenched lattice nonrelativistic QCD to calculate the masses of ground state singly bottom baryons. In 2004, C. Albertus *et al.* [42] utilized a Faddeev approach to study the ground states of the singly heavy baryons. This model was later extended in references [43–45] to investigate the excited states of singly heavy baryons. Some other examples of the recent literature on theoretical investigations of the heavy baryon spectroscopy are the following: references [46, 47] use the relativistic quark-diquark description; references [48–50] use the non-relativistic quark model (NRQM); reference [51] use the Regge phenomenology; references [52–55] use the Hypercentral Constituent Quark Model(HCQM) and reference [56] applies it to study the excited Ω_b states; references [57–61] use the QCD sum rules (QCDSR); and reference [62] employs the symmetry-preserving Schwinger-Dyson equation approach. More discussions employing other models can be found in references [63–68]. For more references, see the review articles [103–108].

Apart from the mass spectra, the decay properties are one of the main physical quantities that are useful when making a consistent assignment of hadrons. A reliable approach to identifying these states involves matching experimental data with the predicted values for both mass spectra and decay widths.

To date, only a limited number of studies have addressed the strong decays of singly bottom baryons [69–81, 109–112]. Among these, the majority have utilized the constituent quark model [69–81]. In 2010, the decay widths of the Ξ_b ground and P-wave excited states were calculated in reference [69] by means of the $^3P_0$ model, with masses taken from Karliner [49] and the PDG. References [70, 71, 73, 74] employed the Elementary Emission Model (EEM) to compute strong decay widths. In 2020, after the discovery of $\Sigma_b(6097)$ by LHCb [26], the strong decay widths of P-wave Σ_b states were calculated in reference [74] within the framework of the χQM. Additionally, references [75–80] used masses from reference [47] to compute strong decay widths via the $^3P_0$ model. The $\Sigma_b^{(*)} \to \Lambda_b \pi$ strong decay widths were also calculated using the MIT bag model in reference [109]. A study of the $\Sigma_b \to \Lambda_b \pi$ and $\Sigma_b^{(*)} \to \Lambda_b \pi$ decays, based on the partial conservation of the axial current, was conducted in reference [110]. The P-wave Ω_b states were investigated using light-cone sum rules within HQET in reference [111]. The strong decay widths of the Σ_b, Σ_b^*, Ξ_b', and Ξ_b^* ground states were analyzed within chiral effective theory in reference [112]. However, none of these studies [69–81, 109–112] addressed decays into bottom baryon–vector meson channels or bottom meson–octet/decuplet baryon channels.

The large number of missing states makes the bottom sector particularly intriguing. Consequently, the primary objective of the study presented in this chapter is to provide predictions for the 1D, 2P, and 2S singly bottom baryons that remain undiscovered. In particular, the study focuses on calculating their partial strong decay widths, including decay channels that have not been explored in the existing literature.

2.1 Quantum Chromodynamics

Quantum Chromodynamics is the theory that describes the strong interactions [113]. It is a Quantum Field Theory characterized by the symmetry group $SU(3)_c$, which is non-Abelian, making QCD a non-Abelian gauge theory. The force carriers of QCD are called gluons, and the associated charge is known as "color." The most important properties of QCD are color confinement, asymptotic freedom, and chiral symmetry breaking.

The QCD Lagrangian is given by [114]:

$$\mathcal{L}_{\text{QCD}} = -\frac{1}{4} G_{\mu\nu\,a} G_a^{\mu\nu} + \bar{q}_i \left(i \not{D}_{\mu\,ij} - m\,\delta_{ij} \right) q_j + \frac{\theta_{QCD}}{32\pi^2} g_s^2 G_{\mu\nu\,a} \tilde{G}_a^{\mu\nu}. \tag{2.1}$$

Here, the non-Abelian gluon field strength tensor $G_{\mu\nu}$ is defined as:

$$G_{\mu\nu\,a} = \partial_\mu G_{\nu\,a} - \partial_\nu G_{\mu\,a} - g_s f_{abc} G_\mu^b G_\nu^c, \tag{2.2}$$

where $G_{\mu\,a}$ are the gluon fields, indexed by a, b, and c running from 1 to 8, and f_{abc} are the structure constants of $SU(3)$. The functions $q_i(x)$ represent the quark fields, where the color indexes i and j run from 1 to 3.

The symbol $\not{D}_\mu$ denotes the gauge covariant derivative in Dirac slash notation, expressed as $\not{D}_\mu = \gamma^\mu(D_\mu)$ where γ^μ are the gamma matrices. The gauge covariant derivative for quarks is defined as:

$$\left(D_\mu\right)_{ij} = \partial_\mu \delta_{ij} - i g_s \left(T_a\right)_{ij} G_{\mu\, a}, \tag{2.3}$$

which couples the quark fields to the gluon fields with a coupling strength g_s via the $SU(3)_c$ generators for quarks in the fundamental representation. These generators are explicitly given by $T_a = \lambda_a/2$, where the $\lambda_a\,(a = 1 \ldots 8)$ are the Gell-Mann matrices. The parameter θ_{QCD} is a dimensionless constant, and the dual field strength tensor is defined as:

$$\tilde{G}_a^{\mu\nu} = \frac{1}{2}\epsilon^{\mu\nu\rho\sigma} G_{\rho\sigma\, a}. \tag{2.4}$$

At low energies, the strong interaction is characterized by a coupling constant significantly larger than those of the electromagnetic and weak interactions. In this nonperturbative regime, where the interaction becomes strongly coupled, confinement occurs, resulting in the formation of hadrons. To study hadronic systems under these conditions, theoretical approaches based on nonperturbative models, such as the constituent quark model, are required.

Although QCD is a relativistic quantum field theory, its low-energy regime is effectively described by massive constituent quarks. The velocities of these constituent quarks inside hadrons are relatively small compared to the speed of light, making relativistic corrections less significant. Consequently, the non-relativistic quark model, which often employs a harmonic oscillator potential to describe quark confinement, provides an effective framework for studying baryon structure and spectra while capturing essential low-energy features of hadronic physics.

2.2 Quark Model

The quark model is a theoretical framework used to explain the behavior of subatomic particles called hadrons, such as protons and neutrons. It was developed in the 1960s by Murray Gell-Mann [5] and George Zweig [6] to explain the increasingly complex list of stable hadrons and hadronic resonances that had been discovered in the new particle accelerators of the 1950s and 1960s [113]. It postulates that hadrons are composed of smaller particles called quarks. This model has since become a cornerstone of particle physics. According to the model, quarks come in six different flavors: up, down, charm, strange, top, and bottom. Each flavor has a corresponding antiparticle, which has the opposite charge.

The quarks are also characterized by their spin and their color charge. The spin can be either up or down, and the color charge comes in three different types: red, green, and blue. Quarks can combine in different ways to form hadrons, which are particles that are bound together by the strong force. The QM has been successful in explaining many properties of hadrons, such as their masses and decay modes. However, there are still many unanswered questions about the nature of quarks and how they interact with each other. Despite these challenges, the

quark model remains an important tool for understanding the behavior of hadrons. The QM is an active area of research, and it continues to play a central role in particle physics.

2.3 Singly bottom baryons wave functions

As previously mentioned, singly bottom baryons consist of one bottom quark and two light quarks. This section presents the construction of the wave functions for these baryonic states. The discussion begins with the total baryon wave function, which incorporates the color, flavor, spin, and spatial degrees of freedom. Regarding the spatial degrees of freedom, two schemes are employed: the first considers singly bottom baryons as three-quark systems, while the second describes them as quark-diquark systems (a more detailed explanation will be provided in Section 2.3.3). Following this, the spin, flavor, and spatial wave functions are discussed in detail. Finally, a general overview of the baryon states is provided, addressing both the three-quark and quark-diquark schemes.

Within the three-quark scheme, singly bottom baryons are described as systems consisting of three quarks in the configuration qqb, where q represents the light quarks (u, d, or s) and b denotes the bottom quark.

The wave function for a generic baryon A in the three-quark scheme is expressed as

$$\mathbf{\Psi}^{\text{Tot}}_{A,J_A,M_{J_A}} = \theta_c \phi_A \sum_{M_{S_A},M_{L_A}} \langle S_A, M_{S_A}, L_A, M_{L_A} | J_A, M_{J_A} \rangle \chi_{S_A,M_{S_A}} \otimes \Psi_{A,L_A,M_{L_A}}(\vec{r}_1, \vec{r}_2, \vec{r}_3), \tag{2.5}$$

where

$$\theta_c = \frac{1}{\sqrt{6}}(rgb - rbg + gbr - grb + brg - bgr) \tag{2.6}$$

is the $SU_c(3)$ color singlet; ϕ_A, $\chi_{S_A,M_{S_A}}$, and $\Psi_{A,L_A,M_{L_A}}(\vec{r}_1, \vec{r}_2, \vec{r}_3)$ are the flavor, spin and spatial wave functions, respectively.

In the quark-diquark scheme, singly bottom baryon states are modeled as a bD system, where b represents the bottom quark and D denotes the diquarks ($D_\Lambda, D_\Xi, D_\Sigma, D_{\Xi'}$, and D_Ω) corresponding to the Λ_b, Ξ_b, Σ_b, Ξ'_b, and Ω_b baryons, respectively.

In this scheme, the wave function for a generic baryon A is expressed as

$$\mathbf{\Psi}^{\text{Tot}}_{A,J_A,M_{J_A}} = \theta_c \phi_A \sum_{M_{S_A},M_{L_A}} \langle S_A, M_{S_A}, L_A, M_{L_A} | J_A, M_{J_A} \rangle \chi_{S_A,M_{S_A}} \otimes \Psi_{A,L_A,M_{L_A}}(\vec{r}_1, \vec{r}_2), \tag{2.7}$$

where θ_c, given by eq. (2.6) is the color singlet wave function of $SU_c(3)$. ϕ_A, $\chi_{S_A,M_{S_A}}$, and $\Psi_{A,L_A,M_{L_A}}(\vec{r}_1, \vec{r}_2)$ are the flavor, spin and spatial wave functions, respectively. In this scheme, the two constituent light quarks are treated as a correlated pair, forming a diquark with no internal spatial excitations.

2.3.1 Spin wave functions of singly bottom baryons

The spin wave functions corresponding to the singly bottom baryons can be constructed by coupling the spins of the three constituent quarks. They are given by

$$\chi_{\rho_{1/2}} : \left|\frac{1}{2},\frac{1}{2}\right\rangle_{\rho} = \frac{1}{\sqrt{2}}\left(|\uparrow\downarrow\uparrow\rangle - |\downarrow\uparrow\uparrow\rangle\right), \tag{2.8}$$

$$\chi_{\rho_{-1/2}} : \left|\frac{1}{2},-\frac{1}{2}\right\rangle_{\rho-} = \frac{1}{\sqrt{2}}\left(|\uparrow\downarrow\downarrow\rangle - |\downarrow\uparrow\downarrow\rangle\right), \tag{2.9}$$

$$\chi_{\lambda_{1/2}} : \left|\frac{1}{2},\frac{1}{2}\right\rangle_{\lambda} = \frac{1}{\sqrt{6}}\left(2|\uparrow\uparrow\downarrow\rangle - |\uparrow\downarrow\uparrow\rangle - |\downarrow\uparrow\uparrow\rangle\right), \tag{2.10}$$

$$\chi_{\lambda_{-1/2}} : \left|\frac{1}{2},-\frac{1}{2}\right\rangle_{\lambda-} = \frac{1}{\sqrt{6}}\left(|\uparrow\downarrow\downarrow\rangle - |\downarrow\uparrow\downarrow\rangle - 2|\downarrow\downarrow\uparrow\rangle\right), \tag{2.11}$$

$$\chi_{s_{3/2}} : \left|\frac{3}{2},\frac{3}{2}\right\rangle_{s} = |\uparrow\uparrow\uparrow\rangle, \tag{2.12}$$

$$\chi_{s_{1/2}} : \left|\frac{3}{2},\frac{1}{2}\right\rangle_{s} = \frac{1}{\sqrt{3}}\left(|\uparrow\uparrow\downarrow\rangle + |\uparrow\downarrow\uparrow\rangle + |\downarrow\uparrow\uparrow\rangle\right), \tag{2.13}$$

$$\chi_{s_{-1/2}} : \left|\frac{3}{2},-\frac{1}{2}\right\rangle_{s} = \frac{1}{\sqrt{3}}\left(|\uparrow\downarrow\downarrow\rangle + |\downarrow\uparrow\downarrow\rangle + |\downarrow\downarrow\uparrow\rangle\right), \tag{2.14}$$

$$\chi_{s_{-3/2}} : \left|\frac{3}{2},-\frac{3}{2}\right\rangle_{s} = |\downarrow\downarrow\downarrow\rangle. \tag{2.15}$$

The mixed symmetric cases (eqs. 2.8-2.11) and the symmetric ones (eqs. 2.12-2.15) exhibit symmetry properties under the permutation group S_3 [115]. The functions $\chi_{\rho_{1/2}}$ and $\chi_{\rho_{-1/2}}$ are anti-symmetric under the interchange of the first two quarks, while on the contrary, $\chi_{\lambda_{1/2}}$, $\chi_{\lambda_{-1/2}}$, $\chi_{s_{3/2}}$, $\chi_{s_{1/2}}$, $\chi_{s_{-1/2}}$ and $\chi_{s_{-3/2}}$ are all symmetric under the same interchange.

2.3.2 Flavor wave functions of singly bottom baryons

In the bottom sector, the $\bar{\mathbf{3}}_{\mathrm{F}}$-plet and the $\mathbf{6}_{\mathrm{F}}$-plet representations of the flavor wave functions are considered. Next, the flavor wave functions of a singly bottom baryon A and its isospin quantum numbers $|A, I, M_I\rangle$ are given [90]:

$\bar{\mathbf{3}}_{\mathrm{F}}$-plet

$$\phi_{\Xi_b^-} : |\Xi_b^-, 1/2, -1/2\rangle = \frac{1}{\sqrt{2}}(|dsb\rangle - |sdb\rangle), \tag{2.16}$$

$$\phi_{\Xi_b^0} : |\Xi_b^0, 1/2, 1/2\rangle = \frac{1}{\sqrt{2}}(|usb\rangle - |sub\rangle), \tag{2.17}$$

$$\phi_{\Lambda_b^0} : |\Lambda_b^0, 0, 0\rangle = \frac{1}{\sqrt{2}}(|udb\rangle - |dub\rangle). \tag{2.18}$$

$\mathbf{6}_{\mathrm{F}}$-plet

$$\phi_{\Omega_b^-} : |\Omega_b^-, 0, 0\rangle : = |ssb\rangle, \tag{2.19}$$

$$\phi_{\Xi_b^{\prime -}} : |\Xi_b^{\prime -}, 1/2, -1/2\rangle = \frac{1}{\sqrt{2}}(|dsb\rangle + |sdb\rangle), \tag{2.20}$$

$$\phi_{\Xi_b^{\prime 0}} : |\Xi_b^{\prime 0}, 1/2, 1/2\rangle = \frac{1}{\sqrt{2}}(|usb\rangle + |sub\rangle), \tag{2.21}$$

$$\phi_{\Sigma_b^+} : |\Sigma_b^+, 1, 1\rangle = |uub\rangle, \tag{2.22}$$

$$\phi_{\Sigma_b^0} : |\Sigma_b^0, 1, 0\rangle = \frac{1}{\sqrt{2}}(|udb\rangle + |dub\rangle), \tag{2.23}$$

$$\phi_{\Sigma_b^-} : |\Sigma_b^-, 1, -1\rangle = |ddb\rangle. \tag{2.24}$$

It can be seen that the functions of the $\bar{\mathbf{3}}_{\mathrm{F}}$-plet are anti-symmetric under the interchange of the first two quarks, whereas, the functions of the $\mathbf{6}_{\mathrm{F}}$-plet are symmetric under the same interchange of the two light quarks.

2.3.3 Spatial wave functions of singly bottom baryons

In this study, a harmonic oscillator quark model is employed to calculate the masses as well as the strong and electromagnetic decay widths of singly bottom baryons. This model assumes that the potential confining the quarks inside a baryon is a harmonic oscillator potential [4, 116].

Spatial wave functions in the three quark scheme

The harmonic oscillator Hamiltonian for the three body system describing baryons in Cartesian coordinates can be written as

$$H = \frac{|\vec{p}_1|^2}{2m_1} + \frac{|\vec{p}_2|^2}{2m_2} + \frac{|\vec{p}_3|^2}{2m_b} + \frac{1}{2}K_b|\vec{r}_1 - \vec{r}_2|^2 + \frac{1}{2}K_b|\vec{r}_1 - \vec{r}_3|^2 + \frac{1}{2}K_b|\vec{r}_2 - \vec{r}_3|^2, \tag{2.25}$$

where $\vec{r}_j$ and $\vec{p}_j$, with $j = 1, 2, 3$ are the coordinate and momentum of the j-th quark, respectively and K_b is the spring constant.

To describe the relative motion of the elements of the system the following coordinate system is used:

$$\vec{\rho} = \frac{1}{\sqrt{2}}(\vec{r}_1 - \vec{r}_2), \qquad \vec{\lambda} = \frac{1}{\sqrt{6}}(\vec{r}_1 + \vec{r}_2 - 2\vec{r}_3), \qquad \vec{R} = \frac{m_\rho(\vec{r}_1 + \vec{r}_2) + m_b\vec{r}_3}{2m_\rho + m_b}, \tag{2.26}$$

where $\vec{\rho}$ and $\vec{\lambda}$ are known as the Jacobi coordinates [4, 33, 83, 90], $\vec{R}$ is the center of mass coordinate, m_ρ is defined as $m_\rho \equiv (m_1 + m_2)/2$ with m_1 and m_2 being the masses of the light quarks and m_b is the mass of the bottom quark. Here the $\vec{\rho}$ coordinate describes the relative motion of the light quark pair while the $\vec{\lambda}$ coordinate describes the relative motion between the light quark pair and the bottom quark, as depicted in Fig. 2.1. Then, the coordinates of the

quarks are given by the following expressions

$$\vec{r}_1 = \vec{R} + \frac{1}{\sqrt{2}}\vec{\rho} + \frac{\sqrt{\frac{3}{2}}m_b}{2m_\rho + m_b}\vec{\lambda}, \quad \vec{r}_2 = \vec{R} - \frac{1}{\sqrt{2}}\vec{\rho} + \frac{\sqrt{\frac{3}{2}}m_b}{2m_\rho + m_b}\vec{\lambda}, \quad \vec{r}_3 = \vec{R} - \frac{\sqrt{6}m_\rho}{2m_\rho + m_b}\vec{\lambda}, \tag{2.27}$$

where the differential volume is given by

$$d^3\vec{r}_1 d^3\vec{r}_2 d^3\vec{r}_3 = 3\sqrt{3}d^3\vec{\rho}d^3\vec{\lambda}d^3\vec{R}. \tag{2.28}$$

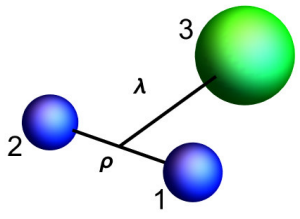

FIGURE 2.1: The $\vec{\rho}$ and $\vec{\lambda}$ coordinates for the singly-bottom baryons. The quarks 1 and 2 represent the light quarks and the quark 3 is the bottom quark.

In this coordinate system the Hamiltonian of eq. (2.25) can be rewritten as

$$H = \frac{|\vec{P}|^2}{2M} + \frac{|\vec{p}_\rho|^2}{2m_\rho} + \frac{|\vec{p}_\lambda|^2}{2m_\lambda} + \frac{3}{2}K_b|\vec{\rho}|^2 + \frac{3}{2}K_b|\vec{\lambda}|^2, \tag{2.29}$$

where the masses M and m_λ are defined as

$$M \equiv 2m_\rho + m_b, \qquad m_\lambda \equiv \frac{3m_\rho m_b}{2m_\rho + m_b}. \tag{2.30}$$

The momenta are defined as

$$\vec{P} = M\frac{d\vec{R}}{dt}, \qquad \vec{p}_\rho = m_\rho\frac{d\vec{\rho}}{dt}, \qquad \vec{p}_\lambda = m_\lambda\frac{d\vec{\lambda}}{dt}, \tag{2.31}$$

which in a more explicit way can be written as

$$\vec{p}_\rho = \frac{1}{\sqrt{2}}(\vec{p}_1 - \vec{p}_2), \qquad \vec{p}_\lambda = \frac{3}{\sqrt{6}}\frac{m_b(\vec{p}_1 + \vec{p}_2) - 2m_\rho\vec{p}_3}{2m_\rho + m_b}, \qquad \vec{P} = \vec{p}_1 + \vec{p}_2 + \vec{p}_3, \tag{2.32}$$

and from these last equations the momentum of each constituent quark is given by

$$\vec{p}_1 = \frac{m_\rho}{M}\vec{P} + \frac{1}{\sqrt{2}}\vec{p}_\rho + \frac{1}{\sqrt{6}}\vec{p}_\lambda, \quad \vec{p}_2 = \frac{m_\rho}{M}\vec{P} - \frac{1}{\sqrt{2}}\vec{p}_\rho + \frac{1}{\sqrt{6}}\vec{p}_\lambda, \quad \vec{p}_3 = \frac{m_b}{M}\vec{P} - \sqrt{\frac{2}{3}}\vec{p}_\lambda. \tag{2.33}$$

The spatial wave function in the coordinate representation is expressed as

$$\Psi_{A,L_A,M_{L_A}}(\vec{r}_1,\vec{r}_2,\vec{r}_3) = \frac{1}{(2\pi)^{3/2}} e^{i\vec{R}\cdot\vec{P}} \psi^{rel}_{k_\rho,l_\rho,m_{l_\rho},k_\lambda,l_\lambda,m_{l_\lambda}}(\vec{\rho},\vec{\lambda}), \tag{2.34}$$

where $\psi^{rel}_{k_\rho,l_\rho,m_{l_\rho},k_\lambda,l_\lambda,m_{l_\lambda}}(\vec{\rho},\vec{\lambda})$ is the relative wave function and is given by

$$\psi^{rel}_{k_\rho,l_\rho,m_{l_\rho},k_\lambda,l_\lambda,m_{l_\lambda}}(\vec{\rho},\vec{\lambda}) = \frac{1}{3^{3/4}} \sum_{m_{l_\rho},m_{l_\lambda}} \langle l_\rho, m_{l_\rho}, l_\lambda, m_{l_\lambda} | L_A, M_{L_A}\rangle \psi_{k_\rho,l_\rho,m_{l_\rho},k_\lambda,l_\lambda,m_{l_\lambda}}(\vec{\rho},\vec{\lambda}). \tag{2.35}$$

In the above expression, $\psi_{k_\rho,l_\rho,m_{l_\rho},k_\lambda,l_\lambda,m_{l_\lambda}}(\vec{\rho},\vec{\lambda})$ represents the harmonic oscillator wave functions. These wave functions can be expressed as the product of the harmonic oscillator wave functions in the $\vec{\rho}$ and $\vec{\lambda}$ coordinates in the following way

$$\psi_{k_\rho,l_\rho,m_{l_\rho},k_\lambda,l_\lambda,m_{l_\lambda}}(\vec{\rho},\vec{\lambda}) = \psi_{k_\rho,l_\rho,m_{l_\rho}}(\vec{\rho}) \otimes \psi_{k_\lambda,l_\lambda,m_{l_\lambda}}(\vec{\lambda}). \tag{2.36}$$

The wave functions of each harmonic oscillator can be written, as it is commonly done in the literature, in terms of their radial and angular parts as

$$\psi_{k_{\rho(\lambda)},l_{\rho(\lambda)},m_{l_{\rho(\lambda)}}}(\vec{\rho}(\vec{\lambda})) = R_{k_{\rho(\lambda)}l_{\rho(\lambda)}}(\vec{\rho}(\vec{\lambda})) Y^{m_{l_{\rho(\lambda)}}}_{l_{\rho(\lambda)}}(\hat{\rho}(\hat{\lambda})), \tag{2.37}$$

where the radial part for the $\vec{\rho}$ coordinate is given by

$$R_{k_\rho l_\rho}(\vec{\rho}) = \sqrt{\frac{\alpha_\rho^3 k_\rho! 2^{l_\rho+k_\rho+2}}{\sqrt{\pi}(2l_\rho+2k_\rho+1)!!}} e^{-\frac{1}{2}\alpha_\rho^2\rho^2} (\alpha_\rho\rho)^{l_\rho} L^{l_\rho+\frac{1}{2}}_{k_\rho}\left(\rho^2\alpha_\rho^2\right), \tag{2.38}$$

and for the $\vec{\lambda}$ coordinate is

$$R_{k_\lambda l_\lambda}(\vec{\lambda}) = \sqrt{\frac{\alpha_\lambda^3 k_\lambda! 2^{l_\lambda+k_\lambda+2}}{\sqrt{\pi}(2l_\lambda+2k_\lambda+1)!!}} e^{-\frac{1}{2}\alpha_\lambda^2\lambda^2} (\alpha_\lambda\lambda)^{l_\lambda} L^{l_\lambda+\frac{1}{2}}_{k_\lambda}\left(\lambda^2\alpha_\lambda^2\right), \tag{2.39}$$

here $L^a_k(x)$ are the generalized Laguerre polynomials. The $\alpha_{\rho(\lambda)}$ are related to the harmonic oscillator frequencies, $\omega_{\rho(\lambda)}$, through the relations $\alpha^2_{\rho(\lambda)} = \omega_{\rho(\lambda)} m_{\rho(\lambda)}$. Thus, $\alpha_{\rho(\lambda)}$ depend on the harmonic oscillator constant K_b and the quark masses, which are fitted to reproduce the bottom baryon mass spectra (see Tab. 2.1). As a result, the harmonic oscillator wave functions do not contain any free parameters.

Spatial wave functions in the quark-diquark scheme

In the quark-diquark scheme the following coordinate system is used [33, 90]:

$$\vec{r} = \vec{r}_1 - \vec{r}_2, \qquad \vec{R} = \frac{m_D\vec{r}_1 + m_b\vec{r}_2}{m_D + m_b}, \tag{2.40}$$

where $\vec{r}_1$ and $\vec{r}_2$ are the diquark and bottom quark coordinates, $\vec{R}$ is the center of mass coordinate, and m_D and m_b are the diquark and bottom quark masses.

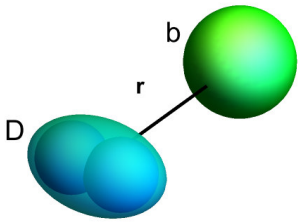

FIGURE 2.2: The $\vec{r}$ coordinate for the singly bottom baryons in the quark-diquark scheme. The D represents the diquark structure made of the 2 light quarks and the quark b is the bottom quark.

The spatial wave functions in the coordinate representation are given by

$$\Psi_{A,L_A,M_{L_A}}(\vec{r}) = \frac{1}{(2\pi)^{3/2}} e^{i\vec{R}\cdot\vec{P}}\, \psi_{k_r,l_r,m_{l_r}}(\vec{r}), \tag{2.41}$$

where $\psi_{k_r,l_r,m_{l_r}}(\vec{r})$ are the harmonic oscillator wave functions, which can be expressed in terms of their radial and angular parts in the form

$$\psi_{k_r,l_r,m_{l_r}}(\vec{r}) = R_{k_r l_r}(\vec{r}) Y_{l_r}^{m_{l_r}}(\hat{r}), \tag{2.42}$$

with the radial part being

$$R_{k_r l_r}(\vec{r}) = \sqrt{\frac{\alpha_r^3 k_r! 2^{l_r+k_r+2}}{\sqrt{\pi}(2l_r+2k_r+1)!!}} e^{-\frac{1}{2}\alpha_r^2 r^2} (\alpha_r r)^{l_r} L_{k_r}^{l_r+\frac{1}{2}}\left(r^2\alpha_r^2\right), \tag{2.43}$$

where, in the same way as for the three-quark scheme, $L_k^a(x)$ are the generalized Laguerre polynomials, and α_r is related to the harmonic oscillator frequency, ω_r, through the relation $\alpha_r^2 = \omega_r m_r$. Thus, α_r depend on the harmonic oscillator constant K_b and the diquark and bottom masses, which are fitted to reproduce the bottom baryon mass spectra (see Tab. 2.1).

2.3.4 General description of states within the three quark scheme

As previously mentioned, in the three quark scheme, the spatial degrees of freedom are expressed in terms of the Jacobi coordinates $\boldsymbol{\rho}$ and $\boldsymbol{\lambda}$, which describes the excitations within the light quark pair, and between the light quark pair and the bottom quark, respectively (see Fig. 2.1).

A three-quark quantum state, written as $\left|l_\lambda, l_\rho, k_\lambda, k_\rho\right\rangle$, is defined by its total angular momentum $\mathbf{J} = \mathbf{L}_{\text{tot}} + \mathbf{S}_{\text{tot}}$, where $\mathbf{L}_{\text{tot}} = \mathbf{l}_{\boldsymbol{\rho}} + \mathbf{l}_{\boldsymbol{\lambda}}$ is the orbital angular momentum and $\mathbf{S}_{\text{tot}} = \mathbf{S}_{12} + \mathbf{1/2}$ is the internal spin, which is the sum of the light quark spin, $\mathbf{S}_{12} = \mathbf{S}_1 + \mathbf{S}_2$, and the b quark

spin ($\mathbf{1/2}$), and the number of nodes is $k_{\lambda,\rho}$. In addition, we assign the flavor multiplet (specified by the symbol $\mathcal{F}$), and the spectroscopic notation $^{2S+1}L_J$ to each of them in order define these states with more precision.

Now, the possible states for the two different flavor representations available for the singly bottom baryons will be constructed.

The states from the ground to the excited states up to the second energy band ($N = 2$), with $N = n_\rho + n_\lambda$, and $n_{\rho(\lambda)} = 2k_{\rho(\lambda)} + l_{\rho(\lambda)}$ will be considered, in order to find S-, P-, D-wave bottom baryon states.

The symmetric $\mathcal{F} = \mathbf{6}_{\rm F}$ multiplet for the three-quark model

The Ω_b, Ξ_b', and Σ_b baryons form a flavor sextet in the bottom baryon sector. These bottom baryons have a symmetric flavor wave function and, in combination with the anti-symmetric color wave function, the final product wave function is anti-symmetric. This fact implies that the product of the spatial and spin wave functions should be symmetric.

- In the energy band $N = 0$, in which $\mathbf{l_\rho} = \mathbf{l_\lambda} = 0$, the spatial wave function of the two light quarks is symmetric implying that their spin-flavor wave function has to be symmetric, meaning that $\mathbf{S}_{12} = \mathbf{1}$. Hence, the ground state baryons made up of a light quark pair with spin symmetric configuration $\mathbf{S}_{12} = \mathbf{1}$, fill one $\mathbf{6}_{\rm F}$-plet with total spin $\mathbf{J} = \mathbf{S}_{\rm tot} = \frac{\mathbf{1}}{\mathbf{2}}$ (shown on the center of Fig. 2.3), and one $\mathbf{6}_{\rm F}$-plet with total spin $\mathbf{J} = \mathbf{S}_{\rm tot} = \frac{\mathbf{3}}{\mathbf{2}}$ (shown on the right-hand side of Fig. 2.3).

- For the energy band $N = 1$, there are two different possibilities. If $\mathbf{l_\rho} = 0$ and $\mathbf{l_\lambda} = 1$, the spatial wave function is symmetric under the interchange of light quarks, implying that their spin-flavor function is also symmetric. This spatial wave function must be coupled with two possible spin configurations, $\mathbf{S}_{\rm tot} = \mathbf{1/2, 3/2}$, with $\mathbf{L}_{\rm tot} = \mathbf{1}$, yielding five P_λ-wave excitations, $\mathbf{J}_{\rm tot} = \mathbf{1 + 3/2} = \mathbf{1/2, 3/2, 1/2, 3/2, 5/2}$. If $\mathbf{l_\rho} = 1$ and $\mathbf{l_\lambda} = 0$, the spatial wave function is anti-symmetric under the interchange of light quarks implying that the spin wave function should be anti-symmetric, meaning $\mathbf{S}_{12} = \mathbf{0}$, which yields to two P_ρ-wave states obtained from $\mathbf{J}_{\rm tot} = \mathbf{1 + 1/2} = \mathbf{1/2, 3/2}$.

- In the energy band $N = 2$, there are three possible cases: the pure $\lambda-$excitations, $\mathbf{l_\rho} = 0$ and $\mathbf{l_\lambda} = 2$, the pure $\rho-$excitations, $\mathbf{l_\rho} = 2$ and $\mathbf{l_\lambda} = 0$, and the mixed case $\mathbf{l_\rho} = 1$ and $\mathbf{l_\lambda} = 1$. In both the pure $\lambda-$excitations and pure $\rho-$excitations cases the total spatial wave function is symmetric under the interchange of light quarks implying that their spin-flavor wave function is also symmetric.

If $\mathbf{l_\rho} = 0$ and $\mathbf{l_\lambda} = 2$, then $\mathbf{L}_{\rm tot} = \mathbf{2}$ is coupled with two possible spin configurations, $\mathbf{S}_{\rm tot} = \frac{\mathbf{1}}{\mathbf{2}}, \frac{\mathbf{3}}{\mathbf{2}}$, giving six D_λ-wave excitations. If $\mathbf{l_\rho} = 2$ and $\mathbf{l_\lambda} = 0$, in a similar way we have six D_ρ-wave excitations.

When $\mathbf{l_\rho} = 1$ and $\mathbf{l_\lambda} = 1$ there are three possible values of the angular momentum $\mathbf{L}_{\rm tot} = \mathbf{0, 1, 2}$. These values are combined with $\mathbf{S}_{\rm tot} = \frac{\mathbf{1}}{\mathbf{2}}$ that come from the light quark spin configuration

$\mathbf{S}_{12} = \mathbf{0}$, producing in this way five possible states: two D-wave states, two P-wave states, and one ground state.

Additionally, there are two possible radial excitation modes in this energy band, $k_\rho = 0, k_\lambda = 1$, and $k_\rho = 1, k_\lambda = 0$, both corresponding to a symmetric light quark wave function since $\mathbf{L}_{\rm tot} = \mathbf{l_\rho} + \mathbf{l_\lambda} = 0$. If $k_\rho = 0$ and $k_\lambda = 1$, in the case of the $\mathbf{6}_{\rm F}$-plet baryons, $\mathbf{L}_{\rm tot} = \mathbf{0}$ is combined with $\mathbf{J} = \mathbf{S}_{\rm tot} = \frac{\mathbf{1}}{\mathbf{2}}, \frac{\mathbf{3}}{\mathbf{2}}$ producing two λ-radial excitations. In a similar way, if $k_\rho = 1$ and $k_\lambda = 1$, in this case we have two ρ-radial excitations.

The anti-symmetric $3_{\rm F}$-plet for the three-quark model

The Λ_b and Ξ_b baryons form a flavor anti-triplet in the bottom baryon sector. These bottom baryons have an anti-symmetric flavor wave function, which, in combination with the anti-symmetric color wave function, produces a symmetric combination. This implies that the product of the spatial and spin wave functions should be anti-symmetric.

- For the energy band $N = 0$, in which ($\mathbf{l_\rho} = \mathbf{l_\lambda} = 0$), the spatial wave function of the two light quarks is symmetric, thus the spin-flavor wave function should be anti-symmetric. Therefore, we can only combine the anti-symmetric $\bar{\mathbf{3}}_{\rm F}$-plet with anti-symmetric-spin configuration $\mathbf{S}_{12} = \mathbf{0}$. This means that the ground state baryons made up of a light quark pair with anti-symmetric spin configuration $\mathbf{S}_{12} = \mathbf{0}$ fill an anti-symmetric $\bar{\mathbf{3}}_{\rm F}$-plet with total spin $\mathbf{J} = \mathbf{S}_{\rm tot} = \frac{\mathbf{1}}{\mathbf{2}}$ (shown on the left-hand side of Fig. 2.3).

- For the energy band $N = 1$, there are two different possibilities. If $\mathbf{l_\rho} = 0$ and $\mathbf{l_\lambda} = 1$, we have a symmetric spatial wave function implying that their spin-flavor wave function is also symmetric. Thus, for the $\bar{\mathbf{3}}_{\rm F}$-plet baryons, the angular momentum $\mathbf{L}_{\rm tot} = \mathbf{1}$ is only coupled with one spin configuration, $\mathbf{S}_{\rm tot} = \frac{\mathbf{1}}{\mathbf{2}}$ that comes from the light quark spin configuration $\mathbf{S}_{12} = \mathbf{0}$, constructing two P_λ-wave excitations. In the case when $\mathbf{l_\rho} = 1$ and $\mathbf{l_\lambda} = 0$, the spatial wave function is anti-symmetric under the interchange of the light quarks implying that the two light quark spin-flavor wave function are also anti-symmetric, hence $\mathbf{L}_{\rm tot} = \mathbf{1}$ is coupled with $\mathbf{S}_{\rm tot} = \frac{\mathbf{1}}{\mathbf{2}}, \frac{\mathbf{3}}{\mathbf{2}}$ yielding to five P_ρ-wave states.

- In the energy band $N = 2$, just like for the $\mathbf{6}_{\rm F}$-plet, there are three possibilities: the pure λ-excitations, the pure ρ-excitations, and the mixed case. In both the $\mathbf{l_\rho} = 0, \mathbf{l_\lambda} = 2$ and $\mathbf{l_\rho} = 2, \mathbf{l_\lambda} = 0$ cases the total spatial wave function is symmetric under the interchange of light quarks implying that their spin-flavor wave function is also symmetric. In the case where $\mathbf{l_\rho} = 0$ and $\mathbf{l_\lambda} = 2$, we have that $\mathbf{L}_{\rm tot} = \mathbf{2}$ is coupled with $\mathbf{S}_{\rm tot} = \frac{\mathbf{1}}{\mathbf{2}}$ giving two D_λ-wave excitations. If $\mathbf{l_\rho} = 2$ and $\mathbf{l_\lambda} = 0$, in a similar way we have two D_ρ-wave excitations.

When $\mathbf{l_\rho} = 1$ and $\mathbf{l_\lambda} = 1$ there are again three possible values of the angular momentum ($\mathbf{L}_{\rm tot} = \mathbf{0}, \mathbf{1}, \mathbf{2}$). In the case of the baryons on the anti-triplet, they are combined with $\mathbf{S}_{\rm tot} = \frac{\mathbf{1}}{\mathbf{2}}, \frac{\mathbf{3}}{\mathbf{2}}$ that comes from the light quark spin configuration $\mathbf{S}_{12} = \mathbf{1}$, producing a total of thirteen mixed excited states: six D-wave states, five P-wave states, and two ground states.

In addition, there are two possible radial excitation modes, $k_\rho = 0, k_\lambda = 1$, and $k_\rho = 1, k_\lambda = 0$, corresponding both of them to a symmetric wave function because $\mathbf{L}_{\rm tot} = \mathbf{l_\rho} + \mathbf{l_\lambda} = 0$. In the

case with $k_\rho = 0$ and $k_\lambda = 1$ the total orbital angular momentum $\mathbf{L}_{\rm tot} = 0$ is combined with $\mathbf{S}_{\rm tot} = \frac{1}{2}$ producing one λ-radial excitation and, if $k_\rho = 1$ and $k_\lambda = 1$ there is one ρ-radial excitation.

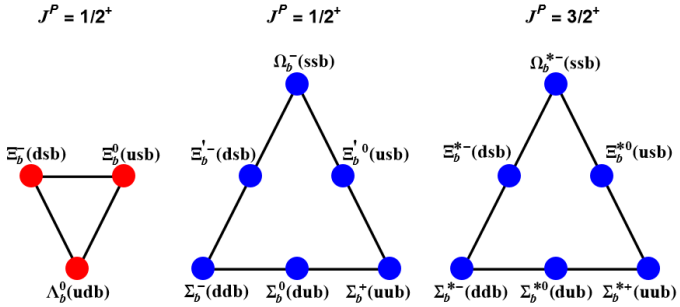

FIGURE 2.3: The singly bottom baryons belong to two $SU_f(3)$ flavor representations: the flavor anti-triplet $\bar{\mathbf{3}}_{\rm F}$ and the flavor sextet $\mathbf{6}_{\rm F}$. Specifically, for ground states, the $\bar{\mathbf{3}}_{\rm F}$-plet, shown on the left side, has spin-parity $\mathbf{J}^P = \frac{1}{2}^+$. The $\mathbf{6}_{\rm F}$-plet has two spin configurations: one with $\mathbf{J}^P = \frac{1}{2}^+$, shown in the center, and another with $\mathbf{J}^P = \frac{3}{2}^+$, shown on the right side.

2.3.5 General description of states within the quark-diquark scheme

In the quark-diquark scheme, the two constituent light quarks of the diquark are considered to be correlated and they have no internal spatial excitations ($\mathbf{l}_\rho = 0$). Then, the quark-diquark states are a subset of the three quark states that were discussed in the previous section. The quark-diquark Hamiltonian is expressed in terms of one spatial coordinate $\boldsymbol{r}$ with an associated reduced mass μ.

A quark-diquark quantum state, written as $|l_r, k_r\rangle$, is defined by its total angular momentum $\mathbf{J}_{\rm tot} = \mathbf{L}_{\rm tot} + \mathbf{S}_{\rm tot}$, where $\mathbf{L}_{\rm tot} = \mathbf{l}_r$ is the orbital angular momentum and $\mathbf{S}_{\rm tot} = \mathbf{S}_{12} + \mathbf{1/2}$ is the internal spin and the number of nodes is k_r. We also report for each state, like for the three quark scheme, the information about the total spin, orbital angular momentum and total angular momentum using the spectroscopic notation.

The symmetric $6_{\rm F}$-multiplet for the quark-diquark model

When the Σ_b, Ξ_b', and Ω_b baryons are considered as quark-diquark systems, it is hypothesized that the system is within the limit where the diquark internal spatial excitations are higher in energy than the scale of the resonances studied [33]. Since the hadron has to be colorless, the diquark transforms as a $\bar{\mathbf{3}}$ under the $SU_c(3)$ group, in this way, the product of the spin and flavor wave functions of the diquark should be symmetric. The flavor wave functions are symmetric, then, only combinations with axial-vector diquarks ($\mathbf{S}_{12} = \mathbf{1}$) can be made.

- In the energy band $N = 0$, the total orbital momentum $\mathbf{L}_{\rm tot} = \mathbf{0}$, and therefore $\mathbf{J}_{\rm tot} = \mathbf{S}_{\rm tot} = \mathbf{1/2}, \mathbf{3/2}$, resulting in two ground states.

- In the band $N = 1$, $\mathbf{L}_{\rm tot} = \mathbf{1}$ has to be coupled with $\mathbf{S}_{\rm tot} = \mathbf{1/2}, \mathbf{3/2}$, then yields to five P-wave excitations.

- In the energy band $N = 2$, $\mathbf{L}_{\rm tot} = \mathbf{2}$, and this value is combined with $\mathbf{S}_{\rm tot} = \mathbf{1/2}, \mathbf{3/2}$, resulting in six D-wave states.

In addition, there is a radial excitation $k_r = 1$ with $\mathbf{L}_{\rm tot} = \mathbf{0}$, then $\mathbf{J}_{\rm tot} = \mathbf{S}_{\rm tot} = \mathbf{1/2}, \mathbf{3/2}$, and therefore there are two radial excited states.

The anti-symmetric $\bar{\mathbf{3}}_{\rm F}$-plet for the quark-diquark model

When the Λ_b and Ξ_b baryons are described as quark-diquark systems, exactly as for the $\mathbf{6}_{\rm F}$-plet described in the above subsection (2.3.5), the diquark presents an S-wave configuration because of the absence internal spatial excitations ($\mathbf{l}_{\boldsymbol{\rho}} = 0$). In this case, the diquark is also $\bar{\mathbf{3}}$ in the $SU_c(3)$ representation, thus the spin-flavor wave functions of the diquark configuration have to be symmetric. In the $\bar{\mathbf{3}}_{\rm f}$-plet representation, the flavor wave function is antisymmetric, therefore, the spin wave function of the diquark corresponds to a scalar configuration ($\mathbf{S}_{12} = \mathbf{0}$).

- For the energy band $N = 0$, the total orbital momentum $\mathbf{L}_{\rm tot} = \mathbf{0}$, then, only exists one ground state $\mathbf{J}_{\rm tot} = \mathbf{S}_{\rm tot} = \mathbf{1/2}$.

- In the band $N = 1$, $\mathbf{L}_{\rm tot} = \mathbf{1}$ has to be combined with $\mathbf{S}_{\rm tot} = \mathbf{1/2}$. This combinations yields two P-wave states.

- In the band $N = 2$, $\mathbf{L}_{\rm tot} = \mathbf{1}$, which, in combination with $\mathbf{S}_{\rm tot} = \mathbf{1/2}$, it yields to two D-wave states.

- Finally, there exists a radial excitation $k_r = 1$, corresponding only to one state because of the fact that $\mathbf{L}_{\rm tot} = \mathbf{0}$.

2.4 Mass spectra of the singly bottom baryons

The masses of the singly bottom baryons are calculated using the model introduced in reference [83]. This model is based on a three-dimensional harmonic oscillator Hamiltonian, supplemented by a perturbation term that accounts for spin, spin-orbit, isospin, and flavor-dependent contributions. The baryon masses are obtained as the eigenvalues of the following Hamiltonian:

$$H = H_{\rm h.o.} + a_{\rm S}\, \mathbf{S}^2_{\rm tot} + a_{\rm SL}\, \mathbf{S}_{\rm tot} \cdot \mathbf{L}_{\rm tot} + a_{\rm I}\, \mathbf{I}^2 + a_{\rm F}\, \hat{\mathbf{C}}_2(SU_F(3)). \tag{2.44}$$

Here, $H_{\rm h.o.}$ represents the sum of the masses of the constituent quarks and the harmonic oscillator Hamiltonian. The terms $\mathbf{S}_{\rm tot}, \mathbf{L}_{\rm tot}, \mathbf{I}$ and $\hat{\mathbf{C}}_2(SU_F(3))$ correspond to the spin, orbital angular momentum, isospin, and the $SU_F(3)$ Casimir operators, respectively. These operators are weighted by the model parameters $a_{\rm S}, a_{\rm SL}, a_{\rm I}$, and $a_{\rm F}$.

2.4.1 Mass spectra within the three-quark scheme

As previously mentioned, when baryons are treated as three-quark systems, the harmonic oscillator term in eq. (2.44), $H_{\text{h.o.}}$, is expressed using the Jacobi coordinates, $\boldsymbol{\rho}$ and $\boldsymbol{\lambda}$, along with their conjugate momenta, $\mathbf{p}_\rho$ and $\mathbf{p}_\lambda$, as follows

$$H^{3q}_{\text{h.o.}} = \sum_{j=1}^{3} m_j + \frac{\mathbf{p}_\rho^2}{2m_\rho} + \frac{\mathbf{p}_\lambda^2}{2m_\lambda} + \frac{1}{2}m_\rho\omega_\rho^2\boldsymbol{\rho}^2 + \frac{1}{2}m_\lambda\omega_\lambda^2\boldsymbol{\lambda}^2. \tag{2.45}$$

Here, m_j denotes the mass of the j-th quark, where $j = 1, 2$ corresponds to the masses of the light quarks, and m_3 represents the mass of the bottom quark. The frequencies of the ρ- and λ-oscillators are given by $\omega_\rho = \sqrt{\frac{3K_b}{m_\rho}}$ and $\omega_\lambda = \sqrt{\frac{3K_b}{m_\lambda}}$, respectively. The eigenstates of the Hamiltonian in eq. (2.45) are provided in Subsection 2.3.3, and its eigenvalues are given by

$$E^{3q}_{\text{h.o.}} = \sum_{j=1}^{3} m_j + \omega_\rho\, n_\rho + \omega_\lambda\, n_\lambda. \tag{2.46}$$

The standard definitions for the harmonic oscillator quantum numbers are used: $n_{\rho(\lambda)} = 2k_{\rho(\lambda)} + l_{\rho(\lambda)}$, where $k_{\rho(\lambda)} = 0, 1, \ldots$ represents the number of nodes (radial excitations) in the $\rho(\lambda)$-oscillator, and $l_{\rho(\lambda)} = 0, 1, \ldots$ corresponds to the orbital angular momentum of the $\rho(\lambda)$-oscillator.

In the three-quark model, the eigenvalues of the Hamiltonian given in eq. (2.44) can be expressed as follows [33, 83, 90]:

$$\begin{aligned} E^{3q} &= \sum_{j=1}^{3} m_j + \omega_\rho n_\rho + \omega_\lambda n_\lambda + a_{\text{S}}\left[S_{\text{tot}}(S_{\text{tot}}+1)\right] + a_{\text{SL}}\frac{1}{2}\Big[J(J+1) - L_{\text{tot}}(L_{\text{tot}}+1) - S_{\text{tot}}(S_{\text{tot}}+1)\Big] \\ &+ a_{\text{I}}\left[I(I+1)\right] + a_{\text{F}}\frac{1}{3}\left[p(p+3) + q(q+3) + pq\right], \end{aligned} \tag{2.47}$$

which is the mass formula used to calculate the spectra in this model. It can be observed that the model is completely analytical, meaning that the Hamiltonian of eq. (2.44), together with eq. (2.45), is completely diagonal in the harmonic oscillator, spin, flavor, and color bases.

In the above expression, the spin-dependent term induces a splitting between states with different total spin, $\mathbf{S}_{\text{tot}}$. The contribution of this term is smaller for bottom baryons compared to the charm baryon sector [90], which is consistent with Heavy Quark Spin Symmetry. The spin-orbit interaction, which is generally negligible in light baryons [34, 46], plays a fundamental role in describing the mass patterns of heavy-light baryons [83]. Specifically, the spin-orbit term splits states with different total angular momentum, $\mathbf{J}$. Furthermore, the effect of the flavor-dependent term is to split the baryons belonging to the flavor sextet, $\mathbf{6}_{\text{F}}$, characterized by $(p, q) = (2, 0)$, from those in the anti-triplet, $\bar{\mathbf{3}}_{\text{F}}$, with $(p, q) = (0, 1)$.

The mass formula given in eq. (2.47) can be employed to calculate the mass splitting between states within the same multiplet:

$$\begin{aligned} m(A) - m(A') &= m_1 + m_2 - m_1' - m_2' + \omega_\rho n_\rho + \omega_\lambda n_\lambda - (\omega_\rho' n_\rho' + \omega_\lambda' n_\lambda') \\ &+ a_{\rm S}\left[S_{\rm tot}(S_{\rm tot}+1) - S'_{\rm tot}(S'_{\rm tot}+1)\right] \\ &+ a_{\rm SL}\frac{1}{2}\Big[J(J+1) - L_{\rm tot}(L_{\rm tot}+1) - S_{\rm tot}(S_{\rm tot}+1) - J'(J'+1) \\ &+ L'_{\rm tot}(L'_{\rm tot}+1) + S'_{\rm tot}(S'_{\rm tot}+1)\Big] + a_{\rm I}\left[I(I+1) - I'(I'+1)\right]. \end{aligned} \tag{2.48}$$

By applying this formula and utilizing the parameter values from reference [33], the following result is obtained:

$$m(^{2S+1}(\Omega_c)_J) - m(^{2S+1}(\Xi'_c)_J) = 115 \pm 30\,\text{MeV}\,,$$

.

This result is consistent with the experimental mass splitting reported by the LHCb collaboration [117] in the charm sector for baryons belonging to the flavor $\mathbf{6}_{\rm F}$-plet

$$\begin{aligned} &m(\Omega_c(3050)) - m(\Xi'_c(2923)) \simeq m(\Omega_c(3065)) - m(\Xi'_c(2939)) \\ &\simeq m(\Omega_c(3090)) - m(\Xi'_c(2965)) \simeq 125\,\text{MeV}. \end{aligned} \tag{2.49}$$

Thus, a similar pattern is expected in the bottom sector, suggesting that the results obtained using equal-spacing rules could serve as a useful guide for future experimental searches in this sector.

For instance, the P_λ-wave excited states follow the equal-spacing rules given by:

$$m(^{2S+1}(\Omega_b)_J) - m(^{2S+1}(\Xi'_b)_J) = m_s - m_n + \omega_\lambda^{\Omega_b} - \omega_\lambda^{\Xi_b} - \frac{3}{4}a_{\rm I} \simeq 117 \pm 20\,\text{MeV}, \tag{2.50}$$

$$m(^{2S+1}(\Xi'_b)_J) - m(^{2S+1}(\Sigma_b)_J) = m_s - m_n + \omega_\lambda^{\Xi_b} - \omega_\lambda^{\Sigma_b} - \frac{5}{4}a_{\rm I} \simeq 100 \pm 26\,\text{MeV}, \tag{2.51}$$

$$m(^{2S+1}(\Xi_b)_J) - m(^{2S+1}(\Lambda_b)_J) = m_s - m_n + \omega_\lambda^{\Xi_b} - \omega_\lambda^{\Sigma_b} + \frac{3}{4}a_{\rm I} \simeq 161 \pm 30\,\text{MeV}\,. \tag{2.52}$$

For P_ρ-wave excited states the expressions

$$m(^{2S+1}(\Omega_b)_J) - m(^{2S+1}(\Xi'_b)_J) = m_s - m_n + \omega_\rho^{\Omega_b} - \omega_\rho^{\Xi_b} - \frac{3}{4}a_{\rm I} \simeq 98 \pm 20\,\text{MeV}, \tag{2.53}$$

$$m(^{2S+1}(\Xi'_b)_J) - m(^{2S+1}(\Sigma_b)_J) = m_s - m_n + \omega_\rho^{\Xi_b} - \omega_\rho^{\Sigma_b} - \frac{5}{4}a_{\rm I} \simeq 63 \pm 26\,\text{MeV}, \tag{2.54}$$

$$m(^{2S+1}(\Xi_b)_J) - m(^{2S+1}(\Lambda_b)_J) = m_s - m_n + \omega_\rho^{\Xi_b} - \omega_\rho^{\Sigma_b} + \frac{3}{4}a_{\rm I} \simeq 134 \pm 30\,\text{MeV}\,, \tag{2.55}$$

are obtained. The D_λ-wave excited states follow the equal-spacing rules given by:

$$m(^{2S+1}(\Omega_b)_J) - m(^{2S+1}(\Xi'_b)_J) = m_s - m_n + 2(\omega_\lambda^{\Omega_b} - \omega_\lambda^{\Xi_b}) - \frac{3}{4}a_{\rm I} \simeq 95 \pm 36\,\text{MeV}, \tag{2.56}$$

$$m(^{2S+1}(\Xi_b')_J) - m(^{2S+1}(\Sigma_b)_J) = m_s - m_n + 2(\omega_\lambda^{\Xi_b} - \omega_\lambda^{\Sigma_b}) - \frac{5}{4}a_{\rm I} \simeq 58 \pm 41\,{\rm MeV}, \quad (2.57)$$

$$m(^{2S+1}(\Xi_b)_J) - m(^{2S+1}(\Lambda_b)_J) = m_s - m_n + 2(\omega_\lambda^{\Xi_b} - \omega_\lambda^{\Sigma_b}) + \frac{3}{4}a_{\rm I} \simeq 129 \pm 26\,{\rm MeV}\,. \quad (2.58)$$

For the D_ρ-wave excited states the relations

$$m(^{2S+1}(\Omega_b)_J) - m(^{2S+1}(\Xi_b')_J) = m_s - m_n + 2(\omega_\rho^{\Omega_b} - \omega_\rho^{\Xi_b}) - \frac{3}{4}a_{\rm I} \simeq 56 \pm 48\,{\rm MeV}, \quad (2.59)$$

$$m(^{2S+1}(\Xi_b')_J) - m(^{2S+1}(\Sigma_b)_J) = m_s - m_n + 2(\omega_\rho^{\Xi_b} - \omega_\rho^{\Sigma_b}) - \frac{5}{4}a_{\rm I} \simeq 4 \pm 40\,{\rm MeV}, \quad (2.60)$$

$$m(^{2S+1}(\Xi_b)_J) - m(^{2S+1}(\Lambda_b)_J) = m_s - m_n + 2(\omega_\rho^{\Xi_b} - \omega_\rho^{\Sigma_b}) + \frac{3}{4}a_{\rm I} \simeq 75 \pm 40\,{\rm MeV}\,, \quad (2.61)$$

are obtained.

All of these calculations are performed using the parameters listed in Table 2.1, with the values of $\omega_{\lambda,\rho}^{B_b}$ computed for each bottom baryon using eq. (2.46). It is important to note that only three distinct labels: Ω_b, Ξ_b, and Σ_b are used, since the relationships $\omega^{\Xi_b} = \omega^{\Xi_b'}$ and $\omega^{\Sigma_b} = \omega^{\Lambda_b}$ hold due to their identical quark content.

2.4.2 Mass spectra within the quark-diquark scheme

When baryons are modeled as quark-diquark systems, the harmonic oscillator term of eq. (2.44) ($H_{\rm h.o.}$) can be expressed using a single relative coordinate, $\boldsymbol{r} = \boldsymbol{r}1 - \boldsymbol{r}2$, and the corresponding conjugate momentum, $\mathbf{p}r = \frac{m_b \mathbf{p}D - m_D \mathbf{p}_b}{m_b + m_D}$ [118].

In this framework (see Figure 2.2), the two light quarks are treated as a single diquark entity that interacts with the heavy quark. Consequently, the term $H_{\rm h.o.}$ in eq. (2.44) can be rewritten in terms of the relative coordinate $\boldsymbol{r}$ and its conjugate momentum $\mathbf{p}_r$ as follows:

$$H_{\rm h.o.}^{qD} = m_D + m_b + \frac{\mathbf{p}_r^2}{2\mu} + \frac{1}{2}\mu\omega_r^2 \boldsymbol{r}^2, \quad (2.62)$$

where m_D and m_b represent the masses of the diquark and the bottom quark, respectively, and $\mu = \frac{m_b m_D}{m_b + m_D}$ denotes the reduced mass of the system.

The eigenstates of the Hamiltonian given in eq. (2.62) are presented in subsection 2.3.3 (eq. (2.41)), and its corresponding eigenvalues are

$$E_{\rm h.o.}^{qD} = m_D + m_b + \omega_r\, n_r;\ \text{with}\ \omega_r = \sqrt{\frac{3K_b}{\mu}}, \quad (2.63)$$

where $n_r = 2k_r + l_r$, with $k_r = 0, 1, \ldots$ representing the number of nodes, and $l_r = 0, 1, \ldots$ denoting the orbital angular momentum of the r-oscillator.

In this scheme, the eigenvalues of the Hamiltonian given in eq. (2.44) are expressed as

$$
\begin{aligned}
E^{qD} &= m_D + m_b + \omega_r\, n_r + a_{\rm S}\left[S_{\rm tot}(S_{\rm tot}+1)\right] + a_{\rm SL}\frac{1}{2}\Big[J(J+1) - L_{\rm tot}(L_{\rm tot}+1) - S_{\rm tot}(S_{\rm tot}+1)\Big] \\
&+ a_{\rm I}\left[I(I+1)\right] + a_{\rm F}\frac{1}{3}\left[p(p+3) + q(q+3) + pq\right], \qquad (2.64)
\end{aligned}
$$

which is the mass formula used to calculate the mass spectra within this scheme.

2.4.3 Parameter determination and uncertainties

In this study, the masses of singly bottom baryons are analyzed by fitting the theoretical predictions obtained from eqs. (2.47) and (2.64) to the experimentally observed values. The aim of this fitting procedure is to determine the values of the constituent quark and diquark masses ($m_{u,d}$, m_s, m_b, $m_{D_{\Sigma,\Lambda}}$, m_{D_Ξ}, and m_{D_Ω}), as well as the model parameters ($a_{\rm S}, a_{\rm SL}, a_{\rm I}, a_{\rm F}$, and K_b), in such a way that the sum of the squared differences between the predicted and experimental baryon masses is minimized. This approach corresponds to the least-squares method.

Experimental measurements of baryon masses include both statistical and systematic uncertainties. Furthermore, the three quark model presented in eq. (2.47) as well as the quark diquark model presented in eq. (2.64) offer approximate descriptions of sinlgy bottom baryons. To account for potential deviations between the models predictions and experimental data, a model uncertainty, denoted as σ_{mod}, is introduced for each model. The computation of σ_{mod} follows the procedure outlined in reference [89], and is adjusted to ensure that the χ^2/NDF value approaches unity, with NDF being the number of degrees of freedom. The χ^2 value is calculated using the following expression:

$$
\chi^2 = \sum_i \frac{(M_{mod,i} - M_{exp,i})^2}{\sigma_{mod}^2 + \sigma_{exp,i}^2}. \qquad (2.65)
$$

Here, $M_{mod,i}$ denotes the predicted masses of the singly bottom baryons, $M_{exp,i}$ represents the corresponding experimental masses used in the fitting procedure, and $\sigma_{exp,i}$ are their associated uncertainties. For the three-quark model, a model uncertainty of $\sigma_{mod} = 12$ MeV is determined, while for the quark-diquark model, $\sigma_{mod} = 20$ MeV is obtained. The model parameters were extracted by fitting only 13 out of the 23 experimentally observed states. The resulting parameters for the bottom baryon masses are listed in Table 2.1. The predictions show good agreement with the experimental data, yielding a root-mean-square deviation of 9.6 MeV.

Comparing the parameters $a_{\rm S}$, $a_{\rm SL}$, $a_{\rm I}$ and $a_{\rm F}$ from Table 2.1 with the corresponding results reported in reference [33] for the charm sector, it is observed that the values of $a_{\rm I}$ and $a_{\rm F}$ are very close in both sectors. In contrast, the values of $a_{\rm S}$ and $a_{\rm SL}$ are considerably smaller in the bottom sector. Specifically, for the parameter $a_{\rm S}$, which appears in the spin-spin interaction term, it is obtained from the fit in the bottom sector a value of $a_{\rm S} = 10^{+2}_{-3}$ MeV, notably lower than the corresponding value of $a_{\rm S} = 23 \pm 3$ MeV found in reference [33] for the charm sector. This reduction is consistent with the expectations of Heavy Quark Spin Symmetry, effectively

TABLE 2.1: *Table from [90] (APS copyright).* Fitted parameters for the three-quark scheme (second column) and the quark-diquark scheme (third column). The symbol "..." indicates that the parameter is absent in that scheme.

Parameter	Three-quark value	Quark-diquark value
m_b	4930^{+12}_{-12} MeV	4677^{+100}_{-64} MeV
m_s	464^{+6}_{-6} MeV	...
m_n	299^{+10}_{-10} MeV	...
m_{D_Ω}	...	1331^{+59}_{-92} MeV
m_{D_Ξ}	...	1185^{+61}_{-92} MeV
$m_{D_{\Sigma,\Lambda}}$	...	1045^{+55}_{-94} MeV
K_b	$0.0254^{+0.0012}_{-0.0012}$ GeV^3	$0.0245^{+0.0023}_{-0.0023}$ GeV^3
a_S	10^{+2}_{-3} MeV	8^{+2}_{-3} MeV
a_{SL}	4^{+2}_{-2} MeV	6^{+3}_{-1} MeV
a_I	36^{+7}_{-7} MeV	19^{+3}_{-2} MeV
a_F	60^{+6}_{-5} MeV	13^{+6}_{-3} MeV

accounting for the fact that the spin-spin interaction is inversely proportional to the product of the interacting quark masses. Regarding the spin-orbit interaction parameter a_{SL}, the value obtained from the fit is $a_{SL} = 4 \pm 2$ MeV, approximately four times smaller than the charm sector value of $a_{SL} = 18 \pm 5$ MeV [33]. The observed reduction in a_{SL} from charm to bottom sector is also consistent with theoretical expectations, since the spin-orbit term $a_{SL}\mathbf{S}_{tot} \cdot \mathbf{L}_{tot}$ is a relativistic interaction and thus suppressed for heavier quark masses.

A statistical simulation using error propagation is performed to incorporate both experimental and model uncertainties into the fitting procedure. This approach involves randomly sampling the experimental masses of singly bottom baryons from Gaussian distributions, where the means correspond to the central experimental values and the widths are given by the quadratic sum of the experimental and model uncertainties. The fitting process is repeated 10^4 times, where in each iteration it is used a sampled mass corresponding to an experimentally observed state included in the fit. The resulting distributions of the fitted model parameters are approximately Gaussian. The model parameters obtained from the 10^4 fits have Gaussian distributions, where the parameter values are the means of these distributions and the parameter uncertainties are defined as the difference from the distribution quantiles at the 68% confidence level to obtain its confidence interval (C.I.). This methodology is known as Monte Carlo bootstrap uncertainty propagation [119, 120]. The fitting and uncertainty propagation are performed using the `MINUIT` [121] minimization library and `NUMPY` [122] for numerical computations.

The thirteen masses and their respective uncertainties used in the fit are taken from the PDG [89], and are indicated with the superscript "*a*" in Tables 2.2–2.6.

2.4.4 Results of the mass spectra

The results for the masses of singly bottom baryons are presented in Tables 2.2–2.6. The fourth column of these tables reports the theoretical masses calculated using the three-quark model Hamiltonian given in eq. (2.47), including their associated uncertainties. The sixth column

TABLE 2.2: *Table from [90] (APS copyright).* Predicted $\Lambda_b(nnb)$ masses and strong decay widths (in MeV). The flavor multiplet is indicated by the symbol $\mathcal{F}$. The first column contains the h.o. three-quark model states, $|l_\lambda, l_\rho, k_\lambda, k_\rho\rangle$, where l_λ and l_ρ are the orbital angular momenta and k_λ, k_ρ the number of nodes of the λ and ρ oscillators, with $N = n_\rho + n_\lambda$. The second column displays the spectroscopic notation $^{2S+1}L_J$ for each state. The third column contains the total angular momentum and parity $\mathbf{J}^P$. In the fourth and eighth columns, the three-quark predicted masses (eq. (2.47)) and their total strong decay widths are shown, respectively. The fifth column contains the h.o. quark-diquark model state, $|l_r, k_r\rangle$, where l_r is the orbital angular momentum and k_r denotes the number of nodes, and $N = n_r$. The sixth column contains the quark-diquark predicted masses (eq. (2.64)). Our theoretical results are compared with the experimental masses and the decay widths from PDG [89] in the seventh and ninth columns, respectively. The "†" indicates that no experimental mass or decay width for that state has yet been reported. The symbol "..." indicates that there is no quark-diquark prediction for that state. The superscript ^{a} indicates the experimental mass and decay width values included in the fits.

$\mathcal{F} = \bar{\mathbf{3}}_\mathrm{F}$	Three-quark			Quark-diquark			Three-quark	
$\Lambda_b(nnb)$			Predicted		Predicted	Exp.	Predicted	Exp.
$\lvert l_\lambda, l_\rho, k_\lambda, k_\rho\rangle$	$^{2S+1}L_J$	$\mathbf{J}^P$	Mass (MeV)	$\lvert l_r, k_r\rangle$	Mass (MeV)	Mass (MeV)	Γ_Strong (MeV)	Γ (MeV)
$N = 0$								
$\lvert 0,0,0,0\rangle$	$^2S_{1/2}$	$\frac{1}{2}^+$	5613^{+9}_{-9}	$\lvert 0,0\rangle$	5611^{+15}_{-16}	5619.60 ± 0.17 [a]	0	≈ 0
$N = 1$								
$\lvert 1,0,0,0\rangle$	$^2P_{1/2}$	$\frac{1}{2}^-$	5918^{+8}_{-8}	$\lvert 1,0\rangle$	5916^{+11}_{-12}	5912.19 ± 0.17 [a]	0	< 0.25
$\lvert 1,0,0,0\rangle$	$^2P_{3/2}$	$\frac{3}{2}^-$	5924^{+8}_{-8}	$\lvert 1,0\rangle$	5925^{+12}_{-12}	5920.09 ± 0.17 [a]	0	< 0.19
$\lvert 0,1,0,0\rangle$	$^2P_{1/2}$	$\frac{1}{2}^-$	6114^{+10}_{-10}	...	...	6072.3 ± 2.9	67^{+16}_{-16}	72 ± 11
$\lvert 0,1,0,0\rangle$	$^4P_{1/2}$	$\frac{1}{2}^-$	6137^{+14}_{-14}	...	...	†	36^{+8}_{-8}	†
$\lvert 0,1,0,0\rangle$	$^2P_{3/2}$	$\frac{3}{2}^-$	6121^{+10}_{-10}	...	...	†	85^{+21}_{-21}	†
$\lvert 0,1,0,0\rangle$	$^4P_{3/2}$	$\frac{3}{2}^-$	6143^{+12}_{-12}	...	...	†	128^{+31}_{-31}	†
$\lvert 0,1,0,0\rangle$	$^4P_{5/2}$	$\frac{5}{2}^-$	6153^{+14}_{-14}	...	...	†	74^{+19}_{-19}	†
$N = 2$								
$\lvert 2,0,0,0\rangle$	$^2D_{3/2}$	$\frac{3}{2}^+$	6225^{+13}_{-13}	$\lvert 2,0\rangle$	6224^{+20}_{-20}	6146.2 ± 0.4	13^{+5}_{-5}	2.9 ± 1.3
$\lvert 2,0,0,0\rangle$	$^2D_{5/2}$	$\frac{5}{2}^+$	6235^{+13}_{-13}	$\lvert 2,0\rangle$	6239^{+20}_{-20}	6152.5 ± 0.4	18^{+12}_{-13}	2.1 ± 0.9
$\lvert 0,0,1,0\rangle$	$^2S_{1/2}$	$\frac{1}{2}^+$	6231^{+12}_{-12}	$\lvert 0,1\rangle$	6233^{+20}_{-20}	†	29^{+14}_{-14}	†
$\lvert 0,0,0,1\rangle$	$^2S_{1/2}$	$\frac{1}{2}^+$	6624^{+21}_{-21}	...	...	†	130^{+32}_{-32}	†
$\lvert 1,1,0,0\rangle$	$^2D_{3/2}$	$\frac{3}{2}^+$	6421^{+16}_{-16}	...	...	†	67^{+17}_{-17}	†
$\lvert 1,1,0,0\rangle$	$^2D_{5/2}$	$\frac{5}{2}^+$	6431^{+17}_{-17}	...	...	†	108^{+28}_{-28}	†
$\lvert 1,1,0,0\rangle$	$^4D_{1/2}$	$\frac{1}{2}^+$	6438^{+22}_{-22}	...	...	†	34^{+9}_{-9}	†
$\lvert 1,1,0,0\rangle$	$^4D_{3/2}$	$\frac{3}{2}^+$	6444^{+19}_{-19}	...	...	†	95^{+25}_{-25}	†
$\lvert 1,1,0,0\rangle$	$^4D_{5/2}$	$\frac{5}{2}^+$	6454^{+17}_{-17}	...	...	†	128^{+34}_{-33}	†
$\lvert 1,1,0,0\rangle$	$^4D_{7/2}$	$\frac{7}{2}^+$	6468^{+23}_{-22}	...	...	†	122^{+34}_{-34}	†
$\lvert 1,1,0,0\rangle$	$^2P_{1/2}$	$\frac{1}{2}^-$	6423^{+16}_{-16}	...	...	†	$0.5^{+0.1}_{-0.1}$	†
$\lvert 1,1,0,0\rangle$	$^2P_{3/2}$	$\frac{3}{2}^-$	6429^{+17}_{-17}	...	...	†	$1.7^{+0.5}_{-0.5}$	†
$\lvert 1,1,0,0\rangle$	$^4P_{1/2}$	$\frac{1}{2}^-$	6446^{+19}_{-18}	...	...	†	$0.3^{+0.1}_{-0.1}$	†
$\lvert 1,1,0,0\rangle$	$^4P_{3/2}$	$\frac{3}{2}^-$	6452^{+17}_{-17}	...	...	†	$1.2^{+0.3}_{-0.3}$	†
$\lvert 1,1,0,0\rangle$	$^4P_{5/2}$	$\frac{5}{2}^-$	6462^{+19}_{-19}	...	...	†	2^{+1}_{-1}	†
$\lvert 1,1,0,0\rangle$	$^4S_{3/2}$	$\frac{3}{2}^+$	6456^{+17}_{-18}	...	...	†	32^{+8}_{-8}	†
$\lvert 1,1,0,0\rangle$	$^2S_{1/2}$	$\frac{1}{2}^+$	6427^{+16}_{-16}	...	...	†	29^{+7}_{-7}	†
$\lvert 0,2,0,0\rangle$	$^2D_{3/2}$	$\frac{3}{2}^+$	6618^{+20}_{-20}	...	...	†	131^{+33}_{-32}	†
$\lvert 0,2,0,0\rangle$	$^2D_{5/2}$	$\frac{5}{2}^+$	6628^{+21}_{-22}	...	...	†	185^{+49}_{-49}	†

TABLE 2.3: *Table from [90] (APS copyright).* Same as Table 2.2, but for $\Xi_b(snb)$ states. The recently discovered $\Xi_b(6087)$ [30], which is not yet on the PDG has been associated with the $1P\,1/2^-$ state; it is reported in the table with the mass and width, as from reference [30]. The recently discovered $\Xi_b(6095)^0$ [30] has been considered by us as the neutral partner of $\Xi_b(6100)^-$ reported by the PDG, and in this Table we reported its width as from LHCb [30].

$\mathcal{F}=\bar{\mathbf{3}}_{\rm F}$	Three-quark			Quark-diquark			Three-quark	
$\Xi_b(snb)$			Predicted		Predicted	Exp.	Predicted	Exp.
$\lvert l_\lambda,l_\rho,k_\lambda,k_\rho\rangle$	$^{2S+1}L_J$	$\mathbf{J}^P$	Mass (MeV)	$\lvert l_r,k_r\rangle$	Mass (MeV)	Mass (MeV)	$\Gamma_{\rm Strong}$ (MeV)	Γ (MeV)
$N=0$								
$\lvert 0,0,0,0\rangle$	$^2S_{1/2}$	$\frac{1}{2}^+$	5806^{+9}_{-9}	$\lvert 0,0\rangle$	5801^{+16}_{-16}	5794.5 ± 0.6 [a]	0	≈ 0
$N=1$								
$\lvert 1,0,0,0\rangle$	$^2P_{1/2}$	$\frac{1}{2}^-$	6079^{+9}_{-9}	$\lvert 1,0\rangle$	6082^{+15}_{-16}	6087.2 ± 0.8	$0.2^{+0.1}_{-0.2}$	2.4 ± 0.6
$\lvert 1,0,0,0\rangle$	$^2P_{3/2}$	$\frac{3}{2}^-$	6085^{+9}_{-9}	$\lvert 1,0\rangle$	6092^{+15}_{-15}	6100.3 ± 0.6 [a]	$1.1^{+0.6}_{-0.6}$	0.9 ± 0.4
$\lvert 0,1,0,0\rangle$	$^2P_{1/2}$	$\frac{1}{2}^-$	6248^{+11}_{-11}	$\cdots$	$\cdots$	†	9^{+2}_{-2}	†
$\lvert 0,1,0,0\rangle$	$^4P_{1/2}$	$\frac{1}{2}^-$	6271^{+15}_{-15}	$\cdots$	$\cdots$	†	6^{+1}_{-2}	†
$\lvert 0,1,0,0\rangle$	$^2P_{3/2}$	$\frac{3}{2}^-$	6255^{+11}_{-11}	$\cdots$	$\cdots$	†	66^{+16}_{-16}	†
$\lvert 0,1,0,0\rangle$	$^4P_{3/2}$	$\frac{3}{2}^-$	6277^{+14}_{-14}	$\cdots$	$\cdots$	†	26^{+7}_{-7}	†
$\lvert 0,1,0,0\rangle$	$^4P_{5/2}$	$\frac{5}{2}^-$	6287^{+15}_{-15}	$\cdots$	$\cdots$	†	68^{+16}_{-16}	†
$N=2$								
$\lvert 2,0,0,0\rangle$	$^2D_{3/2}$	$\frac{3}{2}^+$	6354^{+13}_{-13}	$\lvert 2,0\rangle$	6368^{+24}_{-21}	6327.3 ± 2.5	$1.9^{+0.8}_{-0.8}$	<2.2
$\lvert 2,0,0,0\rangle$	$^2D_{5/2}$	$\frac{5}{2}^+$	6364^{+13}_{-13}	$\lvert 2,0\rangle$	6383^{+23}_{-21}	6332.7 ± 2.5	$1.5^{+0.5}_{-0.5}$	<1.6
$\lvert 0,0,1,0\rangle$	$^2S_{1/2}$	$\frac{1}{2}^+$	6360^{+12}_{-13}	$\lvert 0,1\rangle$	6377^{+23}_{-21}	†	5^{+2}_{-2}	†
$\lvert 0,0,0,1\rangle$	$^2S_{1/2}$	$\frac{1}{2}^+$	6699^{+19}_{-19}	$\cdots$	$\cdots$	†	179^{+28}_{-28}	†
$\lvert 1,1,0,0\rangle$	$^2D_{3/2}$	$\frac{3}{2}^+$	6524^{+16}_{-16}	$\cdots$	$\cdots$	†	46^{+12}_{-12}	†
$\lvert 1,1,0,0\rangle$	$^2D_{5/2}$	$\frac{5}{2}^+$	6534^{+17}_{-17}	$\cdots$	$\cdots$	†	108^{+27}_{-27}	†
$\lvert 1,1,0,0\rangle$	$^4D_{1/2}$	$\frac{1}{2}^+$	6540^{+22}_{-22}	$\cdots$	$\cdots$	†	20^{+5}_{-5}	†
$\lvert 1,1,0,0\rangle$	$^4D_{3/2}$	$\frac{3}{2}^+$	6546^{+19}_{-19}	$\cdots$	$\cdots$	†	67^{+18}_{-18}	†
$\lvert 1,1,0,0\rangle$	$^4D_{5/2}$	$\frac{5}{2}^+$	6556^{+17}_{-18}	$\cdots$	$\cdots$	†	100^{+26}_{-26}	†
$\lvert 1,1,0,0\rangle$	$^4D_{7/2}$	$\frac{7}{2}^+$	6570^{+22}_{-22}	$\cdots$	$\cdots$	†	114^{+30}_{-30}	†
$\lvert 1,1,0,0\rangle$	$^2P_{1/2}$	$\frac{1}{2}^-$	6526^{+16}_{-16}	$\cdots$	$\cdots$	†	$0.3^{+0.1}_{-0.1}$	†
$\lvert 1,1,0,0\rangle$	$^2P_{3/2}$	$\frac{3}{2}^-$	6532^{+16}_{-16}	$\cdots$	$\cdots$	†	2^{+1}_{-1}	†
$\lvert 1,1,0,0\rangle$	$^4P_{1/2}$	$\frac{1}{2}^-$	6548^{+19}_{-19}	$\cdots$	$\cdots$	†	$0.2^{+0.1}_{-0.1}$	†
$\lvert 1,1,0,0\rangle$	$^4P_{3/2}$	$\frac{3}{2}^-$	6554^{+18}_{-17}	$\cdots$	$\cdots$	†	$0.9^{+0.3}_{-0.3}$	†
$\lvert 1,1,0,0\rangle$	$^4P_{5/2}$	$\frac{5}{2}^-$	6564^{+19}_{-19}	$\cdots$	$\cdots$	†	3^{+1}_{-1}	†
$\lvert 1,1,0,0\rangle$	$^4S_{3/2}$	$\frac{3}{2}^+$	6558^{+18}_{-18}	$\cdots$	$\cdots$	†	33^{+8}_{-8}	†
$\lvert 1,1,0,0\rangle$	$^2S_{1/2}$	$\frac{1}{2}^+$	6530^{+16}_{-16}	$\cdots$	$\cdots$	†	31^{+7}_{-8}	†
$\lvert 0,2,0,0\rangle$	$^2D_{3/2}$	$\frac{3}{2}^+$	6693^{+20}_{-19}	$\cdots$	$\cdots$	†	127^{+31}_{-31}	†
$\lvert 0,2,0,0\rangle$	$^2D_{5/2}$	$\frac{5}{2}^+$	6703^{+20}_{-20}	$\cdots$	$\cdots$	†	98^{+25}_{-25}	†

TABLE 2.4: *Table from [90] (APS copyright).* Same as Table 2.2, but for $\Sigma_b(nnb)$ states.

$\mathcal{F}=\mathbf{6}_{\rm F}$	Three-quark			Quark-diquark			Three-quark	
$\Sigma_b(nnb)$			Predicted		Predicted	Exp.	Predicted	Exp.
$\lvert l_\lambda,l_\rho,k_\lambda,k_\rho\rangle$	$^{2S+1}L_J$	$\mathbf{J}^P$	Mass (MeV)	$\lvert l_r,k_r\rangle$	Mass (MeV)	Mass (MeV)	$\Gamma_{\rm Strong}$ (MeV)	Γ (MeV)
$N=0$								
$\lvert 0,0,0,0\rangle$	$^2S_{1/2}$	$\frac{1}{2}^+$	5804^{+8}_{-8}	$\lvert 0,0\rangle$	5811^{+13}_{-14}	5813.1 ± 0.3 [a]	4^{+2}_{-2}	5.0 ± 0.5
$\lvert 0,0,0,0\rangle$	$^4S_{3/2}$	$\frac{3}{2}^+$	5832^{+8}_{-8}	$\lvert 0,0\rangle$	5835^{+14}_{-13}	5832.5 ± 0.5 [a]	10^{+3}_{-3}	9.9 ± 0.9 [a]
$N=1$								
$\lvert 1,0,0,0\rangle$	$^2P_{1/2}$	$\frac{1}{2}^-$	6108^{+10}_{-10}	$\lvert 1,0\rangle$	6098^{+14}_{-13}	6096.9 ± 1.8 [a]	24^{+6}_{-6}	30 ± 7
$\lvert 1,0,0,0\rangle$	$^4P_{1/2}$	$\frac{1}{2}^-$	6131^{+12}_{-13}	$\lvert 1,0\rangle$	6113^{+15}_{-14}	†	13^{+3}_{-3}	†
$\lvert 1,0,0,0\rangle$	$^2P_{3/2}$	$\frac{3}{2}^-$	6114^{+10}_{-10}	$\lvert 1,0\rangle$	6107^{+14}_{-14}	†	84^{+20}_{-20}	†
$\lvert 1,0,0,0\rangle$	$^4P_{3/2}$	$\frac{3}{2}^-$	6137^{+10}_{-10}	$\lvert 1,0\rangle$	6122^{+14}_{-13}	†	57^{+14}_{-14}	†
$\lvert 1,0,0,0\rangle$	$^4P_{5/2}$	$\frac{5}{2}^-$	6147^{+12}_{-12}	$\lvert 1,0\rangle$	6137^{+15}_{-14}	†	96^{+23}_{-23}	†
$\lvert 0,1,0,0\rangle$	$^2P_{1/2}$	$\frac{1}{2}^-$	6304^{+13}_{-13}	$\cdots$	$\cdots$	†	134^{+31}_{-32}	†
$\lvert 0,1,0,0\rangle$	$^2P_{3/2}$	$\frac{3}{2}^-$	6311^{+13}_{-13}	$\cdots$	$\cdots$	†	129^{+32}_{-32}	†
$N=2$								
$\lvert 2,0,0,0\rangle$	$^2D_{3/2}$	$\frac{3}{2}^+$	6415^{+15}_{-15}	$\lvert 2,0\rangle$	6388^{+22}_{-22}	†	58^{+15}_{-15}	†
$\lvert 2,0,0,0\rangle$	$^2D_{5/2}$	$\frac{5}{2}^+$	6425^{+16}_{-16}	$\lvert 2,0\rangle$	6404^{+22}_{-22}	†	130^{+33}_{-33}	†
$\lvert 2,0,0,0\rangle$	$^4D_{1/2}$	$\frac{1}{2}^+$	6431^{+21}_{-21}	$\lvert 2,0\rangle$	6393^{+22}_{-22}	†	78^{+19}_{-20}	†
$\lvert 2,0,0,0\rangle$	$^4D_{3/2}$	$\frac{3}{2}^+$	6437^{+17}_{-17}	$\lvert 2,0\rangle$	6403^{+21}_{-21}	†	106^{+27}_{-27}	†
$\lvert 2,0,0,0\rangle$	$^4D_{5/2}$	$\frac{5}{2}^+$	6448^{+15}_{-15}	$\lvert 2,0\rangle$	6418^{+20}_{-21}	†	133^{+33}_{-33}	†
$\lvert 2,0,0,0\rangle$	$^4D_{7/2}$	$\frac{7}{2}^+$	6462^{+20}_{-20}	$\lvert 2,0\rangle$	6440^{+23}_{-22}	†	145^{+38}_{-39}	†
$\lvert 0,0,1,0\rangle$	$^2S_{1/2}$	$\frac{1}{2}^+$	6421^{+15}_{-15}	$\lvert 0,1\rangle$	6397^{+22}_{-21}	†	119^{+29}_{-29}	†
$\lvert 0,0,1,0\rangle$	$^4S_{3/2}$	$\frac{3}{2}^+$	6450^{+15}_{-15}	$\lvert 0,1\rangle$	6421^{+20}_{-21}	†	121^{+30}_{-30}	†
$\lvert 0,0,0,1\rangle$	$^2S_{1/2}$	$\frac{1}{2}^+$	6813^{+24}_{-24}	$\cdots$	$\cdots$	†	710^{+156}_{-184}	†
$\lvert 0,0,0,1\rangle$	$^4S_{3/2}$	$\frac{3}{2}^+$	6842^{+24}_{-23}	$\cdots$	$\cdots$	†	973^{+243}_{-243}	†
$\lvert 1,1,0,0\rangle$	$^2D_{3/2}$	$\frac{3}{2}^+$	6611^{+19}_{-19}	$\cdots$	$\cdots$	†	376^{+93}_{-95}	†
$\lvert 1,1,0,0\rangle$	$^2D_{5/2}$	$\frac{5}{2}^+$	6621^{+20}_{-20}	$\cdots$	$\cdots$	†	252^{+67}_{-66}	†
$\lvert 1,1,0,0\rangle$	$^2P_{1/2}$	$\frac{1}{2}^-$	6613^{+19}_{-19}	$\cdots$	$\cdots$	†	4^{+1}_{-1}	†
$\lvert 1,1,0,0\rangle$	$^2P_{3/2}$	$\frac{3}{2}^-$	6619^{+20}_{-20}	$\cdots$	$\cdots$	†	5^{+1}_{-1}	†
$\lvert 1,1,0,0\rangle$	$^2S_{1/2}$	$\frac{1}{2}^+$	6617^{+19}_{-19}	$\cdots$	$\cdots$	†	58^{+15}_{-16}	†
$\lvert 0,2,0,0\rangle$	$^2D_{3/2}$	$\frac{3}{2}^+$	6807^{+23}_{-23}	$\cdots$	$\cdots$	†	549^{+130}_{-130}	†
$\lvert 0,2,0,0\rangle$	$^2D_{5/2}$	$\frac{5}{2}^+$	6817^{+24}_{-25}	$\cdots$	$\cdots$	†	616^{+172}_{-170}	†
$\lvert 0,2,0,0\rangle$	$^4D_{1/2}$	$\frac{1}{2}^+$	6824^{+27}_{-27}	$\cdots$	$\cdots$	†	1349^{+320}_{-321}	†
$\lvert 0,2,0,0\rangle$	$^4D_{3/2}$	$\frac{3}{2}^+$	6830^{+24}_{-24}	$\cdots$	$\cdots$	†	741^{+176}_{-175}	†
$\lvert 0,2,0,0\rangle$	$^4D_{5/2}$	$\frac{5}{2}^+$	6840^{+23}_{-23}	$\cdots$	$\cdots$	†	376^{+90}_{-89}	†
$\lvert 0,2,0,0\rangle$	$^4D_{7/2}$	$\frac{7}{2}^+$	6854^{+28}_{-28}	$\cdots$	$\cdots$	†	1178^{+331}_{-334}	†

TABLE 2.5: *Table from [90] (APS copyright).* Same as Table 2.2, but for $\Xi_b'(snb)$ states.

$\mathcal{F}=\mathbf{6}_{\rm F}$	Three-quark			Quark-diquark			Three-quark	
$\Xi_b'(snb)$			Predicted		Predicted	Exp.	Predicted	Exp.
$\lvert l_\lambda,l_\rho,k_\lambda,k_\rho\rangle$	$^{2S+1}L_J$	$\mathbf{J}^P$	Mass (MeV)	$\lvert l_r,k_r\rangle$	Mass (MeV)	Mass (MeV)	$\Gamma_{\rm Strong}$ (MeV)	Γ (MeV)
$N=0$								
$\lvert 0,0,0,0\rangle$	$^2S_{1/2}$	$\frac{1}{2}^+$	5925^{+6}_{-6}	$\lvert 0,0\rangle$	5927^{+13}_{-13}	5935.02 ± 0.05 [a]	0	<0.08
$\lvert 0,0,0,0\rangle$	$^4S_{3/2}$	$\frac{3}{2}^+$	5953^{+7}_{-7}	$\lvert 0,0\rangle$	5951^{+13}_{-14}	5953.8 ± 0.6 [a]	$0.2^{+0.1}_{-0.1}$	0.90 ± 0.18
$N=1$								
$\lvert 1,0,0,0\rangle$	$^2P_{1/2}$	$\frac{1}{2}^-$	6198^{+7}_{-7}	$\lvert 1,0\rangle$	6199^{+14}_{-15}	†	3^{+1}_{-1}	†
$\lvert 1,0,0,0\rangle$	$^4P_{1/2}$	$\frac{1}{2}^-$	6220^{+10}_{-10}	$\lvert 1,0\rangle$	6213^{+14}_{-14}	†	4^{+1}_{-1}	†
$\lvert 1,0,0,0\rangle$	$^2P_{3/2}$	$\frac{3}{2}^-$	6204^{+7}_{-7}	$\lvert 1,0\rangle$	6208^{+14}_{-14}	†	29^{+7}_{-7}	†
$\lvert 1,0,0,0\rangle$	$^4P_{3/2}$	$\frac{3}{2}^-$	6226^{+7}_{-7}	$\lvert 1,0\rangle$	6223^{+14}_{-13}	†	8^{+2}_{-2}	†
$\lvert 1,0,0,0\rangle$	$^4P_{5/2}$	$\frac{5}{2}^-$	6237^{+10}_{-10}	$\lvert 1,0\rangle$	6238^{+14}_{-14}	6227.9 ± 1.6	31^{+8}_{-8}	19.9 ± 2.6
$\lvert 0,1,0,0\rangle$	$^2P_{1/2}$	$\frac{1}{2}^-$	6367^{+9}_{-9}	$\cdots$	$\cdots$	†	197^{+48}_{-49}	†
$\lvert 0,1,0,0\rangle$	$^2P_{3/2}$	$\frac{3}{2}^-$	6374^{+10}_{-10}	$\cdots$	$\cdots$	†	97^{+24}_{-24}	†
$N=2$								
$\lvert 2,0,0,0\rangle$	$^2D_{3/2}$	$\frac{3}{2}^+$	6473^{+12}_{-12}	$\lvert 2,0\rangle$	6474^{+20}_{-22}	†	14^{+5}_{-5}	†
$\lvert 2,0,0,0\rangle$	$^2D_{5/2}$	$\frac{5}{2}^+$	6483^{+13}_{-13}	$\lvert 2,0\rangle$	6489^{+21}_{-22}	†	30^{+11}_{-11}	†
$\lvert 2,0,0,0\rangle$	$^4D_{1/2}$	$\frac{1}{2}^+$	6489^{+18}_{-18}	$\lvert 2,0\rangle$	6479^{+22}_{-22}	†	25^{+10}_{-10}	†
$\lvert 2,0,0,0\rangle$	$^4D_{3/2}$	$\frac{3}{2}^+$	6495^{+14}_{-14}	$\lvert 2,0\rangle$	6488^{+21}_{-21}	†	35^{+12}_{-12}	†
$\lvert 2,0,0,0\rangle$	$^4D_{5/2}$	$\frac{5}{2}^+$	6506^{+11}_{-11}	$\lvert 2,0\rangle$	6504^{+20}_{-21}	†	46^{+13}_{-13}	†
$\lvert 2,0,0,0\rangle$	$^4D_{7/2}$	$\frac{7}{2}^+$	6520^{+18}_{-18}	$\lvert 2,0\rangle$	6526^{+20}_{-22}	†	47^{+14}_{-14}	†
$\lvert 0,0,1,0\rangle$	$^2S_{1/2}$	$\frac{1}{2}^+$	6479^{+11}_{-12}	$\lvert 0,1\rangle$	6483^{+21}_{-22}	†	47^{+14}_{-14}	†
$\lvert 0,0,1,0\rangle$	$^4S_{3/2}$	$\frac{3}{2}^+$	6508^{+12}_{-12}	$\lvert 0,1\rangle$	6507^{+20}_{-21}	†	79^{+26}_{-26}	†
$\lvert 0,0,0,1\rangle$	$^2S_{1/2}$	$\frac{1}{2}^+$	6818^{+19}_{-19}	$\cdots$	$\cdots$	†	599^{+149}_{-149}	†
$\lvert 0,0,0,1\rangle$	$^4S_{3/2}$	$\frac{3}{2}^+$	6847^{+19}_{-19}	$\cdots$	$\cdots$	†	630^{+157}_{-157}	†
$\lvert 1,1,0,0\rangle$	$^2D_{3/2}$	$\frac{3}{2}^+$	6642^{+15}_{-15}	$\cdots$	$\cdots$	†	234^{+59}_{-60}	†
$\lvert 1,1,0,0\rangle$	$^2D_{5/2}$	$\frac{5}{2}^+$	6653^{+17}_{-17}	$\cdots$	$\cdots$	†	116^{+30}_{-29}	†
$\lvert 1,1,0,0\rangle$	$^2P_{1/2}$	$\frac{1}{2}^-$	6644^{+15}_{-15}	$\cdots$	$\cdots$	†	3^{+1}_{-1}	†
$\lvert 1,1,0,0\rangle$	$^2P_{3/2}$	$\frac{3}{2}^-$	6651^{+16}_{-16}	$\cdots$	$\cdots$	†	3^{+1}_{-1}	†
$\lvert 1,1,0,0\rangle$	$^2S_{1/2}$	$\frac{1}{2}^+$	6649^{+15}_{-15}	$\cdots$	$\cdots$	†	59^{+14}_{-14}	†
$\lvert 0,2,0,0\rangle$	$^2D_{3/2}$	$\frac{3}{2}^+$	6812^{+19}_{-19}	$\cdots$	$\cdots$	†	315^{+81}_{-85}	†
$\lvert 0,2,0,0\rangle$	$^2D_{5/2}$	$\frac{5}{2}^+$	6822^{+20}_{-20}	$\cdots$	$\cdots$	†	209^{+54}_{-55}	†
$\lvert 0,2,0,0\rangle$	$^4D_{1/2}$	$\frac{1}{2}^+$	6828^{+22}_{-22}	$\cdots$	$\cdots$	†	529^{+156}_{-151}	†
$\lvert 0,2,0,0\rangle$	$^4D_{3/2}$	$\frac{3}{2}^+$	6834^{+20}_{-20}	$\cdots$	$\cdots$	†	364^{+94}_{-93}	†
$\lvert 0,2,0,0\rangle$	$^4D_{5/2}$	$\frac{5}{2}^+$	6845^{+19}_{-19}	$\cdots$	$\cdots$	†	194^{+48}_{-47}	†
$\lvert 0,2,0,0\rangle$	$^4D_{7/2}$	$\frac{7}{2}^+$	6859^{+24}_{-24}	$\cdots$	$\cdots$	†	349^{+98}_{-98}	†

TABLE 2.6: *Table from [90] (APS copyright)*. Same as Table 2.2, but for $\Omega_b(ssb)$ states.

$\mathcal{F}=\mathbf{6}_{\rm F}$	Three-quark			Quark-diquark			Three-quark	
$\Omega_b(ssb)$			Predicted		Predicted	Exp.	Predicted	Exp.
$\lvert l_\lambda,l_\rho,k_\lambda,k_\rho\rangle$	$^{2S+1}L_J$	$\mathbf{J}^P$	Mass (MeV)	$\lvert l_r,k_r\rangle$	Mass (MeV)	Mass (MeV)	$\Gamma_{\rm Strong}$ (MeV)	Γ (MeV)
$N=0$								
$\lvert 0,0,0,0\rangle$	$^2S_{1/2}$	$\frac{1}{2}^+$	6064^{+8}_{-8}	$\lvert 0,0\rangle$	6059^{+13}_{-12}	6045.2 ± 1.2 [a]	0	≈ 0
$\lvert 0,0,0,0\rangle$	$^4S_{3/2}$	$\frac{3}{2}^+$	6093^{+9}_{-8}	$\lvert 0,0\rangle$	6083^{+13}_{-14}	†	0	†
$N=1$								
$\lvert 1,0,0,0\rangle$	$^2P_{1/2}$	$\frac{1}{2}^-$	6315^{+7}_{-7}	$\lvert 1,0\rangle$	6318^{+9}_{-10}	6315.6 ± 0.6 [a]	5^{+1}_{-1}	<4.2
$\lvert 1,0,0,0\rangle$	$^4P_{1/2}$	$\frac{1}{2}^-$	6337^{+10}_{-10}	$\lvert 1,0\rangle$	6333^{+11}_{-11}	6330.3 ± 0.6 [a]	11^{+3}_{-3}	<4.7
$\lvert 1,0,0,0\rangle$	$^2P_{3/2}$	$\frac{3}{2}^-$	6321^{+8}_{-8}	$\lvert 1,0\rangle$	6328^{+10}_{-10}	6339.7 ± 0.6	24^{+6}_{-6}	<1.8
$\lvert 1,0,0,0\rangle$	$^4P_{3/2}$	$\frac{3}{2}^-$	6343^{+7}_{-7}	$\lvert 1,0\rangle$	6342^{+10}_{-10}	6349.8 ± 0.6	6^{+2}_{-2}	<3.2
$\lvert 1,0,0,0\rangle$	$^4P_{5/2}$	$\frac{5}{2}^-$	6353^{+11}_{-11}	$\lvert 1,0\rangle$	6358^{+11}_{-10}	†	40^{+10}_{-10}	†
$\lvert 0,1,0,0\rangle$	$^2P_{1/2}$	$\frac{1}{2}^-$	6465^{+9}_{-8}	⋯	⋯	†	10^{+2}_{-2}	†
$\lvert 0,1,0,0\rangle$	$^2P_{3/2}$	$\frac{3}{2}^-$	6471^{+10}_{-10}	⋯	⋯	†	54^{+14}_{-14}	†
$N=2$								
$\lvert 2,0,0,0\rangle$	$^2D_{3/2}$	$\frac{3}{2}^+$	6568^{+11}_{-11}	$\lvert 2,0\rangle$	6581^{+14}_{-15}	†	4^{+1}_{-1}	†
$\lvert 2,0,0,0\rangle$	$^2D_{5/2}$	$\frac{5}{2}^+$	6578^{+12}_{-12}	$\lvert 2,0\rangle$	6596^{+15}_{-15}	†	10^{+2}_{-2}	†
$\lvert 2,0,0,0\rangle$	$^4D_{1/2}$	$\frac{1}{2}^+$	6584^{+17}_{-17}	$\lvert 2,0\rangle$	6585^{+17}_{-17}	†	$1.0^{+0.3}_{-0.3}$	†
$\lvert 2,0,0,0\rangle$	$^4D_{3/2}$	$\frac{3}{2}^+$	6590^{+13}_{-13}	$\lvert 2,0\rangle$	6595^{+16}_{-16}	†	3^{+1}_{-1}	†
$\lvert 2,0,0,0\rangle$	$^4D_{5/2}$	$\frac{5}{2}^+$	6600^{+10}_{-10}	$\lvert 2,0\rangle$	6610^{+15}_{-15}	†	8^{+2}_{-2}	†
$\lvert 2,0,0,0\rangle$	$^4D_{7/2}$	$\frac{7}{2}^+$	6614^{+18}_{-18}	$\lvert 2,0\rangle$	6632^{+17}_{-16}	†	18^{+10}_{-9}	†
$\lvert 0,0,1,0\rangle$	$^2S_{1/2}$	$\frac{1}{2}^+$	6574^{+11}_{-11}	$\lvert 0,1\rangle$	6590^{+15}_{-15}	†	20^{+6}_{-6}	†
$\lvert 0,0,1,0\rangle$	$^4S_{3/2}$	$\frac{3}{2}^+$	6602^{+11}_{-11}	$\lvert 0,1\rangle$	6614^{+15}_{-15}	†	17^{+6}_{-6}	†
$\lvert 0,0,0,1\rangle$	$^2S_{1/2}$	$\frac{1}{2}^+$	6874^{+17}_{-17}	⋯	⋯	†	398^{+119}_{-119}	†
$\lvert 0,0,0,1\rangle$	$^4S_{3/2}$	$\frac{3}{2}^+$	6902^{+17}_{-17}	⋯	⋯	†	257^{+64}_{-64}	†
$\lvert 1,1,0,0\rangle$	$^2D_{3/2}$	$\frac{3}{2}^+$	6718^{+14}_{-14}	⋯	⋯	†	116^{+39}_{-39}	†
$\lvert 1,1,0,0\rangle$	$^2D_{5/2}$	$\frac{5}{2}^+$	6728^{+15}_{-15}	⋯	⋯	†	82^{+22}_{-23}	†
$\lvert 1,1,0,0\rangle$	$^2P_{1/2}$	$\frac{1}{2}^-$	6720^{+14}_{-14}	⋯	⋯	†	$1.1^{+0.4}_{-0.4}$	†
$\lvert 1,1,0,0\rangle$	$^2P_{3/2}$	$\frac{3}{2}^-$	6726^{+15}_{-15}	⋯	⋯	†	2^{+1}_{-1}	†
$\lvert 1,1,0,0\rangle$	$^2S_{1/2}$	$\frac{1}{2}^+$	6724^{+14}_{-14}	⋯	⋯	†	72^{+21}_{-21}	†
$\lvert 0,2,0,0\rangle$	$^2D_{3/2}$	$\frac{3}{2}^+$	6868^{+17}_{-17}	⋯	⋯	†	180^{+56}_{-54}	†
$\lvert 0,2,0,0\rangle$	$^2D_{5/2}$	$\frac{5}{2}^+$	6878^{+19}_{-19}	⋯	⋯	†	157^{+39}_{-39}	†
$\lvert 0,2,0,0\rangle$	$^4D_{1/2}$	$\frac{1}{2}^+$	6884^{+21}_{-21}	⋯	⋯	†	126^{+31}_{-32}	†
$\lvert 0,2,0,0\rangle$	$^4D_{3/2}$	$\frac{3}{2}^+$	6890^{+18}_{-18}	⋯	⋯	†	195^{+47}_{-47}	†
$\lvert 0,2,0,0\rangle$	$^4D_{5/2}$	$\frac{5}{2}^+$	6900^{+17}_{-17}	⋯	⋯	†	172^{+41}_{-41}	†
$\lvert 0,2,0,0\rangle$	$^4D_{7/2}$	$\frac{7}{2}^+$	6914^{+23}_{-23}	⋯	⋯	†	230^{+62}_{-63}	†

TABLE 2.7: *Table from [90] (APS copyright).* Comparison of our predicted three-quark $\Lambda_b(nnb)$ masses with other three-quark model predictions (in MeV). The flavor multiplet is indicated by the symbol $\mathcal{F}$. The first column contains the three-quark model state, $|l_\lambda, l_\rho, k_\lambda, k_\rho\rangle$, where $l_{\lambda,\rho}$ are the orbital angular momenta and $k_{\lambda,\rho}$ the number of nodes of the λ and ρ oscillators. The second column displays the spectroscopic notation $^{2S+1}L_J$ for each state. The third column reports our predicted masses, computed within the three-quark model. Our results are compared with those of references [50] (fourth column), [57, 59, 60] (fifth column), [48] (sixth column), [65] (seventh column), [68] (eighth column), [44] (ninth column), [42] (tenth column), and [35] (eleventh column). Our theoretical results are also compared with the experimental masses as from PDG [89] (twelfth column). The symbol "..." indicates that there is no prediction for that state. The "†" indicates that there is no reported experimental mass for that state up to now.

$\Lambda_b(snb)$	$\mathcal{F}=\bar{\mathbf{3}}_F$	This	NRQM	QCDSR	NRQM	χQM	LQCD	CQC	NRQM	RQM	
$\lvert l_\lambda, l_\rho, k_\lambda, k_\rho\rangle$	$^{2S+1}L_J$	work	[50]	[57, 59, 60]	[48]	[65]	[68]	[44]	[42]	[35]	Exp.
$N=0$											
$\lvert 0,0,0,0\rangle$	$^2S_{1/2}$	5613^{+9}_{-9}	5618	5637	5612	5620	5667	5624	5629	5585	5619.60 ± 0.17
$N=1$											
$\lvert 1,0,0,0\rangle$	$^2P_{1/2}$	5918^{+8}_{-8}	5938	6010	5939	5914	...	5947	...	5912	5912.19 ± 0.17
$\lvert 1,0,0,0\rangle$	$^2P_{3/2}$	5924^{+8}_{-8}	5939	6010	5941	5927	...	...	...	5920	5920.09 ± 0.17
$\lvert 0,1,0,0\rangle$	$^2P_{1/2}$	6114^{+10}_{-10}	6236	...	6180	6207	...	6245	...	6100	†
$\lvert 0,1,0,0\rangle$	$^4P_{1/2}$	6137^{+14}_{-14}	6273	5870	...	6233	...	...	...	6165	†
$\lvert 0,1,0,0\rangle$	$^2P_{3/2}$	6121^{+10}_{-10}	6273	...	6191	...	...	...	...	6185	†
$\lvert 0,1,0,0\rangle$	$^4P_{3/2}$	6143^{+12}_{-12}	6285	5880	...	...	...	...	...	6190	†
$\lvert 0,1,0,0\rangle$	$^4P_{5/2}$	6153^{+14}_{-14}	6289	...	6206	...	...	...	...	6205	†
$N=2$											
$\lvert 2,0,0,0\rangle$	$^2D_{3/2}$	6225^{+13}_{-13}	6211	6010	6181	6172	...	6388	...	6145	6146.2 ± 0.4
$\lvert 2,0,0,0\rangle$	$^2D_{5/2}$	6235^{+13}_{-13}	6212	6010	6183	6178	...	...	...	6165	6152.5 ± 0.4
$\lvert 0,0,1,0\rangle$	$^2S_{1/2}$	6231^{+12}_{-12}	6153	...	6107	6121	...	6106	...	6045	†
$\lvert 0,0,0,1\rangle$	$^2S_{1/2}$	6624^{+21}_{-21}	...	...	...	...	...	...	...	...	†
$\lvert 1,1,0,0\rangle$	$^2D_{3/2}$	6421^{+16}_{-16}	6488	...	6401	...	...	...	...	...	†
$\lvert 1,1,0,0\rangle$	$^2D_{5/2}$	6431^{+17}_{-17}	6530	6560	6422	...	...	...	...	...	†
$\lvert 1,1,0,0\rangle$	$^4D_{1/2}$	6438^{+22}_{-22}	6467	...	...	...	...	...	...	...	†
$\lvert 1,1,0,0\rangle$	$^4D_{3/2}$	6444^{+19}_{-19}	6511	6360	...	...	...	...	...	...	†
$\lvert 1,1,0,0\rangle$	$^4D_{5/2}$	6454^{+17}_{-17}	6539	6360	...	...	...	...	...	...	†
$\lvert 1,1,0,0\rangle$	$^4D_{7/2}$	6468^{+23}_{-22}	...	6560	6433	...	...	...	...	...	†
$\lvert 1,1,0,0\rangle$	$^2P_{1/2}$	6423^{+16}_{-16}	...	...	...	...	...	...	...	6260	†
$\lvert 1,1,0,0\rangle$	$^2P_{3/2}$	6429^{+17}_{-17}	...	...	...	...	...	...	...	6265	†
$\lvert 1,1,0,0\rangle$	$^4P_{1/2}$	6446^{+19}_{-18}	...	6220	...	...	...	...	...	6470	†
$\lvert 1,1,0,0\rangle$	$^4P_{3/2}$	6452^{+17}_{-17}	...	6230	...	...	...	...	...	6510	†
$\lvert 1,1,0,0\rangle$	$^4P_{5/2}$	6462^{+19}_{-19}	...	...	...	...	...	...	...	6360	†
$\lvert 1,1,0,0\rangle$	$^4S_{3/2}$	6456^{+17}_{-18}	...	...	...	...	...	...	...	...	†
$\lvert 1,1,0,0\rangle$	$^2S_{1/2}$	6427^{+16}_{-16}	...	...	...	...	...	...	...	...	†
$\lvert 0,2,0,0\rangle$	$^2D_{3/2}$	6618^{+20}_{-20}	...	6520	...	...	...	6637	...	...	†
$\lvert 0,2,0,0\rangle$	$^2D_{5/2}$	6628^{+21}_{-22}	...	6520	...	...	...	...	...	...	†

TABLE 2.8: *Table from [90] (APS copyright).* Same as Table 2.7, but for $\Xi_b(snb)$ states.

$\Xi_b(snb)$	$\mathcal{F}=\bar{\mathbf{3}}_F$	This	NRQM	QCDSR	NRQM	χQM	LQCD	CQC	NRQM	RQM	
$\lvert l_\lambda,l_\rho,k_\lambda,k_\rho\rangle$	$^{2S+1}L_J$	work	[50]	[57, 59, 60]	[48]	[65]	[68]	[44]	[42]	[35]	Exp.
$N=0$											
$\lvert 0,0,0,0\rangle$	$^2S_{1/2}$	5806^{+9}_{-9}	...	5780	5844	5796	5901	5801	5800	...	5794.5 ± 0.6
$N=1$											
$\lvert 1,0,0,0\rangle$	$^2P_{1/2}$	6079^{+9}_{-9}	...	6270	6108	6069	...	6109	...	...	†
$\lvert 1,0,0,0\rangle$	$^2P_{3/2}$	6085^{+9}_{-9}	...	6280	6110	6080	...	...	...	...	6100.3 ± 0.6
$\lvert 0,1,0,0\rangle$	$^2P_{1/2}$	6248^{+11}_{-11}	...	...	...	6084	...	6223	...	...	†
$\lvert 0,1,0,0\rangle$	$^4P_{1/2}$	6271^{+15}_{-15}	...	6060	...	6540	...	...	...	...	†
$\lvert 0,1,0,0\rangle$	$^2P_{3/2}$	6255^{+11}_{-11}	...	...	...	...	...	...	...	...	†
$\lvert 0,1,0,0\rangle$	$^4P_{3/2}$	6277^{+14}_{-14}	...	6070	...	6554	...	...	...	...	†
$\lvert 0,1,0,0\rangle$	$^4P_{5/2}$	6287^{+15}_{-15}	...	...	6312	...	...	...	...	...	†
$N=2$											
$\lvert 2,0,0,0\rangle$	$^2D_{3/2}$	6354^{+13}_{-13}	...	6190	6294	6307	...	...	...	...	6327.3 ± 2.5
$\lvert 2,0,0,0\rangle$	$^2D_{5/2}$	6364^{+13}_{-13}	...	6190	6333	6313	...	...	...	...	6332.7 ± 2.5
$\lvert 0,0,1,0\rangle$	$^2S_{1/2}$	6360^{+12}_{-13}	...	...	...	6260	...	6258	...	...	†
$\lvert 0,0,0,1\rangle$	$^2S_{1/2}$	6699^{+19}_{-19}	...	...	...	...	...	...	...	...	†
$\lvert 1,1,0,0\rangle$	$^2D_{3/2}$	6524^{+16}_{-16}	...	...	...	...	...	...	...	...	†
$\lvert 1,1,0,0\rangle$	$^2D_{5/2}$	6534^{+17}_{-17}	...	6860	...	...	...	...	...	...	†
$\lvert 1,1,0,0\rangle$	$^4D_{1/2}$	6540^{+22}_{-22}	...	...	...	...	...	...	...	...	†
$\lvert 1,1,0,0\rangle$	$^4D_{3/2}$	6546^{+19}_{-19}	...	6840	...	...	...	...	...	...	†
$\lvert 1,1,0,0\rangle$	$^4D_{5/2}$	6556^{+17}_{-18}	...	6840	...	...	...	...	...	...	†
$\lvert 1,1,0,0\rangle$	$^4D_{7/2}$	6570^{+22}_{-22}	...	6860	6524	...	...	...	...	...	†
$\lvert 1,1,0,0\rangle$	$^2P_{1/2}$	6526^{+16}_{-16}	...	...	...	...	...	...	...	...	†
$\lvert 1,1,0,0\rangle$	$^2P_{3/2}$	6532^{+16}_{-16}	...	...	...	...	...	...	...	...	†
$\lvert 1,1,0,0\rangle$	$^4P_{1/2}$	6548^{+19}_{-19}	...	6820	...	...	...	...	...	...	†
$\lvert 1,1,0,0\rangle$	$^4P_{3/2}$	6554^{+18}_{-17}	...	6820	...	...	...	...	...	...	†
$\lvert 1,1,0,0\rangle$	$^4P_{5/2}$	6564^{+19}_{-19}	...	...	...	...	...	...	...	...	†
$\lvert 1,1,0,0\rangle$	$^4S_{3/2}$	6558^{+18}_{-18}	...	...	...	...	...	...	...	...	†
$\lvert 1,1,0,0\rangle$	$^2S_{1/2}$	6530^{+16}_{-16}	...	...	...	...	...	...	...	...	†
$\lvert 0,2,0,0\rangle$	$^2D_{3/2}$	6693^{+20}_{-19}	...	6570	...	...	...	...	...	...	†
$\lvert 0,2,0,0\rangle$	$^2D_{5/2}$	6703^{+20}_{-20}	...	6570	...	...	...	...	...	...	†

TABLE 2.9: *Table from [90] (APS copyright).* Same as Table 2.7, but for $\Sigma_b(nnb)$ states.

$\Sigma_b(nnb)$	$\mathcal{F}=\mathbf{6}_\mathrm{F}$	This	NRQM	QCDSR	NRQM	χQM	LQCD	CQC	NRQM	RQM	
$\lvert l_\lambda,l_\rho,k_\lambda,k_\rho\rangle$	$^{2S+1}L_J$	work	[50]	[57, 59, 60]	[48]	[65]	[68]	[44]	[42]	[35]	Exp.
$N=0$											
$\lvert 0,0,0,0\rangle$	$^2S_{1/2}$	5804^{+8}_{-8}	5823	5809	5833	5810	5820	5807	5844	5795	5813.1 ± 0.3
$\lvert 0,0,0,0\rangle$	$^4S_{3/2}$	5832^{+8}_{-8}	5845	5835	5858	5829	5836	5829	5874	5805	5832.5 ± 0.5
$N=1$											
$\lvert 1,0,0,0\rangle$	$^2P_{1/2}$	6108^{+10}_{-10}	6127	...	6099	6043	...	6103	...	6070	6096.9 ± 1.8
$\lvert 1,0,0,0\rangle$	$^4P_{1/2}$	6131^{+12}_{-13}	6135	6020	6106	6065	...	...	...	6070	†
$\lvert 1,0,0,0\rangle$	$^2P_{3/2}$	6114^{+10}_{-10}	6132	...	6101	6079	...	...	...	6070	†
$\lvert 1,0,0,0\rangle$	$^4P_{3/2}$	6137^{+10}_{-10}	6141	5960	6105	6117	...	...	...	6085	†
$\lvert 1,0,0,0\rangle$	$^4P_{5/2}$	6147^{+12}_{-12}	6144	5980	6172	6129	...	...	...	6090	†
$\lvert 0,1,0,0\rangle$	$^2P_{1/2}$	6304^{+13}_{-13}	6246	5910	...	...	...	6241	...	6170	†
$\lvert 0,1,0,0\rangle$	$^2P_{3/2}$	6311^{+13}_{-13}	6246	5920	...	...	...	...	...	6180	†
$N=2$											
$\lvert 2,0,0,0\rangle$	$^2D_{3/2}$	6415^{+15}_{-15}	6356	...	6308	6316	...	6260	...	6250	†
$\lvert 2,0,0,0\rangle$	$^2D_{5/2}$	6425^{+16}_{-16}	6397	...	6325	6341	...	...	...	6325	†
$\lvert 2,0,0,0\rangle$	$^4D_{1/2}$	6431^{+21}_{-21}	6343	...	...	6304	...	...	...	6300	†
$\lvert 2,0,0,0\rangle$	$^4D_{3/2}$	6437^{+17}_{-17}	6393	...	...	6330	...	...	...	6320	†
$\lvert 2,0,0,0\rangle$	$^4D_{5/2}$	6448^{+15}_{-15}	6402	...	6328	6365	...	...	...	6335	†
$\lvert 2,0,0,0\rangle$	$^4D_{7/2}$	6462^{+20}_{-20}	...	...	6333	6373	...	...	...	6340	†
$\lvert 0,0,1,0\rangle$	$^2S_{1/2}$	6421^{+15}_{-15}	6395	...	6294	6274	...	6247	...	6290	†
$\lvert 0,0,1,0\rangle$	$^4S_{3/2}$	6450^{+15}_{-15}	...	...	...	6286	...	...	...	...	†
$\lvert 0,0,0,1\rangle$	$^2S_{1/2}$	6813^{+24}_{-24}	...	...	...	...	...	...	...	6400	†
$\lvert 0,0,0,1\rangle$	$^4S_{3/2}$	6842^{+24}_{-23}	...	...	...	...	...	...	...	...	†
$\lvert 1,1,0,0\rangle$	$^2D_{3/2}$	6611^{+19}_{-19}	...	...	...	...	...	...	...	...	†
$\lvert 1,1,0,0\rangle$	$^2D_{5/2}$	6621^{+20}_{-20}	6505	...	...	...	...	...	...	...	†
$\lvert 1,1,0,0\rangle$	$^2P_{1/2}$	6613^{+19}_{-19}	...	...	...	...	...	...	...	6440	†
$\lvert 1,1,0,0\rangle$	$^2P_{3/2}$	6619^{+20}_{-20}	...	...	...	...	...	...	...	6445	†
$\lvert 1,1,0,0\rangle$	$^2S_{1/2}$	6617^{+19}_{-19}	...	...	...	...	...	...	...	...	†
$\lvert 0,2,0,0\rangle$	$^2D_{3/2}$	6807^{+23}_{-23}	...	...	...	...	...	...	...	...	†
$\lvert 0,2,0,0\rangle$	$^2D_{5/2}$	6817^{+24}_{-25}	...	...	...	...	...	...	...	...	†
$\lvert 0,2,0,0\rangle$	$^4D_{1/2}$	6824^{+27}_{-27}	...	...	...	...	...	...	...	...	†
$\lvert 0,2,0,0\rangle$	$^4D_{3/2}$	6830^{+24}_{-24}	...	...	...	...	...	...	...	...	†
$\lvert 0,2,0,0\rangle$	$^4D_{5/2}$	6840^{+23}_{-23}	...	...	...	...	...	...	...	...	†
$\lvert 0,2,0,0\rangle$	$^4D_{7/2}$	6854^{+28}_{-28}	...	...	6554	...	...	...	...	6535	†

TABLE 2.10: *Table from [90] (APS copyright).* Same as Table 2.7, but for $\Xi_b'(snb)$ states.

$\Xi_b'(snb)$	$\mathcal{F}=\mathbf{6}_{\rm F}$	This	NRQM	QCDSR	NRQM	χQM	LQCD	CQC	NRQM	RQM	
$\lvert l_\lambda,l_\rho,k_\lambda,k_\rho\rangle$	$^{2S+1}L_J$	work	[50]	[57, 59, 60]	[48]	[65]	[68]	[44]	[42]	[35]	Exp.
$N=0$											
$\lvert 0,0,0,0\rangle$	$^2S_{1/2}$	5925^{+6}_{-6}	...	5903	5958	5934	5946	5939	5939	...	5935.02 ± 0.05
$\lvert 0,0,0,0\rangle$	$^4S_{3/2}$	5954^{+7}_{-7}	...	...	...	5952	...	5961	5970	...	5953.8 ± 0.6
$N=1$											
$\lvert 1,0,0,0\rangle$	$^2P_{1/2}$	6198^{+7}_{-7}	...	...	6192	6164	...	...	...	...	†
$\lvert 1,0,0,0\rangle$	$^4P_{1/2}$	6220^{+10}_{-10}	...	6240	...	6183	...	...	...	...	†
$\lvert 1,0,0,0\rangle$	$^2P_{3/2}$	6204^{+7}_{-7}	...	...	6194	6195	...	...	...	...	†
$\lvert 1,0,0,0\rangle$	$^4P_{3/2}$	6227^{+7}_{-7}	...	6170	...	6227	...	...	...	...	†
$\lvert 1,0,0,0\rangle$	$^4P_{5/2}$	6237^{+10}_{-10}	...	6180	6204	6238	...	...	...	...	6227.9 ± 1.6
$\lvert 0,1,0,0\rangle$	$^2P_{1/2}$	6367^{+9}_{-9}	...	6110	...	...	...	...	...	...	†
$\lvert 0,1,0,0\rangle$	$^2P_{3/2}$	6373^{+10}_{-10}	...	6110	...	...	...	...	...	...	†
$N=2$											
$\lvert 2,0,0,0\rangle$	$^2D_{3/2}$	6473^{+12}_{-12}	...	...	5982	6423	...	...	...	...	†
$\lvert 2,0,0,0\rangle$	$^2D_{5/2}$	6483^{+13}_{-13}	...	...	6402	6444	...	...	...	...	†
$\lvert 2,0,0,0\rangle$	$^4D_{1/2}$	6489^{+18}_{-18}	...	...	...	6411	...	...	...	...	†
$\lvert 2,0,0,0\rangle$	$^4D_{3/2}$	6495^{+14}_{-14}	...	...	...	6434	...	...	...	...	†
$\lvert 2,0,0,0\rangle$	$^4D_{5/2}$	6506^{+11}_{-11}	...	...	...	6465	...	...	...	...	†
$\lvert 2,0,0,0\rangle$	$^4D_{7/2}$	6520^{+18}_{-18}	...	...	6405	6472	...	...	...	...	†
$\lvert 0,0,1,0\rangle$	$^2S_{1/2}$	6479^{+11}_{-12}	...	...	...	6381	...	6360	...	...	†
$\lvert 0,0,1,0\rangle$	$^4S_{3/2}$	6508^{+12}_{-11}	...	...	...	6392	...	...	...	...	†
$\lvert 0,0,0,1\rangle$	$^2S_{1/2}$	6818^{+19}_{-19}	...	...	...	...	...	...	...	...	†
$\lvert 0,0,0,1\rangle$	$^4S_{3/2}$	6847^{+19}_{-19}	...	...	...	...	...	...	...	...	†
$\lvert 1,1,0,0\rangle$	$^2D_{3/2}$	6642^{+15}_{-15}	...	...	...	...	...	...	...	...	†
$\lvert 1,1,0,0\rangle$	$^2D_{5/2}$	6653^{+16}_{-16}	...	...	...	...	...	...	...	...	†
$\lvert 1,1,0,0\rangle$	$^2P_{1/2}$	6644^{+15}_{-15}	...	...	...	...	...	...	...	...	†
$\lvert 1,1,0,0\rangle$	$^2P_{3/2}$	6650^{+16}_{-16}	...	...	...	...	...	...	...	...	†
$\lvert 1,1,0,0\rangle$	$^2S_{1/2}$	6648^{+15}_{-15}	...	...	...	...	...	...	...	...	†
$\lvert 0,2,0,0\rangle$	$^2D_{3/2}$	6812^{+19}_{-19}	...	...	...	...	...	...	...	...	†
$\lvert 0,2,0,0\rangle$	$^2D_{5/2}$	6822^{+20}_{-20}	...	...	...	...	...	...	...	...	†
$\lvert 0,2,0,0\rangle$	$^4D_{1/2}$	6828^{+22}_{-22}	...	...	...	...	...	...	...	...	†
$\lvert 0,2,0,0\rangle$	$^4D_{3/2}$	6834^{+20}_{-20}	...	...	...	...	...	...	...	...	†
$\lvert 0,2,0,0\rangle$	$^4D_{5/2}$	6845^{+19}_{-19}	...	...	...	...	...	...	...	...	†
$\lvert 0,2,0,0\rangle$	$^4D_{7/2}$	6859^{+24}_{-25}	...	...	...	...	...	...	...	...	†

TABLE 2.11: *Table from [90] (APS copyright).* Same as Table 2.7, but for $\Omega_b(ssb)$ states.

$\Omega_b(ssb)$	$\mathcal{F}=\mathbf{6}_\mathrm{F}$	This	NRQM	QCDSR	NRQM	χQM	LQCD	CQC	NRQM	RQM	
$\lvert l_\lambda,l_\rho,k_\lambda,k_\rho\rangle$	$^{2S+1}L_J$	work	[50]	[57, 59, 60]	[48]	[65]	[68]	[44]	[42]	[35]	Exp.
$N=0$											
$\lvert 0,0,0,0\rangle$	$^2S_{1/2}$	6064^{+8}_{-8}	6076	6036	6081	6047	6014	6056	6030	...	6045.2 ± 1.2
$\lvert 0,0,0,0\rangle$	$^4S_{3/2}$	6093^{+9}_{-8}	6094	6063	6102	6064	6019	6079	6061	...	†
$N=1$											
$\lvert 1,0,0,0\rangle$	$^2P_{1/2}$	6315^{+7}_{-7}	6333	...	6301	6273	...	6340	...	...	6315.6 ± 0.6
$\lvert 1,0,0,0\rangle$	$^4P_{1/2}$	6337^{+10}_{-10}	6340	6500	6312	6290	...	...	...	...	6330.3 ± 0.6
$\lvert 1,0,0,0\rangle$	$^2P_{3/2}$	6321^{+8}_{-8}	6336	...	6304	6301	...	...	...	...	6339.7 ± 0.6
$\lvert 1,0,0,0\rangle$	$^4P_{3/2}$	6343^{+7}_{-7}	6344	6430	6311	6329	...	...	...	...	6349.8 ± 0.6
$\lvert 1,0,0,0\rangle$	$^4P_{5/2}$	6353^{+11}_{-11}	6345	6430	6311	6339	...	...	...	...	†
$\lvert 0,1,0,0\rangle$	$^2P_{1/2}$	6465^{+9}_{-8}	6437	6340	...	...	...	6458	...	...	†
$\lvert 0,1,0,0\rangle$	$^2P_{3/2}$	6471^{+10}_{-10}	6438	6340	...	...	...	...	...	...	†
$N=2$											
$\lvert 2,0,0,0\rangle$	$^2D_{3/2}$	6568^{+11}_{-11}	6528	...	6478	6522	...	6493	...	...	†
$\lvert 2,0,0,0\rangle$	$^2D_{5/2}$	6578^{+12}_{-12}	6561	...	6492	6541	...	...	...	...	†
$\lvert 2,0,0,0\rangle$	$^4D_{1/2}$	6584^{+17}_{-17}	6517	...	...	6511	...	...	...	...	†
$\lvert 2,0,0,0\rangle$	$^4D_{3/2}$	6590^{+13}_{-13}	6559	...	...	6532	...	...	...	...	†
$\lvert 2,0,0,0\rangle$	$^4D_{5/2}$	6600^{+10}_{-10}	6566	...	6494	6559	...	...	...	...	†
$\lvert 2,0,0,0\rangle$	$^4D_{7/2}$	6614^{+18}_{-18}	...	...	6497	6567	...	...	...	...	†
$\lvert 0,0,1,0\rangle$	$^2S_{1/2}$	6574^{+11}_{-11}	6561	...	6472	6480	...	6479	...	...	†
$\lvert 0,0,1,0\rangle$	$^4S_{3/2}$	6602^{+11}_{-11}	...	...	...	6491	...	...	...	...	†
$\lvert 0,0,0,1\rangle$	$^2S_{1/2}$	6874^{+17}_{-17}	...	...	...	...	...	...	...	...	†
$\lvert 0,0,0,1\rangle$	$^4S_{3/2}$	6902^{+17}_{-17}	...	...	...	...	...	...	...	...	†
$\lvert 1,1,0,0\rangle$	$^2D_{3/2}$	6718^{+14}_{-14}	...	...	...	...	...	...	...	...	†
$\lvert 1,1,0,0\rangle$	$^2D_{5/2}$	6728^{+15}_{-15}	6657	...	...	...	...	...	...	...	†
$\lvert 1,1,0,0\rangle$	$^2P_{1/2}$	6720^{+14}_{-14}	...	...	...	...	...	...	...	...	†
$\lvert 1,1,0,0\rangle$	$^2P_{3/2}$	6726^{+15}_{-15}	...	...	...	...	...	...	...	...	†
$\lvert 1,1,0,0\rangle$	$^2S_{1/2}$	6724^{+14}_{-14}	...	...	...	...	...	...	...	...	†
$\lvert 0,2,0,0\rangle$	$^2D_{3/2}$	6868^{+17}_{-17}	...	...	...	...	...	...	...	...	†
$\lvert 0,2,0,0\rangle$	$^2D_{5/2}$	6878^{+19}_{-19}	...	...	...	...	...	...	...	...	†
$\lvert 0,2,0,0\rangle$	$^4D_{1/2}$	6884^{+21}_{-21}	...	...	...	...	...	...	...	...	†
$\lvert 0,2,0,0\rangle$	$^4D_{3/2}$	6890^{+18}_{-18}	...	...	...	...	...	...	...	...	†
$\lvert 0,2,0,0\rangle$	$^4D_{5/2}$	6900^{+17}_{-17}	...	...	...	...	...	...	...	...	†
$\lvert 0,2,0,0\rangle$	$^4D_{7/2}$	6914^{+23}_{-23}	...	...	6667	...	...	...	...	...	†

presents the theoretical masses obtained within the quark-diquark model using the Hamiltonian in eq. (2.64). In the seventh column, the corresponding experimental values, as reported by the PDG [89], are listed. Additionally, a comparison between our theoretical predictions and the experimental data [89] is shown in Figs. 2.4–2.8, for both the three-quark and quark-diquark models.

It can be observed that our mass predictions show good agreement with the available experimental data. It is noteworthy that the model presented in reference [83] relies on a relatively small number of parameters. The fit is performed using the data from only 13 of the 23 well-established singly bottom baryons states; these states are indicated with the superscript "*a*" in Tables 2.2–2.6. Therefore, the remaining states constitute predictions of the model.

Furthermore, Tables 2.7–2.11 present a comparison between our predicted mass spectra and previous three-quark model studies, including the NRQM [42, 48, 50], QCDSR [57, 59, 60], χQM [65], and LQCD [68]. However, these previous works did not provide the explicit internal structure of the baryon states, specifying only their flavor content and total angular momentum J. As a result, a tentative assignment was made based on the mass values and total spin J.

Due to the limited available data, it is not possible to draw definitive conclusions regarding the differences in the predictions of each model. It is important to emphasize that validating the model proposed in reference [83] requires the identification of singly bottom baryon multiplets through additional experimental observations.

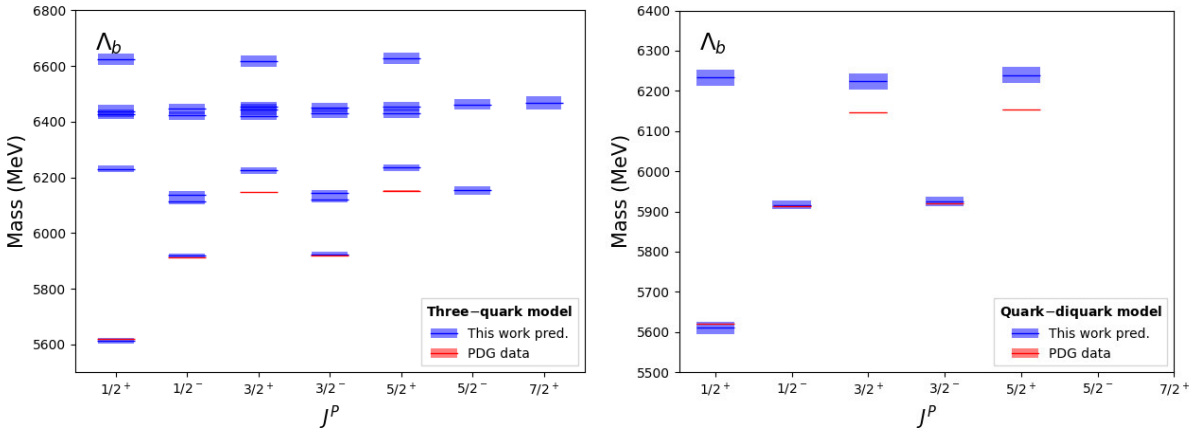

FIGURE 2.4: *Figure taken from [90] (APS copyright).* Λ_b mass spectra and tentative quantum number assignments based on the three-quark model Hamiltonian of Eqs. 2.44 and 2.45 (left) and based on the quark-diquark model Hamiltonian of Eqs. 2.44 and 2.62 (right). The theoretical predictions and their uncertainties (blue lines and bands) are compared with the experimental results (red lines and bands) given in the PDG [89]. The experimental errors are too small to be reported on this energy scale.

2.5 Strong decay widths

It is worth noting that the experimentally measured decay widths include contributions from strong, electromagnetic, and weak interactions. However, the dominant contribution typically arises from the strong decay process.

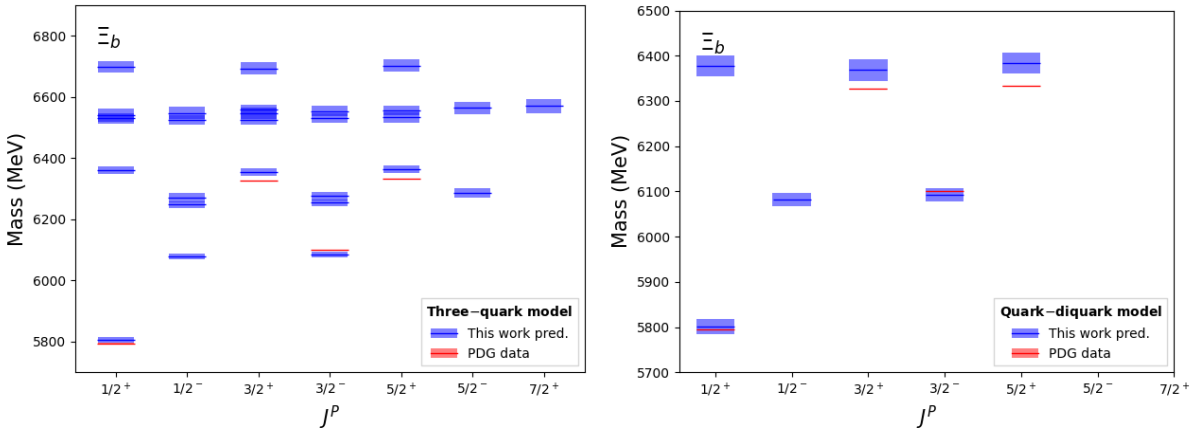

FIGURE 2.5: *Figure taken from [90] (APS copyright).* Same as Figure 2.4, but for Ξ_b states.

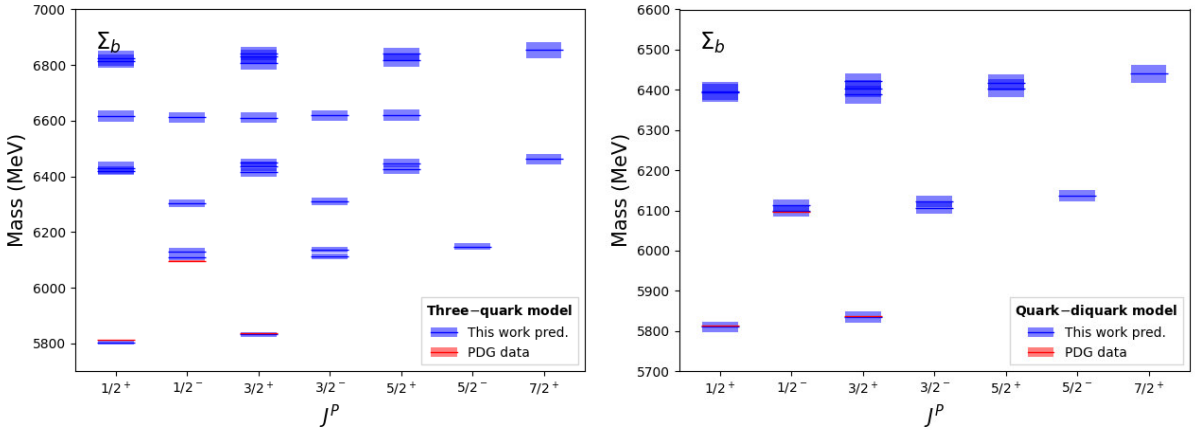

FIGURE 2.6: *Figure taken from [90] (APS copyright).* Same as Figure 2.4, but for Σ_b states.

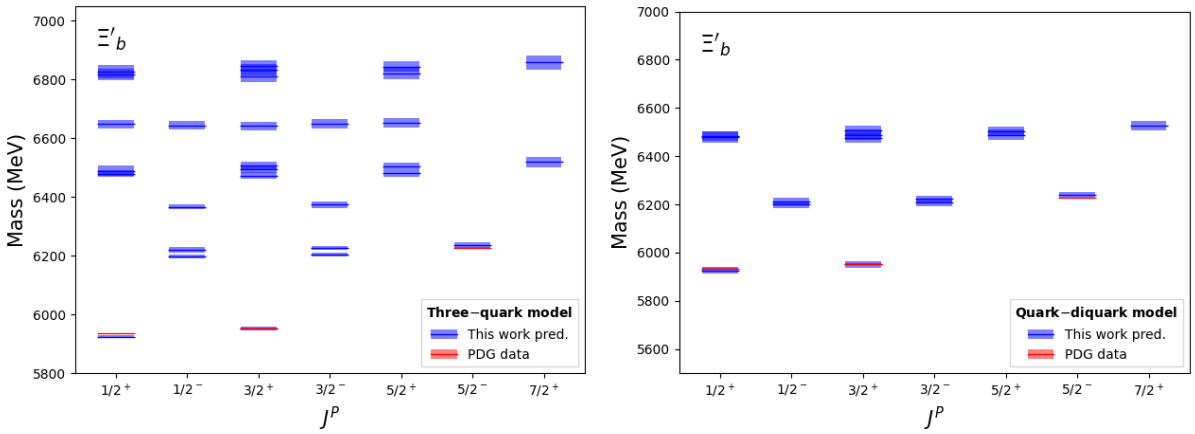

FIGURE 2.7: *Figure taken from [90] (APS copyright).* Same as Figure 2.4, but for Ξ'_b states.

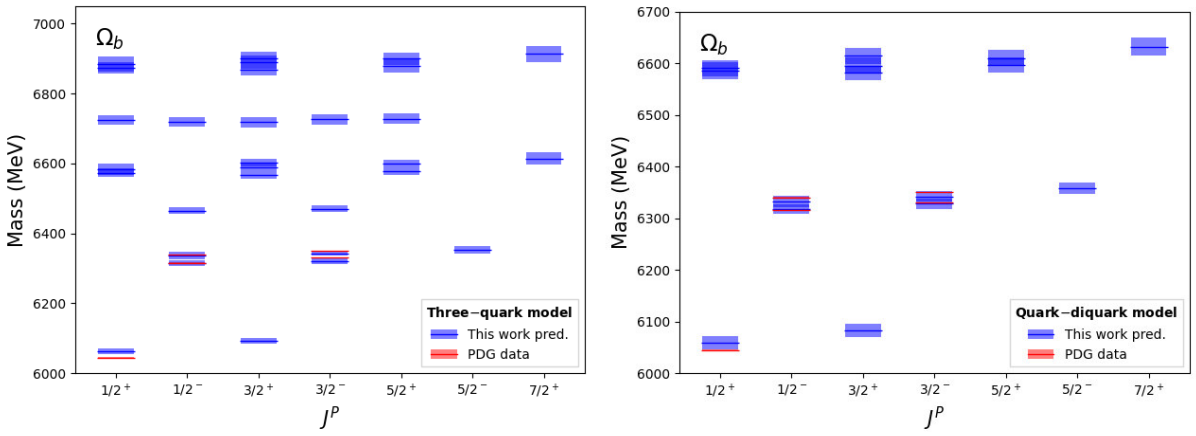

FIGURE 2.8: *Figure taken from [90] (APS copyright).* Same as Figure 2.4, but for Ω_b states.

In this section, the open-flavor strong decay widths of the singly bottom baryons are investigated. The decay widths in the three-quark picture are computed using the $^3P_0$ model. In this framework, the transition operator is defined as follows [33, 84, 85, 87, 88, 123]:

$$T^\dagger = -3\gamma_0 \int d\mathbf{p}_4\, d\mathbf{p}_5\, \delta(\mathbf{p}_4+\mathbf{p}_5)\, C_{45}\, F_{45}\, [\chi_{45} \times \mathcal{Y}_1(\mathbf{p}_4-\mathbf{p}_5)]_0^{(0)}\; b_4^\dagger(\mathbf{p}_4)\, d_5^\dagger(\mathbf{p}_5), \quad (2.66)$$

where γ_0 is the pair-creation strength, and $b_4^\dagger(\mathbf{p}_4)$ and $d_5^\dagger(\mathbf{p}_5)$ denote the creation operators for a quark and an antiquark with momenta $\mathbf{p}_4$ and $\mathbf{p}_5$, respectively. The created $q\bar{q}$ pair is characterized by a color-singlet wave function C_{45}, a flavor-singlet wave function F_{45}, a spin-triplet wave function χ_{45} with spin $\mathbf{S}_{45} = \mathbf{1}$ and a solid harmonic $\mathcal{Y}_1(\mathbf{p}_4 - \mathbf{p}_5)$, reflecting the fact that the quark and antiquark are in a relative P-wave.

In the framework of the $^3P_0$ model, the decay of the baryon A occurs via the creation of a $q\bar{q}$ pair from the vacuum. This pair subsequently recombines with the remaining quarks to form an outgoing baryon B and a meson C, as illustrated in Fig. 2.9.

The total strong decay width of a singly bottom baryon A is given by the sum of the partial widths corresponding to its decays into all open-flavor channels BC. This can be expressed as:

$$\Gamma_{\text{Strong}} = \sum_{BC} \Gamma_{\text{Strong}}(A \to BC), \quad (2.67)$$

where the strong partial decay widths $\Gamma_{\text{Strong}}(A \to BC)$ are calculated using

$$\Gamma_{\text{Strong}}(A \to BC) = \frac{2\pi\gamma_0^2}{2J_A+1}\, \Phi_{A\to BC} \sum_{M_{J_A}, M_{J_B}} \left|\mathcal{M}^{M_{J_A}, M_{J_B}}\right|^2, \quad (2.68)$$

here, $\Phi_{A\to BC}$ is the phase space factor [88, 123] and the transition amplitude

$$\mathcal{M}^{M_{J_A}, M_{J_B}} = \langle \Psi_B \Psi_C | T^\dagger | \Psi_A \rangle, \quad (2.69)$$

is calculated using the eigenstates of the Hamiltonian operator in eq. (2.45), denoted by Ψ_A, Ψ_B

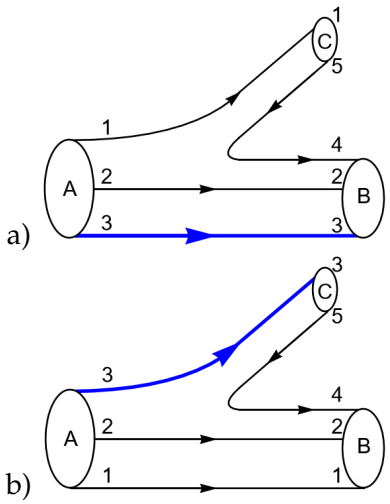

FIGURE 2.9: *Figure taken from [90] (APS copyright).* The $^3P_0$ pair-creation model. The blue line 3 denotes a bottom quark, while the remaining black lines denote light quarks. In diagram a) the bottom baryon A decays to a bottom baryon B and a light meson C. In diagram b) the bottom baryon A decays to a light baryon B and a bottom meson C.

and Ψ_C, which correspond to harmonic oscillator wave functions. In the above equation, $T^\dagger$ is the $^3P_0$ transition operator defined in eq. (2.66). In eq. (2.68), the summation runs over the third components M_{J_A} and M_{J_B} of the total angular momenta J_A and J_B of baryons A and B, respectively.

As previously mentioned, the harmonic oscillator wave functions do not depend on any free parameters, and the parameters $\alpha_{\rho(\lambda)}$ depend on the harmonic oscillator constant K_b and the quark masses. In the Λ_b and Σ_b sectors, the values are $\alpha_\rho = 381$ MeV and $\alpha_\lambda = 487$ MeV. For the Ξ_b and $\Xi_b^{'}$ sectors, the parameters are $\alpha_\rho = 403$ MeV and $\alpha_\lambda = 512$ MeV, while in the Ω_b sector, they are $\alpha_\rho = 425$ MeV and $\alpha_\lambda = 536$ MeV. The only free parameter in the $^3P_0$ model is the pair-creation strength γ_0, which is fitted to reproduce the experimental strong decay width of the channel $\Sigma_b^* \to \Lambda_b\pi$ [89]. The resulting value is $\gamma_0 = 21 \pm 3$. All other strong decay widths presented in this work are therefore predictions of the model.

In the computation of the strong decay widths, an additional parameter R, which is related to the meson size, is employed. In this study, the value $R = 2.1$ GeV^{-1} is adopted [33, 124, 125]. The decay widths are calculated for the $1S$, $1P$, $1D$, $2P$, and $2S$ singly bottom baryons. The available open-flavor decay channels include multiplets of light pseudoscalar and vector mesons, as well as heavy bottom mesons. The flavor wave functions of the baryons and mesons are provided in Appendices B and C of reference [90], respectively. The corresponding flavor couplings, given by $\mathcal{F}_{A\to BC} = \langle\phi_B\phi_C|\phi_0\phi_A\rangle$, are listed in Appendix D of the same reference. The masses of the decay products used in the calculations are compiled in Table 2.12.

2.5.1 Results of strong decay widths

Our theoretical strong decay widths are presented in the eighth column of Tables 2.2-2.6. These results show good agreement with the experimental values reported in the ninth column of the

TABLE 2.12: *Table from [90] (APS copyright).* Masses as from PDG [89] of the final baryon and meson states used in the calculation of the decay widths.

	Mass in GeV
m_π	0.13725 ± 0.00295
m_K	0.49564 ± 0.00279
m_η	0.54786 ± 0.00002
$m_{\eta'}$	0.95778 ± 0.00006
m_ρ	0.77518 ± 0.00045
m_{K^*}	0.89555 ± 0.00100
m_ω	0.78266 ± 0.00002
m_ϕ	1.01946 ± 0.00002
m_B	5.27966 ± 0.00012
m_{B_s}	5.36692 ± 0.00010
m_{B^*}	5.32471 ± 0.00021
m_N	0.93891 ± 0.00091
$m_{N(1520)}$	1.51500 ± 0.00500
$m_{N(1535)}$	1.53000 ± 0.01500
$m_{N(1680)}$	1.68500 ± 0.00500
$m_{N(1720)}$	1.72000 ± 0.03500
m_Δ	1.23200 ± 0.00200
m_Λ	1.11568 ± 0.00001
$m_{\Lambda(1520)}$	1.51900 ± 0.00010
m_{Ξ_8}	1.31820 ± 0.00360
$m_{\Xi_{10}}$	1.53370 ± 0.00250
m_{Σ_8}	1.11932 ± 0.00340
$m_{\Sigma_{10}}$	1.38460 ± 0.00460
m_{Λ_b}	5.61960 ± 0.00010
m_{Ξ_b}	5.79700 ± 0.00060
$m_{\Xi_b'}$	5.93502 ± 0.00005
$m_{\Xi_b^*}$	6.07800 ± 0.00006
m_{Σ_b}	5.81056 ± 0.00025
$m_{\Sigma_b^*}$	5.83032 ± 0.00030
m_{Ω_b}	6.04520 ± 0.00120
$m_{\Omega_b^*}$	6.09300 ± 0.00060

same tables [89]. This level of agreement is particularly noteworthy given that the $^3P_0$ model includes only a single free parameter.

Additionally, our theoretical predictions are compared with previous studies based on various models, including the NRQM [69], χQM [70, 71], and other implementations of the $^3P_0$ model [75–77, 79, 80, 83, 126]. These comparisons are shown in Tables 2.13-2.17. From these tables, it can be observed that the previous studies considered only a subset of the possible meson channels in their calculations.

TABLE 2.13: *Table from [90] (APS copyright).* Comparison of our predicted $\Lambda_b(nnb)$ strong decay widths with those of other theoretical studies (in MeV). The flavor multiplet is indicated by the symbol $\mathcal{F}$. The first column contains the three-quark model state, $|l_\lambda, l_\rho, k_\lambda, k_\rho\rangle$, where $l_{\lambda,\rho}$ are the orbital angular momenta and $k_{\lambda,\rho}$ the number of nodes of the λ and ρ oscillators. The second column displays each state's spectroscopic notation $^{2S+1}L_J$. In the third column, our predicted strong decay widths, computed within the $^3P_0$ model and the baryon-meson channels included in the calculation, are shown. Our results are compared with those of references [76] (fourth column), [71] (fifth column), and [80] (sixth column). Our theoretical results are also compared with the experimental decay widths from PDG [89] (seventh column). The symbol "..." indicates that there is no prediction for that state. The "†" indicates that there is no reported experimental decay width for that state up to now.

$\Lambda_b(nnb)$	$\mathcal{F}=\bar{\mathbf{3}}_F$	This work	[76]	[71]	[80]	Exp.
$\lvert l_\lambda, l_\rho, k_\lambda, k_\rho\rangle$	$^{2S+1}L_J$	Γ (MeV)	Γ (MeV)	Γ (MeV)	Γ (MeV)	Γ (MeV)
Channels		$\Sigma_b\pi, \Sigma_b^*\pi, \Lambda_b\eta, \Sigma_b\rho$ $\Sigma_b^*\rho, \Lambda_b\eta, \Lambda_b\omega, \Xi_bK$ $\Xi_b'K, \Xi_b^*K, \Xi_bK^*$ $\Xi_b'K^*, \Xi_b^*K^*, NB$	$\Sigma_b\pi, \Sigma_b^*\pi$	$\Sigma_b\pi, \Sigma_b^*\pi$	$\Sigma_b\pi, \Sigma_b^*\pi$	
$N=0$						
$\lvert 0,0,0,0\rangle$	$^2S_{1/2}$	0	...	...	...	≈ 0
$N=1$						
$\lvert 1,0,0,0\rangle$	$^2P_{1/2}$	0	...	...	...	< 0.25
$\lvert 1,0,0,0\rangle$	$^2P_{3/2}$	0	...	...	...	< 0.19
$\lvert 0,1,0,0\rangle$	$^2P_{1/2}$	67	...	...	...	†
$\lvert 0,1,0,0\rangle$	$^4P_{1/2}$	36	523	...	...	†
$\lvert 0,1,0,0\rangle$	$^2P_{3/2}$	85	460	...	...	†
$\lvert 0,1,0,0\rangle$	$^4P_{3/2}$	128	4	...	...	†
$\lvert 0,1,0,0\rangle$	$^4P_{5/2}$	74	3	...	...	†
$N=2$						
$\lvert 2,0,0,0\rangle$	$^2D_{3/2}$	13	...	9	...	2.9 ± 1.3
$\lvert 2,0,0,0\rangle$	$^2D_{5/2}$	18	...	9	...	2.1 ± 0.9
$\lvert 0,0,1,0\rangle$	$^2S_{1/2}$	29	9	...	36	†
$\lvert 0,0,0,1\rangle$	$^2S_{1/2}$	130	...	...	...	†
$\lvert 1,1,0,0\rangle$	$^2D_{3/2}$	67	...	...	...	†
$\lvert 1,1,0,0\rangle$	$^2D_{5/2}$	108	...	...	...	†
$\lvert 1,1,0,0\rangle$	$^4D_{1/2}$	34	...	...	...	†
$\lvert 1,1,0,0\rangle$	$^4D_{3/2}$	95	...	...	...	†
$\lvert 1,1,0,0\rangle$	$^4D_{5/2}$	128	...	...	...	†
$\lvert 1,1,0,0\rangle$	$^4D_{7/2}$	122	...	...	...	†
$\lvert 1,1,0,0\rangle$	$^2P_{1/2}$	0	...	...	...	†
$\lvert 1,1,0,0\rangle$	$^2P_{3/2}$	2	...	...	...	†
$\lvert 1,1,0,0\rangle$	$^4P_{1/2}$	0	...	...	...	†
$\lvert 1,1,0,0\rangle$	$^4P_{3/2}$	1	...	...	...	†
$\lvert 1,1,0,0\rangle$	$^4P_{5/2}$	2	...	...	...	†
$\lvert 1,1,0,0\rangle$	$^4S_{3/2}$	32	...	...	...	†
$\lvert 1,1,0,0\rangle$	$^2S_{1/2}$	29	...	...	...	†
$\lvert 0,2,0,0\rangle$	$^2D_{3/2}$	131	...	...	...	†
$\lvert 0,2,0,0\rangle$	$^2D_{5/2}$	185	...	...	...	†

Furthermore, the strong partial decay widths $\Gamma_{\text{Strong}}(A \to BC)$ for an initial baryon A decaying into a final baryon B and a meson C, across all open-flavor channels, are presented in Tables 2.18-2.22. The partial decay widths obtained in this study provide valuable input for

TABLE 2.14: *Table from [90] (APS copyright).* Comparison of our predicted $\Xi_b(snb)$ strong decay widths with those of other theoretical studies (in MeV). The flavor multiplet is indicated by the symbol $\mathcal{F}$. The first column contains the three-quark model state, $|l_\lambda, l_\rho, k_\lambda, k_\rho\rangle$, where $l_{\lambda,\rho}$ are the orbital angular momenta and $k_{\lambda,\rho}$ the number of nodes of the λ and ρ oscillators. The second column displays each state's spectroscopic notation $^{2S+1}L_J$. In the third column, our predicted strong decay widths, computed within the $^3P_0$ model and the baryon-meson channels included in the calculation, are shown. Our results are compared with those of references [69] (fourth column), [71] (fifth column), [70] (sixth column), [77] (seventh column), [79] (eighth column), and [126] (ninth column). The experimental widths, as from PDG [89], are reported in the tenth column. The symbol "..." indicates that there is no prediction for that state. The "†" indicates that there is no reported experimental decay width for that state up to now.

$\Xi_b(snb)$ $\lvert l_\lambda, l_\rho, k_\lambda, k_\rho\rangle$	$\mathcal{F}=\bar{\mathbf{3}}_F$ $^{2S+1}L_J$	This work Γ (MeV)	[69] Γ (MeV)	[71] Γ (MeV)	[70] Γ (MeV)	[77] Γ (MeV)	[79] Γ (MeV)	[126] Γ (MeV)	Exp. Γ (MeV)
Channels		$\Lambda_b K, \Xi_b \pi, \Xi_b' \pi$ $\Xi_b^* \pi, \Sigma_b K, \Sigma_b^* K$ $\Xi_b \eta, \Lambda_b K^*, \Xi_b \rho$ $\Xi_b' \rho, \Xi_b^* \rho, \Sigma_b K^*$ $\Sigma_b^* K^*, \Xi_b' \eta, \Xi_b^* \eta$ $\Xi_b \eta', \Xi_b' \eta', \Xi_b^* \eta'$ $\Xi_b \omega, \Xi_b' \omega, \Xi_b^* \omega$ $\Xi_b \phi, \Xi_b' \phi, \Xi_b^* \phi$ $\Lambda_8 B, \Lambda_8 B^*, \Sigma_8 B$ $\Lambda_8^* B$	$\Xi_b \pi$ $\Xi_b' \pi$	$\Xi_b' \pi$ $\Xi_b^* \pi$ $\Sigma_b K$ $\Sigma_b^* K$	$\Xi_b' \pi$ $\Xi_b^* \pi$	$\Xi_b' \pi$ $\Xi_b^* \pi$ $\Sigma_b K$ $\Sigma_b^* K$	$\Xi_b \pi$ $\Xi_b' \pi$ $\Xi_b^* \pi$	$\Sigma_b \bar{K}, \Xi_b' \pi$ $\Sigma_b^* \bar{K}, \Xi_b^* \pi$ $\Lambda_b \bar{K}, \Xi_b \pi$ $\Xi_b \eta$	
$N=0$									
$\lvert 0,0,0,0\rangle$	$^2S_{1/2}$	0	...	...	...	...	...	0	≈ 0
$N=1$									
$\lvert 1,0,0,0\rangle$	$^2P_{1/2}$	0	11	...	3	18	4	0	†
$\lvert 1,0,0,0\rangle$	$^2P_{3/2}$	1	≈ 0	...	3	16	3	0	< 1.9
$\lvert 0,1,0,0\rangle$	$^2P_{1/2}$	9	223	...	...	...	...	0.55	†
$\lvert 0,1,0,0\rangle$	$^4P_{1/2}$	6	10	...	...	...	...	0.36	†
$\lvert 0,1,0,0\rangle$	$^2P_{3/2}$	66	...	...	...	...	...	1.90	†
$\lvert 0,1,0,0\rangle$	$^4P_{3/2}$	26	...	...	...	...	...	1.90	†
$\lvert 0,1,0,0\rangle$	$^4P_{5/2}$	68	...	...	...	...	...	2.16	†
$N=2$									
$\lvert 2,0,0,0\rangle$	$^2D_{3/2}$	2	...	7	...	7	...	0.19	< 2.2
$\lvert 2,0,0,0\rangle$	$^2D_{5/2}$	2	...	7	...	6	...	0.10	< 1.6
$\lvert 0,0,1,0\rangle$	$^2S_{1/2}$	5	...	...	...	7	16	...	†
$\lvert 0,0,0,1\rangle$	$^2S_{1/2}$	179	...	...	...	...	...	...	†
$\lvert 1,1,0,0\rangle$	$^2D_{3/2}$	46	...	...	...	...	...	...	†
$\lvert 1,1,0,0\rangle$	$^2D_{5/2}$	108	...	...	...	...	...	...	†
$\lvert 1,1,0,0\rangle$	$^4D_{1/2}$	20	...	...	...	...	...	...	†
$\lvert 1,1,0,0\rangle$	$^4D_{3/2}$	67	...	...	...	...	...	...	†
$\lvert 1,1,0,0\rangle$	$^4D_{5/2}$	100	...	...	...	...	...	...	†
$\lvert 1,1,0,0\rangle$	$^4D_{7/2}$	114	...	...	...	...	...	...	†
$\lvert 1,1,0,0\rangle$	$^2P_{1/2}$	0	...	...	...	...	...	...	†
$\lvert 1,1,0,0\rangle$	$^2P_{3/2}$	2	...	...	...	...	...	...	†
$\lvert 1,1,0,0\rangle$	$^4P_{1/2}$	0	...	...	...	...	...	...	†
$\lvert 1,1,0,0\rangle$	$^4P_{3/2}$	1	...	...	...	...	...	...	†
$\lvert 1,1,0,0\rangle$	$^4P_{5/2}$	2	...	...	...	...	...	...	†
$\lvert 1,1,0,0\rangle$	$^4S_{3/2}$	33	...	...	...	...	...	...	†
$\lvert 1,1,0,0\rangle$	$^2S_{1/2}$	31	...	...	...	...	...	...	†
$\lvert 0,2,0,0\rangle$	$^2D_{3/2}$	127	...	...	...	...	...	...	†
$\lvert 0,2,0,0\rangle$	$^2D_{5/2}$	98	...	...	...	...	...	...	†

TABLE 2.15: *Table from [90] (APS copyright).* Comparison of our predicted $\Sigma_b(nnb)$ strong decay widths with those of other theoretical studies (in MeV). The flavor multiplet is indicated by the symbol $\mathcal{F}$. The first column contains the three-quark model state, $|l_\lambda, l_\rho, k_\lambda, k_\rho\rangle$, where $l_{\lambda,\rho}$ are the orbital angular momenta and $k_{\lambda,\rho}$ the number of nodes of the λ and ρ oscillators. The second column displays each state's spectroscopic notation $^{2S+1}L_J$. In the third column, our predicted strong decay widths, computed within the $^3P_0$ model and the baryon-meson channels included in the calculation, are shown. Our results are compared with those of references [76] (fourth column), [71] (fifth column), [70] (sixth column), [79] (seventh column), and [80] (eighth column). The experimental widths, as from PDG [89], are reported in the ninth column. The symbol "..." indicates that there is no prediction for that state. N_1^*, N_2^*, N_3^*, and N_4^* represent $N(1520)$, $N(1535)$, $N(1680)$, and $N(1720)$, respectively. The "†" indicates that there is no reported experimental decay width for that state up to now.

$\Sigma_b(nnb)$	$\mathcal{F}=\mathbf{6}_\mathrm{F}$	This work	[76]	[71]	[70]	[79]	[80]	Exp.
$\lvert l_\lambda, l_\rho, k_\lambda, k_\rho\rangle$	$^{2S+1}L_J$	Γ (MeV)	Γ (MeV)	Γ (MeV)	Γ (MeV)	Γ (MeV)	Γ (MeV)	Γ (MeV)
Channels		$\Sigma_b\pi, \Sigma_b^*\pi, \Lambda_b\pi$ $\Sigma_b\eta, \Xi_bK, \Sigma_b\rho$ $\Sigma_b^*\rho, \Lambda_b\rho, \Sigma_b^*\eta$ $\Sigma_b\eta', \Sigma_b^*\eta', \Xi_b'K$ $\Xi_b^*K, \Xi_bK^*, \Xi_b'K^*$ $\Xi_b^*K^*, \Sigma_b\omega, \Sigma_b^*\omega$ NB, Σ_8B_s, NB^* $\Delta B, N_1^*B, N_2^*B$ N_3^*B, N_4^*B	$\Sigma_b\pi, \Sigma_b^*\pi$ $\Lambda_b\pi$	$\Sigma_b\pi, \Sigma_b^*\pi$	$\Sigma_b\pi, \Sigma_b^*\pi$ $\Lambda_b\pi$	$\Lambda_b\pi$	$\Sigma_b\pi, \Sigma_b^*\pi$ $\Lambda_b\pi, NB$ NB^*	
$N=0$								
$\lvert 0,0,0,0\rangle$	$^2S_{1/2}$	4	...	...	...	5	...	5.0 ± 0.5
$\lvert 0,0,0,0\rangle$	$^4S_{3/2}$	10	...	...	...	9	...	9.9 ± 0.9
$N=1$								
$\lvert 1,0,0,0\rangle$	$^2P_{1/2}$	24	264	...	23	...	27	30 ± 7
$\lvert 1,0,0,0\rangle$	$^4P_{1/2}$	13	209	...	14	...	109	†
$\lvert 1,0,0,0\rangle$	$^2P_{3/2}$	84	181	...	39	...	114	†
$\lvert 1,0,0,0\rangle$	$^4P_{3/2}$	57	9	...	26	...	42	†
$\lvert 1,0,0,0\rangle$	$^4P_{5/2}$	96	9	...	38	...	43	†
$\lvert 0,1,0,0\rangle$	$^2P_{1/2}$	134	261	...	...	...	...	†
$\lvert 0,1,0,0\rangle$	$^2P_{3/2}$	129	268	...	...	...	...	†
$N=2$								
$\lvert 2,0,0,0\rangle$	$^2D_{3/2}$	58	...	121	...	...	...	†
$\lvert 2,0,0,0\rangle$	$^2D_{5/2}$	130	...	48	...	...	...	†
$\lvert 2,0,0,0\rangle$	$^4D_{1/2}$	78	...	148	...	...	...	†
$\lvert 2,0,0,0\rangle$	$^4D_{3/2}$	106	...	85	...	...	...	†
$\lvert 2,0,0,0\rangle$	$^4D_{5/2}$	133	...	48	...	...	...	†
$\lvert 2,0,0,0\rangle$	$^4D_{7/2}$	145	...	53	...	...	...	†
$\lvert 0,0,1,0\rangle$	$^2S_{1/2}$	119	...	...	...	...	116	†
$\lvert 0,0,1,0\rangle$	$^4S_{3/2}$	121	...	...	...	...	122	†
$\lvert 0,0,0,1\rangle$	$^2S_{1/2}$	710	...	...	...	...	...	†
$\lvert 0,0,0,1\rangle$	$^4S_{3/2}$	973	...	...	...	...	...	†
$\lvert 1,1,0,0\rangle$	$^2D_{3/2}$	376	...	...	...	...	...	†
$\lvert 1,1,0,0\rangle$	$^2D_{5/2}$	252	...	...	...	...	...	†
$\lvert 1,1,0,0\rangle$	$^2P_{1/2}$	4	...	...	...	...	...	†
$\lvert 1,1,0,0\rangle$	$^2P_{3/2}$	5	...	...	...	...	...	†
$\lvert 1,1,0,0\rangle$	$^2S_{1/2}$	58	...	...	...	...	...	†
$\lvert 0,2,0,0\rangle$	$^2D_{3/2}$	549	...	...	...	...	...	†
$\lvert 0,2,0,0\rangle$	$^2D_{5/2}$	616	...	...	...	...	...	†
$\lvert 0,2,0,0\rangle$	$^4D_{1/2}$	1349	...	...	...	...	...	†
$\lvert 0,2,0,0\rangle$	$^4D_{3/2}$	741	...	...	...	...	...	†
$\lvert 0,2,0,0\rangle$	$^4D_{5/2}$	376	...	...	...	...	...	†
$\lvert 0,2,0,0\rangle$	$^4D_{7/2}$	1178	...	...	...	...	...	†

TABLE 2.16: *Table from [90] (APS copyright).* Comparison of our predicted $\Xi_b'(snb)$ strong decay widths with those of other theoretical studies (in MeV). The flavor multiplet is indicated by the symbol $\mathcal{F}$. The first column contains the three-quark model state, $|l_\lambda, l_\rho, k_\lambda, k_\rho\rangle$, where $l_{\lambda,\rho}$ are the orbital angular momenta and $k_{\lambda,\rho}$ the number of nodes of the λ and ρ oscillators. The second column displays each state's spectroscopic notation $^{2S+1}L_J$. In the third column, our predicted strong decay widths, computed within the $^3P_0$ model and the baryon-meson channels included in the calculation, are shown. Our results are compared with those of references [69] (fourth column), [71] (fifth column), [70] (sixth column), [77] (seventh column), [79] (eighth column), and [126] (ninth column). The experimental widths, as from PDG [89], are reported in the tenth column. The symbol "..." indicates that there is no prediction for that state. The "†" indicates that there is no reported experimental decay width for that state up to now.

$\Xi_b'(snb)$ $\lvert l_\lambda, l_\rho, k_\lambda, k_\rho\rangle$	$\mathcal{F}=\mathbf{6}_\mathrm{F}$ $^{2S+1}L_J$	This work Γ (MeV)	[69] Γ (MeV)	[71] Γ (MeV)	[70] Γ (MeV)	[77] Γ (MeV)	[79] Γ (MeV)	[126] Γ (MeV)	Exp. Γ (MeV)
Channels		$\Lambda_b K, \Xi_b \pi, \Xi_b' \pi$ $\Xi_b^* \pi, \Sigma_b K, \Sigma_b^* K$ $\Xi_b \eta, \Lambda_b K^*, \Xi_b \rho$ $\Xi_b' \rho, \Xi_b^* \rho, \Sigma_b K^*$ $\Sigma_b^* K^*, \Xi_b' \eta, \Xi_b^* \eta$ $\Xi_b \eta', \Xi_b' \eta', \Xi_b^* \eta'$ $\Xi_b \omega, \Xi_b' \omega, \Xi_b^* \omega$ $\Xi_b \phi, \Xi_b' \phi, \Xi_b^* \phi$ $\Sigma_8 B, \Xi_8 B_s$ $\Sigma_8 B^*, \Sigma_{10} B$	$\Xi_b \pi$	$\Lambda_b K$ $\Xi_b \pi$ $\Xi_b' \pi$ $\Xi_b^* \pi$ $\Sigma_b K$ $\Sigma_b^* K$	$\Lambda_b K$ $\Xi_b \pi$ $\Xi_b' \pi$	$\Lambda_b K$ $\Xi_b \pi$ $\Xi_b' \pi$ $\Xi_b^* \pi$ $\Sigma_b K$ $\Sigma_b^* K$	$\Lambda_b K$ $\Xi_b \pi$ $\Xi_b' \pi$ $\Xi_b^* \pi$	$\Sigma_b \bar{K}$ $\Xi_b' \pi$ $\Sigma_b^* \bar{K}$ $\Xi_b^* \pi$ $\Lambda_b \bar{K}$ $\Xi_b \pi$ $\Xi_b \eta$	
$N=0$									
$\lvert 0,0,0,0\rangle$	$^2S_{1/2}$	0	≈ 0	...	...	...	≈ 0	0	< 0.08
$\lvert 0,0,0,0\rangle$	$^4S_{3/2}$	0.2	2	...	...	...	1	0.02	0.90 ± 0.18
$N=1$									
$\lvert 1,0,0,0\rangle$	$^2P_{1/2}$	3	...	...	27	371	10	0.86	†
$\lvert 1,0,0,0\rangle$	$^4P_{1/2}$	4	...	...	32	91	17	0.65	†
$\lvert 1,0,0,0\rangle$	$^2P_{3/2}$	29	...	...	24	86	25	2.92	†
$\lvert 1,0,0,0\rangle$	$^4P_{3/2}$	8	...	...	16	7	24	1.83	†
$\lvert 1,0,0,0\rangle$	$^4P_{5/2}$	31	...	...	24	7	25	3.36	19.9 ± 2.6
$\lvert 0,1,0,0\rangle$	$^2P_{1/2}$	197	...	...	...	...	...	5.88	†
$\lvert 0,1,0,0\rangle$	$^2P_{3/2}$	97	...	...	...	...	...	3.08	†
$N=2$									
$\lvert 2,0,0,0\rangle$	$^2D_{3/2}$	14	...	101	...	40	...	...	†
$\lvert 2,0,0,0\rangle$	$^2D_{5/2}$	30	...	25	...	19	...	...	†
$\lvert 2,0,0,0\rangle$	$^4D_{1/2}$	25	...	109	...	39	...	...	†
$\lvert 2,0,0,0\rangle$	$^4D_{3/2}$	35	...	58	...	22	...	...	†
$\lvert 2,0,0,0\rangle$	$^4D_{5/2}$	46	...	28	...	2	...	...	†
$\lvert 2,0,0,0\rangle$	$^4D_{7/2}$	47	...	41	...	2	...	...	†
$\lvert 0,0,1,0\rangle$	$^2S_{1/2}$	47	...	...	...	34	56	...	†
$\lvert 0,0,1,0\rangle$	$^4S_{3/2}$	79	...	...	...	36	58	...	†
$\lvert 0,0,0,1\rangle$	$^2S_{1/2}$	599	...	...	...	...	...	...	†
$\lvert 0,0,0,1\rangle$	$^4S_{3/2}$	630	...	...	...	...	...	...	†
$\lvert 1,1,0,0\rangle$	$^2D_{3/2}$	234	...	...	...	...	...	...	†
$\lvert 1,1,0,0\rangle$	$^2D_{5/2}$	116	...	...	...	...	...	...	†
$\lvert 1,1,0,0\rangle$	$^2P_{1/2}$	3	...	...	...	...	...	...	†
$\lvert 1,1,0,0\rangle$	$^2P_{3/2}$	3	...	...	...	...	...	...	†
$\lvert 1,1,0,0\rangle$	$^2S_{1/2}$	59	...	...	...	...	...	...	†
$\lvert 0,2,0,0\rangle$	$^2D_{3/2}$	315	...	...	...	...	...	...	†
$\lvert 0,2,0,0\rangle$	$^2D_{5/2}$	209	...	...	...	...	...	...	†
$\lvert 0,2,0,0\rangle$	$^4D_{1/2}$	529	...	...	...	...	...	...	†
$\lvert 0,2,0,0\rangle$	$^4D_{3/2}$	364	...	...	...	...	...	...	†
$\lvert 0,2,0,0\rangle$	$^4D_{5/2}$	194	...	...	...	...	...	...	†
$\lvert 0,2,0,0\rangle$	$^4D_{7/2}$	349	...	...	...	...	...	...	†

TABLE 2.17: *Table from [90] (APS copyright).* Comparison of our predicted $\Omega_b(ssb)$ strong decay widths with those of other theoretical studies (in MeV). The flavor multiplet is indicated by the symbol $\mathcal{F}$. The first column contains the three-quark model state, $|l_\lambda, l_\rho, k_\lambda, k_\rho\rangle$, where $l_{\lambda,\rho}$ are the orbital angular momenta and $k_{\lambda,\rho}$ the number of nodes of the λ and ρ oscillators. The second column displays each state's spectroscopic notation $^{2S+1}L_J$. In the third column, our predicted strong decay widths, computed within the $^3P_0$ model and the baryon-meson channels included in the calculation, are shown. Our results are compared with those of references [71] (fourth column), [70] (fifth column), [75] (sixth column), [80] (seventh column), and [83] (eigth column). The experimental widths, as from PDG [89], are reported in the ninth column. The symbol "..." indicates that there is no prediction for that state. The "†" indicates that there is no reported experimental decay width for that state up to now.

$\Omega_b(ssb)$	$\mathcal{F}=\mathbf{6}_\mathrm{F}$	This work	[71]	[70]	[75]	[80]	[83]	Exp.
$\lvert l_\lambda, l_\rho, k_\lambda, k_\rho\rangle$	$^{2S+1}L_J$	Γ (MeV)	Γ (MeV)	Γ (MeV)	Γ (MeV)	Γ (MeV)	Γ (MeV)	Γ (MeV)
Channels		$\Xi_bK, \Xi_b'K, \Xi_b^*K$ $\Xi_bK^*, \Xi_b'K^*, \Xi_b^*K^*$ $\Omega_b\eta, \Omega_b^*\eta, \Omega_b\phi$ $\Omega_b^*\phi, \Omega_b\eta', \Omega_b^*\eta'$ $\Xi_8B, \Xi_{10}B$	$\Xi_bK, \Xi_b'K$ Ξ_b^*K	Ξ_bK	$\Xi_bK, \Xi_b'K$ Ξ_b^*K	$\Xi_bK, \Xi_b'K$ Ξ_b^*K	$\Xi_b^0K^-$	
$N=0$								
$\lvert 0,0,0,0\rangle$	$^2S_{1/2}$	0	...	...	...	...	0	≈ 0
$\lvert 0,0,0,0\rangle$	$^4S_{3/2}$	0	...	...	...	...	0	†
$N=1$								
$\lvert 1,0,0,0\rangle$	$^2P_{1/2}$	5	...	49	...	33	0.5	< 4.2
$\lvert 1,0,0,0\rangle$	$^4P_{1/2}$	11	...	95	...	...	2.79	< 4.7
$\lvert 1,0,0,0\rangle$	$^2P_{3/2}$	24	...	2	...	...	1.14	< 1.8
$\lvert 1,0,0,0\rangle$	$^4P_{3/2}$	6	...	≈ 0	...	2	0.62	< 3.2
$\lvert 1,0,0,0\rangle$	$^4P_{5/2}$	40	...	2	...	3	4.28	†
$\lvert 0,1,0,0\rangle$	$^2P_{1/2}$	10	...	...	...	...	0	†
$\lvert 0,1,0,0\rangle$	$^2P_{3/2}$	54	...	...	...	...	0	†
$N=2$								
$\lvert 2,0,0,0\rangle$	$^2D_{3/2}$	4	20	...	108	...	...	†
$\lvert 2,0,0,0\rangle$	$^2D_{5/2}$	10	8	...	21	...	...	†
$\lvert 2,0,0,0\rangle$	$^4D_{1/2}$	1	29	...	106	...	...	†
$\lvert 2,0,0,0\rangle$	$^4D_{3/2}$	3	20	...	27	...	...	†
$\lvert 2,0,0,0\rangle$	$^4D_{5/2}$	8	7	...	3	...	...	†
$\lvert 2,0,0,0\rangle$	$^4D_{7/2}$	18	9	...	3	...	...	†
$\lvert 0,0,1,0\rangle$	$^2S_{1/2}$	20	...	...	50	16	...	†
$\lvert 0,0,1,0\rangle$	$^4S_{3/2}$	17	...	...	53	16	...	†
$\lvert 0,0,0,1\rangle$	$^2S_{1/2}$	398	...	...	...	...	...	†
$\lvert 0,0,0,1\rangle$	$^4S_{3/2}$	257	...	...	...	...	...	†
$\lvert 1,1,0,0\rangle$	$^2D_{3/2}$	116	...	...	...	...	...	†
$\lvert 1,1,0,0\rangle$	$^2D_{5/2}$	82	...	...	...	...	...	†
$\lvert 1,1,0,0\rangle$	$^2P_{1/2}$	1	...	...	...	...	...	†
$\lvert 1,1,0,0\rangle$	$^2P_{3/2}$	2	...	...	...	...	...	†
$\lvert 1,1,0,0\rangle$	$^2S_{1/2}$	72	...	...	...	...	...	†
$\lvert 0,2,0,0\rangle$	$^2D_{3/2}$	180	...	...	...	...	...	†
$\lvert 0,2,0,0\rangle$	$^2D_{5/2}$	157	...	...	...	...	...	†
$\lvert 0,2,0,0\rangle$	$^4D_{1/2}$	126	...	...	...	...	...	†
$\lvert 0,2,0,0\rangle$	$^4D_{3/2}$	195	...	...	...	...	...	†
$\lvert 0,2,0,0\rangle$	$^4D_{5/2}$	172	...	...	...	...	...	†
$\lvert 0,2,0,0\rangle$	$^4D_{7/2}$	230	...	...	...	...	...	†

TABLE 2.18: *Table from [90] (APS copyright).* Predicted $\Lambda_b(nnb)$ strong partial decay widths (in MeV). The flavor multiplet is denoted by the symbol $\mathcal{F}$. The first column reports the baryon name with its predicted mass, calculated by using the three-quark model Hamiltonian given by Eqs. 2.44 and 2.45. The second column displays $\mathbf{J}^{\mathrm{P}}$, the third column shows the three-quark model state, $|l_\lambda, l_\rho, k_\lambda, k_\rho\rangle$, where $l_{\lambda,\rho}$ represent the orbital angular momenta and $k_{\lambda,\rho}$ denote the number of nodes of the λ and ρ oscillators. The fourth column presents the spectroscopic notation $^{2S+1}L_J$. The value of $N = n_\rho + n_\lambda$ distinguishes the $N = 0, 1, 2$ energy bands. Starting from the fifth column, we provide the strong partial decay widths calculated by means of eq. (2.68). Each column corresponds to an open-flavor strong decay channel, and the specific decay channels are indicated at the top of each column. The masses of the decay products are given in Table 2.12. The values for the strong decay widths are given in MeV. The decay widths denoted by 0 are either too small to be shown on this scale or forbidden by phase space, while the decay widths denoted by the symbol "..." are forbidden by selection rules. Finally, the last column represents the sum of the strong partial decay widths over all the decay channels.

$\mathcal{F} = \bar{\mathbf{3}}_{\mathrm{F}}$				$\Sigma_b\pi$	$\Sigma_b^*\pi$	$\Lambda_b\eta$	$\Sigma_b\rho$	$\Sigma_b^*\rho$	$\Lambda_b\eta'$	$\Lambda_b\omega$	$\Xi_b K$	$\Xi_b' K$	$\Xi_b^* K$	$\Xi_b K^*$	$\Xi_b' K^*$	$\Xi_b^* K^*$	NB	Γ^{Strong}
$\Lambda_b(nnb)$	$\mathbf{J}^P$	$\lvert l_\lambda, l_\rho, k_\lambda, k_\rho\rangle$	$^{2S+1}L_J$	MeV	MeV	MeV	MeV	MeV	MeV	MeV	MeV	MeV	MeV	MeV	MeV	MeV	MeV	MeV
$N=0$																		
$\Lambda_b(5613)$	$\frac{1}{2}^+$	$\lvert 0,0,0,0\rangle$	$^2S_{1/2}$	0	0	0	0	0	0	0	0	0	0	0	0	0	0	0
$N=1$																		
$\Lambda_b(5918)$	$\frac{1}{2}^-$	$\lvert 1,0,0,0\rangle$	$^2P_{1/2}$	0	0	0	0	0	0	0	0	0	0	0	0	0	0	0
$\Lambda_b(5924)$	$\frac{3}{2}^-$	$\lvert 1,0,0,0\rangle$	$^2P_{3/2}$	0	0	0	0	0	0	0	0	0	0	0	0	0	0	0
$\Lambda_b(6114)$	$\frac{1}{2}^-$	$\lvert 0,1,0,0\rangle$	$^2P_{1/2}$	9.3	57.5	0	0	0	0	0	0	0	0	0	0	0	0	66.8
$\Lambda_b(6137)$	$\frac{1}{2}^-$	$\lvert 0,1,0,0\rangle$	$^4P_{1/2}$	4.2	31.3	0	0	0	0	0	0	0	0	0	0	0	0	35.5
$\Lambda_b(6121)$	$\frac{3}{2}^-$	$\lvert 0,1,0,0\rangle$	$^2P_{3/2}$	76.9	7.8	0	0	0	0	0	0	0	0	0	0	0	0	84.7
$\Lambda_b(6143)$	$\frac{3}{2}^-$	$\lvert 0,1,0,0\rangle$	$^4P_{3/2}$	4.2	123.6	0	0	0	0	0	0	0	0	0	0	0	0	127.8
$\Lambda_b(6153)$	$\frac{5}{2}^-$	$\lvert 0,1,0,0\rangle$	$^4P_{5/2}$	26.4	47.9	0	0	0	0	0	0	0	0	0	0	0	0	74.3
$N=2$																		
$\Lambda_b(6225)$	$\frac{3}{2}^+$	$\lvert 2,0,0,0\rangle$	$^2D_{3/2}$	1.4	8.3	...	0	0	0	0	0	0	0	0	0	0	3.3	13.0
$\Lambda_b(6235)$	$\frac{5}{2}^+$	$\lvert 2,0,0,0\rangle$	$^2D_{5/2}$	3.1	1.2	...	0	0	0	0	0	0	0	0	0	0	13.2	17.5
$\Lambda_b(6231)$	$\frac{1}{2}^+$	$\lvert 0,0,1,0\rangle$	$^2S_{1/2}$	6.2	11.1	...	0	0	0	0	0	0	0	0	0	0	11.5	28.9
$\Lambda_b(6624)$	$\frac{1}{2}^+$	$\lvert 0,0,0,1\rangle$	$^2S_{1/2}$	9.3	24.2	...	27.0	2.6	...	48.7	...	13.0	5.6	0	0	0	...	130.5
$\Lambda_b(6421)$	$\frac{3}{2}^+$	$\lvert 1,1,0,0\rangle$	$^2D_{3/2}$	11.4	48.7	1.3	0	0	0	3.2	2.5	0	0	0	0	0	...	67.1
$\Lambda_b(6431)$	$\frac{5}{2}^+$	$\lvert 1,1,0,0\rangle$	$^2D_{5/2}$	81.4	8.0	8.3	0	0	0	0.7	9.4	0.3	0	0	0	0	...	108.1
$\Lambda_b(6438)$	$\frac{1}{2}^+$	$\lvert 1,1,0,0\rangle$	$^4D_{1/2}$	2.2	23.5	1.1	0	0	0	3.3	4.3	0.1	0	0	0	0	...	34.5
$\Lambda_b(6444)$	$\frac{3}{2}^+$	$\lvert 1,1,0,0\rangle$	$^4D_{3/2}$	2.8	75.5	1.2	0	0	0	12.5	2.9	0.1	0	0	0	0	...	95.0
$\Lambda_b(6454)$	$\frac{5}{2}^+$	$\lvert 1,1,0,0\rangle$	$^4D_{5/2}$	9.0	95.1	3.7	0	0	0	15.6	4.5	0.1	0	0	0	0	...	128.0
$\Lambda_b(6468)$	$\frac{7}{2}^+$	$\lvert 1,1,0,0\rangle$	$^4D_{7/2}$	29.1	59.4	12.1	0	0	0	4.8	16.3	0.7	0	0	0	0	...	122.4
$\Lambda_b(6423)$	$\frac{1}{2}^-$	$\lvert 1,1,0,0\rangle$	$^2P_{1/2}$	0	0.5	0	0	0	0	0	0	0	0	0	0	0	...	0.5
$\Lambda_b(6429)$	$\frac{3}{2}^-$	$\lvert 1,1,0,0\rangle$	$^2P_{3/2}$	1.2	0.3	0.1	0	0	0	0	0.1	0	0	0	0	0	...	1.7
$\Lambda_b(6446)$	$\frac{1}{2}^-$	$\lvert 1,1,0,0\rangle$	$^4P_{1/2}$	0	0.3	0	0	0	0	0	0	0	0	0	0	0	...	0.3
$\Lambda_b(6452)$	$\frac{3}{2}^-$	$\lvert 1,1,0,0\rangle$	$^4P_{3/2}$	0.1	1.0	0	0	0	0	0.1	0	0	0	0	0	0	...	1.2
$\Lambda_b(6462)$	$\frac{5}{2}^-$	$\lvert 1,1,0,0\rangle$	$^4P_{5/2}$	0.4	1.3	0.2	0	0	0	0.2	0.2	0	0	0	0	0	...	2.3
$\Lambda_b(6456)$	$\frac{3}{2}^+$	$\lvert 1,1,0,0\rangle$	$^4S_{3/2}$	2.3	14.1	1.1	0	0	0	8.2	5.8	0.3	0	0	0	0	...	31.8
$\Lambda_b(6427)$	$\frac{1}{2}^+$	$\lvert 1,1,0,0\rangle$	$^2S_{1/2}$	12.2	7.0	1.5	0	0	0	3.5	5.2	0	0	0	0	0	...	29.4
$\Lambda_b(6618)$	$\frac{3}{2}^+$	$\lvert 0,2,0,0\rangle$	$^2D_{3/2}$	21.5	53.1	...	9.3	0.1	...	40.7	...	3.1	3.6	0	0	0	...	131.4
$\Lambda_b(6628)$	$\frac{5}{2}^+$	$\lvert 0,2,0,0\rangle$	$^2D_{5/2}$	52.9	93.0	...	1.0	1.1	...	29.2	...	7.5	0.5	0	0	0	...	185.2

TABLE 2.19: *Table from [90] (APS copyright).* Same as 2.18, but for $\Xi_b(snb)$ states.

$\mathcal{F}=\bar{\mathbf{3}}_{\mathrm{F}}$				$\Lambda_b K$	$\Xi_b\pi$	$\Xi_b'\pi$	$\Xi_b^*\pi$	$\Sigma_b K$	$\Sigma_b^* K$	$\Xi_b\eta$	$\Lambda_b K^*$	$\Xi_b\rho$	$\Xi_b'\rho$	$\Xi_b^*\rho$	$\Sigma_b K^*$	$\Sigma_b^* K^*$	$\Xi_b'\eta$	$\Xi_b^*\eta$	$\Xi_b\eta'$	$\Xi_b'\eta'$	$\Xi_b^*\eta'$	$\Xi_b\omega$	$\Xi_b'\omega$	$\Xi_b^*\omega$	$\Xi_b\phi$	$\Xi_b'\phi$	$\Xi_b^*\phi$	$\Lambda_8 B$	$\Lambda_8 B^*$	$\Sigma_8 B$	$\Lambda_8^* B$	Γ^{Strong}
$\Xi_b(snb)$	$\mathbf{J}^P$	$\lvert l_\lambda,l_\rho,k_\lambda,k_\rho\rangle$	$^{2S+1}L_J$	MeV	MeV	MeV	MeV	MeV	MeV	MeV	MeV	MeV	MeV	MeV	MeV	MeV	MeV	MeV	MeV	MeV	MeV	MeV	MeV	MeV	MeV	MeV	MeV	MeV	MeV	MeV	MeV	MeV
$N=0$																																
$\Xi_b(5806)$	$\frac{1}{2}^+$	$\lvert 0,0,0,0\rangle$	$^2S_{1/2}$	0	0	0	0	0	0	0	0	0	0	0	0	0	0	0	0	0	0	0	0	0	0	0	0	0	0	0	0	0
$N=1$																																
$\Xi_b(6079)$	$\frac{1}{2}^-$	$\lvert 1,0,0,0\rangle$	$^2P_{1/2}$	0	0	0.2	0	0	0	0	0	0	0	0	0	0	0	0	0	0	0	0	0	0	0	0	0	0	0	0	0	0.2
$\Xi_b(6085)$	$\frac{3}{2}^-$	$\lvert 1,0,0,0\rangle$	$^2P_{3/2}$	0	0	1.1	0	0	0	0	0	0	0	0	0	0	0	0	0	0	0	0	0	0	0	0	0	0	0	0	0	1.1
$\Xi_b(6248)$	$\frac{1}{2}^-$	$\lvert 0,1,0,0\rangle$	$^2P_{1/2}$	1.0	0.4	2.5	4.8	0	0	0	0	0	0	0	0	0	0	0	0	0	0	0	0	0	0	0	0	0	0	0	0	8.7
$\Xi_b(6271)$	$\frac{1}{2}^-$	$\lvert 0,1,0,0\rangle$	$^4P_{1/2}$	1.1	0.3	1.1	3.5	0	0	0	0	0	0	0	0	0	0	0	0	0	0	0	0	0	0	0	0	0	0	0	0	6.0
$\Xi_b(6255)$	$\frac{3}{2}^-$	$\lvert 0,1,0,0\rangle$	$^2P_{3/2}$	21.1	23.7	20.5	0.6	0	0	0	0	0	0	0	0	0	0	0	0	0	0	0	0	0	0	0	0	0	0	0	0	65.9
$\Xi_b(6277)$	$\frac{3}{2}^-$	$\lvert 0,1,0,0\rangle$	$^4P_{3/2}$	4.4	5.0	1.1	15.6	0	0	0	0	0	0	0	0	0	0	0	0	0	0	0	0	0	0	0	0	0	0	0	0	26.1
$\Xi_b(6287)$	$\frac{5}{2}^-$	$\lvert 0,1,0,0\rangle$	$^4P_{5/2}$	26.9	30.5	7.0	4.1	0	0	0	0	0	0	0	0	0	0	0	0	0	0	0	0	0	0	0	0	0	0	0	0	68.5
$N=2$																																
$\Xi_b(6354)$	$\frac{3}{2}^+$	$\lvert 2,0,0,0\rangle$	$^2D_{3/2}$	$\cdots$	$\cdots$	0.3	0.5	0.2	0.8	$\cdots$	0	0	0	0	0	0	0	0	0	0	0	0	0	0	0	0	0	0	0	0	0	1.8
$\Xi_b(6364)$	$\frac{5}{2}^+$	$\lvert 2,0,0,0\rangle$	$^2D_{5/2}$	$\cdots$	$\cdots$	0.8	0.1	0.6	0.1	$\cdots$	0	0	0	0	0	0	0	0	0	0	0	0	0	0	0	0	0	0	0	0	0	1.6
$\Xi_b(6360)$	$\frac{1}{2}^+$	$\lvert 0,0,1,0\rangle$	$^2S_{1/2}$	$\cdots$	$\cdots$	1.7	0.9	1.4	1.4	$\cdots$	0	0	0	0	0	0	0	0	0	0	0	0	0	0	0	0	0	0	0	0	0	5.4
$\Xi_b(6699)$	$\frac{1}{2}^+$	$\lvert 0,0,0,1\rangle$	$^2S_{1/2}$	$\cdots$	$\cdots$	7.2	20.6	18.9	41.8	$\cdots$	34.8	40.1	0	0	0	0	1.4	0.9	0	0	0	12.9	0	0	0	0	0	$\cdots$	$\cdots$	$\cdots$	0	178.8
$\Xi_b(6524)$	$\frac{3}{2}^+$	$\lvert 1,1,0,0\rangle$	$^2D_{3/2}$	1.6	2.1	3.1	6.4	7.7	23.6	0.3	1.0	0	0	0	0	0	0.1	0	0	0	0	0	0	0	0	0	0	$\cdots$	$\cdots$	$\cdots$	0	45.9
$\Xi_b(6534)$	$\frac{5}{2}^+$	$\lvert 1,1,0,0\rangle$	$^2D_{5/2}$	21.2	24.4	19.3	0.6	37.6	2.3	1.4	0.3	0	0	0	0	0	0.3	0	0	0	0	0	0	0	0	0	0	$\cdots$	$\cdots$	$\cdots$	0	107.4
$\Xi_b(6540)$	$\frac{1}{2}^+$	$\lvert 1,1,0,0\rangle$	$^4D_{1/2}$	0.1	0.5	0.9	3.1	2.7	11.1	0.5	1.3	0	0	0	0	0	0.1	0	0	0	0	0	0	0	0	0	0	$\cdots$	$\cdots$	$\cdots$	0	20.3
$\Xi_b(6546)$	$\frac{3}{2}^+$	$\lvert 1,1,0,0\rangle$	$^4D_{3/2}$	1.6	2.0	0.8	12.2	2.0	42.7	0.3	5.3	0	0	0	0	0	0	0	0	0	0	0	0	0	0	0	0	$\cdots$	$\cdots$	$\cdots$	0	66.9
$\Xi_b(6556)$	$\frac{5}{2}^+$	$\lvert 1,1,0,0\rangle$	$^4D_{5/2}$	8.9	10.2	2.0	14.8	4.0	52.3	0.6	7.3	0	0	0	0	0	0	0	0	0	0	0	0	0	0	0	0	$\cdots$	$\cdots$	$\cdots$	0	100.1
$\Xi_b(6570)$	$\frac{7}{2}^+$	$\lvert 1,1,0,0\rangle$	$^4D_{7/2}$	29.8	34.2	7.0	4.3	14.4	19.5	2.2	2.2	0	0	0	0	0	0.2	0	0	0	0	0	0	0	0	0	0	$\cdots$	$\cdots$	$\cdots$	0	113.8
$\Xi_b(6526)$	$\frac{1}{2}^-$	$\lvert 1,1,0,0\rangle$	$^2P_{1/2}$	0	0	0	0.1	0	0.2	0	0	0	0	0	0	0	0	0	0	0	0	0	0	0	0	0	0	$\cdots$	$\cdots$	$\cdots$	0	0.3
$\Xi_b(6532)$	$\frac{3}{2}^-$	$\lvert 1,1,0,0\rangle$	$^2P_{3/2}$	0.4	0.5	0.3	0	0.6	0.1	0	0	0	0	0	0	0	0	0	0	0	0	0	0	0	0	0	0	$\cdots$	$\cdots$	$\cdots$	0	1.9
$\Xi_b(6548)$	$\frac{1}{2}^-$	$\lvert 1,1,0,0\rangle$	$^4P_{1/2}$	0	0	0	0	0	0.1	0	0	0	0	0	0	0	0	0	0	0	0	0	0	0	0	0	0	$\cdots$	$\cdots$	$\cdots$	0	0.1
$\Xi_b(6554)$	$\frac{3}{2}^-$	$\lvert 1,1,0,0\rangle$	$^4P_{3/2}$	0.1	0.1	0	0.1	0	0.5	0	0.1	0	0	0	0	0	0	0	0	0	0	0	0	0	0	0	0	$\cdots$	$\cdots$	$\cdots$	0	0.9
$\Xi_b(6564)$	$\frac{5}{2}^-$	$\lvert 1,1,0,0\rangle$	$^4P_{5/2}$	0.5	0.6	0.1	0.2	0.2	0.7	0	0.1	0	0	0	0	0	0	0	0	0	0	0	0	0	0	0	0	$\cdots$	$\cdots$	$\cdots$	0	2.4
$\Xi_b(6558)$	$\frac{3}{2}^+$	$\lvert 1,1,0,0\rangle$	$^4S_{3/2}$	0	0.3	1.1	6.1	3.3	17.2	0.6	4.0	0	0	0	0	0	0.1	0	0	0	0	0	0	0	0	0	0	$\cdots$	$\cdots$	$\cdots$	0	32.7
$\Xi_b(6530)$	$\frac{1}{2}^+$	$\lvert 1,1,0,0\rangle$	$^2S_{1/2}$	0.2	0.9	4.8	2.2	13.9	7.0	0.6	1.3	0	0	0	0	0	0.2	0	0	0	0	0	0	0	0	0	0	$\cdots$	$\cdots$	$\cdots$	0	31.1
$\Xi_b(6693)$	$\frac{3}{2}^+$	$\lvert 0,2,0,0\rangle$	$^2D_{3/2}$	$\cdots$	$\cdots$	4.2	17.3	9.1	42.9	$\cdots$	22.8	22.9	0	0	0	0	0.3	0.6	0	0	0	7.3	0	0	0	0	0	$\cdots$	$\cdots$	$\cdots$	0	127.4
$\Xi_b(6703)$	$\frac{5}{2}^+$	$\lvert 0,2,0,0\rangle$	$^2D_{5/2}$	$\cdots$	$\cdots$	11.3	6.3	24.9	30.4	$\cdots$	12.6	8.4	0	0	0	0	0.8	0.1	0	0	0	2.6	0	0	0	0	0	$\cdots$	$\cdots$	$\cdots$	0	97.4

TABLE 2.20: *Table from [90] (APS copyright).* Predicted $\Sigma_b(nnb)$ strong partial decay widths (in MeV). The flavor multiplet is denoted by the symbol $\mathcal{F}$. The first column reports the baryon name with its predicted mass, calculated by using the three-quark model Hamiltonian given by Eqs. 2.44 and 2.45. The second column displays $\mathbf{J}^{\mathrm{P}}$, the third column shows the three-quark model state, $|l_\lambda, l_\rho, k_\lambda, k_\rho\rangle$, where $l_{\lambda,\rho}$ represent the orbital angular momenta and $k_{\lambda,\rho}$ denote the number of nodes of the λ and ρ oscillators. The fourth column presents the spectroscopic notation $^{2S+1}L_J$. The value of $N = n_\rho + n_\lambda$ distinguishes the $N = 0, 1, 2$ energy bands. Starting from the fifth column, we provide the strong partial decay widths calculated using eq. (2.68). Each column corresponds to an open flavor strong decay channel, and the specific decay channels are indicated at the top of each column. The masses of the decay products are given in Table 2.12. The values for the strong decay widths are given in MeV. The decay widths denoted by 0 are either too small to be shown in this scale or forbidden by phase space, while the decay widths denoted by the symbol "..." are forbidden by selection rules. Finally, the last column represents the sum of the strong partial decay widths over all the decay channels. N_1^*, N_2^*, N_3^*, and N_4^* represent $N(1520)$, $N(1535)$, $N(1680)$, and $N(1720)$, respectively.

$\mathcal{F} = \mathbf{6}_{\mathrm{F}}$				$\Sigma_b\pi$	$\Sigma_b^*\pi$	$\Lambda_b\pi$	$\Sigma_b\eta$	Ξ_bK	$\Sigma_b\rho$	$\Sigma_b^*\rho$	$\Lambda_b\rho$	$\Sigma_b^*\eta$	$\Sigma_b\eta'$	$\Sigma_b^*\eta'$	$\Xi_b'K$	Ξ_b^*K	Ξ_bK^*	$\Xi_b'K^*$	$\Xi_b^*K^*$	$\Sigma_b\omega$	$\Sigma_b^*\omega$	NB	Σ_8B_s	NB^*	ΔB	N_1^*B	N_2^*B	N_3^*B	N_4^*B	Γ^{Strong}
$\Sigma_b(nnb)$	$\mathbf{J}^P$	$\lvert l_\lambda, l_\rho, k_\lambda, k_\rho\rangle$	$^{2S+1}L_J$	MeV	MeV	MeV	MeV	MeV	MeV	MeV	MeV	MeV	MeV	MeV	MeV	MeV	MeV	MeV	MeV	MeV	MeV	MeV	MeV	MeV	MeV	MeV	MeV	MeV	MeV	MeV
$N=0$																														
$\Sigma_b(5804)$	$\frac{1}{2}^+$	$\lvert 0,0,0,0\rangle$	$^2S_{1/2}$	0	0	3.9	0	0	0	0	0	0	0	0	0	0	0	0	0	0	0	0	0	0	0	0	0	0	0	3.9
$\Sigma_b(5832)$	$\frac{3}{2}^+$	$\lvert 0,0,0,0\rangle$	$^4S_{3/2}$	0	0	10.0	0	0	0	0	0	0	0	0	0	0	0	0	0	0	0	0	0	0	0	0	0	0	0	10.0
$N=1$																														
$\Sigma_b(6108)$	$\frac{1}{2}^-$	$\lvert 1,0,0,0\rangle$	$^2P_{1/2}$	3.4	20.1	0	0	0	0	0	0	0	0	0	0	0	0	0	0	0	0	0	0	0	0	0	0	0	0	23.5
$\Sigma_b(6131)$	$\frac{1}{2}^-$	$\lvert 1,0,0,0\rangle$	$^4P_{1/2}$	1.6	11.1	0.5	0	0	0	0	0	0	0	0	0	0	0	0	0	0	0	0	0	0	0	0	0	0	0	0	13.2
$\Sigma_b(6114)$	$\frac{3}{2}^-$	$\lvert 1,0,0,0\rangle$	$^2P_{3/2}$	27.2	2.7	54.0	0	0	0	0	0	0	0	0	0	0	0	0	0	0	0	0	0	0	0	0	0	0	0	0	83.9
$\Sigma_b(6137)$	$\frac{3}{2}^-$	$\lvert 1,0,0,0\rangle$	$^4P_{3/2}$	1.5	44.1	11.3	0	0	0	0	0	0	0	0	0	0	0	0	0	0	0	0	0	0	0	0	0	0	0	0	56.9
$\Sigma_b(6147)$	$\frac{5}{2}^-$	$\lvert 1,0,0,0\rangle$	$^4P_{5/2}$	9.4	16.7	69.8	0	0	0	0	0	0	0	0	0	0	0	0	0	0	0	0	0	0	0	0	0	0	0	0	95.9
$\Sigma_b(6304)$	$\frac{1}{2}^-$	$\lvert 0,1,0,0\rangle$	$^2P_{1/2}$	0.1	134.1	...	0	...	0	0	0	0	0	0	0	0	0	0	0	0	0	0	...	0	...	0	0	0	0	0	134.2
$\Sigma_b(6311)$	$\frac{3}{2}^-$	$\lvert 0,1,0,0\rangle$	$^2P_{3/2}$	67.1	62.2	...	0	...	0	0	0	0	0	0	0	0	0	0	0	0	0	0	...	0	...	0	0	0	0	0	129.3
$N=2$																														
$\Sigma_b(6415)$	$\frac{3}{2}^+$	$\lvert 2,0,0,0\rangle$	$^2D_{3/2}$	2.7	4.2	6.0	0.1	0.6	0	0	1.0	0.1	0	0	0	0	0	0	0	0	0	0	4.3	0	38.6	0	0	0	0	0	57.6
$\Sigma_b(6425)$	$\frac{5}{2}^+$	$\lvert 2,0,0,0\rangle$	$^2D_{5/2}$	7.3	1.5	15.1	0.3	1.3	0	0	0.1	0	0	0	0	0	0	0	0	0	0	0	11.0	0	93.3	0	0	0	0	0	129.9
$\Sigma_b(6431)$	$\frac{1}{2}^+$	$\lvert 2,0,0,0\rangle$	$^4D_{1/2}$	0.1	6.7	2.2	0	0.5	0	0	2.3	0.2	0	0	0	0	0	0	0	0	0	0	4.5	0	61.3	0	0	0	0	0	77.8
$\Sigma_b(6437)$	$\frac{3}{2}^+$	$\lvert 2,0,0,0\rangle$	$^4D_{3/2}$	0.7	7.3	6.6	0	0.7	0	0	5.0	0.4	0	0	0	0	0	0	0	0	0	0	18.7	0	66.5	0	0	0	0	0	105.9
$\Sigma_b(6448)$	$\frac{5}{2}^+$	$\lvert 2,0,0,0\rangle$	$^4D_{5/2}$	1.6	6.6	12.5	0.1	1.2	0	0	4.1	0.4	0	0	0	0	0	0	0	0	0	0	39.1	0	67.1	0	0	0	0	0	132.7
$\Sigma_b(6462)$	$\frac{7}{2}^+$	$\lvert 2,0,0,0\rangle$	$^4D_{7/2}$	2.2	7.8	18.5	0.1	2.0	0	0	2.5	0.2	0	0	0.1	0	0	0	0	0	0	0	55.8	0	56.0	0	0	0	0	0	145.2
$\Sigma_b(6421)$	$\frac{1}{2}^+$	$\lvert 0,0,1,0\rangle$	$^2S_{1/2}$	8.5	4.3	3.2	0.6	2.8	0	0	3.3	0.2	0	0	0	0	0	0	0	0	0	0	7.9	0	88.4	0	0	0	0	0	119.2
$\Sigma_b(6450)$	$\frac{3}{2}^+$	$\lvert 0,0,1,0\rangle$	$^4S_{3/2}$	2.0	10.5	2.0	0.2	3.4	0	0	8.6	0.9	0	0	0.1	0	0	0	0	0	0	0	28.6	0	64.8	0	0	0	0	0	121.2
$\Sigma_b(6813)$	$\frac{1}{2}^+$	$\lvert 0,0,0,1\rangle$	$^2S_{1/2}$	5.5	1.5	81.7	0.9	0.4	357.9	6.0	1.3	0.7	7.4	1.8	11.1	9.4	36.4	0	0	184.2	3.1	...	...	...	...	...	...	0	0	709.8
$\Sigma_b(6842)$	$\frac{3}{2}^+$	$\lvert 0,0,0,1\rangle$	$^4S_{3/2}$	2.7	8.7	100.0	0.1	0	18.1	497.3	0.1	0.9	3.1	11.4	2.1	23.2	38.7	0.8	0	9.4	256.9	...	...	...	...	...	...	0	0	973.5
$\Sigma_b(6611)$	$\frac{3}{2}^+$	$\lvert 1,1,0,0\rangle$	$^2D_{3/2}$	7.0	117.8	...	1.3	...	9.0	0.1	209.2	20.1	0	0	3.3	5.1	0	0	0	3.3	0	...	...	...	...	...	0	0	0	376.2
$\Sigma_b(6621)$	$\frac{5}{2}^+$	$\lvert 1,1,0,0\rangle$	$^2D_{5/2}$	77.8	77.0	...	8.3	...	1.7	1.1	66.6	2.9	0	0	14.6	0.5	0	0	0	0.7	0.4	...	...	...	...	...	0	0	0	251.6
$\Sigma_b(6613)$	$\frac{1}{2}^-$	$\lvert 1,1,0,0\rangle$	$^2P_{1/2}$	0	2.2	...	0	...	0	0	1.8	0.2	0	0	0	0	0	0	0	0	0	...	...	...	...	...	0	0	0	4.2
$\Sigma_b(6619)$	$\frac{3}{2}^-$	$\lvert 1,1,0,0\rangle$	$^2P_{3/2}$	1.2	1.1	...	0.1	...	0	0	1.9	0.1	0	0	0.2	0	0	0	0	0	0	...	...	...	...	...	0	0	0	4.6
$\Sigma_b(6617)$	$\frac{1}{2}^+$	$\lvert 1,1,0,0\rangle$	$^2S_{1/2}$	2.0	1.5	...	1.5	...	9.0	1.0	26.2	3.5	0	0	6.1	2.9	0	0	0	3.5	0.3	...	...	...	...	...	0	0	0	57.5
$\Sigma_b(6807)$	$\frac{3}{2}^+$	$\lvert 0,2,0,0\rangle$	$^2D_{3/2}$	49.8	3.7	120.5	4.3	11.8	213.3	0.4	2.2	2.1	1.4	1.2	8.0	8.4	13.6	0	0	108.3	0.2	...	...	...	...	...	...	0	0	549.2
$\Sigma_b(6817)$	$\frac{5}{2}^+$	$\lvert 0,2,0,0\rangle$	$^2D_{5/2}$	85.6	54.0	160.6	10.1	25.4	116.2	1.4	73.8	4.7	3.6	0.2	21.8	2.4	0.9	0	0	54.9	0.7	...	...	...	...	...	...	0	0	616.3
$\Sigma_b(6824)$	$\frac{1}{2}^+$	$\lvert 0,2,0,0\rangle$	$^4D_{1/2}$	17.2	15.6	213.5	0.7	10.6	13.2	676.3	13.9	5.0	0.4	2.8	0.2	13.4	18.5	0	0	6.6	340.9	...	...	...	...	...	...	0	0	1348.8
$\Sigma_b(6830)$	$\frac{3}{2}^+$	$\lvert 0,2,0,0\rangle$	$^4D_{3/2}$	14.0	4.2	130.3	1.2	13.5	25.2	291.0	38.8	2.4	0.6	4.9	2.2	15.4	35.7	0	0	12.7	148.4	...	...	...	...	...	...	0	0	740.5
$\Sigma_b(6840)$	$\frac{5}{2}^+$	$\lvert 0,2,0,0\rangle$	$^4D_{5/2}$	13.6	75.2	77.8	2.0	19.0	15.4	29.5	66.0	6.9	1.0	5.1	4.7	13.4	22.1	0.7	0	7.7	15.6	...	...	...	...	...	...	0	0	375.7
$\Sigma_b(6854)$	$\frac{7}{2}^+$	$\lvert 0,2,0,0\rangle$	$^4D_{7/2}$	27.8	173.6	211.6	3.2	32.3	32.3	235.6	267.6	18.6	1.9	2.5	6.6	14.1	24.8	0.6	0	15.6	109.8	...	...	...	...	...	...	0	0	1178.5

TABLE 2.21: *Table from [90] (APS copyright).* Same as 2.18, but for $\Xi_b'(snb)$ states.

$\mathcal{F}=\mathbf{6}_\mathrm{F}$				$\Lambda_b K$	$\Xi_b\pi$	$\Xi_b'\pi$	$\Xi_b^*\pi$	$\Sigma_b K$	$\Sigma_b^* K$	$\Xi_b\eta$	$\Lambda_b K^*$	$\Xi_b\rho$	$\Xi_b'\rho$	$\Xi_b^*\rho$	$\Sigma_b K^*$	$\Sigma_b^* K^*$	$\Xi_b'\eta$	$\Xi_b^*\eta$	$\Xi_b\eta'$	$\Xi_b'\eta'$	$\Xi_b^*\eta'$	$\Xi_b\omega$	$\Xi_b'\omega$	$\Xi_b^*\omega$	$\Xi_b\phi$	$\Xi_b'\phi$	$\Xi_b^*\phi$	$\Sigma_8 B$	$\Xi_8 B_s$	$\Sigma_8 B^*$	$\Sigma_{10} B$	Γ^{Strong}
$\Xi_b'(snb)$	$\mathbf{J}^P$	$\lvert l_\lambda,l_\rho,k_\lambda,k_\rho\rangle$	$^{2S+1}L_J$	MeV	MeV	MeV	MeV	MeV	MeV	MeV	MeV	MeV	MeV	MeV	MeV	MeV	MeV	MeV	MeV	MeV	MeV	MeV	MeV	MeV	MeV	MeV	MeV	MeV	MeV	MeV	MeV	MeV	MeV
$N=0$																																	
$\Xi_b'(5925)$	$\frac{1}{2}^+$	$\lvert 0,0,0,0\rangle$	$^2S_{1/2}$	0	0	0	0	0	0	0	0	0	0	0	0	0	0	0	0	0	0	0	0	0	0	0	0	0	0	0	0	0	0
$\Xi_b'(5953)$	$\frac{3}{2}^+$	$\lvert 0,0,0,0\rangle$	$^4S_{3/2}$	0	0.2	0	0	0	0	0	0	0	0	0	0	0	0	0	0	0	0	0	0	0	0	0	0	0	0	0	0	0	0.2
$N=1$																																	
$\Xi_b'(6198)$	$\frac{1}{2}^-$	$\lvert 1,0,0,0\rangle$	$^2P_{1/2}$	1.1	0.5	1.4	0	0	0	0	0	0	0	0	0	0	0	0	0	0	0	0	0	0	0	0	0	0	0	0	0	0	3.0
$\Xi_b'(6220)$	$\frac{1}{2}^-$	$\lvert 1,0,0,0\rangle$	$^4P_{1/2}$	1.8	0.8	0.7	0.4	0	0	0	0	0	0	0	0	0	0	0	0	0	0	0	0	0	0	0	0	0	0	0	0	0	0	3.7
$\Xi_b'(6204)$	$\frac{3}{2}^-$	$\lvert 1,0,0,0\rangle$	$^2P_{3/2}$	9.9	11.2	8.4	0	0	0	0	0	0	0	0	0	0	0	0	0	0	0	0	0	0	0	0	0	0	0	0	0	0	0	29.5
$\Xi_b'(6226)$	$\frac{3}{2}^-$	$\lvert 1,0,0,0\rangle$	$^4P_{3/2}$	2.1	2.4	0.5	2.6	0	0	0	0	0	0	0	0	0	0	0	0	0	0	0	0	0	0	0	0	0	0	0	0	0	0	7.6
$\Xi_b'(6237)$	$\frac{5}{2}^-$	$\lvert 1,0,0,0\rangle$	$^4P_{5/2}$	13.0	14.6	3.0	0.8	0	0	0	0	0	0	0	0	0	0	0	0	0	0	0	0	0	0	0	0	0	0	0	0	0	0	31.4
$\Xi_b'(6367)$	$\frac{1}{2}^-$	$\lvert 0,1,0,0\rangle$	$^2P_{1/2}$	$\cdots$	$\cdots$	0.6	44.8	7.2	144.0	$\cdots$	0	0	0	0	0	0	0	0	0	0	0	0	0	0	0	0	0	0	0	0	0	0	0	196.6
$\Xi_b'(6374)$	$\frac{3}{2}^-$	$\lvert 0,1,0,0\rangle$	$^2P_{3/2}$	$\cdots$	$\cdots$	22.8	6.1	50.1	18.2	$\cdots$	0	0	0	0	0	0	0	0	0	0	0	0	0	0	0	0	0	0	0	0	0	0	0	97.2
$N=2$																																	
$\Xi_b'(6473)$	$\frac{3}{2}^+$	$\lvert 2,0,0,0\rangle$	$^2D_{3/2}$	0.8	0.9	0.8	0.7	1.6	2.4	0.1	0	0	0	0	0	0	0	0	0	0	0	0	0	0	0	0	0	0	1.6	0	4.8	0	13.7
$\Xi_b'(6483)$	$\frac{5}{2}^+$	$\lvert 2,0,0,0\rangle$	$^2D_{5/2}$	2.2	2.5	2.0	0.1	3.6	0.4	0.1	0	0	0	0	0	0	0	0	0	0	0	0	0	0	0	0	0	0	3.6	0	15.7	0	30.2
$\Xi_b'(6489)$	$\frac{1}{2}^+$	$\lvert 2,0,0,0\rangle$	$^4D_{1/2}$	0	0	0.1	1.0	0.3	3.6	0	0	0	0	0	0	0	0	0	0	0	0	0	0	0	0	0	0	0	6.2	0	13.5	0	24.7
$\Xi_b'(6495)$	$\frac{3}{2}^+$	$\lvert 2,0,0,0\rangle$	$^4D_{3/2}$	0.9	1.0	0.2	1.4	0.5	5.1	0.1	0	0	0	0	0	0	0	0	0	0	0	0	0	0	0	0	0	0	8.5	0	17.7	0	35.4
$\Xi_b'(6506)$	$\frac{5}{2}^+$	$\lvert 2,0,0,0\rangle$	$^4D_{5/2}$	1.9	2.2	0.4	1.3	0.8	4.5	0.1	0	0	0	0	0	0	0	0	0	0	0	0	0	0	0	0	0	0	14.2	0	20.9	0	46.3
$\Xi_b'(6520)$	$\frac{7}{2}^+$	$\lvert 2,0,0,0\rangle$	$^4D_{7/2}$	2.6	3.0	0.6	0.6	1.3	2.4	0.2	0.1	0	0	0	0	0	0	0	0	0	0	0	0	0	0	0	0	0	24.6	0	11.4	0	46.8
$\Xi_b'(6479)$	$\frac{1}{2}^+$	$\lvert 0,0,1,0\rangle$	$^2S_{1/2}$	2.1	2.8	3.7	0.9	7.8	3.5	0.3	0	0	0	0	0	0	0	0	0	0	0	0	0	0	0	0	0	0	5.0	0	21.2	0	47.4
$\Xi_b'(6508)$	$\frac{3}{2}^+$	$\lvert 0,0,1,0\rangle$	$^4S_{3/2}$	1.8	2.6	0.9	2.9	2.2	10.2	0.3	0	0	0	0	0	0	0	0	0	0	0	0	0	0	0	0	0	0	26.2	0	31.7	0	79
$\Xi_b'(6818)$	$\frac{1}{2}^+$	$\lvert 0,0,0,1\rangle$	$^2S_{1/2}$	1.9	0.2	3.0	5.4	7.4	5.1	0.4	12.7	29.7	133.6	0	331.3	4.5	1.7	0.9	8.5	0	0	10.1	42.3	0	0.1	0	0	$\cdots$	$\cdots$	$\cdots$	$\cdots$	599
$\Xi_b'(6847)$	$\frac{3}{2}^+$	$\lvert 0,0,0,1\rangle$	$^4S_{3/2}$	3.4	0.9	0.4	11.7	1.0	7.8	0.2	9.0	26.5	9.4	0	22.2	504.4	0.4	2.4	12.2	0	0	9.1	3.1	0	5.8	0	0	$\cdots$	$\cdots$	$\cdots$	$\cdots$	630.2
$\Xi_b'(6642)$	$\frac{3}{2}^+$	$\lvert 1,1,0,0\rangle$	$^2D_{3/2}$	$\cdots$	$\cdots$	2.1	35.8	5.4	113.8	$\cdots$	43.4	25.7	0	0	0	0	0.3	0.2	0	0	0	7.5	0	0	0	0	0	$\cdots$	0	$\cdots$	0	234.2
$\Xi_b'(6653)$	$\frac{5}{2}^+$	$\lvert 1,1,0,0\rangle$	$^2D_{5/2}$	$\cdots$	$\cdots$	22.9	4.4	49.4	21.7	$\cdots$	9.1	5.3	0	0	0	0	1.2	0	0	0	0	1.6	0	0	0	0	0	$\cdots$	0	$\cdots$	0	115.6
$\Xi_b'(6644)$	$\frac{1}{2}^-$	$\lvert 1,1,0,0\rangle$	$^2P_{1/2}$	$\cdots$	$\cdots$	0	0.4	0	1.6	$\cdots$	0.3	0.2	0	0	0	0	0	0	0	0	0	0.1	0	0	0	0	0	$\cdots$	0	$\cdots$	0	2.6
$\Xi_b'(6651)$	$\frac{3}{2}^-$	$\lvert 1,1,0,0\rangle$	$^2P_{3/2}$	$\cdots$	$\cdots$	0.4	0.2	0.9	0.8	$\cdots$	0.4	0.2	0	0	0	0	0	0	0	0	0	0.1	0	0	0	0	0	$\cdots$	0	$\cdots$	0	3.0
$\Xi_b'(6649)$	$\frac{1}{2}^+$	$\lvert 1,1,0,0\rangle$	$^2S_{1/2}$	$\cdots$	$\cdots$	1.3	7.7	4.9	12.6	$\cdots$	14.5	13.2	0	0	0	0	0.6	0.1	0	0	0	4.0	0	0	0	0	0	$\cdots$	0	$\cdots$	0	58.9
$\Xi_b'(6812)$	$\frac{3}{2}^+$	$\lvert 0,2,0,0\rangle$	$^2D_{3/2}$	13.5	13.7	9.3	5.9	20.4	10.0	0.8	4.1	10.0	57.7	0	145.2	0.1	0.6	0.7	1.5	0	0	3.4	18.1	0	0	0	0	$\cdots$	$\cdots$	$\cdots$	$\cdots$	315.0
$\Xi_b'(6822)$	$\frac{5}{2}^+$	$\lvert 0,2,0,0\rangle$	$^2D_{5/2}$	22.0	24.8	21.8	5.0	48.6	23.0	2.0	6.9	2.8	11.1	0	29.8	1.0	1.7	0.1	3.7	0	0	0.9	3.4	0	0.1	0	0	$\cdots$	$\cdots$	$\cdots$	$\cdots$	208.7
$\Xi_b'(6828)$	$\frac{1}{2}^+$	$\lvert 0,2,0,0\rangle$	$^4D_{1/2}$	20.2	17.4	1.5	11.0	3.1	23.6	0.4	9.1	15.7	3.5	0	8.7	404.9	0	1.0	1.6	0	0	5.3	1.1	0	1.1	0	0	$\cdots$	$\cdots$	$\cdots$	$\cdots$	529.2
$\Xi_b'(6834)$	$\frac{3}{2}^+$	$\lvert 0,2,0,0\rangle$	$^4D_{3/2}$	15.2	15.4	2.6	8.7	5.8	11.3	0.9	18.5	30.4	6.9	0	17.0	212.1	0.2	1.3	2.2	0	0	10.2	2.2	0	2.7	0	0	$\cdots$	$\cdots$	$\cdots$	$\cdots$	363.6
$\Xi_b'(6845)$	$\frac{5}{2}^+$	$\lvert 0,2,0,0\rangle$	$^4D_{5/2}$	13.2	16.4	4.3	10.7	9.6	33.0	1.6	13.8	18.5	4.5	0	10.9	41.8	0.4	1.1	3.8	0	0	6.2	1.4	0	2.6	0	0	$\cdots$	$\cdots$	$\cdots$	$\cdots$	193.8
$\Xi_b'(6859)$	$\frac{7}{2}^+$	$\lvert 0,2,0,0\rangle$	$^4D_{7/2}$	28.8	32.0	6.7	22.3	15.1	89.3	2.5	46.1	38.1	3.7	0.2	10.2	31.2	0.5	0.8	6.7	0	0	12.3	1.1	0	1.8	0	0	$\cdots$	$\cdots$	$\cdots$	$\cdots$	349.4

TABLE 2.22: *Table from [90] (APS copyright).* Same as 2.18, but for $\Omega_b(ssb)$ states.

$\mathcal{F}=\mathbf{6}_{\rm F}$				$\Xi_b K$	$\Xi_b' K$	$\Xi_b^* K$	$\Xi_b K^*$	$\Xi_b' K^*$	$\Xi_b^* K^*$	$\Omega_b \eta$	$\Omega_b^* \eta$	$\Omega_b \phi$	$\Omega_b^* \phi$	$\Omega_b \eta'$	$\Omega_b^* \eta'$	$\Xi_8 B$	$\Xi_{10} B$	$\Gamma^{\rm Strong}$
$\Omega_b(ssb)$	$\mathbf{J}^P$	$\lvert l_\lambda, l_\rho, k_\lambda, k_\rho\rangle$	$^{2S+1}L_J$	MeV	MeV	MeV	MeV	MeV	MeV	MeV	MeV	MeV	MeV	MeV	MeV	MeV	MeV	MeV
$N=0$																		
$\Omega_b(6064)$	$\frac{1}{2}^+$	$\lvert 0,0,0,0\rangle$	$^2S_{1/2}$	0	0	0	0	0	0	0	0	0	0	0	0	0	0	0
$\Omega_b(6093)$	$\frac{3}{2}^+$	$\lvert 0,0,0,0\rangle$	$^4S_{3/2}$	0	0	0	0	0	0	0	0	0	0	0	0	0	0	0
$N=1$																		
$\Omega_b(6315)$	$\frac{1}{2}^-$	$\lvert 1,0,0,0\rangle$	$^2P_{1/2}$	4.6	0	0	0	0	0	0	0	0	0	0	0	0	0	4.6
$\Omega_b(6337)$	$\frac{1}{2}^-$	$\lvert 1,0,0,0\rangle$	$^4P_{1/2}$	10.7	0	0	0	0	0	0	0	0	0	0	0	0	0	10.7
$\Omega_b(6321)$	$\frac{3}{2}^-$	$\lvert 1,0,0,0\rangle$	$^2P_{3/2}$	24.0	0	0	0	0	0	0	0	0	0	0	0	0	0	24.0
$\Omega_b(6343)$	$\frac{3}{2}^-$	$\lvert 1,0,0,0\rangle$	$^4P_{3/2}$	6.3	0	0	0	0	0	0	0	0	0	0	0	0	0	6.3
$\Omega_b(6353)$	$\frac{5}{2}^-$	$\lvert 1,0,0,0\rangle$	$^4P_{5/2}$	40.5	0	0	0	0	0	0	0	0	0	0	0	0	0	40.5
$\Omega_b(6465)$	$\frac{1}{2}^-$	$\lvert 0,1,0,0\rangle$	$^2P_{1/2}$	-	9.8	0	0	0	0	0	0	0	0	0	0	0	0	9.8
$\Omega_b(6471)$	$\frac{3}{2}^-$	$\lvert 0,1,0,0\rangle$	$^2P_{3/2}$	-	53.5	0	0	0	0	0	0	0	0	0	0	0	0	53.5
$N=2$																		
$\Omega_b(6568)$	$\frac{3}{2}^+$	$\lvert 2,0,0,0\rangle$	$^2D_{3/2}$	2.4	1.6	0	0	0	0	0	0	0	0	0	0	0	0	4.0
$\Omega_b(6578)$	$\frac{5}{2}^+$	$\lvert 2,0,0,0\rangle$	$^2D_{5/2}$	6.2	3.5	0	0	0	0	0	0	0	0	0	0	0	0	9.7
$\Omega_b(6584)$	$\frac{1}{2}^+$	$\lvert 2,0,0,0\rangle$	$^4D_{1/2}$	0.5	0.3	0.1	0	0	0	0	0	0	0	0	0	0	0	0.9
$\Omega_b(6590)$	$\frac{3}{2}^+$	$\lvert 2,0,0,0\rangle$	$^4D_{3/2}$	2.6	0.5	0.3	0	0	0	0	0	0	0	0	0	0	0	3.4
$\Omega_b(6600)$	$\frac{5}{2}^+$	$\lvert 2,0,0,0\rangle$	$^4D_{5/2}$	5.5	0.8	0.4	0	0	0	0	0	0	0	0	0	1.0	0	7.7
$\Omega_b(6614)$	$\frac{7}{2}^+$	$\lvert 2,0,0,0\rangle$	$^4D_{7/2}$	7.7	1.3	0.2	0	0	0	0.1	0	0	0	0	0	8.2	0	17.5
$\Omega_b(6574)$	$\frac{1}{2}^+$	$\lvert 0,0,1,0\rangle$	$^2S_{1/2}$	11.3	8.9	0	0	0	0	0	0	0	0	0	0	0	0	20.3
$\Omega_b(6602)$	$\frac{3}{2}^+$	$\lvert 0,0,1,0\rangle$	$^4S_{3/2}$	11.4	2.7	1.2	0	0	0	0	0	0	0	0	0	1.44	0	16.8
$\Omega_b(6874)$	$\frac{1}{2}^+$	$\lvert 0,0,0,1\rangle$	$^2S_{1/2}$	5.2	36.1	27.1	107.6	166.8	0	37.5	17.9	0	0	0	0	$\cdots$	$\cdots$	398.3
$\Omega_b(6902)$	$\frac{3}{2}^+$	$\lvert 0,0,0,1\rangle$	$^4S_{3/2}$	2.2	7.4	66.5	107.1	18.2	0	9.2	46.6	0	0	0	0	$\cdots$	$\cdots$	257.3
$\Omega_b(6718)$	$\frac{3}{2}^+$	$\lvert 1,1,0,0\rangle$	$^2D_{3/2}$	$\cdots$	8.5	61.6	22.3	0	0	3.7	19.8	0	0	0	0	$\cdots$	0	115.9
$\Omega_b(6728)$	$\frac{5}{2}^+$	$\lvert 1,1,0,0\rangle$	$^2D_{5/2}$	$\cdots$	55.3	5.4	6.0	0	0	13.8	1.8	0	0	0	0	$\cdots$	0	82.3
$\Omega_b(6720)$	$\frac{1}{2}^-$	$\lvert 1,1,0,0\rangle$	$^2P_{1/2}$	$\cdots$	0	0.7	0.2	0	0	0	0.2	0	0	0	0	$\cdots$	0	1.1
$\Omega_b(6726)$	$\frac{3}{2}^-$	$\lvert 1,1,0,0\rangle$	$^2P_{3/2}$	$\cdots$	1.1	0.4	0.2	0	0	0.2	0.1	0	0	0	0	$\cdots$	0	2.0
$\Omega_b(6724)$	$\frac{1}{2}^+$	$\lvert 1,1,0,0\rangle$	$^2S_{1/2}$	$\cdots$	13.7	24.7	16.0	0	0	8.2	9.9	0	0	0	0	$\cdots$	0	72.5
$\Omega_b(6868)$	$\frac{3}{2}^+$	$\lvert 0,2,0,0\rangle$	$^2D_{3/2}$	27.3	19.1	20.1	33.1	59.4	0	8.5	12.4	0	0	0	0	$\cdots$	$\cdots$	179.9
$\Omega_b(6878)$	$\frac{5}{2}^+$	$\lvert 0,2,0,0\rangle$	$^2D_{5/2}$	58.4	51.2	6.8	3.1	12.1	0	22.0	3.0	0	0	0	0	$\cdots$	$\cdots$	156.6
$\Omega_b(6884)$	$\frac{1}{2}^+$	$\lvert 0,2,0,0\rangle$	$^4D_{1/2}$	23.1	0.6	32.1	46.2	4.7	0	0.3	19.1	0	0	0	0	$\cdots$	$\cdots$	126.1
$\Omega_b(6890)$	$\frac{3}{2}^+$	$\lvert 0,2,0,0\rangle$	$^4D_{3/2}$	30.7	5.2	35.2	88.4	9.8	0	2.3	23.4	0	0	0	0	$\cdots$	$\cdots$	195.0
$\Omega_b(6900)$	$\frac{5}{2}^+$	$\lvert 0,2,0,0\rangle$	$^4D_{5/2}$	44.2	11.0	31.1	53.0	7.4	0	4.9	19.9	0	0	0	0	$\cdots$	$\cdots$	171.5
$\Omega_b(6914)$	$\frac{7}{2}^+$	$\lvert 0,2,0,0\rangle$	$^4D_{7/2}$	74.1	15.6	37.0	74.7	4.6	0	6.8	17.7	0	0	0	0	$\cdots$	$\cdots$	230.5

experimental efforts aimed at identifying bottom baryons. Knowledge of the possible decay channels can significantly aid in the interpretation of experimental data and guide the search for yet-unobserved states.

Nevertheless, there are a few cases in which strong decays are forbidden due to the lack of phase space, resulting in the dominance of electromagnetic or even weak interactions. Specifically, the ground states Λ_b, Ξ_b, and Ω_b can decay only via the weak interaction. For states such as Ξ_b', and Ω_b^*, all strong decay channels are kinematically closed, making the electromagnetic interaction the dominant decay mechanism. These cases motivate the study of electromagnetic decay widths, which is the focus of the next chapter.

2.6 Assignments

Based on our theoretical results, the assignments of the singly bottom baryons reported in PDG [89] will be made. The mass spectrum is used as the primary criterion for identifying resonances of singly bottom baryons, while the decay widths serve as a secondary criterion to support these assignments.

2.6.1 Λ_b baryons

In particular, the assignment of the six Λ_b states listed by the PDG [89] is made using our theoretical predictions presented in Table 2.2.

The Λ_b^0 is identified as the ground state with quantum numbers $\mathbf{J}^P = \frac{\mathbf{1}}{\mathbf{2}}^+$, and its mass is accurately reproduced by both the three-quark and quark-diquark models.

The $\Lambda_b(5912)^0$ and $\Lambda_b(5920)^0$ states are identified as the two P_λ-wave excitations with quantum numbers $\mathbf{J}^P = \frac{\mathbf{1}}{\mathbf{2}}^-$ and $\mathbf{J}^P = \frac{\mathbf{3}}{\mathbf{2}}^-$, respectively. Our theoretical mass predictions for these states are in good agreement with the experimental values. Since there are no available strong decay channels for these states, their strong decay widths are predicted to be zero.

The $\Lambda_b(6070)^0$ state was observed by LHCb [28] with mass and decay width

$$m[\Lambda_b(6072)^0] = 6072.3 \pm 2.9 \ \pm 0.6 \pm 0.2 \text{ MeV}, \tag{2.70}$$

$$\Gamma[\Lambda_b(6072)^0] = 72 \pm 11 \ \pm 2 \text{ MeV}, \tag{2.71}$$

and was suggested to be the first radial excitation of the Λ_b with $\mathbf{J}^P = \frac{\mathbf{1}}{\mathbf{2}}^+$. However, its quantum numbers have not yet been determined experimentally.

Assuming it is a Roper-like state and employing the model from reference [83], the mass shows a deviation of approximately 3% from the experimental value, and the calculated width is 29 ± 14 MeV. Due to the limitations of the harmonic oscillator model in accurately reproducing the masses of Roper-like states, the decay width of $\Lambda_b(6072)$ is also calculated using its experimental mass as input, under the assumption that it is a $2S$ state. The resulting width is 3.1

MeV, having a reduction of 90% compared to the previous estimate, caused by the closure of dominant open-flavor channels. This value is significantly lower than the experimental decay width of 72 MeV, suggesting that $\Lambda_b(6072)$ cannot be conclusively identified as a $2S$ state. Alternatively, $\Lambda_b(6072)$ can be interpreted as a P_ρ state with $\mathbf{J}^P = \frac{\mathbf{1}}{\mathbf{2}}^-$, and internal spin $\mathbf{S}_{\rm tot} = \frac{\mathbf{1}}{\mathbf{2}}$. Under this interpretation, the experimental decay width is well reproduced, although the mass remains slightly overestimated.

The $\Lambda_b(6146)^0$ and $\Lambda_b(6152)^0$ states are identified as the two D_λ excitations, with quantum numbers $\mathbf{J}^P = \frac{\mathbf{3}}{\mathbf{2}}^+$ and $\mathbf{J}^P = \frac{\mathbf{5}}{\mathbf{2}}^+$, respectively. However, their quantum numbers have not yet been experimentally determined. In this case, our theoretical mass predictions deviate by only about 1%, and the predicted decay widths are slightly larger than the corresponding experimental values.

2.6.2 Ξ_b and Ξ_b' baryons

The assignments for the Ξ_b and Ξ_b' states reported by the PDG [89] are made using our theoretical results presented in Tables 2.3 and 2.5, respectively. The invariance of the strong interaction under $SU_I(2)$ isospin transformations leads to isospin conservation and the formation of degenerate isospin multiplets. Both Ξ_b and Ξ_b' baryons belong to isospin doublets. In this context, assigning quantum numbers becomes more challenging due to the presence of several excited states in the same energy region for both Ξ_b and Ξ_b', making a clear distinction between them more complex.

The masses of the Ξ_b^0 and Ξ_b^- are degenerate in both the three-quark and quark–diquark schemes, in agreement with experimental observations [89]. In this work, the quantum numbers $\mathbf{J}^P = \frac{\mathbf{1}}{\mathbf{2}}^+$ are assigned to these states, although these quantum numbers have not yet been directly measured.

The $\Xi_b'(5935)^-$ is considered the ground state belonging to the flavor sextet. Its predicted mass, in both the three-quark and quark-diquark models, is in agreement with the experimental data. It is assigned quantum numbers $\mathbf{J}^P = \frac{\mathbf{1}}{\mathbf{2}}^+$; however, these quantum numbers have not yet been experimentally confirmed. Moreover, its neutral charge partner, the $\Xi_b'(5935)^0$, has not yet been observed.

The $\Xi_b'(5955)^-$ and $\Xi_b'(5945)^0$ are identified as spin excitations of the $\Xi_b'(5935)^-$. They are assigned quantum numbers $\mathbf{J}^P = \frac{\mathbf{3}}{\mathbf{2}}^+$, although these assignments are based on quark model expectations and have not yet been experimentally measured. The predicted masses of the $\Xi_b'(5955)^-$ and $\Xi_b'(5945)^0$ are degenerate and agree well with experimental data. Additionally, their decay widths are accurately reproduced in our study.

The $\Xi_b'(6100)^-$ is identified as a P-wave state with quantum numbers $\mathbf{J}^P = \frac{\mathbf{1}}{\mathbf{2}}^-$, although this assignment remains to be experimentally confirmed. It is identified as one of the two P_λ excitations of the Ξ_b, belonging to the flavor antitriplet, with total spin $\mathbf{S}_{\rm tot} = \frac{\mathbf{1}}{\mathbf{2}}$. Both its mass and decay width are well reproduced in this study.

The $\Xi_b'(6227)^-$ and $\Xi_b'(6227)^0$ are identified in our study as the fifth P_λ excitation of the Ξ_b', with quantum numbers $\mathbf{J}^P = \frac{5}{2}^-$ and total spin $\mathbf{S}_{\rm tot} = \frac{3}{2}$. The computed mass is consistent with the experimental value, and the decay width is well reproduced. However, an alternative assignment with $\mathbf{J}^P = \frac{3}{2}^-$ is also possible, as the predicted mass for this state is similar. In that case, though, the decay width deviates from the experimental value by approximately 6 MeV.

The two states $\Xi_b(6327)^0$ and $\Xi_b(6333)^0$ were observed by the LHCb Collaboration [29]. In this study, they are identified as the two D_λ excitations with quantum numbers $\mathbf{J}^P = \frac{3}{2}^+$ and $\mathbf{J}^P = \frac{5}{2}^+$, respectively, belonging to the flavor $\bar{\mathbf{3}}_{\rm F}$-plet.

Finally, the LHCb Collaboration reported the discovery of the $\Xi_b(6087)^0$ and $\Xi_b(6095)^0$ states [30]. The $\Xi_b(6087)^0$ is associated with the $1P$, $\mathbf{J}^P = \frac{1}{2}^-$ state. Our theoretical prediction for its mass is in good agreement with the experimental value, although the predicted decay width is slightly lower than the experimental value. The $\Xi_b(6095)^0$ is interpreted as the $1P$, $\mathbf{J}^P = \frac{3}{2}^-$ neutral partner of the $\Xi_b(6100)^-$. Our predicted mass shows good agreement with the experimental measurement, and the predicted width is also consistent with the observed width.

2.6.3 Σ_b baryons

The PDG [89] reports only four Σ_b states, and their quantum numbers have not yet been experimentally determined. In this work, our theoretical results for the Σ_b baryons, presented in Table 2.4, are used to propose their assignments.

The Σ_b is identified as the ground state with quantum numbers $\mathbf{J}^P = \frac{1}{2}^+$. Its theoretical mass, as calculated in both the three-quark and quark-diquark models, shows good agreement with the experimental value. Furthermore, the predicted decay width is in agreement with the experimental measurement.

The spin excitation Σ_b^* is identified with quantum numbers $\mathbf{J}^P = \frac{3}{2}^+$. Our theoretical predictions for its mass and decay width are in good agreement with the experimental data.

The $\Sigma_b(6097)^-$ and $\Sigma_b(6097)^+$ states are two of the three charge states of the $\Sigma_b(6097)$, which are degenerate in the model proposed in reference [83]. Our predicted mass and decay width for the $\Sigma_b(6097)$ are in good agreement with the experimental data. According to our calculations, this state is identified as the first P_λ excitation of the Σ_b, with quantum numbers $\mathbf{J}^P = \frac{1}{2}^-$ and total spin $\mathbf{S}_{\rm tot} = \mathbf{1/2}$.

2.6.4 Ω_b baryons

The predicted mass spectra and strong decay widths for the Ω_b states, presented in Table 2.6, are used to propose assignments for the experimentally observed states. Our calculations are in good agreement with the earlier results reported in reference [83]. Furthermore, compared to that previous study, the present work extends the analysis to include the $1D$, $2P$, and $2S$-wave excitations.

The Ω_b^- baryon is identified as a $\mathbf{J}^P = \frac{1}{2}^+$ state. Its experimental mass is well reproduced within the quark-diquark model. In the three-quark model, the predicted mass shows a slight

deviation of approximately 10 MeV. Since the Ω_b^- can only decay via the weak interaction, its strong decay width is zero.

The Ω_b^{*-}, identified as the spin excitation of the Ω_b^- with quantum numbers $\mathbf{J}^P = \frac{3}{2}^+$, has not yet been observed experimentally. Therefore, the radiative decay mode $\Omega_b^* \to \Omega_b^- \gamma$ is proposed as a "golden channel" for the discovery of this state.

The LHCb Collaboration [27] reported the discovery of four Ω_b resonances, namely $\Omega_b(6316)^-$, $\Omega_b(6330)^-$, $\Omega_b(6340)^-$, and $\Omega_b(6350)^-$. These states still require confirmation by other experiments, and their quantum numbers have not yet been determined. In our study, they are identified as four of the five P_λ excitations of the Ω_b.

The mass and width of the $\Omega_b(6316)^-$ are well reproduced in our calculations. This state is assigned as $\mathbf{J}^P = \frac{1}{2}^-$, with total spin $\mathbf{S}_{\rm tot} = \frac{1}{2}$. The $\Omega_b(6330)^-$ is also assigned $\mathbf{J}^P = \frac{1}{2}^-$, but with $\mathbf{S}_{\rm tot} = \frac{3}{2}$. Its mass is well described in both the three-quark and quark-diquark models, and the predicted width is consistent with the experimental data. The mass of the $\Omega_b(6340)^-$ is similarly well reproduced by both models, although the decay width is slightly overestimated. Our assignment for this state is $\mathbf{J}^P = \frac{3}{2}^-$, with $\mathbf{S}_{\rm tot} = \frac{1}{2}$. Finally, the $\Omega_b(6350)^-$ is well described in terms of both mass and width, and is assigned $\mathbf{J}^P = \frac{3}{2}^-$ with $\mathbf{S}_{\rm tot} = \frac{3}{2}$.

For the fifth Ω_b^- P_λ excitation, a large decay width is predicted, which implies that a high statistical significance would be required for its observation at the LHC. This state is expected to lie in the mass range of 6345-6365 MeV, with a width of approximately 40 MeV.

In the three-quark model, two additional P_ρ excitations are predicted, which do not appear in the quark-diquark scheme. These states do not couple to the $\Xi_b^0 K^-$ channel, that is the channel in which the LHCb Collaboration observed the four excited Ω_b^- states, but instead exhibit a strong coupling to the $\Xi_b^{\prime 0} K^-$ channel. Therefore, the experimental search for these two P_ρ excitations is a crucial step toward determining whether singly bottom baryons are better described as genuine three-quark systems or as quark-diquark configurations.

2.7 Discussion

Our theoretical strong decay widths, calculated using the $^3P_0$ model, show good agreement with the experimental values reported in the PDG [89]. This agreement is particularly noteworthy given that the $^3P_0$ model involves only a single free parameter, which is fitted to reproduce the experimental decay width of the process $\Sigma_b^* \to \Lambda_b \pi$ [89].

Moreover, the predicted mass spectrum successfully reproduces the trend observed in the available experimental data, as illustrated in Fig. 2.10, where the spectra of singly bottom baryons computed using the three-quark model is presented. States belonging to the flavor antitriplet are shown in purple, with corresponding mass predictions represented by purple lines. States from the flavor sextet are shown in teal, with their theoretical masses indicated by teal lines. The experimentally established states and their measured masses, as reported in the PDG [89], are shown in black.

Furthermore, many strong decay channels that had not been previously investigated were studied in this work [90].

It is well known in the study of light baryons that the harmonic oscillator quark model fails to reproduce the order of the Roper and $1P$ states. For instance, the Roper resonance $N(1440)$ lies below the $1P$ wave excitations $N(1520)$ and $N(1535)$, while it provides a good description of the remaining states.

The situation is markedly different in the heavy baryon sector. A key distinction is that the Roper-like candidates (identified as $2S$ excitations) lie above the $1P$ states. In the charm sector, for example, the Roper-like candidate $\Lambda_c(2765)$ [127] lies approximately 150 MeV above the P-wave excitations $\Lambda_c(2595)$ and $\Lambda_c(2625)$ [128]. Similarly, in the bottom sector, the Roper-like candidate $\Lambda_b(6070)$ lies about 100 MeV above the P-wave excitations $\Lambda_b(5912)$ and $\Lambda_b(5920)$.

Therefore, in the heavy sector, the harmonic oscillator quark model, which is known to work well for the rest of the spectrum, can also be applied to Roper-like states. However, it is important to remain cautious about the model's limitations in accurately reproducing the properties of $2S$ states. Additional experimental data will be crucial for determining the quantum numbers and decay modes of the Roper-like candidates. Such information will be essential for confirming whether these states are indeed genuine $2S$ excitations.

2.8 Conclusions of the chapter

In this chapter, the mass spectra and strong decay widths of singly bottom baryons have been calculated. Both the three-quark and quark-diquark schemes were employed to describe the mass spectra, predicting the $1S$, $1P$, $1D$, $2P$, and $2S$ states, thereby extending the model proposed in reference [83]. A Monte Carlo bootstrap method was used to account for the propagation of parameter uncertainties. Notably, the harmonic oscillator approach enables a comprehensive description of singly bottom baryons through a global fit in which the same model predicts the masses, strong partial decay widths, and electromagnetic decay widths of bottom baryons. Since all the parameters of the model Hamiltonian in eq. (2.44) were fitted to 13 of the 23 experimental mass values reported in the PDG [89], the harmonic oscillator wave functions used in the model do not rely on any additional free parameters.

Our theoretical mass spectra successfully reproduce the overall trend observed in the experimental data. To date, only λ-mode excited singly bottom baryons have been experimentally identified. However, based on our strong decay calculations, a tentative assignment of the Λ_b as a P_ρ-wave excited state with quantum numbers $\mathbf{J}^P = \frac{\mathbf{1}}{\mathbf{2}}^-$ is proposed, rather than as a $2S$ radial excitation. Therefore, an experimental determination of its quantum numbers is essential to clarify whether this state corresponds to a true radial excitation or to the first P_ρ-wave excitation of the Λ_b. The identification of ρ-mode excitations would significantly improve our understanding of the internal structure of singly bottom baryons, especially in distinguishing between three-quark configurations and quark-diquark models.

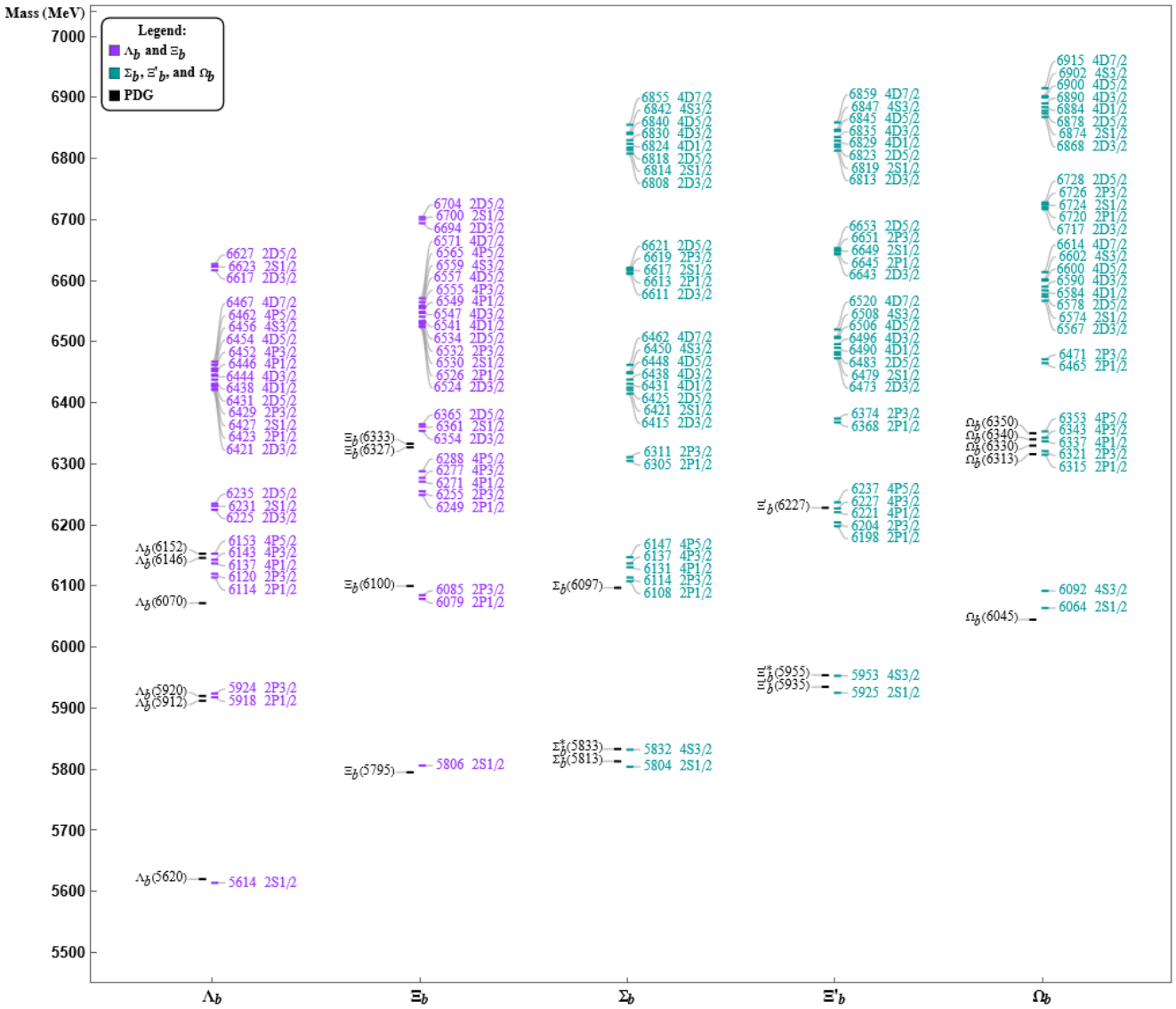

FIGURE 2.10: *Figure taken from [90] (APS copyright)* Comparison between the singly bottom baryon mass predictions, obtained using the three-quark model Hamiltonian of eqs. (2.44) and (2.45), with the experimental data from PDG [89]. The predicted masses for the $\bar{\mathbf{3}}_{\mathrm{F}}$ and $\mathbf{6}_{\mathrm{F}}$ states are displayed in purple and teal, respectively, while the experimental masses are reported in black [89].

The strong decay widths of the three-quark excited $1P$, $1D$, $2P$, and $2S$ singly bottom baryons, including both ρ- and λ-mode excitations, are calculated using the $^3P_0$ model. The decays are studied into final states composed of singly bottom baryons and pseudoscalar/vector mesons, as well as into pairs of light octet/decuplet baryons and bottom pseudoscalar/vector mesons. To further support experimental efforts in identifying bottom baryons, the partial decay widths for all open-flavor channels are provided in Tables 2.18-2.22.

Our predictions for the masses and strong decay widths of singly bottom baryons show good agreement with the available experimental data. Notably, the mass formula proposed in reference [83], together with the $^3P_0$ model, successfully describes the recently observed D-wave excitations such as $\Lambda_b(6146)^0$ and $\Lambda_b(6152)^0$, which are identified as D_λ states with quantum numbers $\mathbf{J}^P = \frac{3}{2}^+$ and $\mathbf{J}^P = \frac{5}{2}^+$, respectively. Similarly, both the three-quark and quark-diquark models account for the $\Xi_b(6327)^0$ and $\Xi_b(6333)^0$ states, recently listed by the PDG [89]. These are also identified as D_λ excitations with $\mathbf{J}^P = \frac{3}{2}^+$ and $\mathbf{J}^P = \frac{5}{2}^+$, respectively, and belong to the flavor $\bar{\mathbf{3}}_\mathrm{F}$-plet. These states were not included in the fitting procedure. Therefore, the agreement between the predicted and experimental masses and widths highlights the strong predictive power of the mass formula from reference [83] and the effectiveness of the $^3P_0$ decay model.

Moreover, the results presented in this chapter, published in *Physical Review D* [90], which include both mass spectra and strong decay widths, provide valuable guidance for experimentalists at collaborations such as LHCb, CMS, and ATLAS. These predictions can assist in identifying the most suitable decay channels for the detection of specific resonances.

Chapter 3

Electromagnetic decays of singly bottom baryons

This chapter presents the calculations of the electromagnetic decay widths for singly bottom baryons within the Quark Model formalism. The calculations employ a harmonic oscillator model and the electromagnetic interaction Hamiltonian in the nonrelativistic approximation. A novel method, introduced in reference [90] and presented in detail in Appendix A, is employed to evaluate the transition amplitudes in an exact and fully analytical manner for the first time, without requiring any additional approximations. This approach contrasts with previous quark model calculations [70, 71, 82], which relied on further approximations to the nonrelativistic Hamiltonian.

The radiative decays of singly bottom baryons have been investigated in several studies [70, 71, 82, 129–142]. Specifically, the analyses in [70, 71, 82] use the constituent quark model, while studies in [129–135] employ Light-Cone QCD sum rules. Heavy Hadron Chiral Perturbation Theory (χPT) is applied in [136–138], and other frameworks include Heavy Quark Symmetry [142], the bound state picture [140], a relativistic three-quark model [141], and modified bag models [139]. Despite the theoretical advancements, no experimental data are currently available for the electromagnetic decays of singly bottom baryons, making it impossible to directly compare theoretical predictions with experimental results.

3.1 Electromagnetic decays widths

In this section the general expressions for computing the electromagnetic amplitudes for singly bottom baryons are derived and the explicit calculations of the electromagnetic decay widths are also performed.

The calculation of the radiative decay width of singly bottom baryons is carried out within the constituent quark model formalism. The case of the emission of a left-handed photon from a singly-bottom baryon (A) to another singly-bottom baryon (A') is considered, i.e.,

$$A \to A' + \gamma. \tag{3.1}$$

The corresponding Feynman diagram for this process is shown in Figure (3.1). The partial decay widths of the electromagnetic transitions are expressed as:

$$\Gamma_{\rm em}(A \to A'\gamma) = \Phi_{A\to A'\gamma}\frac{1}{(2\pi)^2}\frac{2}{2J_A+1}\sum_{M_{J_A}>0}\left|\mathcal{A}_{M_{J_A}}\right|^2, \tag{3.2}$$

where J_A is the initial singly bottom baryon total angular momentum; the sum runs over the helicities M_{J_A} of the initial baryon A; $\Phi_{A\to A'\gamma}$ is the phase space factor, which in the rest frame of the initial baryon is expressed as

$$\Phi_{A\to A'\gamma} = 4\pi\frac{E_{A'}}{m_A}\mathrm{k}^2, \tag{3.3}$$

here the energy of the final state $E_{A'}$ is given by the expression

$$E_{A'} = \sqrt{m_{A'}^2+\mathrm{k}^2}, \tag{3.4}$$

being m_A and m'_A the masses of the initial and final baryon, respectively, and the photon energy k is given by

$$\mathrm{k} = \frac{m_A^2 - m_{A'}^2}{2m_A}. \tag{3.5}$$

The transition amplitude for a given helicity M_{J_A} is defined as

$$\mathcal{A}_{M_{J_A}} = \langle\phi_{A'}, J_{A'}, M_{J_A}-1, k_{A'}|\mathcal{H}_{\rm em}|\phi_A, J_A, M_{J_A}, k_A\rangle. \tag{3.6}$$

Here, $\mathcal{H}_{\rm em}$ represents the nonrelativistic Hamiltonian governing the electromagnetic transitions. It is derived from the interaction Hamiltonian that describes the electromagnetic coupling between photons and quarks. At tree level, this Hamiltonian is expressed as

$$H = -\sum_j \mathrm{e}_j\bar{q}_j\gamma^\mu A_\mu q_j, \tag{3.7}$$

where e_j and q_j denote the charge and the quark field associated with the j-th quark, respectively, γ^μ are the Dirac matrices, and A_μ represents the electromagnetic field. By taking the nonrelativistic limit and retaining terms up to the order m_j^{-1}, the interaction Hamiltonian derived from the original interaction takes the following form:

$$\begin{aligned}\mathcal{H}_{\rm em} &= \sum_{j=1}^{3}\frac{1}{(2\pi)^{3/2}}\frac{\mathrm{e}_j}{(2\mathrm{k})^{1/2}}\Bigg\{\varepsilon^0 e^{-i\mathbf{k}\cdot\mathbf{r}_j} \\ &- \frac{[\mathbf{p}_j\cdot\boldsymbol{\varepsilon}e^{-i\mathbf{k}\cdot\mathbf{r}_j} + e^{-i\mathbf{k}\cdot\mathbf{r}_j}\boldsymbol{\varepsilon}\cdot\mathbf{p}_j]}{2m_j} - \frac{i\boldsymbol{\sigma}\cdot(\mathbf{k}\times\boldsymbol{\varepsilon})e^{-i\mathbf{k}\cdot\mathbf{r}_j}}{2m_j}\Bigg\}.\end{aligned} \tag{3.8}$$

Here, $\mathbf{r}_j$ and $\mathbf{p}_j$, represent the coordinate and momentum of the j-th quark, respectively, k

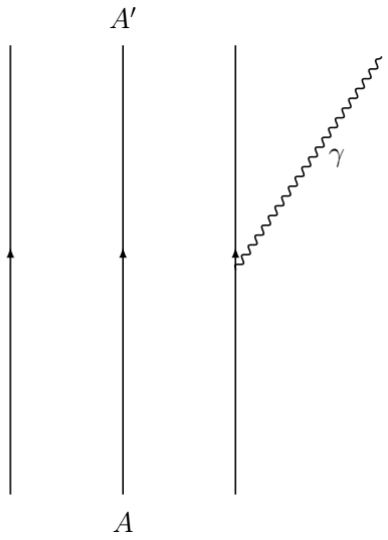

FIGURE 3.1: Feynman diagram illustrating the electromagnetic transition between singly bottom baryons. The diagram shows the emission of a photon γ in the radiative decay $A \to A' + \gamma$.

denotes the photon energy, and $\mathbf{k} = \mathrm{k}\hat{\mathbf{z}}$ corresponds to the momentum of a photon emitted in the positive z-direction. The polarization vector for radiative decays can be expressed as $\varepsilon^{\mu} = (0, 1, -i, 0)/\sqrt{2}$. One can notice that the zeroth component vanishes ($\varepsilon^0 = 0$) because radiative decays involve real photons [86]. Consequently, the first term in eq. (3.8) becomes identically zero. By substituting the explicit form of the polarization vector, the interaction Hamiltonian that describes the electromagnetic decays of baryons can be written as

$$\mathcal{H}_{\mathrm{em}} = 2\sqrt{\frac{\pi}{\mathrm{k}_0}} \sum_{j=1}^{3} \mu_j \left[\mathrm{k}\mathbf{s}_{j,-} e^{-i\mathbf{k}\cdot\mathbf{r}_j} - \frac{1}{2} \left(\mathbf{p}_{j,-} e^{-i\mathbf{k}\cdot\mathbf{r}_j} + e^{-i\mathbf{k}\cdot\mathbf{r}_j} \mathbf{p}_{j,-} \right) \right], \tag{3.9}$$

where $\mu_j \equiv \mathrm{e}_j/(2m_j)$, $\mathbf{s}_{j,-} \equiv \mathbf{s}_{j,x} - i\mathbf{s}_{j,y}$, and $\mathbf{p}_{j,-} \equiv \mathbf{p}_{j,x} - i\mathbf{p}_{j,y}$, represent the magnetic moment, the spin ladder, and the momentum ladder operator of the j-th quark, respectively.

It can be seen that the Hamiltonian in eq. (3.9) consists of two parts. The first part is proportional to the operator

$$\mathrm{k}\mathbf{s}_{j,-} \hat{U}_j \equiv \mathrm{k}\mathbf{s}_{j,-} \exp[-i\mathbf{k}\cdot\mathbf{r}_j], \tag{3.10}$$

that corresponds to the spin-flip contribution. This part can be evaluated straightforwardly by observing that the operators $\hat{U}_j$ can be written for each quark in the following way

$$\hat{U}_1 = \exp[-i\mathbf{k}\cdot\mathbf{r}_1] = \exp\left[-i\frac{1}{\sqrt{2}}\mathbf{k}\cdot\boldsymbol{\rho} - i\frac{\sqrt{\frac{3}{2}}m_b}{2m_\rho + m_b}\mathbf{k}\cdot\boldsymbol{\lambda} \right], \tag{3.11}$$

$$\hat{U}_2 = \exp[-i\mathbf{k}\cdot\mathbf{r}_2] = \exp\left[i\frac{1}{\sqrt{2}}\mathbf{k}\cdot\boldsymbol{\rho} - i\frac{\sqrt{\frac{3}{2}}m_b}{2m_\rho + m_b}\mathbf{k}\cdot\boldsymbol{\lambda} \right], \tag{3.12}$$

$$\hat{U}_3 = \exp[-i\mathbf{k}\cdot\mathbf{r}_3] = \exp\left[i\frac{\sqrt{6}m_\rho}{2m_\rho + m_b}\mathbf{k}\cdot\boldsymbol{\lambda}\right]. \tag{3.13}$$

The second part of the Hamiltonian is proportional to the operator

$$\hat{T}_{j,-} \equiv \mathbf{p}_{j,-}\,\hat{U}_j + \hat{U}_j\,\mathbf{p}_{j,-}, \tag{3.14}$$

that corresponds to the orbit-flip contribution. Here $\mathbf{p}_{j,-}$ denotes the momentum ladder operator, which is defined as

$$\mathbf{p}_{j,-} = \mathbf{p}_{j,x} - i\mathbf{p}_{j,y}, \tag{3.15}$$

whose components are given by

$$\begin{aligned}
\mathbf{p}_{1,-} &= \frac{1}{\sqrt{2}}\mathbf{p}_{\rho,-} + \frac{1}{\sqrt{6}}\mathbf{p}_{\lambda,-}\,,\\
\mathbf{p}_{2,-} &= -\frac{1}{\sqrt{2}}\mathbf{p}_{\rho,-} + \frac{1}{\sqrt{6}}\mathbf{p}_{\lambda,-}\,,\\
\mathbf{p}_{3,-} &= -\sqrt{\frac{2}{3}}\mathbf{p}_{\lambda,-}\,,
\end{aligned} \tag{3.16}$$

for $j = 1, 2$ and 3, respectively. Using the above equations, the $\hat{T}_{j,-}$ operators can be expressed as

$$\hat{T}_{1,-} = \left(\frac{1}{\sqrt{2}}\mathbf{p}_{\rho,-} + \frac{1}{\sqrt{6}}\mathbf{p}_{\lambda,-}\right)\hat{U}_1 + \hat{U}_1\left(\frac{1}{\sqrt{2}}\mathbf{p}_{\rho,-} + \frac{1}{\sqrt{6}}\mathbf{p}_{\lambda,-}\right), \tag{3.17}$$

$$\hat{T}_{2,-} = \left(-\frac{1}{\sqrt{2}}\mathbf{p}_{\rho,-} + \frac{1}{\sqrt{6}}\mathbf{p}_{\lambda,-}\right)\hat{U}_2 + \hat{U}_2\left(-\frac{1}{\sqrt{2}}\mathbf{p}_{\rho,-} + \frac{1}{\sqrt{6}}\mathbf{p}_{\lambda,-}\right), \tag{3.18}$$

$$\hat{T}_{3,-} = -\sqrt{\frac{2}{3}}\mathbf{p}_{\lambda,-}\hat{U}_3 - \hat{U}_3\sqrt{\frac{2}{3}}\mathbf{p}_{\lambda,-}. \tag{3.19}$$

In this way, the Hamiltonian of eq. (3.9) can be rewritten in terms of the operators $\hat{U}_j$ and $\hat{T}_{j,-}$ in the following way

$$\mathcal{H}_{\rm em} = 2\sqrt{\frac{\pi}{\mathrm{k}}}\sum_{j=1}^{3}\hat{\mu}_j\left[\mathrm{k}\mathbf{s}_{j,-}\hat{U}_j - \frac{1}{2}\hat{T}_{j,-}\right]. \tag{3.20}$$

In this study the compact expression of eq. (3.20) is used to write the transition amplitudes in function of the $\hat{U}_j$ and $\hat{T}_{j,-}$ operators in the following way:

$$\begin{aligned}
\mathcal{A}_{M_{J_A}} &= 2\sqrt{\frac{\pi}{\mathrm{k}_0}}\mathrm{k}\sum_{j=1}^{3}\langle\phi_{A'}, J_{A'}, M_{J_A}-1, k_{A'}|\hat{\mu}_j\mathbf{s}_{j,-}\hat{U}_j|\phi_A, J_A, M_{J_A}, k_A\rangle\\
&- \sqrt{\frac{\pi}{\mathrm{k}_0}}\sum_{j=1}^{3}\langle\phi_{A'}, J_{A'}, M_{J_A}-1, k_{A'}|\hat{\mu}_j\hat{T}_{j,-}|\phi_A, J_A, M_{J_A}, k_A\rangle.
\end{aligned} \tag{3.21}$$

The evaluation of the transition amplitudes is discussed in detail in Appendix A. The explicit evaluation in spin, flavor and spatial spaces in Sections A.1, A.2 and A.3.

In this Appendix the procedure of evaluating the matrix elements for the $\hat{T}_{j,-}$ operators in the electromagnetic transitions from P-wave states to ground states is exposed. This is accomplished by expressing the matrix elements of the $\hat{T}_{j,-}$ operators as a sum of matrix elements of the $\hat{U}_j$ operators. To make this transformation, the action of the ladder operators $\mathbf{p}_{\lambda/\rho,-}$ on the wave functions has to be evaluated (see Appendix A) and the analytical formulas are obtained.

The $\hat{U}_j$ matrix elements from the ground states to ground states are given by

$$\langle 0,0,0,0,0,0|\hat{U}_1|0,0,0,0,0,0\rangle = \langle 0,0,0,0,0,0|\hat{U}_2|0,0,0,0,0,0\rangle = e^{-\frac{1}{8}k^2\left(\frac{1}{\alpha_\rho^2}+\frac{3m_b{}^2}{\alpha_\lambda^2(2m_\rho+m_b)^2}\right)}, \tag{3.22}$$

$$\langle 0,0,0,0,0,0|\hat{U}_3|0,0,0,0,0,0\rangle = e^{-\frac{3k^2m_\rho^2}{2\alpha_\lambda^2(2m_\rho+m_b)^2}}. \tag{3.23}$$

The $\hat{T}_{j,-}$ matrix elements from the ground states to ground states are all 0, i.e.

$$\begin{aligned}&\langle 0,0,0,0,0,0|\hat{T}_{1,-}|0,0,0,0,0,0\rangle = \langle 0,0,0,0,0,0|\hat{T}_{2,-}|0,0,0,0,0,0\rangle \\ &= \langle 0,0,0,0,0,0|\hat{T}_{3,-}|0,0,0,0,0,0\rangle = 0.\end{aligned} \tag{3.24}$$

The $\hat{U}_j$ matrix elements from P_ρ-wave states to ground states are

$$\langle 0,0,0,0,0,0|\hat{U}_1|0,1,m_{l_\rho},0,0,0\rangle = -\langle 0,0,0,0,0,0|\hat{U}_2|0,1,m_{l_\rho},0,0,0\rangle = -\frac{ike^{-\frac{1}{8}k^2\left(\frac{1}{\alpha_\rho^2}+\frac{3m_b{}^2}{\alpha_\lambda^2(2m_\rho+m_b)^2}\right)}}{2\alpha_\rho}, \tag{3.25}$$

$$\langle 0,0,0,0,0,0|\hat{U}_3|0,1,m_{l_\rho},0,0,0\rangle = 0, \tag{3.26}$$

and from the P_λ-wave states to ground states

$$\langle 0,0,0,0,0,0|\hat{U}_1|0,0,0,0,1,m_{l_\lambda}\rangle = \langle 0,0,0,0,0,0|\hat{U}_2|0,0,0,0,1,m_{l_\lambda}\rangle = -\frac{i\sqrt{3}km_b e^{-\frac{1}{8}k^2\left(\frac{1}{\alpha_\rho^2}+\frac{3m_b{}^2}{\alpha_\lambda^2(2m_\rho+m_b)^2}\right)}}{2\alpha_\lambda(2m_\rho+m_b)}, \tag{3.27}$$

$$\langle 0,0,0,0,0,0|\hat{U}_3|0,0,0,0,1,m_{l_\lambda}\rangle = \frac{i\sqrt{3}km_\rho e^{-\frac{3k^2m_\rho^2}{2\alpha_\lambda^2(2m_\rho+m_b)^2}}}{\alpha_\lambda(2m_\rho+m_b)}. \tag{3.28}$$

The $\hat{T}_{j,-}$ matrix elements from P_ρ-wave states to ground states are

$$\langle 0,0,0,0,0,0|\hat{T}_{1,-}|0,1,m_{l_\rho},0,0,0\rangle = -\langle 0,0,0,0,0,0|\hat{T}_{2,-}|0,1,m_{l_\rho},0,0,0\rangle = i\sqrt{2}\alpha_\rho e^{-\frac{1}{8}k^2\left(\frac{1}{\alpha_\rho^2}+\frac{3m_b{}^2}{\alpha_\lambda^2(2m_\rho+m_b)^2}\right)}\delta_{m_{l_\rho},1}, \tag{3.29}$$

$$\langle 0,0,0,0,0,0|\hat{T}_{3,-}|0,1,m_{l_\rho},0,0,0\rangle = 0, \tag{3.30}$$

and finally from P_λ-wave states to ground states we have

$$\langle 0,0,0,0,0,0|\hat{T}_{1,-}|0,0,0,0,1,m_{l\lambda}\rangle = \langle 0,0,0,0,0,0|\hat{T}_{2,-}|0,0,0,0,1,m_{l\lambda}\rangle = i\sqrt{\tfrac{2}{3}}\alpha_\lambda e^{\frac{-k^2}{8}\left(\frac{1}{\alpha_\rho^2}+\frac{3m_b^2}{\alpha_\lambda^2(2m_\rho+m_b)^2}\right)}\delta_{m_{l_\lambda},1}, \tag{3.31}$$

$$\langle 0,0,0,0,0,0|\hat{T}_{3,-}|0,0,0,0,1,m_{l\lambda}\rangle = -2i\sqrt{\tfrac{2}{3}}\alpha_\lambda e^{\frac{-3k^2m_\rho^2}{2\alpha_\lambda^2(2m_\rho+m_b)^2}}\delta_{m_{l_\lambda},1}. \tag{3.32}$$

Further details on the relationship between the matrix elements of $\hat{T}_{j,-}$, expressed as a sum of matrix elements involving the $\hat{U}_j$ operators, are provided in Appendix A.3.3. The methodology outlined in this work enables the exact analytical evaluation of the matrix elements associated with the $\hat{T}_{j,-}$ operators.

When calculating the electromagnetic decay widths, the uncertainties associated with both the mass model parameters and the decay product masses are taken into account. The experimental values of the decay product masses, along with their corresponding uncertainties, are listed in Table 2.12. The propagation of errors was performed using the Monte Carlo method described in Section 2.4.3.

3.1.1 Results of electromagnetic decay widths

Tables 3.1-3.5 present the results obtained for the electromagnetic decay widths of the Λ_b, Ξ_b, Σ_b, Ξ_b', and Ω_b baryons, calculated using eq. (3.2) for transitions from P-wave excited states to ground states, as well as ground-to-ground state transitions. These results expand upon those reported in previous studies on the subject [70, 71, 82, 129–142]. Furthermore, our theoretical predictions are compared with previous results obtained using models such as the CQM [70] and NRQM [115], as shown in the same tables.

3.2 Discussion and Conclusions of the chapter

The experimental widths of hadronic states include contributions from strong, electromagnetic, and weak interactions, with the dominant component typically arising from strong decays. In contrast, our computed electromagnetic decay widths constitute only a small fraction of the total decay width, as expected.

Nevertheless, electromagnetic decays are particularly important in scenarios where strong decays are forbidden. A notable example is the spin excitation of the Ω_b^- baryon, denoted as Ω_b^*, which has not yet been observed experimentally. The strong decay $\Omega_b^* \to \Omega_b^-\pi$ is kinematically forbidden due to the lack of phase space and isospin conservation constraints. Given that the $\Omega_b(6093)$ state has not been discovered, an intriguing experimental opportunity exists to search for this resonance via the electromagnetic decay channel $\Omega_b^* \to \Omega_b^-\gamma$. Moreover, electromagnetic decay widths can assist with the assignments when different states have comparable masses and total widths, thus providing an additional discriminating tool in hadron spectroscopy.

It is important to note that alternative approaches have been employed in the literature to evaluate electromagnetic transitions. One such method was introduced by Close and Copley in 1970 [143]. In their work, they used the well-known commutation relation $i[H_0, \mathbf{r}_j] = \mathbf{p}_j/m_j$, where $H_0 = \sum_i \mathbf{p}_i^2/(2m_i)$ is the free Hamiltonian of constituent quarks. By approximating

TABLE 3.1: *Table from [90] (APS copyright).* Predicted electromagnetic decay widths (in KeV) for $\Lambda_b(nnb)$ states belonging to the flavor multiplet $\mathcal{F} = \bar{\mathbf{3}}_{\mathrm{F}}$. The first column reports the baryon name with its predicted mass, calculated by using the three-quark model Hamiltonian given by eqs. (2.44) and (2.45). The second column displays $\mathbf{J}^{\mathrm{P}}$, the third column shows the internal configuration of the baryon $|l_\lambda, l_\rho, k_\lambda, k_\rho\rangle$ within the three-quark model, where $l_{\lambda,\rho}$ represent the orbital angular momenta and $k_{\lambda,\rho}$ denote the number of nodes of the λ and ρ oscillators. The fourth column presents the spectroscopic notation $^{2S+1}L_J$ for each state. Furthermore, $N = n_\rho + n_\lambda$ separates the $N = 0, 1$ energy bands. Starting from the fifth column, the electromagnetic decay widths, computed by using eq. (3.2), are presented. Each column corresponds to an electromagnetic decay channel, the decay products are indicated at the top of the column and their masses are shown in Table 2.12. The zero values are electromagnetic decay widths that are either too small to be shown on this scale or not permitted by phase space. Our results are compared with those of references [70] and [115]. The symbol "..." indicates that there is no prediction for that state in reference [70].

$\mathcal{F} = \bar{\mathbf{3}}_{\mathrm{F}}$							
$\Lambda_b(nnb)$	$\mathbf{J}^{\mathbf{P}}$	$\lvert l_\lambda, l_\rho, k_\lambda, k_\rho\rangle$	$^{2S+1}L_J$	$\Lambda_b^0\gamma$	$\Sigma_b^0\gamma$	$\Sigma_b^*\gamma$	
$N = 0$							
$\Lambda_b(5613)$	$\frac{1}{2}^+$	$\lvert 0, 0, 0, 0\rangle$	$^2S_{1/2}$	0	0	0	
$N = 1$							
$\Lambda_b(5918)$	$\frac{1}{2}^-$	$\lvert 1, 0, 0, 0\rangle$	$^2P_{1/2}$	64^{+5}_{-4}	$0.4^{+0.1}_{-0.1}$	0	
				50.2	0.14	0.09	[70]
				40.7	0.2	0.0	[115]
$\Lambda_b(5924)$	$\frac{3}{2}^-$	$\lvert 1, 0, 0, 0\rangle$	$^2P_{3/2}$	65^{+5}_{-5}	$0.5^{+0.2}_{-0.2}$	$0.1^{+0.03}_{-0.03}$	
				52.8	0.21	0.15	[70]
				43.4	0.3	0.0	[115]
$\Lambda_b(6114)$	$\frac{1}{2}^-$	$\lvert 0, 1, 0, 0\rangle$	$^2P_{1/2}$	15^{+2}_{-2}	519^{+40}_{-39}	3^{+1}_{-1}	
				1.62	16.2	0.02	[70]
				10.2	93.3	2.0	[115]
$\Lambda_b(6137)$	$\frac{1}{2}^-$	$\lvert 0, 1, 0, 0\rangle$	$^4P_{1/2}$	9^{+2}_{-1}	6^{+2}_{-2}	76^{+16}_{-17}	
				0.81	0.02	8.25	[70]
				5.6	3.5	6.2	[115]
$\Lambda_b(6121)$	$\frac{3}{2}^-$	$\lvert 0, 1, 0, 0\rangle$	$^2P_{3/2}$	16^{+2}_{-2}	1025^{+101}_{-94}	3^{+1}_{-1}	
				1.81	15.1	0.03	[70]
				10.6	315.6	2.2	[115]
$\Lambda_b(6143)$	$\frac{3}{2}^-$	$\lvert 0, 1, 0, 0\rangle$	$^4P_{3/2}$	25^{+4}_{-4}	17^{+6}_{-4}	382^{+30}_{-30}	
				2.54	0.07	9.90	[70]
				16.2	10.6	73.9	[115]
$\Lambda_b(6153)$	$\frac{5}{2}^-$	$\lvert 0, 1, 0, 0\rangle$	$^4P_{5/2}$	17^{+3}_{-3}	12^{+4}_{-4}	1023^{+111}_{-108}	
				...	...	...	[70]
				11.0	7.8	216.5	[115]

TABLE 3.2: *Table from [90] (APS copyright).* Same as Table 3.1, but for $\Xi_b(snb)$ states belonging to the flavor multiplet $\mathcal{F} = \bar{\mathbf{3}}_{\mathrm{F}}$.

$\mathcal{F} = \bar{\mathbf{3}}_{\mathrm{F}}$											
$\Xi_b(snb)$	$\mathbf{J^P}$	$\lvert l_\lambda, l_\rho, k_\lambda, k_\rho\rangle$	$^{2S+1}L_J$	$\Xi_b^0\gamma$	$\Xi_b^-\gamma$	$\Xi_b'^0\gamma$	$\Xi_b'^-\gamma$	$\Xi_b'^{*0}\gamma$	$\Xi_b'^{*-}\gamma$	
$N = 0$										
$\Xi_b(5806)$	$\frac{1}{2}^+$	$\lvert 0, 0, 0, 0\rangle$	$^2S_{1/2}$	0	0	0	0	0	0	
$N = 1$										
$\Xi_b(6079)$	$\frac{1}{2}^-$	$\lvert 1, 0, 0, 0\rangle$	$^2P_{1/2}$	122^{+16}_{-13}	126^{+10}_{-10}	$1.1^{+0.3}_{-0.3}$	0	$0.2^{+0.06}_{-0.06}$	0	
				63.6	135	1.32	0.0	2.04	0.0	[70]
				83.1	91.5	0.6	0.0	0.1	0.0	[115]
$\Xi_b(6085)$	$\frac{3}{2}^-$	$\lvert 1, 0, 0, 0\rangle$	$^2P_{3/2}$	125^{+16}_{-13}	126^{+10}_{-10}	$1.3^{+0.4}_{-0.4}$	0	$0.2^{+0.06}_{-0.06}$	0	
				68.3	147	1.68	0.0	2.64	0.0	[70]
				88.9	96.1	0.7	0.0	0.2	0.0	[115]
$\Xi_b(6248)$	$\frac{1}{2}^-$	$\lvert 0, 1, 0, 0\rangle$	$^2P_{1/2}$	19^{+5}_{-4}	28^{+6}_{-5}	494^{+36}_{-34}	9^{+2}_{-1}	$2^{+0.6}_{-0.6}$	0	
				1.86	7.19	94.3	0.0	0.62	0.0	[70]
				13.3	21.8	144.5	3.1.	1.7	0.0	[115]
$\Xi_b(6271)$	$\frac{1}{2}^-$	$\lvert 0, 1, 0, 0\rangle$	$^4P_{1/2}$	11^{+4}_{-3}	17^{+4}_{-4}	5^{+2}_{-2}	$0.1^{+0.03}_{-0.03}$	75^{+14}_{-15}	$1.4^{+0.4}_{-0.4}$	
				0.93	3.59	0.16	0.0	80.0	0.0	[70]
				7.5	12.3	2.9	0.1	14.7	0.3	[115]
$\Xi_b(6255)$	$\frac{3}{2}^-$	$\lvert 0, 1, 0, 0\rangle$	$^2P_{3/2}$	20^{+5}_{-4}	29^{+6}_{-5}	950^{+98}_{-89}	17^{+4}_{-3}	3^{+1}_{-1}	0	
				2.10	8.13	69.4	0.0	0.80	0.0	[70]
				14.0	23.0	377.2	8.0	1.9	0.0	[115]
$\Xi_b(6277)$	$\frac{3}{2}^-$	$\lvert 0, 1, 0, 0\rangle$	$^4P_{3/2}$	33^{+9}_{-7}	48^{+11}_{-10}	14^{+5}_{-4}	$0.3^{+0.1}_{-0.1}$	363^{+28}_{-27}	7^{+1}_{-1}	
				2.94	11.4	0.8	0.0	78.0	0.0	[70]
				22.2	36.3	8.8	0.2	109.7	2.3	[115]
$\Xi_b(6287)$	$\frac{5}{2}^-$	$\lvert 0, 1, 0, 0\rangle$	$^4P_{5/2}$	23^{+6}_{-5}	34^{+8}_{-7}	10^{+4}_{-3}	$0.2^{+0.06}_{-0.06}$	945^{+106}_{-99}	17^{+4}_{-3}	
				...	...	...	...	...	...	[70]
				15.4	25.3	6.5	0.1	245.2	5.2	[115]

TABLE 3.3: *Table from [90] (APS copyright).* Same as Table 3.1, but for $\Sigma_b(nnb)$ states belonging to the flavor multiplet $\mathcal{F} = \mathbf{6}_{\rm F}$.

$\mathcal{F} = \mathbf{6}_{\rm F}$												
$\Sigma_b(nnb)$	$\mathbf{J^P}$	$\lvert l_\lambda, l_\rho, k_\lambda, k_\rho\rangle$	$^{2S+1}L_J$	$\Sigma_b^+\gamma$	$\Sigma_b^0\gamma$	$\Sigma_b^-\gamma$	$\Lambda_b^0\gamma$	$\Sigma_b^{*+}\gamma$	$\Sigma_b^{*0}\gamma$	$\Sigma_b^{*-}\gamma$	
$N=0$											
$\Sigma_b(5804)$	$\frac{1}{2}^+$	$\lvert 0,0,0,0\rangle$	$^2S_{1/2}$	0	0	0	150^{+46}_{-40}	0	0	0	
$\Sigma_b(5832)$	$\frac{3}{2}^+$	$\lvert 0,0,0,0\rangle$	$^4S_{3/2}$	$0.5^{+0.2}_{-0.2}$	0	$0.1^{+0.03}_{-0.03}$	215^{+56}_{-51}	0	0	0	
$N=1$											
$\Sigma_b(6108)$	$\frac{1}{2}^-$	$\lvert 1,0,0,0\rangle$	$^2P_{1/2}$	407^{+46}_{-47}	34^{+3}_{-3}	73^{+10}_{-10}	195^{+32}_{-27}	6^{+3}_{-2}	$0.4^{+0.1}_{-0.1}$	$2^{+1}_{-0.6}$	
				1016	74.9	212	133	16.9	1.03	4.36	[70]
				267.7	21.3	50.9	156.2	5.3	0.3	1.5	[115]
$\Sigma_b(6131)$	$\frac{1}{2}^-$	$\lvert 1,0,0,0\rangle$	$^4P_{1/2}$	13^{+5}_{-4}	$0.8^{+0.2}_{-0.2}$	3^{+1}_{-1}	111^{+19}_{-17}	36^{+18}_{-17}	4^{+1}_{-1}	5^{+2}_{-2}	
				5.31	0.32	1.37	63.6	867	63.6	182	[70]
				8.9	0.5	2.5	85.3	19.2	1.9	2.7	[115]
$\Sigma_b(6114)$	$\frac{3}{2}^-$	$\lvert 1,0,0,0\rangle$	$^2P_{3/2}$	1202^{+132}_{-122}	89^{+10}_{-9}	252^{+28}_{-26}	202^{+31}_{-28}	7^{+3}_{-2}	$0.4^{+0.1}_{-0.1}$	$2^{+0.6}_{-0.6}$	
				483	37.9	94	129	15.6	0.95	4.02	[70]
				864.7	59.3	196.2	162.2	5.8	0.3	1.6	[115]
$\Sigma_b(6137)$	$\frac{3}{2}^-$	$\lvert 1,0,0,0\rangle$	$^4P_{3/2}$	40^{+12}_{-10}	$2^{+0.6}_{-0.6}$	10^{+3}_{-3}	321^{+46}_{-42}	316^{+31}_{-32}	26^{+2}_{-2}	59^{+7}_{-7}	
				13.1	0.8	3.39	170	527	39.8	107	[70]
				27.2	1.5	7.7	247.4	209.6	16.2	41.6	[115]
$\Sigma_b(6147)$	$\frac{5}{2}^-$	$\lvert 1,0,0,0\rangle$	$^4P_{5/2}$	29^{+10}_{-8}	$2^{+0.6}_{-0.6}$	7^{+2}_{-2}	218^{+34}_{-30}	1222^{+151}_{-141}	90^{+11}_{-10}	256^{+33}_{-30}	
				8.07	0.49	2.08	83.3	426	32.6	85.3	[70]
				20.0	1.1	5.7	168.2	589.4	39.5	137.0	[115]
$\Sigma_b(6304)$	$\frac{1}{2}^-$	$\lvert 0,1,0,0\rangle$	$^2P_{1/2}$	247^{+45}_{-40}	15^{+3}_{-2}	62^{+11}_{-10}	424^{+42}_{-42}	103^{+22}_{-19}	6^{+1}_{-1}	26^{+5}_{-5}	
				...	...	...	...	...	...	...	[70]
				182.1	10.3	50.2	526.5	79.3	4.5	21.9	[115]
$\Sigma_b(6311)$	$\frac{3}{2}^-$	$\lvert 0,1,0,0\rangle$	$^2P_{3/2}$	256^{+46}_{-41}	16^{+3}_{-3}	64^{+12}_{-10}	414^{+39}_{-39}	107^{+22}_{-19}	7^{+1}_{-1}	27^{+5}_{-5}	
				...	...	...	...	...	...	...	[70]
				189.2	10.7	52.1	523.1	82.8	4.7	22.8	[115]

TABLE 3.4: *Table from [90] (APS copyright).* Same as Table 3.1, but for $\Xi_b'(snb)$ states belonging to the flavor multiplet $\mathcal{F} = \mathbf{6}_{\rm F}$.

$\mathcal{F} = \mathbf{6}_{\rm F}$											
$\Xi_b'(snb)$	$\mathbf{J^P}$	$\lvert l_\lambda, l_\rho, k_\lambda, k_\rho\rangle$	$^{2S+1}L_J$	$\Xi_b^0\gamma$	$\Xi_b^-\gamma$	$\Xi_b'^0\gamma$	$\Xi_b'^-\gamma$	$\Xi_b'^{*0}\gamma$	$\Xi_b'^{*-}\gamma$	
$N = 0$										
$\Xi_b'(5925)$	$\frac{1}{2}^+$	$\lvert 0,0,0,0\rangle$	$^2S_{1/2}$	33^{+16}_{-13}	$0.6^{+0.2}_{-0.2}$	0	0	0	0	
$\Xi_b'(5953)$	$\frac{3}{2}^+$	$\lvert 0,0,0,0\rangle$	$^4S_{3/2}$	60^{+24}_{-20}	$1.1^{+0.3}_{-0.3}$	$0.1^{+0.03}_{-0.03}$	$0.1^{+0.03}_{-0.03}$	0	0	
$N = 1$										
$\Xi_b'(6198)$	$\frac{1}{2}^-$	$\lvert 1,0,0,0\rangle$	$^2P_{1/2}$	65^{+13}_{-11}	$1.2^{+0.3}_{-0.3}$	78^{+9}_{-8}	71^{+7}_{-6}	$0.4^{+0.1}_{-0.1}$	$0.6^{+0.2}_{-0.2}$	
				72.2	0.0	76.3	190	0.89	3.54	[70]
				50.7	1.1	52.9	50.8	0.3	0.5	[115]
$\Xi_b'(6220)$	$\frac{1}{2}^-$	$\lvert 1,0,0,0\rangle$	$^4P_{1/2}$	40^{+9}_{-8}	$0.7^{+0.2}_{-0.2}$	$1^{+0.3}_{-0.3}$	$1.4^{+0.4}_{-0.4}$	11^{+2}_{-2}	9^{+2}_{-2}	
				34	0.0	0.25	1.48	69.5	164	[70]
				29.3	0.6	0.6	1.0	6.9	5.6	[115]
$\Xi_b'(6204)$	$\frac{3}{2}^-$	$\lvert 1,0,0,0\rangle$	$^2P_{3/2}$	68^{+13}_{-12}	$1.3^{+0.4}_{-0.4}$	157^{+18}_{-15}	167^{+15}_{-15}	$0.4^{+0.1}_{-0.1}$	$1^{+0.3}_{-0.3}$	
				72.8	0.0	43.9	92.3	0.9	3.6	[70]
				53.9	1.1	111.5	128.1	0.3	0.6	[115]
$\Xi_b'(6226)$	$\frac{3}{2}^-$	$\lvert 1,0,0,0\rangle$	$^4P_{3/2}$	117^{+21}_{-19}	$2^{+0.6}_{-0.6}$	3^{+1}_{-1}	4^{+1}_{-1}	57^{+6}_{-5}	54^{+5}_{-4}	
				94.0	0.0	0.67	2.94	47.5	104	[70]
				87.1	1.8	1.7	3.0	38.8	38.5	[115]
$\Xi_b'(6237)$	$\frac{5}{2}^-$	$\lvert 1,0,0,0\rangle$	$^4P_{5/2}$	82^{+18}_{-15}	$2^{+0.6}_{-0.6}$	$2^{+0.6}_{-0.6}$	3^{+1}_{-1}	157^{+21}_{-18}	168^{+19}_{-17}	
				47.7	0.0	0.44	1.88	41.5	88.2	[70]
				61.6	1.3	1.3	2.2	69.4	82.7	[115]
$\Xi_b'(6367)$	$\frac{1}{2}^-$	$\lvert 0,1,0,0\rangle$	$^2P_{1/2}$	644^{+54}_{-52}	12^{+3}_{-2}	19^{+3}_{-3}	28^{+5}_{-4}	7^{+1}_{-1}	11^{+2}_{-2}	
				...	...	...	...	...	...	[70]
				708.1	15.0	13.4	21.9	5.5	9.0	[115]
$\Xi_b'(6374)$	$\frac{3}{2}^-$	$\lvert 0,1,0,0\rangle$	$^2P_{3/2}$	637^{+52}_{-50}	12^{+3}_{-2}	20^{+4}_{-3}	29^{+5}_{-5}	8^{+2}_{-1}	12^{+2}_{-2}	
				...	...	...	...	...	...	[70]
				714.7	15.2	14.1	23.0	5.9	9.6	[115]

TABLE 3.5: *Table from [90] (APS copyright).* Same as Table 3.1, but for $\Omega_b(ssb)$ states belonging to the flavor multiplet $\mathcal{F} = \mathbf{6}_{\rm F}$.

$\mathcal{F} = \mathbf{6}_{\rm F}$						
$\Omega_b(ssb)$	$\mathbf{J^P}$	$\vert l_\lambda, l_\rho, k_\lambda, k_\rho\rangle$	$^{2S+1}L_J$	$\Omega_b\gamma$	$\Omega_b^*\gamma$	
$N = 0$						
$\Omega_b(6064)$	$\frac{1}{2}^+$	$\vert 0,0,0,0\rangle$	$^2S_{1/2}$	0	0	
$\Omega_b(6093)$	$\frac{3}{2}^+$	$\vert 0,0,0,0\rangle$	$^4S_{3/2}$	$0.1^{+0.03}_{-0.03}$	0	
$N = 1$						
$\Omega_b(6315)$	$\frac{1}{2}^-$	$\vert 1,0,0,0\rangle$	$^2P_{1/2}$	51^{+5}_{-4}	$0.2^{+0.06}_{-0.06}$	
				154	1.49	[70]
				36.0	0.2	[115]
$\Omega_b(6337)$	$\frac{1}{2}^-$	$\vert 1,0,0,0\rangle$	$^4P_{1/2}$	$0.5^{+0.2}_{-0.2}$	8^{+2}_{-2}	
				0.64	99.23	[70]
				0.4	5.1	[115]
$\Omega_b(6321)$	$\frac{3}{2}^-$	$\vert 1,0,0,0\rangle$	$^2P_{3/2}$	99^{+10}_{-10}	$0.2^{+0.06}_{-0.06}$	
				83.4	1.51	[70]
				73.7	0.2	[115]
$\Omega_b(6343)$	$\frac{3}{2}^-$	$\vert 1,0,0,0\rangle$	$^4P_{3/2}$	$2^{+0.6}_{-0.6}$	38^{+3}_{-3}	
				1.81	70.68	[70]
				1.1	26.7	[115]
$\Omega_b(6353)$	$\frac{5}{2}^-$	$\vert 1,0,0,0\rangle$	$^4P_{5/2}$	$1^{+0.2}_{-0.3}$	99^{+12}_{-12}	
				1.21	63.26	[70]
				0.9	45.1	[115]
$\Omega_b(6465)$	$\frac{1}{2}^-$	$\vert 0,1,0,0\rangle$	$^2P_{1/2}$	12^{+2}_{-2}	4^{+1}_{-1}	
				...	...	[70]
				8.7	3.4	[115]
$\Omega_b(6471)$	$\frac{3}{2}^-$	$\vert 0,1,0,0\rangle$	$^2P_{3/2}$	12^{+3}_{-2}	5^{+1}_{-1}	
				...	...	[70]
				9.2	3.7	[115]

$i[H_0, \mathbf{r}_j] \approx i\mathrm{k}\mathbf{r}_j$, they effectively rewrote the convective term of the electromagnetic Hamiltonian in eq. (3.8), substituting $\mathbf{p}_j/m_j$ with $i\mathrm{k}\mathbf{r}_j$, as follows:

$$\begin{aligned}\mathcal{H}_{\text{conv}} &= -\sum_{j=1}^{3} \frac{1}{(2\pi)^{3/2}} \frac{\mathrm{e}_j}{(2\mathrm{k})^{1/2}} \left\{ \frac{\mathbf{p}_j \cdot \boldsymbol{\varepsilon} e^{-i\mathbf{k}\cdot\mathbf{r}_j} + e^{-i\mathbf{k}\cdot\mathbf{r}_j} \boldsymbol{\varepsilon} \cdot \mathbf{p}_j}{2m_j} \right\} \\ &\approx -i \sum_{j=1}^{3} \frac{\mathrm{e}_j}{2(2\pi)^{3/2}} \sqrt{\frac{\mathrm{k}}{2}} \left\{ \mathbf{r}_j \cdot \boldsymbol{\varepsilon} e^{-i\mathbf{k}\cdot\mathbf{r}_j} + e^{-i\mathbf{k}\cdot\mathbf{r}_j} \boldsymbol{\varepsilon} \cdot \mathbf{r}_j \right\} \\ &\approx -i \sum_{j=1}^{3} \frac{\mathrm{e}_j}{(2\pi)^{3/2}} \sqrt{\frac{\mathrm{k}}{2}} \mathbf{r}_j \cdot \boldsymbol{\varepsilon} e^{-i\mathbf{k}\cdot\mathbf{r}_j}.\end{aligned} \tag{3.33}$$

It should be noted that the approximation $i[H_0, \mathbf{r}_j] \approx i\mathrm{k}\mathbf{r}_j$ cannot be derived rigorously but rather stems from dimensional analysis. As a result, employing eq. (3.33) in the study of electromagnetic transitions inevitably entails the loss of important information inherent to the original system. Despite this limitation, the approximation has been widely adopted in the literature. For instance, Iachello and Kusnesov used it in reference [144] to calculate radiative transitions in light mesons. More recently, this method has been extensively applied in electromagnetic studies of both mesons and baryons [70, 82, 145–148].

A different approach was employed in reference [115] to calculate the electromagnetic decays of heavy baryons. In this method, the authors replaced $\mathbf{p}_\lambda$ with $im_\lambda \mathrm{k}_0 \boldsymbol{\lambda}$ and $\mathbf{p}_\rho$ with $im_\rho \mathrm{k}_0 \boldsymbol{\rho}$. It is worth noting that this substitution does not precisely correspond to the approximation $\mathbf{p}_j/m_j \to i\mathrm{k}\mathbf{r}_j$, originally introduced by Close and Copley [143] and commonly accepted in the literature. This distinction highlights subtle differences in how the convective term is treated across other models.

In this chapter, the electromagnetic decay widths obtained using eq. (3.9) are compared with those reported in reference [70], which were calculated using the approximation given in eq. (3.33), and reference [115], which applies the substitution discussed previously. These comparisons highlight the advantages of our full calculation based on eq. (3.9), which avoids additional approximations and therefore yields more robust and reliable results.

In summary, the electromagnetic decay widths of singly bottom baryons were calculated using eq. (3.2). It was demonstrated that the convective term in the nonrelativistic Hamiltonian given in eq. (3.9) can be evaluated in a fully analytical and exact manner, without the need for any additional approximations. This rigorous treatment of the transition amplitudes ensures that the results presented in this work are more robust than those obtained in previous studies, such as references [70, 115]. Importantly, the analytical nature of our approach eliminates the necessity for further approximations, underscoring the reliability and precision of the present method. The results reported in this chapter have been published in *Physical Review D* [90].

Chapter 4

Electromagnetic decays of the second shell singly bottom baryons

This Chapter is devoted to the calculations of the electromagnetic decay widths of singly bottom baryons within the constituent quark model formalism. These decays are computed from the states of the second shell to the ground states and P-wave states.

The electromagnetic decays are useful to confirm the existence of some resonances. As mentioned in Chapter 3, when the strong decays are not allowed the electromagnetic decays play a dominant role. They can also help with the assignments when states have the same mass and total decay widths.

4.1 Electromagnetic decay widths

In this section, the electromagnetic decay widths of the singly bottom baryons from the states of the second shell to the ground states and P-wave states are calculated. These decay widths are calculated by means of eq. (3.2) following the same procedure employed in Chapter 3. In the spin and flavor spaces the matrix elements are the same as those used in Chapter 3 (see Sections A.1 and A.2 of Appendix A for more details). The matrix elements in the spatial space have to be calculated to be able to calculate the decay widths.

To date, the radiative decays of second shell singly bottom baryons remain largely unexplored. Only references [71] and [82], have addressed these processes. In reference [71], the authors considered only transitions from pure D_λ states to P_λ states within the framework of the NRQM. Meanwhile, reference [82] investigated decays from D_λ-wave and λ-mode radial excitations to ground-state singly bottom baryons using the Gaussian Expansion Method (GEM). This work extend the electromagnetic decays for all second shell states to the ground states and P-wave states.

4.1.1 Spatial matrix elements

To calculate the electromagnetic decay widths of second shell singly bottom baryons to ground and P-wave states it is first required to compute matrix elements of the form

TABLE 4.1: Predicted electromagnetic decay widths (in KeV) for second shell $\Lambda_b^0(nnb)$ states belonging to the flavor multiplet $\mathcal{F} = \bar{\mathbf{3}}_{\mathrm{F}}$. The first column reports the baryon name with its predicted mass, calculated in [90]. The second column displays $\mathbf{J}^{\mathrm{P}}$, the third column shows the internal configuration of the baryon $|l_\lambda, l_\rho, k_\lambda, k_\rho\rangle$ within the three-quark model, where $l_{\lambda,\rho}$ represent the orbital angular momenta and $k_{\lambda,\rho}$ denote the number of nodes of the λ and ρ oscillators. The fourth column presents the spectroscopic notation $^{2S+1}L_J$ for each state. Furthermore, $N = n_\rho + n_\lambda$ separates the $N = 0, 1$ energy bands. Starting from the fifth column, the electromagnetic decay widths, computed by using eq. (3.2), are presented. Each column corresponds to an electromagnetic decay channel, the decay products are indicated at the top of the column and their masses are shown in Table 2.12. The zero values are electromagnetic decay widths that are either too small to be shown on this scale or not permitted by phase space.

$\mathcal{F} = \bar{\mathbf{3}}_{\mathrm{F}}$				$\Lambda_b^0\gamma$	$\Sigma_b^0\gamma$	$\Sigma_b^{*0}\gamma$	$\Lambda_b^0\gamma$	$\Lambda_b^0\gamma$	$\Lambda_b^0\gamma$	$\Lambda_b^0\gamma$	$\Lambda_b^0\gamma$	$\Lambda_b^0\gamma$	$\Lambda_b^0\gamma$	$\Sigma_b^0\gamma$	$\Sigma_b^0\gamma$	$\Sigma_b^0\gamma$	$\Sigma_b^0\gamma$	$\Sigma_b^0\gamma$	$\Sigma_b^0\gamma$	$\Sigma_b^0\gamma$
$\Lambda_b^0(nnb)$	$\mathbf{J}^{\mathbf{P}}$	$\lvert l_\lambda, l_\rho, k_\lambda, k_\rho\rangle$	$^{2S+1}L_J$	$^2S_{1/2}$	$^2S_{1/2}$	$^4S_{3/2}$	$^2_\lambda P_{1/2}$	$^2_\lambda P_{3/2}$	$^2_\rho P_{1/2}$	$^4_\rho P_{1/2}$	$^2_\rho P_{3/2}$	$^4_\rho P_{3/2}$	$^4_\rho P_{5/2}$	$^2_\lambda P_{1/2}$	$^4_\lambda P_{1/2}$	$^2_\lambda P_{3/2}$	$^4_\lambda P_{3/2}$	$^4_\lambda P_{5/2}$	$^2_\rho P_{1/2}$	$^2_\rho P_{3/2}$
$N = 2$																				
$\Lambda_b(6225)^0$	$\frac{3}{2}^+$	$\lvert 2,0,0,0\rangle$	$^2D_{3/2}$	15.36	9.2	3.1	92.2	14.5	0	0	0	0	0	0.2	0.21	0.2	0.04	0.003	0	0
$\Lambda_b(6235)^0$	$\frac{5}{2}^+$	$\lvert 2,0,0,0\rangle$	$^2D_{5/2}$	15.28	10.4	3.6	0.4	107.4	0	0	0	0	0	0.5	0.02	0.4	0.1	0.07	0	0
$\Lambda_b(6231)^0$	$\frac{1}{2}^+$	$\lvert 0,0,1,0\rangle$	$^2S_{1/2}$	0	24.8	8.5	53.2	24.8	0	0	0	0	0	2.05	0	4.8	0.02	0.4	0	0
$\Lambda_b(6624)^0$	$\frac{1}{2}^+$	$\lvert 0,0,0,1\rangle$	$^2S_{1/2}$	0	157.3	72.9	2.2	1.1	41.1	0.3	118.0	1.2	39.3	36.1	0.2	98.4	0.8	23.9	640.9	317.3
$\Lambda_b(6421)^0$	$\frac{3}{2}^+$	$\lvert 1,1,0,0\rangle$	$^2D_{3/2}$	19.6	123.8	10.7	1.9	1.6	29.8	0.58	3.8	0.17	0.02	417.4	3.9	58.8	1.2	0.1	0.1	0.1
$\Lambda_b(6431)^0$	$\frac{5}{2}^+$	$\lvert 1,1,0,0\rangle$	$^2D_{5/2}$	20.2	688.6	11.6	4.8	2.9	4.8	0.06	59.2	0.3	0.2	38.9	0.5	700.3	2.0	1.5	0.2	0.2
$\Lambda_b(6438)^0$	$\frac{1}{2}^+$	$\lvert 1,1,0,0\rangle$	$^4D_{1/2}$	10.2	14.4	40.2	4.1	0.2	0.5	19.4	0.001	6.2	0.4	3.6	322.1	0	67.3	6.6	0.3	0.004
$\Lambda_b(6444)^0$	$\frac{3}{2}^+$	$\lvert 1,1,0,0\rangle$	$^4D_{3/2}$	20.7	29.8	100.4	10.2	1.4	1.37	20.7	0.08	10.4	1.6	8.8	254.8	0.5	168.8	21.4	0.91	0.05
$\Lambda_b(6454)^0$	$\frac{5}{2}^+$	$\lvert 1,1,0,0\rangle$	$^4D_{5/2}$	28.8	42.9	194.0	3.9	8.8	0.5	3.3	1.2	36.7	6.2	3.5	24.4	7.7	457.7	95.5	0.5	0.9
$\Lambda_b(6468)^0$	$\frac{7}{2}^+$	$\lvert 1,1,0,0\rangle$	$^4D_{7/2}$	18.7	29.4	708.0	1.03	9.5	0.01	0.2	1.5	4.3	65.7	0.15	5.7	9.4	36.3	747.5	0	1.4
$\Lambda_b(6423)^0$	$\frac{1}{2}^-$	$\lvert 1,1,0,0\rangle$	$^2P_{1/2}$	0	33.9	0	0	0	46.9	0.69	7.2	0.5	0.1	498.9	4.8	46.8	3.6	0.8	0	0
$\Lambda_b(6429)^0$	$\frac{3}{2}^-$	$\lvert 1,1,0,0\rangle$	$^2P_{3/2}$	0	33.9	0	8.2	3.9	25.3	0.2	33.8	0.3	0.1	225.6	1.7	350.6	2.3	0.8	0.3	0.1
$\Lambda_b(6446)^0$	$\frac{1}{2}^-$	$\lvert 1,1,0,0\rangle$	$^4P_{1/2}$	0	0	8.5	13.5	6.5	1.3	11.7	0.6	3.6	0.5	8.8	124.7	4.1	65.8	0.7	0.8	0.3
$\Lambda_b(6452)^0$	$\frac{3}{2}^-$	$\lvert 1,1,0,0\rangle$	$^4P_{3/2}$	0	0	23.7	7.4	3.6	0.7	44.8	0.3	4.1	2.38	5.1	431.3	2.4	52.8	20.9	0.5	0.2
$\Lambda_b(6462)^0$	$\frac{5}{2}^-$	$\lvert 1,1,0,0\rangle$	$^4P_{5/2}$	0	0	32.2	2.9	15.7	0.3	0.8	1.6	37.9	22.8	2.1	1.08	10.9	348.4	243.2	0.3	1.2
$\Lambda_b(6456)^0$	$\frac{3}{2}^+$	$\lvert 1,1,0,0\rangle$	$^4S_{3/2}$	0	0	0	0.8	1.7	0.4	26.4	0.8	23.5	2.9	2.3	253.9	4.4	256.8	50.3	0.4	0.7
$\Lambda_b(6427)^0$	$\frac{1}{2}^+$	$\lvert 1,1,0,0\rangle$	$^2S_{1/2}$	0	0	0	0.9	1.9	46.7	0.1	5.8	0.02	0.2	467.4	0.7	91.4	0.1	1.1	0.2	0.3
$\Lambda_b(6618)^0$	$\frac{3}{2}^+$	$\lvert 0,2,0,0\rangle$	$^2D_{3/2}$	9.3	62.0	28.7	12.2	10.08	5.9	17.7	6.8	5.8	0.6	2.26	0.8	4.18	0.15	1.18	1206.3	186.6
$\Lambda_b(6628)^0$	$\frac{5}{2}^+$	$\lvert 0,2,0,0\rangle$	$^2D_{5/2}$	9.0	63.6	29.6	5.1	17.5	11.8	1.9	9.8	8.5	7.2	2.6	0.9	4.8	0.2	1.4	2.9	1390.6

TABLE 4.2: Same as Table 4.1, but for $\Xi_b^0(snb)$ states belonging to the flavor multiplet $\mathcal{F} = \bar{\mathbf{3}}_{\mathrm{F}}$.

$\mathcal{F} = \bar{\mathbf{3}}_{\mathrm{F}}$				$\Xi_b^0\gamma$	$\Xi_b^{\prime 0}\gamma$	$\Xi_b^{*0}\gamma$	$\Xi_b^0\gamma$	$\Xi_b^0\gamma$	$\Xi_b^0\gamma$	$\Xi_b^0\gamma$	$\Xi_b^0\gamma$	$\Xi_b^0\gamma$	$\Xi_b^0\gamma$	$\Xi_b^{\prime 0}\gamma$	$\Xi_b^{*0}\gamma$	$\Xi_b^{\prime 0}\gamma$	$\Xi_b^{*0}\gamma$	$\Xi_b^{*0}\gamma$	$\Xi_b^{\prime 0}\gamma$	$\Xi_b^{\prime 0}\gamma$
$\Xi_b^0(snb)$	$\mathbf{J^P}$	$\lvert l_\lambda, l_\rho, k_\lambda, k_\rho\rangle$	$^{2S+1}L_J$	$^2S_{1/2}$	$^2S_{1/2}$	$^4S_{3/2}$	$^2_\lambda P_{1/2}$	$^2_\lambda P_{3/2}$	$^2_\rho P_{1/2}$	$^4_\rho P_{1/2}$	$^2_\rho P_{3/2}$	$^4_\rho P_{3/2}$	$^4_\rho P_{5/2}$	$^2_\lambda P_{1/2}$	$^4_\lambda P_{1/2}$	$^2_\lambda P_{3/2}$	$^4_\lambda P_{3/2}$	$^4_\lambda P_{5/2}$	$^2_\rho P_{1/2}$	$^2_\rho P_{3/2}$
$N = 2$																				
$\Xi_b(6354)^0$	$\frac{3}{2}^+$	$\lvert 2,0,0,0\rangle$	$^2D_{3/2}$	30.3	6.4	2.2	184.8	27.8	0	0	0	0	0	0.5	0.8	0.6	0.2	0.02	0	0
$\Xi_b(6364)^0$	$\frac{5}{2}^+$	$\lvert 2,0,0,0\rangle$	$^2D_{5/2}$	30.63	7.2	2.49	0.37	214.6	0	0	0	0	0	1.19	0.07	0.98	0.4	0.27	0	0
$\Xi_b(6360)^0$	$\frac{1}{2}^+$	$\lvert 0,0,1,0\rangle$	$^2S_{1/2}$	0	17.14	5.9	96.7	45.8	0	0	0	0	0	4.99	0.018	12.37	0.067	1.55	0	0
$\Xi_b(6699)^0$	$\frac{1}{2}^+$	$\lvert 0,0,0,1\rangle$	$^2S_{1/2}$	0	114.3	51.04	3.53	1.72	59.17	0.37	166.8	1.58	50.9	17.38	0.09	47.12	0.37	11.03	595.02	294.38
$\Xi_b(6524)^0$	$\frac{3}{2}^+$	$\lvert 1,1,0,0\rangle$	$^2D_{3/2}$	26.19	131.9	6.5	2.9	2.9	66.8	0.6	8.2	0.16	0.017	401.26	3.55	54.5	1.12	0.1	0.25	0.27
$\Xi_b(6534)^0$	$\frac{5}{2}^+$	$\lvert 1,1,0,0\rangle$	$^2D_{5/2}$	27.4	558.65	7.06	6.63	4.7	5.17	0.06	115.3	0.29	0.23	32.09	0.4	665.49	1.75	1.36	0.59	0.47
$\Xi_b(6540)^0$	$\frac{1}{2}^+$	$\lvert 1,1,0,0\rangle$	$^4D_{1/2}$	14.13	9.1	57.1	6.45	0.058	0.62	50.96	0.003	9.7	0.43	3.12	314.15	0.001	60.65	5.45	0.73	0.008
$\Xi_b(6546)^0$	$\frac{3}{2}^+$	$\lvert 1,1,0,0\rangle$	$^4D_{3/2}$	29.01	18.96	90.01	15.64	1.23	1.54	40.96	0.089	25.6	2.37	7.6	242.2	0.45	162.4	18.6	1.94	0.1
$\Xi_b(6556)^0$	$\frac{5}{2}^+$	$\lvert 1,1,0,0\rangle$	$^4D_{5/2}$	41.09	27.48	170.9	5.9	13.19	0.64	3.6	1.36	73.1	14.13	3.02	20.29	6.6	435.08	90.47	0.92	1.79
$\Xi_b(6570)^0$	$\frac{7}{2}^+$	$\lvert 1,1,0,0\rangle$	$^4D_{7/2}$	27.47	18.96	572.4	0.64	14.97	0.006	0.17	1.69	4.5	124.17	0.1	4.27	7.95	29.27	707.89	0.001	2.58
$\Xi_b(6526)^0$	$\frac{1}{2}^-$	$\lvert 1,1,0,0\rangle$	$^2P_{1/2}$	0	28.8	0	0	0	88.18	0.69	12.7	0.49	0.1	471.28	4.27	45.6	3.14	0.67	0	0
$\Xi_b(6532)^0$	$\frac{3}{2}^-$	$\lvert 1,1,0,0\rangle$	$^2P_{3/2}$	0	28.96	0	10.34	4.93	40.04	0.25	66.5	0.32	0.11	207.86	1.54	335.4	1.99	0.73	0.72	0.29
$\Xi_b(6548)^0$	$\frac{1}{2}^-$	$\lvert 1,1,0,0\rangle$	$^4P_{1/2}$	0	0	7.16	17.49	8.37	1.4	22.0	0.63	10.73	0.52	7.44	117.84	3.47	64.8	0.66	1.69	0.7
$\Xi_b(6554)^0$	$\frac{3}{2}^-$	$\lvert 1,1,0,0\rangle$	$^4P_{3/2}$	0	0	20.17	9.7	4.66	0.8	76.03	0.36	8.5	6.01	4.24	401.74	1.98	50.3	21.8	1.049	0.43
$\Xi_b(6564)^0$	$\frac{5}{2}^-$	$\lvert 1,1,0,0\rangle$	$^4P_{5/2}$	0	0	27.6	3.9	20.6	0.34	0.86	1.7	61.9	46.26	1.77	1.0	9.13	322.1	234.14	0.49	2.3
$\Xi_b(6558)^0$	$\frac{3}{2}^+$	$\lvert 1,1,0,0\rangle$	$^4S_{3/2}$	0	0	0	2.66	5.3	0.53	42.58	0.97	40.64	6.85	2.07	232.4	3.97	235.77	46.74	0.86	1.46
$\Xi_b(6530)^0$	$\frac{1}{2}^+$	$\lvert 1,1,0,0\rangle$	$^2S_{1/2}$	0	0	0	2.55	5.03	76.76	0.13	12.8	0.02	0.18	428.23	0.66	84.76	0.12	0.98	0.42	0.69
$\Xi_b(6693)^0$	$\frac{3}{2}^+$	$\lvert 0,2,0,0\rangle$	$^2D_{3/2}$	37.49	44.7	19.9	18.8	15.17	7.8	21.58	9.3	6.6	0.69	1.09	0.39	2.0	0.07	0.54	1134.02	174.3
$\Xi_b(6703)^0$	$\frac{5}{2}^+$	$\lvert 0,2,0,0\rangle$	$^2D_{5/2}$	36.7	46.4	20.76	7.98	27.06	15.45	2.1	13.3	10.29	8.88	1.26	0.46	2.32	0.08	0.64	2.54	1307.29

TABLE 4.3: Same as Table 4.1, but for $\Xi_b^-(snb)$ states belonging to the flavor multiplet $\mathcal{F} = \bar{\mathbf{3}}_{\mathrm{F}}$.

$\mathcal{F} = \bar{\mathbf{3}}_{\mathrm{F}}$				$\Xi_b^-\gamma$	$\Xi_b^{\prime-}\gamma$	$\Xi_b^{*-}\gamma$	$\Xi_b^-\gamma$	$\Xi_b^-\gamma$	$\Xi_b^-\gamma$	$\Xi_b^-\gamma$	$\Xi_b^-\gamma$	$\Xi_b^-\gamma$	$\Xi_b^-\gamma$	$\Xi_b^{\prime-}\gamma$	$\Xi_b^{*-}\gamma$	$\Xi_b^{\prime-}\gamma$	$\Xi_b^{*-}\gamma$	$\Xi_b^{*-}\gamma$	$\Xi_b^{\prime-}\gamma$	$\Xi_b^{\prime-}\gamma$
$\Xi_b^-(snb)$	$\mathbf{J^P}$	$\lvert l_\lambda, l_\rho, k_\lambda, k_\rho\rangle$	$^{2S+1}L_J$	$^2S_{1/2}$	$^2S_{1/2}$	$^4S_{3/2}$	$^2_\lambda P_{1/2}$	$^2_\lambda P_{3/2}$	$^2_\rho P_{1/2}$	$^4_\rho P_{1/2}$	$^2_\rho P_{3/2}$	$^4_\rho P_{3/2}$	$^4_\rho P_{5/2}$	$^2_\lambda P_{1/2}$	$^4_\lambda P_{1/2}$	$^2_\lambda P_{3/2}$	$^4_\lambda P_{3/2}$	$^4_\lambda P_{5/2}$	$^2_\rho P_{1/2}$	$^2_\rho P_{3/2}$
$N = 2$																				
$\Xi_b(6354)^-$	$\frac{3}{2}^+$	$\lvert 2,0,0,0\rangle$	$^2D_{3/2}$	47.9	0.1	0.04	184.5	28.7	0	0	0	0	0	0.01	0.01	0.01	0	0	0	0
$\Xi_b(6364)^-$	$\frac{5}{2}^+$	$\lvert 2,0,0,0\rangle$	$^2D_{5/2}$	48.9	0.13	0.045	0.47	212.4	0	0	0	0	0	0.02	0.001	0.017	0.007	0.005	0	0
$\Xi_b(6360)^-$	$\frac{1}{2}^+$	$\lvert 0,0,1,0\rangle$	$^2S_{1/2}$	0	0.3	0.1	98.25	50.26	0	0	0	0	0	0.09	0	0.22	0.001	0.028	0	0
$\Xi_b(6699)^-$	$\frac{1}{2}^+$	$\lvert 0,0,0,1\rangle$	$^2S_{1/2}$	0	2.08	0.93	5.17	2.5	86.7	0.54	244.6	2.32	74.7	0.31	0.001	0.85	0.006	0.2	10.8	5.37
$\Xi_b(6524)^-$	$\frac{3}{2}^+$	$\lvert 1,1,0,0\rangle$	$^2D_{3/2}$	38.4	2.4	0.1	4.33	4.26	61.6	0.93	7.7	0.26	0.026	7.32	0.064	0.9	0.02	0.001	0.004	0.005
$\Xi_b(6534)^-$	$\frac{5}{2}^+$	$\lvert 1,1,0,0\rangle$	$^2D_{5/2}$	40.23	10.19	0.12	9.7	6.9	7.66	0.093	116.38	0.45	0.37	0.58	0.007	12.14	0.032	0.024	0.01	0.008
$\Xi_b(6540)^-$	$\frac{1}{2}^+$	$\lvert 1,1,0,0\rangle$	$^4D_{1/2}$	20.71	0.16	1.04	9.45	0.08	0.98	43.96	0.005	11.08	0.62	0.056	5.7	0	1.1	0.09	0.013	0
$\Xi_b(6546)^-$	$\frac{3}{2}^+$	$\lvert 1,1,0,0\rangle$	$^4D_{3/2}$	42.5	0.34	1.64	22.9	1.8	2.4	40.67	0.14	22.87	2.74	0.14	4.4	0.008	2.96	0.33	0.035	0.002
$\Xi_b(6556)^-$	$\frac{5}{2}^+$	$\lvert 1,1,0,0\rangle$	$^4D_{5/2}$	60.24	0.5	3.11	8.67	19.34	1.0	5.23	2.12	72.4	13.03	0.05	0.37	0.12	7.9	1.65	0.016	0.032
$\Xi_b(6570)^-$	$\frac{7}{2}^+$	$\lvert 1,1,0,0\rangle$	$^4D_{7/2}$	40.27	0.34	10.44	0.94	21.9	0.008	0.25	2.64	6.52	126.7	0.002	0.07	0.14	0.53	12.9	0	0.047
$\Xi_b(6526)^-$	$\frac{1}{2}^-$	$\lvert 1,1,0,0\rangle$	$^2P_{1/2}$	0	0.52	0	0	0	90.45	1.07	13.48	0.77	0.16	8.59	0.078	0.83	0.057	0.012	0	0
$\Xi_b(6532)^-$	$\frac{3}{2}^-$	$\lvert 1,1,0,0\rangle$	$^2P_{3/2}$	0	0.5	0	15.16	7.2	45.6	0.39	66.28	0.49	0.17	3.79	0.028	6.12	0.036	0.013	0.013	0.005
$\Xi_b(6548)^-$	$\frac{1}{2}^-$	$\lvert 1,1,0,0\rangle$	$^4P_{1/2}$	0	0	0.13	25.65	12.27	2.17	22.57	0.98	8.8	0.75	0.13	2.14	0.06	1.18	0.012	0.03	0.013
$\Xi_b(6554)^-$	$\frac{3}{2}^-$	$\lvert 1,1,0,0\rangle$	$^4P_{3/2}$	0	0	0.36	14.26	6.8	1.26	82.18	0.57	8.3	5.37	0.07	7.32	0.036	0.9	0.39	0.019	0.008
$\Xi_b(6564)^-$	$\frac{5}{2}^-$	$\lvert 1,1,0,0\rangle$	$^4P_{5/2}$	0	0	0.5	5.7	30.2	0.5	1.24	2.7	68.3	45.64	0.03	0.018	0.16	5.8	4.27	0.009	0.04
$\Xi_b(6558)^-$	$\frac{3}{2}^+$	$\lvert 1,1,0,0\rangle$	$^4S_{3/2}$	0	0	0	3.9	7.7	0.8	48.1	1.5	43.77	6.19	0.037	4.24	0.07	4.3	0.85	0.015	0.026
$\Xi_b(6530)^-$	$\frac{1}{2}^+$	$\lvert 1,1,0,0\rangle$	$^2S_{1/2}$	0	0	0	3.7	7.37	86.4	0.2	11.5	0.038	0.29	7.8	0.012	1.54	0.002	0.017	0.007	0.012
$\Xi_b(6693)^-$	$\frac{3}{2}^+$	$\lvert 0,2,0,0\rangle$	$^2D_{3/2}$	54.97	0.8	0.36	27.59	22.2	11.48	31.64	13.6	9.7	1.02	0.02	0.007	0.036	0.001	0.01	20.68	3.17
$\Xi_b(6703)^-$	$\frac{5}{2}^+$	$\lvert 0,2,0,0\rangle$	$^2D_{5/2}$	53.86	0.84	0.37	11.7	39.67	22.65	3.08	19.5	15.09	13.02	0.022	0.008	0.04	0.0015	0.011	0.046	23.85

TABLE 4.4: Same as Table 4.1, but for $\Sigma_b^+(nnb)$ states belonging to the flavor multiplet $\mathcal{F} = \mathbf{6}_F$.

$\mathcal{F} = \mathbf{6}_F$				$\Sigma_b^+\gamma$	$\Sigma_b^{*+}\gamma$	$\Sigma_b^+\gamma$	$\Sigma_b^+\gamma$	$\Sigma_b^+\gamma$	$\Sigma_b^+\gamma$	$\Sigma_b^+\gamma$	$\Sigma_b^+\gamma$	$\Sigma_b^+\gamma$
$\Sigma_b^+(uub)$	$\mathbf{J^P}$	$\lvert l_\lambda, l_\rho, k_\lambda, k_\rho\rangle$	$^{2S+1}L_J$	$^2S_{1/2}$	$^4S_{3/2}$	$^2_\lambda P_{1/2}$	$^4_\lambda P_{1/2}$	$^2_\lambda P_{3/2}$	$^4_\lambda P_{3/2}$	$^4_\lambda P_{5/2}$	$^2_\rho P_{1/2}$	$^2_\rho P_{3/2}$
$N = 2$												
$\Sigma_b(6415)^+$	$\frac{3}{2}^+$	$\lvert 2,0,0,0\rangle$	$^2D_{3/2}$	70.4	13.4	850.4	20.1	76.1	5.7	0.5	0	0
$\Sigma_b(6425)^+$	$\frac{5}{2}^+$	$\lvert 2,0,0,0\rangle$	$^2D_{5/2}$	611.3	14.2	107.3	1.9	1779.7	9.5	7.9	0	0
$\Sigma_b(6431)^+$	$\frac{1}{2}^+$	$\lvert 2,0,0,0\rangle$	$^4D_{1/2}$	18.2	7.9	19.7	553.4	0.1	120.1	7.1	0	0
$\Sigma_b(6437)^+$	$\frac{3}{2}^+$	$\lvert 2,0,0,0\rangle$	$^4D_{3/2}$	37.6	82.9	47.3	589.2	2.8	261.4	26.2	0	0
$\Sigma_b(6448)^+$	$\frac{5}{2}^+$	$\lvert 2,0,0,0\rangle$	$^4D_{5/2}$	53.6	157.1	18.9	61.0	41.2	1109.0	137.8	0	0
$\Sigma_b(6462)^+$	$\frac{7}{2}^+$	$\lvert 2,0,0,0\rangle$	$^4D_{7/2}$	36.2	631.5	0.1	3.1	49.0	75.1	1978.4	0	0
$\Sigma_b(6421)^+$	$\frac{1}{2}^+$	$\lvert 0,0,1,0\rangle$	$^2S_{1/2}$	335.5	34.8	1838.9	0.3	76.6	1.5	46.1	0	0
$\Sigma_b(6450)^+$	$\frac{3}{2}^+$	$\lvert 0,0,1,0\rangle$	$^4S_{3/2}$	99.8	294.8	91.4	425.0	254.0	528.4	68.7	0	0
$\Sigma_b(6813)^+$	$\frac{1}{2}^+$	$\lvert 0,0,0,1\rangle$	$^2S_{1/2}$	452.9	56.7	296.3	0.8	1862.1	3.5	113.2	656.0	1883.5
$\Sigma_b(6842)^+$	$\frac{3}{2}^+$	$\lvert 0,0,0,1\rangle$	$^4S_{3/2}$	111.9	396.4	163.1	3.6	462.7	47.6	1199.6	721.9	2085.4
$\Sigma_b(6611)^+$	$\frac{3}{2}^+$	$\lvert 1,1,0,0\rangle$	$^2D_{3/2}$	316.6	146.5	31.7	112.5	25.2	53.8	5.7	513.7	104.3
$\Sigma_b(6621)^+$	$\frac{5}{2}^+$	$\lvert 1,1,0,0\rangle$	$^2D_{5/2}$	323.4	150.2	77.0	24.3	46.8	60.0	37.7	9.4	611.7
$\Sigma_b(6613)^+$	$\frac{1}{2}^-$	$\lvert 1,1,0,0\rangle$	$^2P_{1/2}$	0	0	0	167.1	0	128.6	30.1	621.1	97.6
$\Sigma_b(6619)^+$	$\frac{3}{2}^-$	$\lvert 1,1,0,0\rangle$	$^2P_{3/2}$	0	0	131.6	57.5	63.6	77.5	31.1	157.7	562.4
$\Sigma_b(6617)^+$	$\frac{1}{2}^+$	$\lvert 1,1,0,0\rangle$	$^2S_{1/2}$	0	0	15.5	8.4	32.0	1.7	15.7	440.1	214.1
$\Sigma_b(6807)^+$	$\frac{3}{2}^+$	$\lvert 0,2,0,0\rangle$	$^2D_{3/2}$	45.6	22.6	77.2	3.7	60.1	0.7	5.9	95.2	110.3
$\Sigma_b(6817)^+$	$\frac{5}{2}^+$	$\lvert 0,2,0,0\rangle$	$^2D_{5/2}$	512.9	22.6	149.5	3.9	546.1	0.7	6.3	188.3	157.4
$\Sigma_b(6824)^+$	$\frac{1}{2}^+$	$\lvert 0,2,0,0\rangle$	$^4D_{1/2}$	22.5	7.2	5.0	26.7	9.7	23.3	4.9	198.0	0.1
$\Sigma_b(6830)^+$	$\frac{3}{2}^+$	$\lvert 0,2,0,0\rangle$	$^4D_{3/2}$	45.0	90.9	10.4	46.3	20.1	0.3	68.9	463.3	28.2
$\Sigma_b(6840)^+$	$\frac{5}{2}^+$	$\lvert 0,2,0,0\rangle$	$^4D_{5/2}$	60.8	134.5	15.0	17.9	28.9	98.2	91.8	173.2	390.1
$\Sigma_b(6854)^+$	$\frac{7}{2}^+$	$\lvert 0,2,0,0\rangle$	$^4D_{7/2}$	38.1	512.0	10.2	135.3	19.7	114.7	466.3	3.8	431.1

$$\langle \text{ground state}|\hat{U}_j|\text{N=2 state}\rangle, \qquad \langle P\text{-wave}|\hat{U}_j|\text{N=2 state}\rangle, \tag{4.1}$$

$$\langle \text{ground state}|\hat{T}_{j,-}|\text{N=2 state}\rangle, \qquad \langle P\text{-wave}|\hat{T}_{j,-}|\text{N=2 state}\rangle, \tag{4.2}$$

where the $N = 2$ sates stands the second shell states which can be pure D_λ-wave or D_ρ-wave, radial λ or ρ excitations and $\rho\lambda$ mixed states.

The procedure for evaluating the matrix elements for the $\hat{T}_{j,-}$ operators in the electromagnetic transitions from second shell states to ground and P-wave states is the same used in Chapter 3, and it is described in details in Appendix A.

4.2 Results of electromagnetic decays of second shell singly bottom baryons

In this section, the results for the electromagnetic decay widths of the second shell singly bottom baryons are presented. These decay widths are computed by using eq. (3.2) for states of the second shell decaying to ground states and P-wave excited states.

The obtained theoretical results for the Λ_b and Ξ_b bottom baryons are reported in Tables 4.1-4.3 and the results for the Σ_b, Ξ_b' and Ω_b bottom baryons are presented in Tables 4.4-4.9. These

TABLE 4.5: Same as Table 4.1, but for $\Sigma_b^0(nnb)$ states belonging to the flavor multiplet $\mathcal{F} = \mathbf{6}_{\rm F}$.

$\mathcal{F}=\mathbf{6}_{\rm F}$				$\Lambda_b^0\gamma$	$\Sigma_b^0\gamma$	$\Sigma_b^{*0}\gamma$	$\Sigma_b^0\gamma$	$\Sigma_b^0\gamma$	$\Sigma_b^0\gamma$	$\Sigma_b^0\gamma$	$\Sigma_b^0\gamma$	$\Sigma_b^0\gamma$	$\Sigma_b^0\gamma$	$\Lambda_b^0\gamma$	$\Lambda_b^0\gamma$	$\Lambda_b^0\gamma$	$\Lambda_b^0\gamma$	$\Lambda_b^0\gamma$	$\Lambda_b^0\gamma$	$\Lambda_b^0\gamma$
$\Sigma_b^0(udb)$	$\mathbf{J^P}$	$\lvert l_\lambda,l_\rho,k_\lambda,k_\rho\rangle$	$^{2S+1}L_J$	$^2S_{1/2}$	$^2S_{1/2}$	$^4S_{3/2}$	$^2_\lambda P_{1/2}$	$^4_\lambda P_{1/2}$	$^2_\lambda P_{3/2}$	$^4_\lambda P_{3/2}$	$^4_\lambda P_{5/2}$	$^2_\rho P_{1/2}$	$^2_\rho P_{3/2}$	$^2_\lambda P_{1/2}$	$^2_\lambda P_{3/2}$	$^2_\rho P_{1/2}$	$^4_\rho P_{1/2}$	$^2_\rho P_{3/2}$	$^4_\rho P_{3/2}$	$^4_\rho P_{5/2}$
$N=2$																				
$\Sigma_b(6415)^0$	$\frac{3}{2}^+$	$\lvert 2,0,0,0\rangle$	$^2D_{3/2}$	4.1	0.8	127.1	68.4	1.2	6.2	0.3	0.03	0	0	67.7	74.0	7.6	0	1.4	0	0
$\Sigma_b(6425)^0$	$\frac{5}{2}^+$	$\lvert 2,0,0,0\rangle$	$^2D_{5/2}$	37.2	0.8	129.9	6.6	0.1	134.5	0.5	0.4	0	0	140.2	110.1	2.0	0	11.7	0	0
$\Sigma_b(6431)^0$	$\frac{1}{2}^+$	$\lvert 2,0,0,0\rangle$	$^4D_{1/2}$	1.1	0.4	66.6	1.2	46.8	0	8.7	0.4	0	0	143.5	0.08	0.01	3.3	0.02	3.05	0.2
$\Sigma_b(6437)^0$	$\frac{3}{2}^+$	$\lvert 2,0,0,0\rangle$	$^4D_{3/2}$	2.3	5.0	134.8	2.8	45.1	0.1	21.9	1.9	0	0	339.1	22.2	0.03	3.7	0.06	0.8	1.4
$\Sigma_b(6448)^0$	$\frac{5}{2}^+$	$\lvert 2,0,0,0\rangle$	$^4D_{5/2}$	3.3	9.5	186.4	1.1	3.8	2.5	84.6	11.4	0	0	125.6	284.0	0.06	2.9	0.1	3.8	1.6
$\Sigma_b(6462)^0$	$\frac{7}{2}^+$	$\lvert 2,0,0,0\rangle$	$^4D_{7/2}$	2.2	38.	120.6	0.01	0.2	2.9	4.7	148.3	0	0	6.06	314.4	0.05	0.3	0.09	4.3	9.9
$\Sigma_b(6421)^0$	$\frac{1}{2}^+$	$\lvert 0,0,1,0\rangle$	$^2S_{1/2}$	20.9	2.1	322.0	128.5	0.02	2.9	0.09	2.8	0	0	412.6	1196.1	1.7	0	12.6	0	0.1
$\Sigma_b(6450)^0$	$\frac{3}{2}^+$	$\lvert 0,0,1,0\rangle$	$^4S_{3/2}$	6.2	18.3	344.7	5.5	31.4	15.3	39.3	3.3	0	0	440.8	1285.6	0.7	2.9	1.8	4.3	7.4
$\Sigma_b(6813)^0$	$\frac{1}{2}^+$	$\lvert 0,0,0,1\rangle$	$^2S_{1/2}$	28.3	3.5	150.2	18.5	0.05	116.3	0.2	7.1	41.0	117.7	592.9	1714.0	2235.5	1.1	700.9	5.1	178.0
$\Sigma_b(6842)^0$	$\frac{3}{2}^+$	$\lvert 0,0,0,1\rangle$	$^4S_{3/2}$	6.9	24.7	140.4	10.2	0.2	28.9	2.9	74.9	45.1	130.3	648.4	1879.8	145.2	343.6	434.3	424.4	519.2
$\Sigma_b(6611)^0$	$\frac{3}{2}^+$	$\lvert 1,1,0,0\rangle$	$^2D_{3/2}$	19.7	9.1	163.5	1.9	7.0	1.5	3.3	0.3	40.3	7.7	139.3	171.5	30.4	100.0	30.0	39.5	3.6
$\Sigma_b(6621)^0$	$\frac{5}{2}^+$	$\lvert 1,1,0,0\rangle$	$^2D_{5/2}$	20.2	9.3	158.3	4.8	1.5	2.9	3.7	2.3	0.6	48.0	82.5	229.5	66.6	15.1	47.6	50.2	36.8
$\Sigma_b(6613)^0$	$\frac{1}{2}^-$	$\lvert 1,1,0,0\rangle$	$^2P_{1/2}$	0	0	15.7	0	10.4	0	8.0	1.8	47.0	7.2	176.8	1.4	0	131.9	0	101.4	23.6
$\Sigma_b(6619)^0$	$\frac{3}{2}^-$	$\lvert 1,1,0,0\rangle$	$^2P_{3/2}$	0	0	15.4	8.2	3.5	3.9	4.8	1.9	12.0	42.3	51.8	125.8	104.4	45.4	50.1	61.2	24.5
$\Sigma_b(6617)^0$	$\frac{1}{2}^+$	$\lvert 1,1,0,0\rangle$	$^2S_{1/2}$	0	0	0	0.9	0.5	2.0	0.1	0.9	32.5	15.6	372.6	187.9	25.9	12.5	51.5	2.4	21.7
$\Sigma_b(6807)^0$	$\frac{3}{2}^+$	$\lvert 0,2,0,0\rangle$	$^2D_{3/2}$	2.8	1.4	60.7	4.8	0.2	3.7	0.04	0.3	5.9	6.8	39.9	78.3	125.5	105.7	73.6	42.4	4.06
$\Sigma_b(6817)^0$	$\frac{5}{2}^+$	$\lvert 0,2,0,0\rangle$	$^2D_{5/2}$	32.0	1.4	59.6	9.3	0.2	34.1	0.04	0.3	11.7	9.8	41.1	80.6	434.07	15.0	905.9	52.4	40.3
$\Sigma_b(6824)^0$	$\frac{1}{2}^+$	$\lvert 0,2,0,0\rangle$	$^4D_{1/2}$	1.4	0.4	29.1	0.3	1.6	0.6	1.4	0.3	12.4	0.009	21.2	41.7	59.4	6.2	0.3	131.3	14.4
$\Sigma_b(6830)^0$	$\frac{3}{2}^+$	$\lvert 0,2,0,0\rangle$	$^4D_{3/2}$	2.8	5.6	57.5	0.6	2.8	1.2	0.02	4.3	28.9	1.7	43.1	84.8	139.2	426.6	10.6	1.4	41.7
$\Sigma_b(6840)^0$	$\frac{5}{2}^+$	$\lvert 0,2,0,0\rangle$	$^4D_{5/2}$	3.8	8.4	76.5	0.9	1.	1.8	6.1	5.7	10.8	24.3	60.1	118.1	49.9	206.2	115.0	647.9	11.6
$\Sigma_b(6854)^0$	$\frac{7}{2}^+$	$\lvert 0,2,0,0\rangle$	$^4D_{7/2}$	2.3	32.0	46.9	0.6	8.4	1.2	7.1	29. 1	0.2	26.9	39.2	77.2	3.8	38.0	122.0	319.1	1229.4

TABLE 4.6: Same as Table 4.1, but for $\Sigma_b^-(nnb)$ states belonging to the flavor multiplet $\mathcal{F} = \mathbf{6_F}$.

$\mathcal{F} = \mathbf{6_F}$				$\Sigma_b^-\gamma$	$\Sigma_b^{*-}\gamma$	$\Sigma_b^-\gamma$	$\Sigma_b^-\gamma$	$\Sigma_b^-\gamma$	$\Sigma_b^-\gamma$	$\Sigma_b^-\gamma$	$\Sigma_b^-\gamma$	$\Sigma_b^-\gamma$
$\Sigma_b^-(ddb)$	$\mathbf{J^P}$	$\vert l_\lambda, l_\rho, k_\lambda, k_\rho\rangle$	$^{2S+1}L_J$	$^2S_{1/2}$	$^4S_{3/2}$	$^2_\lambda P_{1/2}$	$^4_\lambda P_{1/2}$	$^2_\lambda P_{3/2}$	$^4_\lambda P_{3/2}$	$^4_\lambda P_{5/2}$	$^2_\rho P_{1/2}$	$^2_\rho P_{3/2}$
$N = 2$												
$\Sigma_b(6415)^-$	$\frac{3}{2}^+$	$\vert 2,0,0,0\rangle$	$^2D_{3/2}$	18.7	3.3	159.2	5.1	14.0	1.4	0.1	0	0
$\Sigma_b(6425)^-$	$\frac{5}{2}^+$	$\vert 2,0,0,0\rangle$	$^2D_{5/2}$	156.8	3.5	26.9	0.4	360.5	2.4	2.0	0	0
$\Sigma_b(6431)^-$	$\frac{1}{2}^+$	$\vert 2,0,0,0\rangle$	$^4D_{1/2}$	4.5	2.4	5.0	96.7	0.02	25.4	1.7	0	0
$\Sigma_b(6437)^-$	$\frac{3}{2}^+$	$\vert 2,0,0,0\rangle$	$^4D_{3/2}$	9.3	21.3	12.1	117.8	0.7	46.2	5.5	0	0
$\Sigma_b(6448)^-$	$\frac{5}{2}^+$	$\vert 2,0,0,0\rangle$	$^4D_{5/2}$	13.3	40.6	4.8	15.1	10.6	222.4	24.6	0	0
$\Sigma_b(6462)^-$	$\frac{7}{2}^+$	$\vert 2,0,0,0\rangle$	$^4D_{7/2}$	9.0	162.3	0.04	0.7	12.6	18.5	404.8	0	0
$\Sigma_b(6421)^-$	$\frac{1}{2}^+$	$\vert 0,0,1,0\rangle$	$^2S_{1/2}$	83.7	8.6	408.3	0.1	28.2	0.3	11.8	0	0
$\Sigma_b(6450)^-$	$\frac{3}{2}^+$	$\vert 0,0,1,0\rangle$	$^4S_{3/2}$	24.8	73.9	23.5	88.3	65.5	109.1	21.8	0	0
$\Sigma_b(6813)^-$	$\frac{1}{2}^+$	$\vert 0,0,0,1\rangle$	$^2S_{1/2}$	113.2	14.2	74.1	0.2	465.5	0.8	28.3	164.0	470.8
$\Sigma_b(6842)^-$	$\frac{3}{2}^+$	$\vert 0,0,0,1\rangle$	$^4S_{3/2}$	27.9	99.1	40.7	0.9	115.6	11.9	299.9	180.4	521.3
$\Sigma_b(6611)^-$	$\frac{3}{2}^+$	$\vert 1,1,0,0\rangle$	$^2D_{3/2}$	79.1	36.6	7.9	28.1	6.3	13.4	1.4	99.4	21.5
$\Sigma_b(6621)^-$	$\frac{5}{2}^+$	$\vert 1,1,0,0\rangle$	$^2D_{5/2}$	80.8	37.5	19.2	6.1	11.7	15.0	9.4	2.2	118.4
$\Sigma_b(6613)^-$	$\frac{1}{2}^-$	$\vert 1,1,0,0\rangle$	$^2P_{1/2}$	0	0	0	41.7	0	32.1	7.5	125.5	20.2
$\Sigma_b(6619)^-$	$\frac{3}{2}^-$	$\vert 1,1,0,0\rangle$	$^2P_{3/2}$	0	0	32.	14.3	15.9	19.3	7.7	31.5	114.5
$\Sigma_b(6617)^-$	$\frac{1}{2}^+$	$\vert 1,1,0,0\rangle$	$^2S_{1/2}$	0	0	3.8	2.1	8.0	0.4	3.9	91.5	45.2
$\Sigma_b(6807)^-$	$\frac{3}{2}^+$	$\vert 0,2,0,0\rangle$	$^2D_{3/2}$	11.4	5.6	19.3	0.9	15.0	0.1	1.4	23.7	27.5
$\Sigma_b(6817)^-$	$\frac{5}{2}^+$	$\vert 0,2,0,0\rangle$	$^2D_{5/2}$	128.2	5.6	37.3	0.9	136.5	0.2	1.5	47.1	39.3
$\Sigma_b(6824)^-$	$\frac{1}{2}^+$	$\vert 0,2,0,0\rangle$	$^4D_{1/2}$	5.6	1.8	1.2	6.6	2.4	5.8	1.2	49.5	0.03
$\Sigma_b(6830)^-$	$\frac{3}{2}^+$	$\vert 0,2,0,0\rangle$	$^4D_{3/2}$	11.2	22.7	2.6	11.5	5.0	0.08	17.2	115.8	7.0
$\Sigma_b(6840)^-$	$\frac{5}{2}^+$	$\vert 0,2,0,0\rangle$	$^4D_{5/2}$	15.2	33.6	3.7	4.4	7.2	24.5	22.9	43.3	97.5
$\Sigma_b(6854)^-$	$\frac{7}{2}^+$	$\vert 0,2,0,0\rangle$	$^4D_{7/2}$	9.5	128.0	2.5	33.8	4.9	28.6	116.5	0.9	107.7

results extend those previously obtained by two other works on the subject. Specifically, the analysis performed in reference [71] employing a constituent quark model for the decays from the low-lying λ-mode D-wave to the λ-mode P-wave singly bottom baryons and the study of reference [82] using the GEM for the decays from the D_λ-wave and λ-mode radial excitations to the ground state singly bottom baryons.

As already mentioned in Chapter 3, the electromagnetic decay widths are particularly valuable in cases where the strong decays are not allowed. They may also be useful to make the assignments of resonances when the states have the same mass and total decay widths.

4.3 Discussion and conclusions

In summary, in this Chapter the electromagnetic decay widths of second shell singly bottom baryons to ground states and P-wave states have been calculated using the formalism introduced in reference [90]. This work presents the first calculations of the electromagnetic decay widths for D_ρ-wave states, $\rho\lambda$ mixed states, and radially excited ρ states. Electromagnetic decay widths may be useful in the assignments of resonances when the states have the same mass and total decay widths.

One example is the case of the Ξ_b $^2D_{3/2}$ $\rho\lambda$ mixed state, which has a mass of 6524 MeV and a strong decay width of 47 MeV, while the Ξ_b' $^4D_{7/2}$ λ state has a mass of 6520 MeV and a strong

TABLE 4.7: Same as Table 4.1, but for $\Xi_b^{\prime 0}(snb)$ states belonging to the flavor multiplet $\mathcal{F} = \mathbf{6}_{\rm F}$.

$\mathcal{F} = \mathbf{6}_{\rm F}$				$\Xi_b^0\gamma$	$\Xi_b^{\prime 0}\gamma$	$\Xi_b^{*0}\gamma$	$\Xi_b^0\gamma$	$\Xi_b^0\gamma$	$\Xi_b^0\gamma$	$\Xi_b^0\gamma$	$\Xi_b^0\gamma$	$\Xi_b^0\gamma$	$\Xi_b^0\gamma$	$\Xi_b^{\prime 0}\gamma$	$\Xi_b^{*0}\gamma$	$\Xi_b^{\prime 0}\gamma$	$\Xi_b^{*0}\gamma$	$\Xi_b^{*0}\gamma$	$\Xi_b^{\prime 0}\gamma$	$\Xi_b^{\prime 0}\gamma$
$\Xi_b^{\prime 0}(sub)$	$\mathbf{J^P}$	$\lvert l_\lambda, l_\rho, k_\lambda, k_\rho\rangle$	$^{2S+1}L_J$	$^2S_{1/2}$	$^2S_{1/2}$	$^4S_{3/2}$	$^2_\lambda P_{1/2}$	$^2_\lambda P_{3/2}$	$^2_\rho P_{1/2}$	$^4_\rho P_{1/2}$	$^2_\rho P_{3/2}$	$^4_\rho P_{3/2}$	$^4_\rho P_{5/2}$	$^2_\lambda P_{1/2}$	$^4_\lambda P_{1/2}$	$^2_\lambda P_{3/2}$	$^4_\lambda P_{3/2}$	$^4_\lambda P_{5/2}$	$^2_\rho P_{1/2}$	$^2_\rho P_{3/2}$
$N = 2$																				
$\Xi_b'(6473)^0$	$\frac{3}{2}^+$	$\lvert 2,0,0,0\rangle$	$^2D_{3/2}$	52.7	11.36	0.76	25.84	30.39	1.56	0	0	0	149.2	1.21	14.8	0.33	0.035	0	0	
$\Xi_b'(6483)^0$	$\frac{5}{2}^+$	$\lvert 2,0,0,0\rangle$	$^2D_{5/2}$	55.9	58.19	0.84	52.4	44.56	0.44	0	2.06	0	0	7.15	0.11	254.44	0.59	0.48	0	0
$\Xi_b'(6489)^0$	$\frac{1}{2}^+$	$\lvert 2,0,0,0\rangle$	$^4D_{1/2}$	29.0	1.14	4.18	56.14	0.16	0	0.67	0.001	0.53	0.059	1.28	116.12	0.01	14.6	0.46	0	0
$\Xi_b'(6495)^0$	$\frac{3}{2}^+$	$\lvert 2,0,0,0\rangle$	$^4D_{3/2}$	60.01	2.4	8.57	134.49	8.03	0.002	0.77	0.003	0.15	0.23	3.16	88.77	0.19	53.35	3.14	0	0
$\Xi_b'(6506)^0$	$\frac{5}{2}^+$	$\lvert 2,0,0,0\rangle$	$^4D_{5/2}$	86.03	3.55	16.7	52.95	117.3	0.004	0.69	0.006	0.72	0.3	1.33	4.2	2.8	163.01	27.14	0	0
$\Xi_b'(6520)^0$	$\frac{7}{2}^+$	$\lvert 2,0,0,0\rangle$	$^4D_{7/2}$	58.46	2.5	60.65	0.79	137.48	0.004	0.048	0.0067	0.95	1.83	0.006	0.17	3.61	5.26	274.43	0	0
$\Xi_b'(6479)^0$	$\frac{1}{2}^+$	$\lvert 0,0,1,0\rangle$	$^2S_{1/2}$	136.58	20.85	2.03	194.25	546.84	0.69	0	1.26	0	0.004	200.05	0.024	0.1	0.09	2.8	0	0
$\Xi_b'(6508)^0$	$\frac{3}{2}^+$	$\lvert 0,0,1,0\rangle$	$^4S_{3/2}$	160.2	6.6	18.4	239.1	677.9	0.04	0.6	0.1	0.8	0.7	6.8	55.9	18.7	70.8	1.3	0	0
$\Xi_b'(6818)^0$	$\frac{1}{2}^+$	$\lvert 0,0,0,1\rangle$	$^2S_{1/2}$	189.8	57.0	6.6	192.6	544.7	2278.8	0.8	427.3	3.8	127.1	9.7	0.03	93.1	0.1	4.7	59.2	166.9
$\Xi_b'(6847)^0$	$\frac{3}{2}^+$	$\lvert 0,0,0,1\rangle$	$^4S_{3/2}$	192.6	15.1	50.1	234.6	666.1	137.8	407.1	400.4	502.9	325.5	8.2	0.6	23.1	3.4	59.4	70.34	199.6
$\Xi_b'(6642)^0$	$\frac{3}{2}^+$	$\lvert 1,1,0,0\rangle$	$^2D_{3/2}$	286.1	26.2	11.3	265.0	123.2	12.1	33.4	13.4	10.9	1.0	2.9	9.3	2.9	3.6	0.3	83.3	14.4
$\Xi_b'(6653)^0$	$\frac{5}{2}^+$	$\lvert 1,1,0,0\rangle$	$^2D_{5/2}$	281.3	27.5	12.0	42.9	344.0	25.3	3.8	20.3	16.5	13.2	6.6	1.4	4.7	4.7	3.4	0.6	98.1
$\Xi_b'(6644)^0$	$\frac{1}{2}^-$	$\lvert 1,1,0,0\rangle$	$^2P_{1/2}$	26.0	0	0	336.5	16.6	0	40.3	0	30.2	6.7	0	12.3	0	9.3	2.1	88.1	12.7
$\Xi_b'(6651)^0$	$\frac{3}{2}^-$	$\lvert 1,1,0,0\rangle$	$^2P_{3/2}$	25.8	0	0	86.9	264.0	35.8	14.3	16.8	18.8	7.2	10.3	4.3	4.9	5.7	2.2	22.5	78.7
$\Xi_b'(6649)^0$	$\frac{1}{2}^+$	$\lvert 1,1,0,0\rangle$	$^2S_{1/2}$	0	0	0	402.2	201.2	14.2	6.0	27.2	1.1	9.5	2.5	1.2	5.0	0.2	2.0	56.7	27.3
$\Xi_b'(6812)^0$	$\frac{3}{2}^+$	$\lvert 0,2,0,0\rangle$	$^2D_{3/2}$	75.6	9.7	2.6	12.6	24.2	392.3	58.9	56.1	19.9	1.9	10.2	0.2	7.2	0.03	0.2	7.8	9.3
$\Xi_b'(6822)^0$	$\frac{5}{2}^+$	$\lvert 0,2,0,0\rangle$	$^2D_{5/2}$	76.1	93.3	2.7	13.6	26.1	257.3	6.5	1365.5	28.4	23.9	11.7	0.2	43.5	0.03	0.2	15.4	13.3
$\Xi_b'(6828)^0$	$\frac{1}{2}^+$	$\lvert 0,2,0,0\rangle$	$^4D_{1/2}$	38.2	2.9	0.4	7.1	13.6	39.1	112.1	0.01	139.6	16.3	0.2	4.6	0.4	3.0	1.8	16.4	0.06
$\Xi_b'(6834)^0$	$\frac{3}{2}^+$	$\lvert 0,2,0,0\rangle$	$^4D_{3/2}$	76.6	5.8	13.2	14.8	28.5	91.6	474.0	5.6	60.1	35.5	0.5	5.3	0.9	0.1	5.7	39.0	2.3
$\Xi_b'(6845)^0$	$\frac{5}{2}^+$	$\lvert 0,2,0,0\rangle$	$^4D_{5/2}$	104.5	8.1	23.9	21.5	41.4	34.2	137.9	77.4	849.8	44.8	0.7	2.5	1.4	9.2	7.7	15.2	33.7
$\Xi_b'(6859)^0$	$\frac{7}{2}^+$	$\lvert 0,2,0,0\rangle$	$^4D_{7/2}$	66.3	5.3	94.3	14.9	28.7	0.9	13.3	85.7	184.6	1646.4	0.5	9.7	1.0	10.8	37.0	0.2	38.6

TABLE 4.8: Same as Table 4.1, but for $\Xi_b'^-(snb)$ states belonging to the flavor multiplet $\mathcal{F} = \mathbf{6}_\mathrm{F}$.

$\mathcal{F}=\mathbf{6}_\mathrm{F}$				$\Xi_b^-\gamma$	$\Xi_b'^-\gamma$	$\Xi_b^{*-}\gamma$	$\Xi_b^-\gamma$	$\Xi_b^-\gamma$	$\Xi_b^-\gamma$	$\Xi_b^-\gamma$	$\Xi_b^-\gamma$	$\Xi_b^-\gamma$	$\Xi_b^-\gamma$	$\Xi_b'^-\gamma$	$\Xi_b^{*-}\gamma$	$\Xi_b'^-\gamma$	$\Xi_b^{*-}\gamma$	$\Xi_b^{*-}\gamma$	$\Xi_b'^-\gamma$	$\Xi_b'^-\gamma$
$\Xi_b'^-(sdb)$	$\mathbf{J^P}$	$\lvert l_\lambda,l_\rho,k_\lambda,k_\rho\rangle$	$^{2S+1}L_J$	$^2S_{1/2}$	$^2S_{1/2}$	$^4S_{3/2}$	$^2_\lambda P_{1/2}$	$^2_\lambda P_{3/2}$	$^2_\rho P_{1/2}$	$^4_\rho P_{1/2}$	$^2_\rho P_{3/2}$	$^4_\rho P_{3/2}$	$^4_\rho P_{5/2}$	$^2_\lambda P_{1/2}$	$^4_\lambda P_{1/2}$	$^2_\lambda P_{3/2}$	$^4_\lambda P_{3/2}$	$^4_\lambda P_{5/2}$	$^2_\rho P_{1/2}$	$^2_\rho P_{3/2}$
$N=2$																				
$\Xi_b'(6473)^-$	$\frac{3}{2}^+$	$\lvert 2,0,0,0\rangle$	$^2D_{3/2}$	0.96	18.8	1.1	0.47	0.55	0.028	0	0.005	0	0	140.9	1.89	13.15	0.5	0.05	0	0
$\Xi_b'(6483)^-$	$\frac{5}{2}^+$	$\lvert 2,0,0,0\rangle$	$^2D_{5/2}$	1.02	90.29	1.22	0.95	0.81	0	0	0.037	0	0	10.59	0.17	262.13	0.92	0.75	0	0
$\Xi_b'(6489)^-$	$\frac{1}{2}^+$	$\lvert 2,0,0,0\rangle$	$^4D_{1/2}$	0.52	1.65	7.29	1.02	0.003	0	0.01	0	0.009	0.001	2.0	104.1	0.018	15.8	0.66	0	0
$\Xi_b'(6495)^-$	$\frac{3}{2}^+$	$\lvert 2,0,0,0\rangle$	$^4D_{3/2}$	1.09	3.49	13.63	2.45	0.14	0	0.014	0	0.002	0.004	4.93	88.77	0.29	48.17	3.39	0	0
$\Xi_b'(6506)^-$	$\frac{5}{2}^+$	$\lvert 2,0,0,0\rangle$	$^4D_{5/2}$	1.56	5.14	26.49	0.96	2.14	0	0.012	0	0.013	0.005	2.08	6.05	4.47	165.14	24.61	0	0
$\Xi_b'(6520)^-$	$\frac{7}{2}^+$	$\lvert 2,0,0,0\rangle$	$^4D_{7/2}$	1.06	3.63	94.32	0.01	2.5	0	0	0	0.017	0.03	0.008	0.26	5.63	7.55	285.68	0	0
$\Xi_b'(6479)^-$	$\frac{1}{2}^+$	$\lvert 0,0,1,0\rangle$	$^2S_{1/2}$	2.5	30.4	2.9	3.5	9.9	0.01	0	0.02	0	0	233.9	0.03	3.1	0.1	4.4	0	0
$\Xi_b'(6508)^-$	$\frac{3}{2}^+$	$\lvert 0,0,1,0\rangle$	$^4S_{3/2}$	2.9	9.6	27.1	4.3	12.3	0	0.01	0.002	0.01	0.01	10.7	59.4	29.3	74.4	3.6	0	0
$\Xi_b'(6818)^-$	$\frac{1}{2}^+$	$\lvert 0,0,0,1\rangle$	$^2S_{1/2}$	3.4	83.6	9.8	3.5	9.9	41.5	0.01	7.7	0.06	2.3	14.2	0.05	136.5	0.2	6.8	86.8	244.7
$\Xi_b'(6847)^-$	$\frac{3}{2}^+$	$\lvert 0,0,0,1\rangle$	$^4S_{3/2}$	3.5	22.1	73.4	4.2	12.1	2.5	7.4	7.3	9.1	5.9	12.1	0.9	33.8	4.9	87.0	103.1	292.7
$\Xi_b'(6642)^-$	$\frac{3}{2}^+$	$\lvert 1,1,0,0\rangle$	$^2D_{3/2}$	5.2	38.4	16.6	4.8	2.2	0.2	0.6	0.2	0.2	0.01	4.3	13.6	4.2	5.3	0.4	81.4	15.0
$\Xi_b'(6653)^-$	$\frac{5}{2}^+$	$\lvert 1,1,0,0\rangle$	$^2D_{5/2}$	5.1	40.4	17.6	0.7	6.2	0.4	0.07	0.3	0.3	0.2	9.7	2.1	6.9	7.0	5.0	0.8	95.4
$\Xi_b'(6644)^-$	$\frac{1}{2}^-$	$\lvert 1,1,0,0\rangle$	$^2P_{1/2}$	0.4	0	0	6.1	0.3	0	0.7	0	0.5	0.1	0	18.1	0	13.7	3.1	90.4	13.4
$\Xi_b'(6651)^-$	$\frac{3}{2}^-$	$\lvert 1,1,0,0\rangle$	$^2P_{3/2}$	0.4	0	0	1.5	4.8	0.6	0.2	0.3	0.3	0.1	15.2	6.3	7.2	8.4	3.3	22.7	81.5
$\Xi_b'(6649)^-$	$\frac{1}{2}^+$	$\lvert 1,1,0,0\rangle$	$^2S_{1/2}$	0	0	0	7.3	3.6	0.2	0.1	0.4	0.02	0.2	3.7	1.7	7.3	0.3	2.9	60.2	29.7
$\Xi_b'(6812)^-$	$\frac{3}{2}^+$	$\lvert 0,2,0,0\rangle$	$^2D_{3/2}$	1.3	14.2	3.8	0.2	0.4	7.1	1.1	1.0	0.3	0.03	15.0	0.2	10.6	0.04	0.3	11.4	13.6
$\Xi_b'(6822)^-$	$\frac{5}{2}^+$	$\lvert 0,2,0,0\rangle$	$^2D_{5/2}$	1.3	136.8	3.9	0.2	0.4	4.6	0.1	24.9	0.5	0.4	17.2	0.2	63.8	0.04	0.4	22.7	19.5
$\Xi_b'(6828)^-$	$\frac{1}{2}^+$	$\lvert 0,2,0,0\rangle$	$^4D_{1/2}$	0.6	4.2	0.6	0.1	0.2	0.7	2.04	0	2.54	0.3	0.3	6.8	0.6	4.4	2.7	24.2	0.1
$\Xi_b'(6834)^-$	$\frac{3}{2}^+$	$\lvert 0,2,0,0\rangle$	$^4D_{3/2}$	1.3	8.6	19.4	0.2	0.5	1.6	8.6	0.1	1.1	0.6	0.7	7.8	1.4	0.2	8.4	57.2	3.4
$\Xi_b'(6845)^-$	$\frac{5}{2}^+$	$\lvert 0,2,0,0\rangle$	$^4D_{5/2}$	1.9	11.9	35.0	0.3	0.7	0.6	2.5	1.4	15.5	0.8	1.1	3.7	2.1	13.5	11.4	22.2	49.4
$\Xi_b'(6859)^-$	$\frac{7}{2}^+$	$\lvert 0,2,0,0\rangle$	$^4D_{7/2}$	1.2	7.7	138.3	0.2	0.5	0.01	0.2	1.5	3.3	30.0	0.8	14.3	1.5	15.8	54.3	0.2	56.7

TABLE 4.9: Same as Table 4.1, but for $\Omega_b^-(ssb)$ states belonging to the flavor multiplet $\mathcal{F} = \mathbf{6}_{\rm F}$.

$\mathcal{F} = \mathbf{6}_{\rm F}$				$\Omega_b^-\gamma$	$\Omega_b^{*-}\gamma$	$\Omega_b^-\gamma$	$\Omega_b^{*-}\gamma$	$\Omega_b^-\gamma$	$\Omega_b^{*-}\gamma$	$\Omega_b^{*-}\gamma$	$\Omega_b^-\gamma$	$\Omega_b^-\gamma$
$\Omega_b^-(ssb)$	$\mathbf{J^P}$	$\lvert l_\lambda, l_\rho, k_\lambda, k_\rho\rangle$	$^{2S+1}L_J$	$^2S_{1/2}$	$^4S_{3/2}$	$^2_\lambda P_{1/2}$	$^4_\lambda P_{1/2}$	$^2_\lambda P_{3/2}$	$^4_\lambda P_{3/2}$	$^4_\lambda P_{5/2}$	$^2_\rho P_{1/2}$	$^2_\rho P_{3/2}$
$N = 2$												
$\Omega_b(6568)^-$	$\frac{3}{2}^+$	$\lvert 2,0,0,0\rangle$	$^2D_{3/2}$	14.06	0.35	97.37	0.72	9.7	0.19	0.02	0	0
$\Omega_b(6578)^-$	$\frac{5}{2}^+$	$\lvert 2,0,0,0\rangle$	$^2D_{5/2}$	46.7	0.4	4.16	0.07	163.27	0.35	0.29	0	0
$\Omega_b(6584)^-$	$\frac{1}{2}^+$	$\lvert 2,0,0,0\rangle$	$^4D_{1/2}$	0.58	7.13	0.8	77.9	0.0	9.04	0.26	0	0
$\Omega_b(6590)^-$	$\frac{3}{2}^+$	$\lvert 2,0,0,0\rangle$	$^4D_{3/2}$	1.23	8.4	2.03	57.25	0.12	35.7	1.9	0	0
$\Omega_b(6600)^-$	$\frac{5}{2}^+$	$\lvert 2,0,0,0\rangle$	$^4D_{5/2}$	1.84	15.6	0.87	2.36	1.86	104.5	18.02	0	0
$\Omega_b(6614)^-$	$\frac{7}{2}^+$	$\lvert 2,0,0,0\rangle$	$^4D_{7/2}$	1.32	48.47	0.002	0.086	2.38	2.9	174.73	0	0
$\Omega_b(6574)^-$	$\frac{1}{2}^+$	$\lvert 0,0,1,0\rangle$	$^2S_{1/2}$	10.52	0.95	125.14	0.015	0.012	0.059	1.7	0	0
$\Omega_b(6602)^-$	$\frac{3}{2}^+$	$\lvert 0,0,1,0\rangle$	$^4S_{3/2}$	3.46	9.27	4.64	35.25	12.56	44.65	0.69	0	0
$\Omega_b(6874)^-$	$\frac{1}{2}^+$	$\lvert 0,0,0,1\rangle$	$^2S_{1/2}$	43.16	4.8	2.27	0.013	38.38	0.054	1.64	39.6	111.25
$\Omega_b(6902)^-$	$\frac{3}{2}^+$	$\lvert 0,0,0,1\rangle$	$^4S_{3/2}$	11.97	37.8	3.33	0.6	9.19	2.01	24.3	49.59	140.02
$\Omega_b(6718)^-$	$\frac{3}{2}^+$	$\lvert 1,1,0,0\rangle$	$^2D_{3/2}$	15.58	6.39	2.04	5.9	2.19	2.04	0.18	54.21	9.3
$\Omega_b(6728)^-$	$\frac{5}{2}^+$	$\lvert 1,1,0,0\rangle$	$^2D_{5/2}$	16.6	6.86	4.4	0.76	3.38	2.94	2.27	0.34	63.14
$\Omega_b(6720)^-$	$\frac{1}{2}^-$	$\lvert 1,1,0,0\rangle$	$^2P_{1/2}$	0	0	0	7.35	0	5.5	1.24	56.08	8.0
$\Omega_b(6726)^-$	$\frac{3}{2}^-$	$\lvert 1,1,0,0\rangle$	$^2P_{3/2}$	0	0	6.45	2.6	3.05	3.43	1.32	14.12	50.35
$\Omega_b(6724)^-$	$\frac{1}{2}^+$	$\lvert 1,1,0,0\rangle$	$^2S_{1/2}$	0	0	2.18	0.95	4.22	0.18	1.53	35.4	17.5
$\Omega_b(6868)^-$	$\frac{3}{2}^+$	$\lvert 0,2,0,0\rangle$	$^2D_{3/2}$	16.05	1.87	8.2	0.057	5.76	0.01	0.08	4.99	6.04
$\Omega_b(6878)^-$	$\frac{5}{2}^+$	$\lvert 0,2,0,0\rangle$	$^2D_{5/2}$	99.76	1.95	7.11	0.06	26.28	0.012	0.09	9.87	8.69
$\Omega_b(6884)^-$	$\frac{1}{2}^+$	$\lvert 0,2,0,0\rangle$	$^4D_{1/2}$	2.24	4.3	0.09	4.1	0.17	2.35	2.0	10.7	0.07
$\Omega_b(6890)^-$	$\frac{3}{2}^+$	$\lvert 0,2,0,0\rangle$	$^4D_{3/2}$	4.59	14.36	0.19	4.16	0.37	0.14	3.8	25.5	1.55
$\Omega_b(6900)^-$	$\frac{5}{2}^+$	$\lvert 0,2,0,0\rangle$	$^4D_{5/2}$	6.45	27.5	0.3	2.25	0.56	6.19	5.12	10.14	22.42
$\Omega_b(6914)^-$	$\frac{7}{2}^+$	$\lvert 0,2,0,0\rangle$	$^4D_{7/2}$	4.27	101.4	0.22	5.39	0.42	7.24	22.23	0.06	26.18

decay width of 46 MeV. Thus if experimentalists find a state with this mass and total decay width they won't be able to distinguish if it is a Ξ_b or a Ξ_b' state only with that information. A possible way to make a conclusive assignment is studying their radiative decay channels. Some useful channels might be the following:

$$\Gamma_{em}[\Xi_b(6524) \to \Xi_b^{\prime 0}\gamma] = 132.5\,\text{KeV} \qquad \Gamma_{em}[\Xi_b'(6520) \to \Xi_b^{\prime 0}\gamma] = 2.4\,\text{KeV}, \tag{4.3}$$

$$\Gamma_{em}[\Xi_b(6524) \to \Xi_b^{*0}\gamma] = 6.3\,\text{KeV} \qquad \Gamma_{em}[\Xi_b'(6520) \to \Xi_b^{*0}\gamma] = 59.7\,\text{KeV}, \tag{4.4}$$

$$\Gamma_{em}[\Xi_b(6524) \to \Xi_b^{-}\gamma] = 37.9\,\text{KeV} \qquad \Gamma_{em}[\Xi_b'(6520) \to \Xi_b^{-}\gamma] = 1.1\,\text{KeV}, \tag{4.5}$$

$$\Gamma_{em}[\Xi_b(6524) \to \Xi_b^{*-}\gamma] = 0.1\,\text{KeV} \qquad \Gamma_{em}[\Xi_b'(6520) \to \Xi_b^{*-}\gamma] = 92.8\,\text{KeV}. \tag{4.6}$$

In this sense, the results obtained in this study may be of importance as a way to make a correct assignment of states similar to the examples just described. These calculations may serve as a valuable reference for experimentalists working on high-energy physics experiments, such as those conducted at the LHC.

The results presented in this Chapter are being prepared for publication in two separated articles: one for the Λ_b and Ξ_b bottom baryons, belonging to the flavor anti-triplet ($\bar{\mathbf{3}}_{\rm F}$) [91], and another one for the Σ_b, Ξ_b' and Ω_b bottom baryons, belonging to the flavor sextet ($\mathbf{6}_{\rm F}$) [92].

Chapter 5

Electromagnetic decays of the Ξ_c baryons

In this Chapter the calculations of the electromagnetic decay widths for the Ξ_c baryons within the constituent quark model formalism are presented. Specifically, the decay widths of the transitions from P-wave states to ground states are determined.

As already mentioned in Chapter 3, the electromagnetic decays play a particularly valuable role when the strong decays are suppressed. One notable example in the charm sector is the Ω_c^*, which is the spin excitation of the Ω_c^0 state. The $\Omega_c^* \to \Omega_c^0 \pi$ strong decay is forbidden due to lack of phase space and isospin conservation in strong interactions. Therefore, the $\Omega_c^* \to \Omega_c^0 \gamma$ decay mode becomes a relevant channel. This resonance was precisely observed in the decay mode channel $\Omega_c^0 \gamma$ by the BABAR collaboration [149] and later confirmed by the Belle Collaboration [150].

In the last few decades, the experimental observation of electromagnetic decays of singly charmed baryons has had more progress [93, 149–151]. In 1999, the CLEO collaboration [151] reported the observation of the Ξ_c' in the electromagnetic decay channel $\Xi_c' \to \Xi_c \gamma$. In 2006, the BABAR collaboration observed for the first time the Ω_c^* state using its radiative decay channel $\Omega_c^* \to \Omega_c^0 \gamma$ [149]. A few years later, in 2008, the Belle Collaboration confirmed this observation in the same electromagnetic channel [150]. However, the electromagnetic decay widths of these ground states were not reported in references [149–151] because of the high difficulty of the measurements.

In a more recent study, in 2020, the Belle collaboration [93] estimated the electromagnetic decay widths of the P-wave $\Xi_c(2790)^{+/0}$ and $\Xi_c(2815)^{+/0}$ singly charmed baryons using the branching ratios of the electromagnetic decays with respect to the total decay widths reported in reference [152].

Regarding theoretical works, the electromagnetic decays of singly charmed baryons have been studied in references [70, 82, 115, 126, 130–142, 153–165]. In references [126, 130–141, 153–162], only the electromagnetic transitions of ground state singly charmed baryons were considered. However, only in references [70, 82, 115, 142, 163–165] the authors have focused on the radiative decays of P-wave charmed baryons. For additional references see the review articles [166–168].

In reference [163], an effective hadron-quark Lagrangian (EHQL) was used to calculate the radiative transitions of some P-wave states. In references [70, 82, 115] the Nonrelativistic Quark Model (NRQM) was used to study singly heavy baryons by means of the nonrelativistic electromagnetic Hamiltonian introduced by Close and Copley [143]. The Coupled-Channel Approach (CCA) was employed in reference [164] to study the radiative decays of the $\Sigma_c(2792)^{\pm,0}$, $\Xi_c(2790)^{+/0}$, $\Xi_c(2970)^{+/0}$, and $\Lambda_c(2595)$ P-wave states. The radiative decays of the $\Sigma_c(2792)^{\pm,0}$, $\Xi_c(2790)^{+/0}$, $\Xi_c(2870)^{+/0}$, and $\Lambda_c(2592)$ states were also studied applying the QCD Sum Rules (QCDSR) approach in reference [165]. The results reported in references [70, 82, 115] followed the experimental trend, but the numerical values were underestimated because the evaluation of the convective term of the electromagnetic interaction Hamiltonian was not done in an exact manner but introducing approximations, as already described in more detail in Chapter 3. The decay widths of the $\Xi_c(2790)^0$ and $\Xi_c(2790)^+$ states obtained in references [164] and [165] followed the opposite trend.

5.1 Singly charmed baryons wave functions

Singly charmed baryons are baryons composed of one charm quark and two light quarks. In this section the wave functions for the singly charmed baryons states are presented. Specifically, only the flavor wave functions are displayed because for the cases of the spin and spatial wave functions, they are exactly the same as for the singly bottom baryons and they are given in sections 2.3.1 and 2.3.3.

In the charm sector, the $\bar{\mathbf{3}}_{\mathrm{F}}$-plet and the $\mathbf{6}_{\mathrm{F}}$-plet representations of the flavor wave functions are considered. Next, the flavor wave functions of a singly charmed baryon A and its isospin quantum numbers $|A, I, M_I\rangle$ are presented [33]:

$\bar{\mathbf{3}}_{\mathrm{F}}$-plet

$$\phi_{\Xi_c^0} : |\Xi_c^0, 1/2, -1/2\rangle = \frac{1}{\sqrt{2}}(|dsc\rangle - |sdc\rangle), \tag{5.1}$$

$$\phi_{\Xi_c^+} : |\Xi_c^+, 1/2, 1/2\rangle = \frac{1}{\sqrt{2}}(|usc\rangle - |suc\rangle), \tag{5.2}$$

$$\phi_{\Lambda_c^+} : |\Lambda_c^+, 0, 0\rangle = \frac{1}{\sqrt{2}}(|udc\rangle - |duc\rangle). \tag{5.3}$$

$\mathbf{6}_{\mathrm{F}}$-plet

$$\phi_{\Omega_c^0} : |\Omega_c, 0, 0\rangle = |ssc\rangle, \tag{5.4}$$

$$\phi_{\Xi_c'^0} : |\Xi_c'^0, 1/2, -1/2\rangle = \frac{1}{\sqrt{2}}(|dsc\rangle + |sdc\rangle), \tag{5.5}$$

$$\phi_{\Xi_c'^+} : |\Xi_c'^+, 1/2, 1/2\rangle = \frac{1}{\sqrt{2}}(|usc\rangle + |suc\rangle), \tag{5.6}$$

$$\phi_{\Sigma_c^{++}} : |\Sigma_c^{++}, 1, 1\rangle = |uuc\rangle, \tag{5.7}$$

$$\phi_{\Sigma_c^{+}} : |\Sigma_c^{+}, 1, 0\rangle = \frac{1}{\sqrt{2}}(|udc\rangle + |duc\rangle), \tag{5.8}$$

$$\phi_{\Sigma_c^{0}} : |\Sigma_c^{0}, 1, -1\rangle = |ddc\rangle. \tag{5.9}$$

It can be seen that, as for the bottom sector, the functions of the $\bar{\mathbf{3}}_{\mathrm{F}}$-plet are anti-symmetric under the interchange of the two light quarks, whereas, the functions of the $\mathbf{6}_{\mathrm{F}}$-plet are symmetric under the same interchange of the two light quarks.

5.2 Electromagnetic decay widths of the Ξ_c baryons

In this section the electromagnetic decay widths for the Ξ_c baryons are calculated using eq. (3.2) presented in Section 3.1 of Chapter 3. The attention was focused on the Ξ_c baryons given that experimental values of electromagnetic decay widths has been reported by the Belle collaboration [93].

The results for our electromagnetic decay widths of the Ξ_c baryons for transitions from P-wave to ground states are shown in Table (5.1). These values are compared with those obtained in references [70, 115]. The errors in the computed values are determined using a Monte Carlo bootstrap method [33]. Our theoretical results for the $\Xi_c(2790)^{+/0}$ and $\Xi_c(2815)^{+/0}$ states are in agreement with the recent data reported by the Belle collaboration [93]. In the following, the obtained theoretical values are discussed.

The Belle collaboration [93] reported for the $\Xi_c(2790)^0$ state a branching ratio of $(7.9 \pm 2.0^{+1.7}_{-2.3})\%$ of the total width corresponding to the electromagnetic decay. This leads to a partial decay width of

$$\Gamma_{em}[\Xi_c(2790)^0 \to \Xi_c^0\gamma] \sim 800 \pm 320 \text{ KeV}. \tag{5.10}$$

Following the assignment made in reference [33], this state corresponds to a P_λ-wave state with $\mathbf{J}^P = \frac{1}{2}^-$ and the decay width calculated in this study is 335^{+23}_{-22} KeV. This value slightly underestimates the value reported by Belle.

The Belle collaboration [93] did not find any signal for the electromagnetic decay of the $\Xi_c(2790)^+$ state, but set an upper limit on the partial width of

$$\Gamma_{em}[\Xi_c(2790)^+ \to \Xi_c^+\gamma] < 350 \text{ KeV}. \tag{5.11}$$

This state was identified as a P_λ-wave state with $\mathbf{J}^P = \frac{1}{2}^-$ in reference [33]. Our result for the electromagnetic decay width is 28^{+17}_{-16} KeV, and this value is compatible with the upper limit set by reference [93].

For the $\Xi_c(2815)^0$ state decaying to $\Xi_c^0\gamma$, the Belle collaboration [93] estimated a partial width of

$$\Gamma_{em}[\Xi_c(2815)^0 \to \Xi_c^0\gamma] = 320 \pm 45^{+45}_{-80}\ \text{KeV}. \tag{5.12}$$

According to reference [33] this state corresponds to a P_λ-wave state with $\mathbf{J}^P = \frac{3}{2}^-$. Our electromagnetic decay width for the $\Xi_c(2815)^0$ state is 380^{+24}_{-23} KeV and this value agrees with the value from reference [93].

Finally, the Belle Collaboration [93] also estimated the upper limit for the partial electromagnetic decay width of the $\Xi_c(2815)^+$ state to the Ξ_c^+ as

$$\Gamma_{em}[\Xi_c(2815)^+ \to \Xi_c^+\gamma] < 80\ \text{KeV}. \tag{5.13}$$

This state is identified as a P_λ-wave state with $\mathbf{J}^P = \frac{3}{2}^-$ in reference [33]. Our computed decay width for this state is 20^{+15}_{-13} KeV. This value is compatible with the upper limit set by the Belle Collaboration [93].

Furthermore, the results of this study for the decay widths of $(\Xi_c(2790)^{+/0} \to \Xi_c^{+/0}\gamma)$ and $(\Xi_c(2815)^{+/0} \to \Xi_c^{+/0}\gamma)$ are compared in Table (5.2) with the experimental values reported by the Belle collaboration [93] and with those obtained in previous theoretical works using different models. Specifically, in reference [163] the Relativistic Quark Model (RQM) was used, NRQM in references [70, 115], the Coupled-Channel Approach (CCA) in reference [164], QCDSR in reference [165], and the GEM in reference [82].

5.3 Summary and conclusions of the chapter

In summary, calculations for the electromagnetic decay widths of the Ξ_c baryons from the P-wave states to the ground states were performed. The values were computed in a new analytical way described in detail in Appendix A and using the masses from reference [33] without introducing any free parameters.

The results of this study for the $\Xi_c(2790)^0$ and $\Xi_c(2815)^0$ states are in good agreement with the values reported by the Belle collaboration in reference [93]. For the $\Xi_c(2790)^+$ and the $\Xi_c(2815)^+$ states, the theoretical decay widths are compatible with the upper limit set by the Belle Collaboration [93]. The trend in the electromagnetic decay widths of the neutral and charged $\Xi_c(2815)$ and $\Xi_c(2790)$ states is well reproduced in our calculations, which are based on the assignment of the $\Xi_c(2790)$ and $\Xi_c(2815)$ as P_λ states made in reference [33].

From Table 5.2, one can see that the results from references [70], and [82] followed the experimental trend, but they underestimated the numerical values. One can also notice that references [164] and [165] followed the opposite trend for the $\Xi_c(2790)^0$ and $\Xi_c(2790)^+$ states. It can be observed that the results of this study also follow the experimental trend, and the numerical values are more compatible with the experimental ones [93]. From Table (5.1), it can be observed that, in general, the results of this work differ from those presented in references [70]

$\mathcal{F}=\bar{\mathbf{3}}_{\mathrm{F}}$				$\Xi_c^+\gamma$	$\Xi_c^0\gamma$	$\Xi_c'^+\gamma$	$\Xi_c'^0\gamma$	$\Xi_c'^{*+}\gamma$	$\Xi_c'^{*0}\gamma$	
$\Xi_c(snc)$	$\mathbf{J^P}$	$\lvert l_\lambda,l_\rho,k_\lambda,k_\rho\rangle$	$^{2S+1}L_J$	KeV	KeV	KeV	KeV	KeV	KeV	
$N=1$										
$\Xi_c(2788)$	$\frac{1}{2}^-$	$\lvert 1,0,0,0\rangle$	$^2P_{1/2}$	28^{+17}_{-16}	335^{+23}_{-22}	$3.6^{+1.5}_{-1.5}$	$0.1^{+0.03}_{-0.02}$	$0.3^{+0.1}_{-0.1}$	0	
				4.65	263	1.43	0	0.44	0	[70]
				7.4	202.5	1.3	0	0.1	0	[115]
$\Xi_c(2815)$	$\frac{3}{2}^-$	$\lvert 1,0,0,0\rangle$	$^2P_{3/2}$	20^{+15}_{-13}	380^{+24}_{-23}	$6^{+2.8}_{-2.6}$	$0.1^{+0.03}_{-0.03}$	$0.7^{+0.3}_{-0.3}$	0	
				2.8	292	2.32	0	0.99	0	[70]
				4.8	292.6	2.9	0.1	0.3	0	[115]
$\Xi_c(2935)$	$\frac{1}{2}^-$	$\lvert 0,1,0,0\rangle$	$^2P_{1/2}$	24^{+11}_{-10}	32^{+12}_{-11}	559^{+46}_{-42}	12^{+3}_{-3}	2.4^{+1}_{-1}	$0.1^{+0.03}_{-0.03}$	
				1.39	5.57	128	0	0.25	0	[70]
				12.3	20.1	145.4	3.1	1.0	0	[115]
$\Xi_c(2977)$	$\frac{1}{2}^-$	$\lvert 0,1,0,0\rangle$	$^4P_{1/2}$	16^{+8}_{-7}	22^{+9}_{-8}	8^{+4}_{-4}	$0.2^{+0.07}_{-0.07}$	86^{+15}_{-17}	$2^{+0.5}_{-0.4}$	
				0.75	3.0	0.41	0	43.4	0	[70]
				7.8	12.8	3.7	0.1	13.7	0.3	[115]
$\Xi_c(2962)$	$\frac{3}{2}^-$	$\lvert 0,1,0,0\rangle$	$^2P_{3/2}$	29^{+13}_{-11}	39^{+14}_{-12}	1218^{+191}_{-194}	26^{+10}_{-9}	$3.4^{+1.5}_{-1.4}$	$0.1^{+0.03}_{-0.03}$	
				1.88	7.5	110	0	0.52	0	[70]
				16.2	26.5	481.6	10.2	1.7	0	[115]
$\Xi_c(3004)$	$\frac{3}{2}^-$	$\lvert 0,1,0,0\rangle$	$^4P_{3/2}$	52^{+23}_{-20}	72^{+25}_{-24}	30^{+14}_{-12}	$0.6^{+0.3}_{-0.2}$	415^{+34}_{-32}	9^{+3}_{-2}	
				2.81	11.2	1.85	0	58.1	0	[70]
				28.0	45.9	15.2	0.3	111.5	2.4	[115]
$\Xi_c(3049)$	$\frac{5}{2}^-$	$\lvert 0,1,0,0\rangle$	$^4P_{5/2}$	43^{+18}_{-16}	59^{+19}_{-18}	28^{+11}_{-10}	$0.6^{+0.3}_{-0.2}$	1258^{+208}_{-214}	27^{+11}_{-10}	
				...	...	...	...	...	...	[70]
				25.7	42.1	16.5	0.4	367.7	7.8	[115]

TABLE 5.1: *Table from [94] (Elsevier copyright).* Predicted $\Xi_c(snc)$ electromagnetic decay widths (in KeV). The first column reports the baryon name with its predicted mass, as from reference [33]. The second column displays $\mathbf{J^P}$. The third column shows the internal configuration of the baryon $\lvert l_\lambda,l_\rho,k_\lambda,k_\rho\rangle$ within the three-quark model, where $l_{\lambda,\rho}$ represent the orbital angular momenta and $k_{\lambda,\rho}$ denote the number of nodes of the λ and ρ oscillators. The fourth column presents the spectroscopic notation $^{2S+1}L_J$ for each state. Furthermore, $N=n_\rho+n_\lambda=1$ is the energy band. Starting from the fifth column, the electromagnetic decay widths, computed by means of eq. (3.2), are presented. Each column corresponds to an electromagnetic decay channel; the decay products are indicated at the top of the column. The zero values are electromagnetic decay widths either too small to be shown on this scale or not permitted by phase space. The results of this work are compared with those of references [70] and [115]. The symbol "..." indicates that there is no prediction for that state in reference [70].

Decay channels	RQM [163]	NRQM [70]	CCA [164]	QCDSR [165]	GEM [82]	this work	Exp. [93]
$\Gamma\left(\Xi_c(2790)^0\to\Xi_c^0\gamma\right)$	...	263	119.3	2.7	217.5	335^{+23}_{-22}	$\sim 800\pm320$
$\Gamma\left(\Xi_c(2790)^+\to\Xi_c^+\gamma\right)$	...	4.65	249.6	265	1.7	28^{+17}_{-16}	<350
$\Gamma\left(\Xi_c(2815)^0\to\Xi_c^0\gamma\right)$	497	292	...	...	243.1	380^{+24}_{-23}	$320\pm45^{+45}_{-80}$
$\Gamma\left(\Xi_c(2815)^+\to\Xi_c^+\gamma\right)$	190	2.8	...	...	1.0	20^{+15}_{-13}	<80

TABLE 5.2: *Table from [94] (Elsevier copyright).* Comparison of the electromagnetic decay widths obtained in this study for the $\Xi_c(2790)^{+/0}$, $\Xi_c(2815)^{+/0}$ baryons (in KeV) with those of previous studies. The first column contains the decay channels. The results of this work are compared with those of references [163] (second column), [70] (third column), [164] (fourth column), , [165] (fifth column) and [82] (sixth column), and they are also compared with the experimental values from [93]. The symbol "..." indicates that there is no prediction for that state in the references.

and [115], as in the present study the evaluation of the convective term is done analytically, without introducing any further approximation as it is described in Appendix A. The origin of the discrepancy between our results and those from references [70] and [115] was already discussed in Chapter 3.

The results presented in this Chapter have been submitted to *Physics Letters B* and are available on arXiv [94]. These calculations demonstrate that the exact evaluation of the convective term plays a crucial role in the evaluation of electromagnetic transitions involving changes in angular momentum between the initial and final states. In such scenarios this term becomes dominant. It can be concluded that the proper treatment of the convective term in the Hamiltonian is essential for achieving results that are in good agreement with the available experimental data.

Chapter 6

Conclusions

In this thesis, the mass spectra, strong and electromagnetic decays of singly bottom baryons have been studied, as well as electromagnetic decays of Ξ_c baryons. Our predictions for the masses and strong decay widths of singly bottom baryons show good agreement with the available experimental data. Additionally, a new analytical method was developed to evaluate the electromagnetic transition amplitudes without introducing further approximations to the non-relativistic electromagnetic interaction Hamiltonian. Using this approach, the electromagnetic decay widths of singly bottom and singly charmed baryons were calculated, yielding results consistent with the available experimental data for singly charmed baryons. This method can be extended to calculate the radiative decays of other hadronic states, such as heavy mesons, doubly and triply heavy baryons, and exotic states like tetraquarks.

The conclusions of this study are divided into three parts:

1. **Mass spectra and strong decays of singly bottom baryons:** In this research, calculations for the mass spectra and strong partial decay widths of singly bottom baryons have been performed. The three-quark and quark-diquark schemes were both utilized to describe the mass spectra, predicting the $1S$, $1P$, $1D$, $2P$, and $2S$ states, extending the model of reference [83]. The three-quark excited $1P$, $1D$, $2P$, and $2S$ singly bottom baryon strong decay widths, within the $^3P_0$ model are also calculated. These results were published in *Physical Review D* [90].

2. **Electromagnetic decays of singly bottom baryons:** Calculations for the electromagnetic decay widths of singly bottom baryons have been performed. The results for the decays of P-wave and ground states to ground states were published in *Physical Review D* [90]. The results for the decays of the second shell singly bottom baryons to ground and P-wave states are being prepared to submit as two separated articles: one for the Λ_b and Ξ_b bottom baryons, belonging to the flavor anti-triplet ($\bar{\mathbf{3}}_{\mathrm{F}}$) [91], and another one for the Σ_b, Ξ_b' and Ω_b bottom baryons, belonging to the flavor sextet ($\mathbf{6}_{\mathrm{F}}$) [92]. The electromagnetic decays are useful to confirm the existence of some resonances. Specifically, when the strong decays are not allowed, the electromagnetic decays play a dominant role. They may also be helpful with the assignments when states have the same mass and total decay widths. Through this study it was possible to arrive at the conclusion that the correct evaluation of the convective term of the nonrelativistic Hamiltonian of eq. (3.9) plays an

important role in the calculation of electromagnetic transitions and that the introduction of any further is unnecessary, as it was demonstrated that an exact analytical evaluation of these transition amplitudes is possible.

3. **Electromagnetic decays of Ξ_c baryons:** Calculations for the electromagnetic decay widths of Ξ_c baryons have been performed using the method introduced in reference [90] and described in Chapter 3. The results of this study for the $\Xi_c(2790)^0$ and $\Xi_c(2815)^0$ states are in good agreement with the values reported by the Belle collaboration in reference [93]. Although the experimental decay widths of the $\Xi_c(2790)^+$ and the $\Xi_c(2815)^+$ states are less precise, our theoretical values are consistent with the upper limit set by Belle [93]. It can be checked once again that the correct evaluation of the convective term of the non-relativistic Hamiltonian for the electromagnetic interactions ensures more precise calculation. Furthermore, our results are in good agreement with the available experimental data. The results for the decays of P-wave Ξ_c states to ground states and their discussion were submitted to *Physics Letters B* and it is available as a pre-print in ArXiv [94].

Appendix A

Electromagnetic transition amplitudes

For the calculation of the transition amplitudes, all of the contributions in the flavor, spin and spatial spaces have to be computed. The explicit evaluations for the flavor and spin spaces are given in the next sections (A.1 and A.2). For the spatial contributions the matrix elements of the operators $\hat{U}_j$ and $\hat{T}_{j,-}$ have to be evaluated. The evaluation of the $\hat{U}_j$ matrix elements is straightforward. The $\hat{T}_{j,-}$ matrix elements are expressed as a sum of matrix elements of the $\hat{U}_j$ operators. To be able of expressing the elements in this way a new method involving the action of the ladder operators $\mathbf{p}_{\lambda/\rho,-}$ on the wave functions is developed. The complete procedure for the evaluation of the matrix elements of $\hat{T}_{j,-}$ are also found in this Appendix in Section A.3.3.

A.1 Evaluation of the matrix elements for the spin space

The matrix elements in the spin space, which are necessary to compute the electromagnetic decay widths, are evaluated. For this evaluation the spin wave functions given in eqs. (2.8-2.15) are used. The following results are obtained for the non-vanishing contributions:

$$\chi^{\dagger}_{s_{1/2}}\mathbf{s}_{1,-}\chi_{s_{3/2}} = \frac{1}{\sqrt{3}}\left[\langle\uparrow\uparrow\downarrow| + \langle\uparrow\downarrow\uparrow| + \langle\downarrow\uparrow\uparrow|\right]\mathbf{s}_{1,-}|\uparrow\uparrow\uparrow\rangle = \frac{1}{\sqrt{3}}, \tag{A.1}$$

$$\chi^{\dagger}_{s_{-1/2}}\mathbf{s}_{1,-}\chi_{s_{1/2}} = \frac{1}{\sqrt{3}}\left[\langle\uparrow\downarrow\downarrow| + \langle\downarrow\uparrow\downarrow| + \langle\downarrow\downarrow\uparrow|\right]\mathbf{s}_{1,-}\frac{1}{\sqrt{3}}\left[|\uparrow\uparrow\downarrow\rangle + |\uparrow\downarrow\uparrow\rangle + |\downarrow\uparrow\uparrow\rangle\right] = \frac{2}{3}, \tag{A.2}$$

$$\chi^{\dagger}_{s_{-3/2}}\mathbf{s}_{1,-}\chi_{s_{-1/2}} = \langle\downarrow\downarrow\downarrow|\mathbf{s}_{1,-}\frac{1}{\sqrt{3}}\left[|\uparrow\downarrow\downarrow\rangle + |\downarrow\uparrow\downarrow\rangle + |\downarrow\downarrow\uparrow\rangle\right] = \frac{1}{\sqrt{3}}, \tag{A.3}$$

$$\chi^{\dagger}_{s_{-1/2}}\mathbf{s}_{1,-}\chi_{\rho_{1/2}} = \frac{1}{\sqrt{3}}\left[\langle\uparrow\downarrow\downarrow| + \langle\downarrow\uparrow\downarrow| + \langle\downarrow\downarrow\uparrow|\right]\mathbf{s}_{1,-}\frac{1}{\sqrt{2}}\left[|\uparrow\downarrow\uparrow\rangle - |\downarrow\uparrow\uparrow\rangle\right] = \frac{1}{\sqrt{6}}, \tag{A.4}$$

$$\chi^{\dagger}_{s_{-3/2}}\mathbf{s}_{1,-}\chi_{\rho_{-1/2}} = \langle\downarrow\downarrow\downarrow|\mathbf{s}_{1,-}\frac{1}{\sqrt{2}}\left[|\uparrow\downarrow\downarrow\rangle - |\downarrow\uparrow\downarrow\rangle\right] = \frac{1}{\sqrt{2}}, \tag{A.5}$$

$$\chi^{\dagger}_{s_{-1/2}}\mathbf{s}_{1,-}\chi_{\lambda_{1/2}} = \frac{1}{\sqrt{3}}\left[\langle\uparrow\downarrow\downarrow| + \langle\downarrow\uparrow\downarrow| + \langle\downarrow\downarrow\uparrow|\right]\mathbf{s}_{1,-}\frac{1}{\sqrt{6}}\left[2|\uparrow\uparrow\downarrow\rangle - |\uparrow\downarrow\uparrow\rangle - |\downarrow\uparrow\uparrow\rangle\right] = \frac{\sqrt{2}}{6}, \tag{A.6}$$

$$\chi^{\dagger}_{s_{-3/2}}\mathbf{s}_{1,-}\chi_{\lambda_{-1/2}} = \langle\downarrow\downarrow\downarrow|\mathbf{s}_{1,-}\frac{1}{\sqrt{6}}\left[|\uparrow\downarrow\downarrow\rangle - |\downarrow\uparrow\downarrow\rangle - 2|\downarrow\downarrow\uparrow\rangle\right] = \frac{1}{\sqrt{6}}, \tag{A.7}$$

$$\chi^{\dagger}_{\rho_{1/2}}\mathbf{s}_{1,-}\chi_{s_{3/2}} = \frac{1}{\sqrt{2}}\left[\langle\uparrow\downarrow\uparrow\,| - \langle\downarrow\uparrow\uparrow\,|\right]\mathbf{s}_{1,-}|\,\uparrow\uparrow\uparrow\rangle = -\frac{1}{\sqrt{2}}, \tag{A.8}$$

$$\chi^{\dagger}_{\rho_{-1/2}}\mathbf{s}_{1,-}\chi_{s_{1/2}} = \frac{1}{\sqrt{2}}\left[\langle\uparrow\downarrow\downarrow\,| - \langle\downarrow\uparrow\downarrow\,|\right]\mathbf{s}_{1,-}\frac{1}{\sqrt{3}}\left[|\,\uparrow\uparrow\downarrow\rangle + |\,\uparrow\downarrow\uparrow\rangle + |\,\downarrow\uparrow\uparrow\rangle\right] = -\frac{1}{\sqrt{6}}, \tag{A.9}$$

$$\chi^{\dagger}_{\rho_{-1/2}}\mathbf{s}_{1,-}\chi_{\lambda_{1/2}} = \frac{1}{\sqrt{2}}\left[\langle\uparrow\downarrow\downarrow\,| - \langle\downarrow\uparrow\downarrow\,|\right]\mathbf{s}_{1,-}\frac{1}{\sqrt{6}}\left[2|\,\uparrow\uparrow\downarrow\rangle - |\,\uparrow\downarrow\uparrow\rangle - |\,\downarrow\uparrow\uparrow\rangle\right] = -\frac{1}{\sqrt{3}}, \tag{A.10}$$

$$\chi^{\dagger}_{\lambda_{1/2}}\mathbf{s}_{1,-}\chi_{s_{3/2}} = \frac{1}{\sqrt{6}}\left[2\langle\uparrow\uparrow\downarrow\,| - \langle\uparrow\downarrow\uparrow\,| - \langle\downarrow\uparrow\uparrow\,|\right]\mathbf{s}_{1,-}|\,\uparrow\uparrow\uparrow\rangle = -\frac{1}{\sqrt{6}}, \tag{A.11}$$

$$\chi^{\dagger}_{\lambda_{-1/2}}\mathbf{s}_{1,-}\chi_{s_{1/2}} = \frac{1}{\sqrt{6}}\left[\langle\uparrow\downarrow\downarrow\,| - \langle\downarrow\uparrow\downarrow\,| - 2\langle\downarrow\downarrow\uparrow\,|\right]\mathbf{s}_{1,-}\frac{1}{\sqrt{3}}\left[|\,\uparrow\uparrow\downarrow\rangle + |\,\uparrow\downarrow\uparrow\rangle + |\,\downarrow\uparrow\uparrow\rangle\right] = -\frac{\sqrt{2}}{6}, \tag{A.12}$$

$$\chi^{\dagger}_{\lambda_{-1/2}}\mathbf{s}_{1,-}\chi_{\rho_{1/2}} = \frac{1}{\sqrt{6}}\left[\langle\uparrow\downarrow\downarrow\,| - \langle\downarrow\uparrow\downarrow\,| - 2\langle\downarrow\downarrow\uparrow\,|\right]\mathbf{s}_{1,-}\frac{1}{\sqrt{2}}\left[|\,\uparrow\downarrow\uparrow\rangle - |\,\downarrow\uparrow\uparrow\rangle\right] = -\frac{1}{\sqrt{3}}, \tag{A.13}$$

$$\chi^{\dagger}_{\lambda_{-1/2}}\mathbf{s}_{1,-}\chi_{\lambda_{1/2}} = \frac{1}{\sqrt{6}}\left[\langle\uparrow\downarrow\downarrow\,| - \langle\downarrow\uparrow\downarrow\,| - 2\langle\downarrow\downarrow\uparrow\,|\right]\mathbf{s}_{1,-}\frac{1}{\sqrt{6}}\left[2|\,\uparrow\uparrow\downarrow\rangle - |\,\uparrow\downarrow\uparrow\rangle - |\,\downarrow\uparrow\uparrow\rangle\right] = \frac{2}{3}, \tag{A.14}$$

$$\chi^{\dagger}_{s_{1/2}}\mathbf{s}_{2,-}\chi_{s_{3/2}} = \frac{1}{\sqrt{3}}\left[\langle\uparrow\uparrow\downarrow\,| + \langle\uparrow\downarrow\uparrow\,| + \langle\downarrow\uparrow\uparrow\,|\right]\mathbf{s}_{2,-}|\,\uparrow\uparrow\uparrow\rangle = \frac{1}{\sqrt{3}}, \tag{A.15}$$

$$\chi^{\dagger}_{s_{-1/2}}\mathbf{s}_{2,-}\chi_{s_{1/2}} = \frac{1}{\sqrt{3}}\left[\langle\uparrow\downarrow\downarrow\,| + \langle\downarrow\uparrow\downarrow\,| + \langle\downarrow\downarrow\uparrow\,|\right]\mathbf{s}_{2,-}\frac{1}{\sqrt{3}}\left[|\,\uparrow\uparrow\downarrow\rangle + |\,\uparrow\downarrow\uparrow\rangle + |\,\downarrow\uparrow\uparrow\rangle\right] = \frac{2}{3}, \tag{A.16}$$

$$\chi^{\dagger}_{s_{-3/2}}\mathbf{s}_{2,-}\chi_{s_{-1/2}} = \langle\downarrow\downarrow\downarrow\,|\mathbf{s}_{2,-}\frac{1}{\sqrt{3}}\left[|\,\uparrow\downarrow\downarrow\rangle + |\,\downarrow\uparrow\downarrow\rangle + |\,\downarrow\downarrow\uparrow\rangle\right] = \frac{1}{\sqrt{3}}, \tag{A.17}$$

$$\chi^{\dagger}_{s_{-1/2}}\mathbf{s}_{2,-}\chi_{\rho_{1/2}} = \frac{1}{\sqrt{3}}\left[\langle\uparrow\downarrow\downarrow\,| + \langle\downarrow\uparrow\downarrow\,| + \langle\downarrow\downarrow\uparrow\,|\right]\mathbf{s}_{2,-}\frac{1}{\sqrt{2}}\left[|\,\uparrow\downarrow\uparrow\rangle - |\,\downarrow\uparrow\uparrow\rangle\right] = -\frac{1}{\sqrt{6}}, \tag{A.18}$$

$$\chi^{\dagger}_{s_{-3/2}}\mathbf{s}_{2,-}\chi_{\rho_{-1/2}} = \langle\downarrow\downarrow\downarrow\,|\mathbf{s}_{2,-}\frac{1}{\sqrt{2}}\left[|\,\uparrow\downarrow\downarrow\rangle - |\,\downarrow\uparrow\downarrow\rangle\right] = -\frac{1}{\sqrt{2}}, \tag{A.19}$$

$$\chi^{\dagger}_{s_{-1/2}}\mathbf{s}_{2,-}\chi_{\lambda_{1/2}} = \frac{1}{\sqrt{3}}\left[\langle\uparrow\downarrow\downarrow\,| + \langle\downarrow\uparrow\downarrow\,| + \langle\downarrow\downarrow\uparrow\,|\right]\mathbf{s}_{2,-}\frac{1}{\sqrt{6}}\left[2|\,\uparrow\uparrow\downarrow\rangle - |\,\uparrow\downarrow\uparrow\rangle - |\,\downarrow\uparrow\uparrow\rangle\right] = \frac{\sqrt{2}}{6}, \tag{A.20}$$

$$\chi^{\dagger}_{s_{-3/2}}\mathbf{s}_{2,-}\chi_{\lambda_{-1/2}} = \langle\downarrow\downarrow\downarrow\,|\mathbf{s}_{2,-}\frac{1}{\sqrt{6}}\left[|\,\uparrow\downarrow\downarrow\rangle - |\,\downarrow\uparrow\downarrow\rangle - 2|\,\downarrow\downarrow\uparrow\rangle\right] = \frac{1}{\sqrt{6}}, \tag{A.21}$$

$$\chi^{\dagger}_{\rho_{1/2}}\mathbf{s}_{2,-}\chi_{s_{3/2}} = \frac{1}{\sqrt{2}}\left[\langle\uparrow\downarrow\uparrow\,| - \langle\downarrow\uparrow\uparrow\,|\right]\mathbf{s}_{2,-}|\,\uparrow\uparrow\uparrow\rangle = \frac{1}{\sqrt{2}}, \tag{A.22}$$

$$\chi^{\dagger}_{\rho_{-1/2}}\mathbf{s}_{2,-}\chi_{s_{1/2}} = \frac{1}{\sqrt{2}}\left[\langle\uparrow\downarrow\downarrow\,| - \langle\downarrow\uparrow\downarrow\,|\right]\mathbf{s}_{2,-}\frac{1}{\sqrt{3}}\left[|\,\uparrow\uparrow\downarrow\rangle + |\,\uparrow\downarrow\uparrow\rangle + |\,\downarrow\uparrow\uparrow\rangle\right] = \frac{1}{\sqrt{6}}, \tag{A.23}$$

$$\chi^{\dagger}_{\rho_{-1/2}}\mathbf{s}_{2,-}\chi_{\lambda_{1/2}} = \frac{1}{\sqrt{2}}\left[\langle\uparrow\downarrow\downarrow\,| - \langle\downarrow\uparrow\downarrow\,|\right]\mathbf{s}_{2,-}\frac{1}{\sqrt{6}}\left[2|\,\uparrow\uparrow\downarrow\rangle - |\,\uparrow\downarrow\uparrow\rangle - |\,\downarrow\uparrow\uparrow\rangle\right] = \frac{1}{\sqrt{3}}, \tag{A.24}$$

$$\chi^{\dagger}_{\lambda_{1/2}}\mathbf{s}_{2,-}\chi_{s_{3/2}} = \frac{1}{\sqrt{6}}\left[2\langle\uparrow\uparrow\downarrow\,| - \langle\uparrow\downarrow\uparrow\,| - \langle\downarrow\uparrow\uparrow\,|\right]\mathbf{s}_{2,-}|\,\uparrow\uparrow\uparrow\rangle = -\frac{1}{\sqrt{6}}, \tag{A.25}$$

$$\chi^{\dagger}_{\lambda_{-1/2}}\mathbf{s}_{2,-}\chi_{s_{1/2}} = \frac{1}{\sqrt{6}}\left[\langle\uparrow\downarrow\downarrow\,| - \langle\downarrow\uparrow\downarrow\,| - 2\langle\downarrow\downarrow\uparrow\,|\right]\mathbf{s}_{2,-}\frac{1}{\sqrt{3}}\left[|\,\uparrow\uparrow\downarrow\rangle + |\,\uparrow\downarrow\uparrow\rangle + |\,\downarrow\uparrow\uparrow\rangle\right] = -\frac{\sqrt{2}}{6}, \tag{A.26}$$

$$\chi^{\dagger}_{\lambda_{-1/2}}\mathbf{s}_{2,-}\chi_{\rho_{1/2}} = \frac{1}{\sqrt{6}}\left[\langle\uparrow\downarrow\downarrow| - \langle\downarrow\uparrow\downarrow| - 2\langle\downarrow\downarrow\uparrow|\right]\mathbf{s}_{2,-}\frac{1}{\sqrt{2}}\left[|\uparrow\downarrow\uparrow\rangle - |\downarrow\uparrow\uparrow\rangle\right] = \frac{1}{\sqrt{3}}, \tag{A.27}$$

$$\chi^{\dagger}_{\lambda_{-1/2}}\mathbf{s}_{2,-}\chi_{\lambda_{1/2}} = \frac{1}{\sqrt{6}}\left[\langle\uparrow\downarrow\downarrow| - \langle\downarrow\uparrow\downarrow| - 2\langle\downarrow\downarrow\uparrow|\right]\mathbf{s}_{2,-}\frac{1}{\sqrt{6}}\left[2|\uparrow\uparrow\downarrow\rangle - |\uparrow\downarrow\uparrow\rangle - |\downarrow\uparrow\uparrow\rangle\right] = \frac{2}{3}, \tag{A.28}$$

$$\chi^{\dagger}_{s_{1/2}}\mathbf{s}_{3,-}\chi_{s_{3/2}} = \frac{1}{\sqrt{3}}\left[\langle\uparrow\uparrow\downarrow| + \langle\uparrow\downarrow\uparrow| + \langle\downarrow\uparrow\uparrow|\right]\mathbf{s}_{3,-}|\uparrow\uparrow\uparrow\rangle = \frac{1}{\sqrt{3}}, \tag{A.29}$$

$$\chi^{\dagger}_{s_{-1/2}}\mathbf{s}_{3,-}\chi_{s_{1/2}} = \frac{1}{\sqrt{3}}\left[\langle\uparrow\downarrow\downarrow| + \langle\downarrow\uparrow\downarrow| + \langle\downarrow\downarrow\uparrow|\right]\mathbf{s}_{3,-}\frac{1}{\sqrt{3}}\left[|\uparrow\uparrow\downarrow\rangle + |\uparrow\downarrow\uparrow\rangle + |\downarrow\uparrow\uparrow\rangle\right] = \frac{2}{3}, \tag{A.30}$$

$$\chi^{\dagger}_{s_{-3/2}}\mathbf{s}_{3,-}\chi_{s_{-1/2}} = \langle\downarrow\downarrow\downarrow|\mathbf{s}_{3,-}\frac{1}{\sqrt{3}}\left[|\uparrow\downarrow\downarrow\rangle + |\downarrow\uparrow\downarrow\rangle + |\downarrow\downarrow\uparrow\rangle\right] = \frac{1}{\sqrt{3}}, \tag{A.31}$$

$$\chi^{\dagger}_{s_{-1/2}}\mathbf{s}_{3,-}\chi_{\lambda_{1/2}} = \frac{1}{\sqrt{3}}\left[\langle\uparrow\downarrow\downarrow| + \langle\downarrow\uparrow\downarrow| + \langle\downarrow\downarrow\uparrow|\right]\mathbf{s}_{3,-}\frac{1}{\sqrt{6}}\left[2|\uparrow\uparrow\downarrow\rangle - |\uparrow\downarrow\uparrow\rangle - |\downarrow\uparrow\uparrow\rangle\right] = -\frac{\sqrt{2}}{3}, \tag{A.32}$$

$$\chi^{\dagger}_{s_{-3/2}}\mathbf{s}_{3,-}\chi_{\lambda_{-1/2}} = \langle\downarrow\downarrow\downarrow|\mathbf{s}_{3,-}\frac{1}{\sqrt{6}}\left[|\uparrow\downarrow\downarrow\rangle - |\downarrow\uparrow\downarrow\rangle - 2|\downarrow\downarrow\uparrow\rangle\right] = -\frac{\sqrt{6}}{3}, \tag{A.33}$$

$$\chi^{\dagger}_{\rho_{-1/2}}\mathbf{s}_{3,-}\chi_{\rho_{1/2}} = \frac{1}{\sqrt{2}}\left[\langle\uparrow\downarrow\downarrow| - \langle\downarrow\uparrow\downarrow|\right]\mathbf{s}_{3,-}\frac{1}{\sqrt{2}}\left[|\uparrow\downarrow\uparrow\rangle - |\downarrow\uparrow\uparrow\rangle\right] = 1, \tag{A.34}$$

$$\chi^{\dagger}_{\lambda_{1/2}}\mathbf{s}_{3,-}\chi_{s_{3/2}} = \frac{1}{\sqrt{6}}\left[2\langle\uparrow\uparrow\downarrow| - \langle\uparrow\downarrow\uparrow| - \langle\downarrow\uparrow\uparrow|\right]\mathbf{s}_{3,-}|\uparrow\uparrow\uparrow\rangle = \frac{\sqrt{6}}{3}, \tag{A.35}$$

$$\chi^{\dagger}_{\lambda_{-1/2}}\mathbf{s}_{3,-}\chi_{s_{1/2}} = \frac{1}{\sqrt{6}}\left[\langle\uparrow\downarrow\downarrow| - \langle\downarrow\uparrow\downarrow| - 2\langle\downarrow\downarrow\uparrow|\right]\mathbf{s}_{3,-}\frac{1}{\sqrt{3}}\left[|\uparrow\uparrow\downarrow\rangle + |\uparrow\downarrow\uparrow\rangle + |\downarrow\uparrow\uparrow\rangle\right] = \frac{\sqrt{2}}{3}, \tag{A.36}$$

$$\chi^{\dagger}_{\lambda_{-1/2}}\mathbf{s}_{3,-}\chi_{\lambda_{1/2}} = \frac{1}{\sqrt{6}}\left[\langle\uparrow\downarrow\downarrow| - \langle\downarrow\uparrow\downarrow| - 2\langle\downarrow\downarrow\uparrow|\right]\mathbf{s}_{3,-}\frac{1}{\sqrt{6}}\left[2|\uparrow\uparrow\downarrow\rangle - |\uparrow\downarrow\uparrow\rangle - |\downarrow\uparrow\uparrow\rangle\right] = -\frac{1}{3}. \tag{A.37}$$

It is important to point out that there are some selection rules which apply to the spin couplings and only the non-vanishing results have been presented. These rules are applied because of the fact that in the electromagnetic decay a left-handed photon is emitted and this photon carries away one unit of angular momentum from the initial state. The selection rules for the ground states are the following:

Initial State	*Final State*
${S_A}^P = \frac{1}{2}^+,\ M_{S_A} = \frac{1}{2}, -\frac{1}{2}$	${S_{A'}}^P = \frac{1}{2}^+,\ M_{S_{A'}} = \frac{1}{2}, -\frac{1}{2},$
${S_A}^P = \frac{3}{2}^+,\ M_{S_A} = \frac{3}{2}, \frac{1}{2}, -\frac{1}{2}, -\frac{3}{2}$	${S_{A'}}^P = \frac{1}{2}^+,\ M_{S_{A'}} = \frac{1}{2}, -\frac{1}{2},$
${S_A}^P = \frac{3}{2}^+,\ M_{S_A} = \frac{3}{2}, \frac{1}{2}, -\frac{1}{2}, -\frac{3}{2}$	${S_{A'}}^P = \frac{3}{2}^+,\ M_{S_{A'}} = \frac{3}{2}, \frac{1}{2}, -\frac{1}{2}, -\frac{3}{2},$

where the allowed transitions are represented with the same color in the initial and in the final states, and the numbers that are in black represent spin transitions that are not allowed.

A.2 Evaluation of the matrix elements for the flavor space

Now the flavor coupling for the singly-bottom baryons are computed. As already defined in Section 3.1, the magnetic moment is given by $\hat{\mu}_j = \frac{\hat{e}_j}{2m_j}$ and the matrix elements in the flavor space are given by

$$\langle \phi_{A'} | \hat{\mu}_j | \phi_A \rangle = \langle \phi_{A'} | \frac{\hat{e}_j}{2m_j} | \phi_A \rangle, \tag{A.38}$$

The results are presented in the following subsections which are divided by its $SU_f(3)$ flavor representations.

A.2.1 Matrix elements of the states belonging to the flavor $\bar{3}_F$-plet

With the flavor wave function of eq. (2.18) the $\hat{\mu}_j$ matrix elements for the $|\phi_{\Lambda_b^0}\rangle$ state is computed and it is obtained

$$\langle \phi_{\Lambda_b^0} | \hat{\mu}_1 | \phi_{\Lambda_b^0} \rangle = \langle \phi_{\Lambda_b^0} | \hat{\mu}_2 | \phi_{\Lambda_b^0} \rangle = \frac{1}{2}(\mu_u + \mu_d), \qquad \langle \phi_{\Lambda_b^0} | \hat{\mu}_3 | \phi_{\Lambda_b^0} \rangle = \mu_b. \tag{A.39}$$

For the $|\phi_{\Xi_b^0}\rangle$ and $|\phi_{\Xi_b^-}\rangle$ states given in eq. (2.17) and eq. (2.16), respectively, the $\hat{\mu}_j$ matrix elements are

$$\langle \phi_{\Xi_b^0} | \hat{\mu}_1 | \phi_{\Xi_b^0} \rangle = \langle \phi_{\Xi_b^0} | \hat{\mu}_2 | \phi_{\Xi_b^0} \rangle = \frac{1}{2}(\mu_u + \mu_s), \qquad \langle \phi_{\Xi_b^0} | \hat{\mu}_3 | \phi_{\Xi_b^0} \rangle = \mu_b, \tag{A.40}$$

and

$$\langle \phi_{\Xi_b^-} | \hat{\mu}_1 | \phi_{\Xi_b^-} \rangle = \langle \phi_{\Xi_b^-} | \hat{\mu}_2 | \phi_{\Xi_b^-} \rangle = \frac{1}{2}(\mu_d + \mu_s), \qquad \langle \phi_{\Xi_b^-} | \hat{\mu}_3 | \phi_{\Xi_b^-} \rangle = \mu_b. \tag{A.41}$$

A.2.2 Matrix elements of the states of the flavor 6_F-plet with the states of the $\bar{3}_F$-plet

With the flavor wave functions of eq. (2.23) and eq. (2.18) the $\hat{\mu}_j$ matrix elements between the $|\phi_{\Sigma_b^0}\rangle$ and the $|\phi_{\Lambda_b^0}\rangle$ states are computed and the results are

$$\langle \phi_{\Lambda_b^0} | \hat{\mu}_1 | \phi_{\Sigma_b^0} \rangle = \frac{1}{2}(\mu_u - \mu_d), \qquad \langle \phi_{\Lambda_b^0} | \hat{\mu}_2 | \phi_{\Sigma_b^0} \rangle = \frac{1}{2}(\mu_d - \mu_u), \qquad \langle \phi_{\Lambda_b^0} | \hat{\mu}_3 | \phi_{\Sigma_b^0} \rangle = 0. \tag{A.42}$$

The matrix elements between the states $|\phi_{\Xi_b^0}\rangle$ and $|\phi_{\Xi_b^{\prime 0}}\rangle$, given by eq. (2.17) and eq. (2.21) are given by

$$\langle\phi_{\Xi_b^0}|\hat{\mu}_1|\phi_{\Xi_b^{\prime 0}}\rangle = \frac{1}{2}(\mu_u - \mu_s), \qquad \langle\phi_{\Xi_b^0}|\hat{\mu}_2|\phi_{\Xi_b^{\prime 0}}\rangle = \frac{1}{2}(\mu_s - \mu_u), \qquad \langle\phi_{\Xi_b^0}|\hat{\mu}_3|\phi_{\Xi_b^{\prime 0}}\rangle = 0. \tag{A.43}$$

And the matrix elements between the states $|\phi_{\Xi_b^-}\rangle$ and $|\phi_{\Xi_b^{\prime -}}\rangle$, given by eq. (2.16) and eq. (2.20) are given by

$$\langle\phi_{\Xi_b^-}|\hat{\mu}_1|\phi_{\Xi_b^{\prime -}}\rangle = \frac{1}{2}(\mu_d - \mu_s), \qquad \langle\phi_{\Xi_b^-}|\hat{\mu}_2|\phi_{\Xi_b^{\prime -}}\rangle = \frac{1}{2}(\mu_s - \mu_d), \qquad \langle\phi_{\Xi_b^-}|\hat{\mu}_3|\phi_{\Xi_b^{\prime -}}\rangle = 0. \tag{A.44}$$

A.2.3 Matrix elements of the states of the flavor 6_F-plet

With the flavor wave function of eq. (2.22) the $\hat{\mu}_j$ matrix elements for the $|\phi_{\Sigma_b^+}\rangle$ state are calculated and they are given by

$$\langle\phi_{\Sigma_b^+}|\hat{\mu}_1|\phi_{\Sigma_b^+}\rangle = \langle\phi_{\Sigma_b^+}|\hat{\mu}_2|\phi_{\Sigma_b^+}\rangle = \mu_u, \qquad \langle\phi_{\Sigma_b^+}|\hat{\mu}_3|\phi_{\Sigma_b^+}\rangle = \mu_b. \tag{A.45}$$

With the flavor wave function of eq. (2.23) the $\hat{\mu}_j$ matrix elements for the $|\phi_{\Sigma_b^0}\rangle$ state are calculated and it is obtained

$$\langle\phi_{\Sigma_b^0}|\hat{\mu}_1|\phi_{\Sigma_b^0}\rangle = \langle\phi_{\Sigma_b^0}|\hat{\mu}_2|\phi_{\Sigma_b^0}\rangle = \frac{1}{2}(\mu_u + \mu_d), \qquad \langle\phi_{\Sigma_b^0}|\hat{\mu}_3|\phi_{\Sigma_b^0}\rangle = \mu_b. \tag{A.46}$$

With the flavor wave function of eq. (2.24) the $\hat{\mu}_j$ matrix elements for the $|\phi_{\Sigma_b^-}\rangle$ state are calculated and it is obtained

$$\langle\phi_{\Sigma_b^-}|\hat{\mu}_1|\phi_{\Sigma_b^-}\rangle = \langle\phi_{\Sigma_b^-}|\hat{\mu}_2|\phi_{\Sigma_b^-}\rangle = \mu_d, \qquad \langle\phi_{\Sigma_b^-}|\hat{\mu}_3|\phi_{\Sigma_b^-}\rangle = \mu_b. \tag{A.47}$$

With the flavor wave function of eq. (2.21) the $\hat{\mu}_j$ matrix elements for the $|\phi_{\Xi_b^{\prime 0}}\rangle$ state are calculated and it is obtained

$$\langle\phi_{\Xi_b^{\prime 0}}|\hat{\mu}_1|\phi_{\Xi_b^{\prime 0}}\rangle = \langle\phi_{\Xi_b^{\prime 0}}|\hat{\mu}_2|\phi_{\Xi_b^{\prime 0}}\rangle = \frac{1}{2}(\mu_u + \mu_s), \qquad \langle\phi_{\Xi_b^{\prime 0}}|\hat{\mu}_3|\phi_{\Xi_b^{\prime 0}}\rangle = \mu_b. \tag{A.48}$$

With the flavor wave function of eq. (2.20) the $\hat{\mu}_j$ matrix elements for the $|\phi_{\Xi_b^{\prime -}}\rangle$ state are calculated and they are given by

$$\langle\phi_{\Xi_b^{\prime -}}|\hat{\mu}_1|\phi_{\Xi_b^{\prime -}}\rangle = \langle\phi_{\Xi_b^{\prime -}}|\hat{\mu}_2|\phi_{\Xi_b^{\prime -}}\rangle = \frac{1}{2}(\mu_d + \mu_s), \qquad \langle\phi_{\Xi_b^{\prime -}}|\hat{\mu}_3|\phi_{\Xi_b^{\prime -}}\rangle = \mu_b. \tag{A.49}$$

With the flavor wave function of eq. (2.19) the $\hat{\mu}_j$ matrix elements for the $|\phi_{\Omega_b^-}\rangle$ state are calculated and it is obtained

$$\langle\phi_{\Omega_b^-}|\hat{\mu}_1|\phi_{\Omega_b^-}\rangle = \langle\phi_{\Omega_b^-}|\hat{\mu}_2|\phi_{\Omega_b^-}\rangle = \mu_s, \qquad \langle\phi_{\Omega_b^-}|\hat{\mu}_3|\phi_{\Omega_b^-}\rangle = \mu_b. \tag{A.50}$$

TABLE A.1: The matrix elements $\langle\phi_{A'}|\hat{\mu}_1|\phi_A\rangle$. The corresponding initial states ($|\phi_A\rangle$) are displayed in the first row and the final states ($|\phi_{A'}\rangle$) in the first column.

States	$\|\phi_{\Lambda_b^0}\rangle$	$\|\phi_{\Xi_b^0}\rangle$	$\|\phi_{\Xi_b^-}\rangle$	$\|\phi_{\Sigma_b^+}\rangle$	$\|\phi_{\Sigma_b^0}\rangle$	$\|\phi_{\Sigma_b^-}\rangle$	$\|\phi_{\Xi_b'^0}\rangle$	$\|\phi_{\Xi_b'^-}\rangle$	$\|\phi_{\Omega_b^-}\rangle$
$\|\phi_{\Lambda_b^0}\rangle$	$\frac{\mu_u+\mu_d}{2}$	0	0	0	$\frac{\mu_u-\mu_d}{2}$	0	0	0	0
$\|\phi_{\Xi_b^0}\rangle$	0	$\frac{\mu_u+\mu_s}{2}$	0	0	0	0	$\frac{\mu_u-\mu_s}{2}$	0	0
$\|\phi_{\Xi_b^-}\rangle$	0	0	$\frac{\mu_d+\mu_s}{2}$	0	0	0	0	$\frac{\mu_d-\mu_s}{2}$	0
$\|\phi_{\Sigma_b^+}\rangle$	0	0	0	μ_u	0	0	0	0	0
$\|\phi_{\Sigma_b^0}\rangle$	$\frac{\mu_u-\mu_d}{2}$	0	0	0	$\frac{\mu_u+\mu_d}{2}$	0	0	0	0
$\|\phi_{\Sigma_b^-}\rangle$	0	0	0	0	0	μ_d	0	0	0
$\|\phi_{\Xi_b'^0}\rangle$	0	$\frac{\mu_u-\mu_s}{2}$	0	0	0	0	$\frac{\mu_u+\mu_s}{2}$	0	0
$\|\phi_{\Xi_b'^-}\rangle$	0	0	$\frac{\mu_d-\mu_s}{2}$	0	0	0	0	$\frac{\mu_d+\mu_s}{2}$	0
$\|\phi_{\Omega_b^-}\rangle$	0	0	0	0	0	0	0	0	μ_s

TABLE A.2: The matrix elements of $\langle\phi_{A'}|\hat{\mu}_2|\phi_A\rangle$. The corresponding initial states ($|\phi_A\rangle$) are displayed in the first row and the final states ($|\phi_{A'}\rangle$) in the first column.

States	$\|\phi_{\Lambda_b^0}\rangle$	$\|\phi_{\Xi_b^0}\rangle$	$\|\phi_{\Xi_b^-}\rangle$	$\|\phi_{\Sigma_b^+}\rangle$	$\|\phi_{\Sigma_b^0}\rangle$	$\|\phi_{\Sigma_b^-}\rangle$	$\|\phi_{\Xi_b'^0}\rangle$	$\|\phi_{\Xi_b'^-}\rangle$	$\|\phi_{\Omega_b^-}\rangle$
$\|\phi_{\Lambda_b^0}\rangle$	$\frac{\mu_u+\mu_d}{2}$	0	0	0	$\frac{\mu_d-\mu_u}{2}$	0	0	0	0
$\|\phi_{\Xi_b^0}\rangle$	0	$\frac{\mu_u+\mu_s}{2}$	0	0	0	0	$\frac{\mu_s-\mu_u}{2}$	0	0
$\|\phi_{\Xi_b^-}\rangle$	0	0	$\frac{\mu_d+\mu_s}{2}$	0	0	0	0	$\frac{\mu_s-\mu_d}{2}$	0
$\|\phi_{\Sigma_b^+}\rangle$	0	0	0	μ_u	0	0	0	0	0
$\|\phi_{\Sigma_b^0}\rangle$	$\frac{\mu_d-\mu_u}{2}$	0	0	0	$\frac{\mu_u+\mu_d}{2}$	0	0	0	0
$\|\phi_{\Sigma_b^-}\rangle$	0	0	0	0	0	μ_d	0	0	0
$\|\phi_{\Xi_b'^0}\rangle$	0	$\frac{\mu_s-\mu_u}{2}$	0	0	0	0	$\frac{\mu_u+\mu_s}{2}$	0	0
$\|\phi_{\Xi_b'^-}\rangle$	0	0	$\frac{\mu_s-\mu_d}{2}$	0	0	0	0	$\frac{\mu_d+\mu_s}{2}$	0
$\|\phi_{\Omega_b^-}\rangle$	0	0	0	0	0	0	0	0	μ_s

Next, summary tables with all of the flavor amplitudes computed above will be shown.

A.3 Evaluation of the matrix elements for the spatial space

A.3.1 Explicit form of the wave functions in coordinates representation

The explicit form of the wave functions of each harmonic oscillator written in eq. (2.37) in terms of their radial and angular parts up to the first radial excitation are given by the following expressions

$$\psi_{0,0,0}(\vec{\rho}(\vec{\lambda})) = \left(\frac{\omega_{\rho(\lambda)} m_{\rho(\lambda)}}{\pi}\right)^{\frac{3}{4}} \exp\left[-\frac{\omega_{\rho(\lambda)} m_{\rho(\lambda)} \vec{\rho}^2(\vec{\lambda}^2)}{2}\right], \tag{A.51}$$

$$\psi_{0,1,m_{l_{\rho(\lambda)}}}(\vec{\rho}(\vec{\lambda})) = \left(\frac{8}{3\sqrt{\pi}}\right)^{1/2} (\omega_{\rho(\lambda)} m_{\rho(\lambda)})^{\frac{5}{4}} \mathcal{Y}_1^{m_{l_{\rho(\lambda)}}}(\vec{\rho}(\vec{\lambda})) \exp\left[-\frac{\omega_{\rho(\lambda)} m_{\rho(\lambda)} \vec{\rho}^2(\vec{\lambda}^2)}{2}\right], \tag{A.52}$$

$$\psi_{0,2,m_{l_{\rho(\lambda)}}}(\vec{\rho}(\vec{\lambda})) = \left(\frac{16}{15\sqrt{\pi}}\right)^{\frac{1}{2}} (\omega_{\rho(\lambda)} m_{\rho(\lambda)})^{\frac{7}{4}} \mathcal{Y}_2^{m_{l_{\rho(\lambda)}}}(\vec{\rho}(\vec{\lambda})) \exp\left[-\frac{\omega_{\rho(\lambda)} m_{\rho(\lambda)} \vec{\rho}^2(\vec{\lambda}^2)}{2}\right], \tag{A.53}$$

TABLE A.3: The matrix elements of $\langle\phi_{A'}|\hat{\mu}_3|\phi_A\rangle$. The corresponding initial states ($|\phi_A\rangle$) are displayed in the first row and the final states ($|\phi_{A'}\rangle$) in the first column.

States	$\|\phi_{\Lambda_b^0}\rangle$	$\|\phi_{\Xi_b^0}\rangle$	$\|\phi_{\Xi_b^-}\rangle$	$\|\phi_{\Sigma_b^+}\rangle$	$\|\phi_{\Sigma_b^0}\rangle$	$\|\phi_{\Sigma_b^-}\rangle$	$\|\phi_{\Xi_b'^0}\rangle$	$\|\phi_{\Xi_b'^-}\rangle$	$\|\phi_{\Omega_b^-}\rangle$
$\|\phi_{\Lambda_b^0}\rangle$	μ_b	0	0	0	0	0	0	0	0
$\|\phi_{\Xi_b^0}\rangle$	0	μ_b	0	0	0	0	0	0	0
$\|\phi_{\Xi_b^-}\rangle$	0	0	μ_b	0	0	0	0	0	0
$\|\phi_{\Sigma_b^+}\rangle$	0	0	0	μ_b	0	0	0	0	0
$\|\phi_{\Sigma_b^0}\rangle$	0	0	0	0	μ_b	0	0	0	0
$\|\phi_{\Sigma_b^-}\rangle$	0	0	0	0	0	μ_b	0	0	0
$\|\phi_{\Xi_b'^0}\rangle$	0	0	0	0	0	0	μ_b	0	0
$\|\phi_{\Xi_b'^-}\rangle$	0	0	0	0	0	0	0	μ_b	0
$\|\phi_{\Omega_b^-}\rangle$	0	0	0	0	0	0	0	0	μ_b

$$\psi_{1,0,0}(\vec{\rho}(\vec{\lambda})) = \left(\frac{2}{3}\right)^{\frac{1}{2}}\left(\frac{3}{2} - \omega_{\rho\,(\lambda)} m_{\rho\,(\lambda)}\vec{\rho}^{\,2}(\vec{\lambda}^2)\right)\left(\frac{\omega_{\rho\,(\lambda)} m_{\rho\,(\lambda)}}{\pi}\right)^{\frac{3}{4}} \exp\left[-\frac{\omega_{\rho\,(\lambda)} m_{\rho\,(\lambda)}\vec{\rho}^{\,2}(\vec{\lambda}^2)}{2}\right]. \quad \text{(A.54)}$$

where

$$\mathcal{Y}_l^m(\vec{\rho}(\vec{\lambda})) = \vec{\rho}^{\,l}(\vec{\lambda}^l) Y_l^{m_{l_{\rho\,(\lambda)}}}(\theta,\phi)$$

are the solid harmonic polynomials and

$$Y_l^m(\theta,\phi)$$

are the spherical harmonics. Next, the explicit form of the harmonic oscillator wave functions, defined in eq. (2.36) are presented. These functions are necessary in order to compute the electromagnetic decay widths.

For the ground bottom baryon, the wave functions are given by

$$\psi_{0,0,0,0,0,0}(\vec{\rho},\vec{\lambda}) = \left(\frac{\omega_\rho m_\rho}{\pi}\right)^{\frac{3}{4}}\left(\frac{\omega_\lambda m_\lambda}{\pi}\right)^{\frac{3}{4}} \exp\left[-\frac{\omega_\rho m_\rho \vec{\rho}^{\,2}}{2} - \frac{\omega_\lambda m_\lambda \vec{\lambda}^2}{2}\right]. \quad \text{(A.55)}$$

For the P-wave bottom baryon

$$\psi_{0,1,m_{l_\rho},0,0,0}(\vec{\rho},\vec{\lambda}) = \left(\frac{8}{3\sqrt{\pi}}\right)^{\frac{1}{2}}(\omega_\rho m_\rho)^{\frac{5}{4}}\,\mathcal{Y}_1^{m_{l_\rho}}(\vec{\rho})\left(\frac{\omega_\lambda m_\lambda}{\pi}\right)^{\frac{3}{4}} \exp\left[-\frac{\omega_\rho m_\rho \vec{\rho}^{\,2}}{2} - \frac{\omega_\lambda m_\lambda \vec{\lambda}^2}{2}\right], \quad \text{(A.56)}$$

$$\psi_{0,0,0,0,1,m_{l_\lambda}}(\vec{\rho},\vec{\lambda}) = \left(\frac{8}{3\sqrt{\pi}}\right)^{\frac{1}{2}}(\omega_\lambda m_\lambda)^{\frac{5}{4}}\,\mathcal{Y}_1^{m_{l_\lambda}}(\vec{\lambda})\left(\frac{\omega_\rho m_\rho}{\pi}\right)^{\frac{3}{4}} \exp\left[-\frac{\omega_\rho m_\rho \vec{\rho}^{\,2}}{2} - \frac{\omega_\lambda m_\lambda \vec{\lambda}^2}{2}\right]. \quad \text{(A.57)}$$

For the D-wave bottom baryon

$$\psi_{0,2,m_{l_\rho},0,0,0}(\vec{\rho},\vec{\lambda}) = \left(\frac{16}{15\sqrt{\pi}}\right)^{\frac{1}{2}}(\omega_\rho m_\rho)^{\frac{7}{4}}\,\mathcal{Y}_2^{m_{l_\rho}}(\vec{\rho})\left(\frac{\omega_\lambda m_\lambda}{\pi}\right)^{\frac{3}{4}} \exp\left[-\frac{\omega_\rho m_\rho \vec{\rho}^{\,2}}{2} - \frac{\omega_\lambda m_\lambda \vec{\lambda}^2}{2}\right], \quad \text{(A.58)}$$

$$\psi_{0,0,0,0,2,m_{l_\lambda}}(\vec{\rho},\vec{\lambda}) = \left(\frac{16}{15\sqrt{\pi}}\right)^{\frac{1}{2}}(\omega_\lambda m_\lambda)^{\frac{7}{4}}\,\mathcal{Y}_2^{m_{l_\lambda}}(\vec{\lambda})\left(\frac{\omega_\rho m_\rho}{\pi}\right)^{\frac{3}{4}} \exp\left[-\frac{\omega_\rho m_\rho \vec{\rho}^{\,2}}{2} - \frac{\omega_\lambda m_\lambda \vec{\lambda}^2}{2}\right] \quad \text{(A.59)}$$

For the $\rho\lambda$ mixed states is given by

$$\begin{aligned}\psi_{0,1,m_{l_\rho},0,1,m_{l_\lambda}}(\vec{\rho},\vec{\lambda}) &= \Big(\frac{8}{3\sqrt{\pi}}\Big)^{\frac{1}{2}}(\omega_\rho m_\rho)^{\frac{5}{4}}\,\mathcal{Y}_1^{m_{l_\rho}}(\vec{\rho})\Big(\frac{8}{3\sqrt{\pi}}\Big)^{\frac{1}{2}}(\omega_\lambda m_\lambda)^{\frac{5}{4}}\mathcal{Y}_1^{m_{l_\lambda}}(\vec{\lambda}) \\ &\times \exp\Big[-\frac{\omega_\rho m_\rho\vec{\rho}^{\,2}}{2}-\frac{\omega_\lambda m_\lambda\vec{\lambda}^2}{2}\Big]. \end{aligned} \tag{A.60}$$

Finally, the wave functions of the first radially excited bottom baryon are given by

$$\psi_{1,0,0,0,0,0}(\vec{\rho},\vec{\lambda}) = \Big(\frac{2}{3}\Big)^{\frac{1}{2}}\Big(\frac{\omega_\lambda m_\lambda\omega_\rho m_\rho}{\pi^2}\Big)^{\frac{3}{4}}\Big(\frac{3}{2}-\omega_\rho m_\rho\vec{\rho}^{\,2}\Big)\exp\Big[-\frac{\omega_\rho m_\rho\vec{\rho}^{\,2}}{2}-\frac{\omega_\lambda m_\lambda\vec{\lambda}^2}{2}\Big], \tag{A.61}$$

$$\psi_{0,0,0,1,0,0}(\vec{\rho},\vec{\lambda}) = \Big(\frac{2}{3}\Big)^{\frac{1}{2}}\Big(\frac{\omega_\lambda m_\lambda\omega_\rho m_\rho}{\pi^2}\Big)^{\frac{3}{4}}\Big(\frac{3}{2}-\omega_\lambda m_\lambda\vec{\lambda}^2\Big)\exp\Big[-\frac{\omega_\rho m_\rho\vec{\rho}^{\,2}}{2}-\frac{\omega_\lambda m_\lambda\vec{\lambda}^2}{2}\Big]. \tag{A.62}$$

A.3.2 Ladder operators in coordinate space

In coordinate representation, the $\mathbf{p}_{j,\pm}$ ladder operator of the j-th quark are

$$\begin{aligned}\langle\vec{r}\,'|\mathbf{p}_{j,\pm}|\vec{r}\rangle &= \langle\vec{r}\,'|\mathbf{p}_{j,x}\pm i\mathbf{p}_{j,y}|\vec{r}\rangle = \left[-i\frac{\partial}{\partial x}\pm i\left(-i\frac{\partial}{\partial y}\right)\right]_j\delta^3(\vec{r}\,'-\vec{r}) \\ &= -i\left[\frac{\partial}{\partial x}\pm i\frac{\partial}{\partial y}\right]_j\delta^3(\vec{r}\,'-\vec{r}), \end{aligned} \tag{A.63}$$

which can be written in spherical coordinates as

$$\langle\vec{r}\,'|\mathbf{p}_{j,\pm}|\vec{r}\rangle = \left[-i\frac{e^{-i\varphi}\cos\theta}{r}\frac{\partial}{\partial\theta}\pm\frac{e^{-i\varphi}}{r\sin\theta}\frac{\partial}{\partial\varphi}-ie^{-i\varphi}\sin\theta\frac{\partial}{\partial r}\right]_j\delta^3(\vec{r}\,'-\vec{r}). \tag{A.64}$$

Using the previous equation in the Jacobi coordinates $\vec{\rho}$ and $\vec{\lambda}$ can be written

$$\langle\vec{\rho}\,'|\mathbf{p}_{\rho,\pm}|\vec{\rho}\rangle = \left[-i\tfrac{e^{-i\varphi}\cos\theta}{\rho}\tfrac{\partial}{\partial\theta}\pm\tfrac{e^{-i\varphi}}{\rho\sin\theta}\tfrac{\partial}{\partial\varphi}-ie^{-i\varphi}\sin\theta\tfrac{\partial}{\partial\rho}\right]\delta^3(\vec{\rho}\,'-\vec{\rho}), \tag{A.65}$$

$$\langle\vec{\lambda}\,'|\mathbf{p}_{\lambda,\pm}|\vec{\lambda}\rangle = \left[-i\tfrac{e^{-i\varphi}\cos\theta}{\lambda}\tfrac{\partial}{\partial\theta}\pm\tfrac{e^{-i\varphi}}{\lambda\sin\theta}\tfrac{\partial}{\partial\varphi}-ie^{-i\varphi}\sin\theta\tfrac{\partial}{\partial\lambda}\right]\delta^3(\vec{\lambda}\,'-\vec{\lambda}). \tag{A.66}$$

The calculation of the case of the ground state $\langle\vec{\rho},\vec{\lambda}|\mathbf{p}_{\rho,\pm}|0,0,0,0,0,0\rangle$ is done to show in detail how is the evaluation done formally. Starting with

$$\begin{aligned}&\langle\vec{\rho},\vec{\lambda}|\mathbf{p}_{\rho,\pm}|0,0,0,0,0,0\rangle = \int d^3\vec{\rho}\,'d^3\vec{\lambda}\,'\langle\vec{\rho},\vec{\lambda}|\mathbf{p}_{\rho,\pm}|\vec{\rho}\,',\vec{\lambda}\,'\rangle\langle\vec{\rho}\,',\vec{\lambda}\,'|0,0,0,0,0,0\rangle \\ &= \left[-i\frac{e^{-i\varphi}\cos\theta}{\rho}\frac{\partial}{\partial\theta}\pm\frac{e^{-i\varphi}}{\rho\sin\theta}\frac{\partial}{\partial\varphi}-ie^{-i\varphi}\sin\theta\frac{\partial}{\partial\rho}\right]\Big(\frac{\omega_\rho m_\rho}{\pi}\Big)^{\frac{3}{4}}\Big(\frac{\omega_\lambda m_\lambda}{\pi}\Big)^{\frac{3}{4}}\exp\Big[-\frac{\omega_\rho m_\rho\vec{\rho}^{\,2}}{2}-\frac{\omega_\lambda m_\lambda\vec{\lambda}^2}{2}\Big] \\ &= \mp i(\omega_\rho m_\rho)^{1/2}\psi_{0,1,\pm1,0,0,0}(\vec{\rho},\vec{\lambda}), \end{aligned} \tag{A.67}$$

where in the second line the fact that the $\mathbf{p}_{\rho(\lambda),\pm}$ operators are diagonal in coordinate space is used, i.e.

$$\langle\vec{\rho},\vec{\lambda}|\mathbf{p}_{\rho(\lambda),\pm}|\vec{\rho}\,',\vec{\lambda}\,'\rangle = \left[-i\frac{e^{-i\varphi}\cos\theta}{\rho}\frac{\partial}{\partial\theta} \pm \frac{e^{-i\varphi}}{\rho\sin\theta}\frac{\partial}{\partial\varphi} - ie^{-i\varphi}\sin\theta\frac{\partial}{\partial\rho}\right]\delta^3(\vec{\rho}-\vec{\rho}\,')\delta^3(\vec{\lambda}-\vec{\lambda}\,'). \tag{A.68}$$

The results for the other cases, obtained using the same method, are reported below.

$$\langle\vec{\rho},\vec{\lambda}|\mathbf{p}_{\lambda,\pm}|0,0,0,0,0,0\rangle = \mp i(\omega_\lambda m_\lambda)^{1/2}\psi_{0,0,0,0,1,\pm1}(\vec{\rho},\vec{\lambda}), \tag{A.69}$$

$$\langle\vec{\rho},\vec{\lambda}|\mathbf{p}_{\rho,\pm}|0,0,0,0,0,0\rangle = \mp i(\omega_\rho m_\rho)^{1/2}\psi_{0,1,\pm1,0,0,0}(\vec{\rho},\vec{\lambda}), \tag{A.70}$$

$$\langle\vec{\rho},\vec{\lambda}|\mathbf{p}_{\lambda,\pm}|0,1,m_{l_\rho},0,0,0\rangle = \mp i(\omega_\lambda m_\lambda)^{1/2}\psi_{0,1,m_{l_\rho},0,1,\pm1}(\vec{\rho},\vec{\lambda}), \tag{A.71}$$

$$\langle\vec{\rho},\vec{\lambda}|\mathbf{p}_{\rho,\pm}|0,0,0,0,1,m_{l_\lambda}\rangle = \mp i(\omega_\rho m_\rho)^{1/2}\psi_{0,1,\pm1,0,1,m_{l_\lambda}}(\vec{\rho},\vec{\lambda}), \tag{A.72}$$

$$\begin{aligned}\langle\vec{\rho},\vec{\lambda}|\mathbf{p}_{\rho,-}|0,1,1,0,0,0\rangle &= \frac{i(\omega_\rho m_\rho)^{1/2}}{\sqrt{3}}\psi_{0,2,0,0,0,0}(\vec{\rho},\vec{\lambda})\\ +i(\omega_\rho m_\rho)^{1/2}\psi_{0,0,0,0,0,0}(\vec{\rho},\vec{\lambda}) &+ i\sqrt{\frac{2}{3}}(\omega_\rho m_\rho)^{1/2}\psi_{1,0,0,0,0,0}(\vec{\rho},\vec{\lambda}),\end{aligned} \tag{A.73}$$

$$\langle\vec{\rho},\vec{\lambda}|\mathbf{p}_{\rho,-}|0,1,-1,0,0,0\rangle = i\sqrt{2}(\omega_\rho m_\rho)^{1/2}\psi_{0,2,-2,0,0,0}(\vec{\rho},\vec{\lambda}), \tag{A.74}$$

$$\langle\vec{\rho},\vec{\lambda}|\mathbf{p}_{\rho,-}|0,1,0,0,0,0\rangle = i(\omega_\rho m_\rho)^{1/2}\psi_{0,2,-1,0,0,0}(\vec{\rho},\vec{\lambda}), \tag{A.75}$$

$$\begin{aligned}\langle\vec{\rho},\vec{\lambda}|\mathbf{p}_{\lambda,-}|0,0,0,0,1,1\rangle &= \frac{i(\omega_\lambda m_\lambda)^{1/2}}{\sqrt{3}}\psi_{0,0,0,0,2,0}(\vec{\rho},\vec{\lambda})\\ +i(\omega_\lambda m_\lambda)^{1/2}\psi_{0,0,0,0,0,0}(\vec{\rho},\vec{\lambda}) &+ i\sqrt{\frac{2}{3}}(\omega_\lambda m_\lambda)^{1/2}\psi_{0,0,0,1,0,0}(\vec{\rho},\vec{\lambda}),\end{aligned} \tag{A.76}$$

$$\langle\vec{\rho},\vec{\lambda}|\mathbf{p}_{\lambda,-}|0,0,0,0,1,-1\rangle = i\sqrt{2}(\omega_\lambda m_\lambda)^{1/2}\psi_{0,0,0,0,2,-2}(\vec{\rho},\vec{\lambda}), \tag{A.77}$$

$$\langle\vec{\rho},\vec{\lambda}|\mathbf{p}_{\lambda,-}|0,0,0,0,1,0\rangle = i(\omega_\lambda m_\lambda)^{1/2}\psi_{0,0,0,0,2,-1}(\vec{\rho},\vec{\lambda}). \tag{A.78}$$

A.3.3 Matrix elements of $\hat{T}_{j,-}$ operators

The previous formulas are applied to evaluate the matrix elements of the $\hat{T}_{1,-}$, $\hat{T}_{2,-}$ and $\hat{T}_{3,-}$ operators in the harmonic oscillator basis. Beginning evaluating the matrix elements for the ρ states. For the operator $\hat{T}_{1,-}$

$$\begin{aligned}&\langle0,0,0,0,0,0|\hat{T}_{1,-}|0,1,m_{l\rho},0,0,0\rangle\\ &= \sqrt{\frac{1}{2}}\langle0,0,0,0,0,0|\mathbf{p}_{\rho,-}\hat{U}_1 + \hat{U}_1\mathbf{p}_{\rho,-}|0,1,1,0,0,0\rangle\\ &+\sqrt{\frac{1}{6}}\langle0,0,0,0,0,0|\mathbf{p}_{\lambda,-}\hat{U}_1 + \hat{U}_1\mathbf{p}_{\lambda,-}|0,1,1,0,0,0\rangle\\ &= \sqrt{\frac{1}{2}}i(\omega_\rho m_\rho)^{1/2}\Big[\langle0,1,1,0,0,0|\hat{U}_1|0,1,1,0,0,0\rangle\\ &+\sqrt{\frac{1}{3}}\langle0,0,0,0,0,0|\hat{U}_1|0,2,0,0,0,0\rangle + \langle0,0,0,0,0,0|\hat{U}_1|0,0,0,0,0,0\rangle\\ +\quad &\sqrt{\frac{2}{3}}\langle0,0,0,0,0,0|\hat{U}_1|1,0,0,0,0,0\rangle\Big] + \sqrt{\frac{1}{6}}i(\omega_\lambda m_\lambda)^{1/2}\end{aligned}$$

$$\times \left[\langle 0,0,0,0,1,1|\hat{U}_1|0,1,1,0,0,0\rangle + \langle 0,0,0,0,0,0|\hat{U}_1|0,1,1,0,1,-1\rangle\right]$$
$$= i\sqrt{2}(\omega_\rho m_\rho)^{1/2} \exp\left[\frac{-\mathrm{k}^2}{8}\left(\frac{1}{\omega_\rho m_\rho} + \frac{3{m_b}^2}{\omega_\lambda m_\lambda (2m_\rho + m_b)^2}\right)\right] \delta_{m_{l_\rho},1}. \tag{A.79}$$

For $\hat{T}_{2,-}$ it is obtained

$$\langle 0,0,0,0,0,0|\hat{T}_{2,-}|0,1,m_{l\rho},0,0,0\rangle$$
$$= -\sqrt{\frac{1}{2}}\langle 0,0,0,0,0,0|\mathbf{p}_{\rho,-}\hat{U}_2 + \hat{U}_2\mathbf{p}_{\rho,-}|0,1,1,0,0,0\rangle$$
$$+\sqrt{\frac{1}{6}}\langle 0,0,0,0,0,0|\mathbf{p}_{\lambda,-}\hat{U}_2 + \hat{U}_2\mathbf{p}_{\lambda,-}|0,1,1,0,0,0\rangle$$
$$= -\sqrt{\frac{1}{2}}i(\omega_\rho m_\rho)^{1/2}\Big[\langle 0,1,1,0,0,0|\hat{U}_2|0,1,1,0,0,0\rangle$$
$$+\sqrt{\frac{1}{3}}\langle 0,0,0,0,0,0|\hat{U}_2|0,2,0,0,0,0\rangle + \langle 0,0,0,0,0,0|\hat{U}_2|0,0,0,0,0,0\rangle$$
$$+\sqrt{\frac{2}{3}}\langle 0,0,0,0,0,0|\hat{U}_2|1,0,0,0,0,0\rangle\Big] + \sqrt{\frac{1}{6}}i(\omega_\lambda m_\lambda)^{1/2}$$
$$\times \left[\langle 0,0,0,0,1,1|\hat{U}_2|0,1,1,0,0,0\rangle + \langle 0,0,0,0,0,0|\hat{U}_2|0,1,1,0,1,-1\rangle\right]$$
$$= -i\sqrt{2}(\omega_\rho m_\rho)^{1/2} \exp\left[\frac{-\mathrm{k}^2}{8}\left(\frac{1}{\omega_\rho m_\rho} + \frac{3{m_b}^2}{\omega_\lambda m_\lambda (2m_\rho + m_b)^2}\right)\right] \delta_{m_{l_\rho},1}. \tag{A.80}$$

Finally, for $\hat{T}_{3,-}$ it is obtained

$$\langle 0,0,0,0,0,0|\hat{T}_{3,-}|0,1,m_{l\rho},0,0,0\rangle$$
$$= -\sqrt{\frac{2}{3}}\langle 0,0,0,0,0,0|\mathbf{p}_{\lambda,-}\hat{U}_3 + \hat{U}_3\mathbf{p}_{\lambda,-}|0,1,1,0,0,0\rangle$$
$$= -\sqrt{\frac{2}{3}}\big[i(\omega_\lambda m_\lambda)^{1/2}\langle 0,0,0,0,1,1|\hat{U}_3|0,1,1,0,0,0\rangle$$
$$+i(\omega_\lambda m_\lambda)^{1/2}\langle 0,0,0,0,0,0|\hat{U}_3|0,1,1,0,1,-1\rangle\big]$$
$$= 0. \tag{A.81}$$

Analog computations are performed for the λ states. For $\hat{T}_{1,-}$ it is obtained

$$\langle 0,0,0,0,0,0|\hat{T}_{1,-}|0,0,0,0,1,m_{l_\lambda}\rangle$$
$$= \sqrt{\frac{1}{6}}\langle 0,0,0,0,0,0|\mathbf{p}_{\lambda,-}\hat{U}_1 + \hat{U}_1\mathbf{p}_{\lambda,-}|0,0,0,0,1,1\rangle$$
$$+\sqrt{\frac{1}{2}}\langle 0,0,0,0,0,0|\mathbf{p}_{\rho,-}\hat{U}_1 + \hat{U}_1\mathbf{p}_{\rho,-}|0,0,0,0,1,1\rangle$$
$$= \sqrt{\frac{1}{6}}i(\omega_\lambda m_\lambda)^{1/2}\big[\langle 0,0,0,0,1,1|\hat{U}_1|0,0,0,0,1,1\rangle$$

$$
\begin{aligned}
&+\sqrt{\frac{1}{3}}\langle 0,0,0,0,0,0|\hat{U}_1|0,0,0,0,2,0\rangle + \langle 0,0,0,0,0,0|\hat{U}_1|0,0,0,0,0,0\rangle \\
&+\sqrt{\frac{2}{3}}\langle 0,0,0,0,0,0|\hat{U}_1|0,0,0,1,0,0\rangle\big] + \sqrt{\frac{1}{2}}i(\omega_\rho m_\rho)^{1/2} \\
&\times\big[\langle 0,1,1,0,0,0|\hat{U}_1|0,0,0,0,1,1\rangle + \langle 0,0,0,0,0,0|\hat{U}_1|0,1,-1,0,1,1\rangle\big] \\
&= i\sqrt{\frac{2}{3}}(\omega_\lambda m_\lambda)^{1/2}\exp\left[\frac{-\mathrm{k}^2}{8}\left(\frac{1}{\omega_\rho m_\rho}+\frac{3{m_b}^2}{\omega_\lambda m_\lambda(2m_\rho+m_b)^2}\right)\right]\delta_{m_{l_\lambda},1}.
\end{aligned}
\tag{A.82}
$$

Next, for $\hat{T}_{2,-}$ it is obtained

$$
\begin{aligned}
&\langle 0,0,0,0,0,0|\hat{T}_{2,-}|0,0,0,0,1,m_{l_\lambda}\rangle \\
&= \sqrt{\frac{1}{6}}\langle 0,0,0,0,0,0|\mathbf{p}_{\lambda,-}\hat{U}_2+\hat{U}_2\mathbf{p}_{\lambda,-}|0,0,0,0,1,1\rangle \\
&-\sqrt{\frac{1}{2}}\langle 0,0,0,0,0,0|\mathbf{p}_{\rho,-}\hat{U}_2+\hat{U}_2\mathbf{p}_{\rho,-}|0,0,0,0,1,1\rangle \\
&= \sqrt{\frac{1}{6}}i(\omega_\lambda m_\lambda)^{1/2}\big[\langle 0,0,0,0,1,1|\hat{U}_2|0,0,0,0,1,1\rangle \\
&+\sqrt{\frac{1}{3}}\langle 0,0,0,0,0,0|\hat{U}_2|0,0,0,0,2,0\rangle + \langle 0,0,0,0,0,0|\hat{U}_2|0,0,0,0,0,0\rangle \\
&+\sqrt{\frac{2}{3}}\langle 0,0,0,0,0,0|\hat{U}_2|0,0,0,1,0,0\rangle\big] - \sqrt{\frac{1}{2}}i(\omega_\rho m_\rho)^{1/2} \\
&\times\big[\langle 0,1,1,0,0,0|\hat{U}_2|0,0,0,0,1,1\rangle + \langle 0,0,0,0,0,0|\hat{U}_2|0,1,-1,0,1,1\rangle\big] \\
&= i\sqrt{\frac{2}{3}}(\omega_\lambda m_\lambda)^{1/2}\exp\left[\frac{-\mathrm{k}^2}{8}\left(\frac{1}{\omega_\rho m_\rho}+\frac{3{m_b}^2}{\omega_\lambda m_\lambda(2m_\rho+m_b)^2}\right)\right]\delta_{m_{l_\lambda},1}.
\end{aligned}
\tag{A.83}
$$

Finally, for $\hat{T}_{3,-}$ it is obtained

$$
\begin{aligned}
&\langle 0,0,0,0,0,0|\hat{T}_{3,-}|0,0,0,0,1,m_{l_\lambda}\rangle \\
&= -\sqrt{\frac{2}{3}}\langle 0,0,0,0,0,0|\mathbf{p}_{\lambda,-}\hat{U}_3+\hat{U}_3\mathbf{p}_{\lambda,-}|0,0,0,0,1,1\rangle \\
&= -\sqrt{\frac{2}{3}}i(\omega_\lambda m_\lambda)^{1/2}\big[\langle 0,0,0,0,1,1|\hat{U}_3|0,0,0,0,1,1\rangle \\
&+\frac{1}{\sqrt{3}}\langle 0,0,0,0,0,0|\hat{U}_3|0,0,0,0,2,0\rangle + \langle 0,0,0,0,0,0|\hat{U}_3|0,0,0,0,0,0\rangle \\
&+\sqrt{\frac{2}{3}}\langle 0,0,0,0,0,0|\hat{U}_3|0,0,0,1,0,0\rangle\big] \\
&= -2i\sqrt{\frac{2}{3}}(\omega_\lambda m_\lambda)^{1/2}\exp\left[\frac{-3\mathrm{k}^2 m_\rho^2}{2\omega_\lambda m_\lambda(2m_\rho+m_b)^2}\right]\delta_{m_{l_\lambda},1}.
\end{aligned}
\tag{A.84}
$$

Bibliography

[1] David J. Gross and Frank Wilczek. "Ultraviolet Behavior of Non-Abelian Gauge Theories". In: *Phys. Rev. Lett.* 30 (26 1973), pp. 1343–1346. DOI: 10.1103/PhysRevLett.30.1343. URL: https://link.aps.org/doi/10.1103/PhysRevLett.30.1343.

[2] H. David Politzer. "Reliable Perturbative Results for Strong Interactions?" In: *Phys. Rev. Lett.* 30 (26 1973), pp. 1346–1349. DOI: 10.1103/PhysRevLett.30.1346. URL: https://link.aps.org/doi/10.1103/PhysRevLett.30.1346.

[3] Atsushi Hosaka et al. *Hadron and Nuclear Physics 09*. WORLD SCIENTIFIC, 2010. DOI: 10.1142/7823. eprint: https://www.worldscientific.com/doi/pdf/10.1142/7823. URL: https://www.worldscientific.com/doi/abs/10.1142/7823.

[4] Hugo García Tecocoatzi. "Propiedades de bariones en el unquenched quark model". PhD thesis. Universidad Nacional Autónoma de México, 2016. URL: https://repositorio.unam.mx/contenidos/75522.

[5] Murray Gell-Mann. "A Schematic Model of Baryons and Mesons". In: *Phys. Lett.* 8 (1964), pp. 214–215. DOI: 10.1016/S0031-9163(64)92001-3.

[6] G. Zweig. "An SU(3) model for strong interaction symmetry and its breaking. Version 2". In: *DEVELOPMENTS IN THE QUARK THEORY OF HADRONS. VOL. 1. 1964 - 1978*. Ed. by D. B. Lichtenberg and Simon Peter Rosen. Feb. 1964, pp. 22–101.

[7] R. Aaij *et al.* [LHCb Collaboration]. "Observation of $J/\psi p$ Resonances Consistent with Pentaquark States in $\Lambda_b^0 \to J/\psi K^- p$ Decays". In: *Phys. Rev. Lett.* 115 (7 2015), p. 072001. DOI: 10.1103/PhysRevLett.115.072001. URL: https://link.aps.org/doi/10.1103/PhysRevLett.115.072001.

[8] R. Aaij *et al.* [LHCb Collaboration]. "Model-Independent Evidence for $J/\psi p$ Contributions to $\Lambda_b^0 \to J/\psi p K^-$ Decays". In: *Phys. Rev. Lett.* 117 (8 2016), p. 082002. DOI: 10.1103/PhysRevLett.117.082002. URL: https://link.aps.org/doi/10.1103/PhysRevLett.117.082002.

[9] R. Aaij *et al.* [LHCb Collaboration]. "Evidence for Exotic Hadron Contributions to $\Lambda_b^0 \to J/\psi p \pi^-$ Decays". In: *Phys. Rev. Lett.* 117 (8 2016), p. 082003. DOI: 10.1103/PhysRevLett.117.082003. URL: https://link.aps.org/doi/10.1103/PhysRevLett.117.082003.

[10] LHCb collaboration. "Observation of structure in the J/Ψ-pair mass spectrum". In: *Science Bulletin* 65.23 (2020), pp. 1983–1993. ISSN: 2095-9273. DOI: https://doi.org/10.1016/j.scib.2020.08.032. URL: https://www.sciencedirect.com/science/article/pii/S2095927320305685.

[11] M. Basile et al. "Evidence for a new particle with naked «beauty» and for its associated production in high-energy (pp) interactions". In: *Lettere al Nuovo Cimento (1971-1985)* 31.4 (1981), pp. 97–111. ISSN: 1827-613X. DOI: 10.1007/BF02822406. URL: https://doi.org/10.1007/BF02822406.

[12] T. Aaltonen *et al.* [CDF Collaboration]. "Observation and Mass Measurement of the Baryon Ξ_b^-". In: *Phys. Rev. Lett.* 99 (5 2007), p. 052002. DOI: 10.1103/PhysRevLett.99.052002. URL: https://link.aps.org/doi/10.1103/PhysRevLett.99.052002.

[13] T. Aaltonen *et al.* [CDF Collaboration]. "First observation of heavy baryons Σ_b and Σ_b^*". In: *Phys. Rev. Lett.* 99 (2007), p. 202001. DOI: 10.1103/PhysRevLett.99.202001. arXiv: 0706.3868 [hep-ex].

[14] T. Aaltonen *et al.* [CDF Collaboration]. "Observation of the Ξ_b^0 Baryon". In: *Phys. Rev. Lett.* 107 (2011), p. 102001. DOI: 10.1103/PhysRevLett.107.102001. arXiv: 1107.4015 [hep-ex].

[15] T. Aaltonen *et al.* [CDF Collaboration]. "Measurement of the masses and widths of the bottom baryons Σ_b^{+-} and Σ_b^{*+-}". In: *Phys. Rev. D* 85 (2012), p. 092011. DOI: 10.1103/PhysRevD.85.092011. arXiv: 1112.2808 [hep-ex].

[16] T. Aaltonen *et al.* [CDF Collaboration]. "Mass and lifetime measurements of bottom and charm baryons in $p\bar{p}$ collisions at $\sqrt{s} = 1.96$ TeV". In: *Phys. Rev. D* 89.7 (2014), p. 072014. DOI: 10.1103/PhysRevD.89.072014. arXiv: 1403.8126 [hep-ex].

[17] V. Abazov *et al.* [D0 Collaboration]. "Direct Observation of the Strange b Baryon Ξ_b^-". In: *Phys. Rev. Lett.* 99 (5 2007), p. 052001. DOI: 10.1103/PhysRevLett.99.052001. URL: https://link.aps.org/doi/10.1103/PhysRevLett.99.052001.

[18] V. Abazov *et al.* [D0 Collaboration]. "Observation of the Doubly Strange b Baryon Ω_b^-". In: *Phys. Rev. Lett.* 101 (23 2008), p. 232002. DOI: 10.1103/PhysRevLett.101.232002. URL: https://link.aps.org/doi/10.1103/PhysRevLett.101.232002.

[19] S. Chatrchyan *et al.* [CMS Collaboration]. "Observation of a new Ξ_b Baryon". In: *Phys. Rev. Lett.* 108 (2012), p. 252002. DOI: 10.1103/PhysRevLett.108.252002. arXiv: 1204.5955 [hep-ex].

[20] A. M. Sirunyan *et al [CMS Collaboration]*. "Study of excited Λ_b^0 states decaying to $\Lambda_b^0\pi^+\pi^-$ in proton-proton collisions at $\sqrt{s} = 13$ TeV". In: *Physics Letters B* 803 (2020), p. 135345. ISSN: 0370-2693. DOI: https://doi.org/10.1016/j.physletb.2020.135345.

[21] R. Aaij *et al.* [LHCb Collaboration]. "Observation of Excited Λ_b^0 Baryons". In: *Phys. Rev. Lett.* 109 (17 2012), p. 172003. DOI: 10.1103/PhysRevLett.109.172003. URL: https://link.aps.org/doi/10.1103/PhysRevLett.109.172003.

[22] R. Aaij *et al.* [LHCb Collaboration]. "Study of beauty hadron decays into pairs of charm hadrons". In: *Phys. Rev. Lett.* 112 (2014), p. 202001. DOI: 10.1103/PhysRevLett.112.202001. arXiv: 1403.3606 [hep-ex].

[23] R. Aaij *et al.* [LHCb Collaboration]. "Observation of two new Ξ_b^- baryon resonances". In: *Phys. Rev. Lett.* 114 (2015), p. 062004. DOI: 10.1103/PhysRevLett.114.062004. arXiv: 1411.4849 [hep-ex].

[24] R. Aaij *et al.* [LHCb Collaboration]. "Observation of the decays $\Lambda_b^0 \to \chi_{c1} p K^-$ and $\Lambda_b^0 \to \chi_{c2} p K^-$". In: *Phys. Rev. Lett.* 119.6 (2017), p. 062001. DOI: 10.1103/PhysRevLett.119.062001. arXiv: 1704.07900 [hep-ex].

[25] R. Aaij *et al.* [LHCb Collaboration]. "Observation of a New Ξ_b^- Resonance". In: *Phys. Rev. Lett.* 121 (7 2018), p. 072002. DOI: 10.1103/PhysRevLett.121.072002. URL: https://link.aps.org/doi/10.1103/PhysRevLett.121.072002.

[26] R. Aaij *et al.* [LHCb Collaboration]. "Observation of Two Resonances in the $\Lambda_b^0 \pi^\pm$ Systems and Precise Measurement of $\Sigma_b^\pm$ and $\Sigma_b^{*\pm}$ Properties". In: *Phys. Rev. Lett.* 122 (1 2019), p. 012001. DOI: 10.1103/PhysRevLett.122.012001. URL: https://link.aps.org/doi/10.1103/PhysRevLett.122.012001.

[27] R. Aaij *et al.* [LHCb Collaboration]. "First Observation of Excited Ω_b^- States". In: *Phys. Rev. Lett.* 124 (8 2020), p. 082002. DOI: 10.1103/PhysRevLett.124.082002. URL: https://link.aps.org/doi/10.1103/PhysRevLett.124.082002.

[28] R. Aaij *et al.* [LHCb Collaboration]. "Observation of a new baryon state in the $\Lambda_b^0 \pi^+ \pi^-$ mass spectrum". In: *JHEP* 06 (2020), p. 136. DOI: 10.1007/JHEP06(2020)136. arXiv: 2002.05112 [hep-ex].

[29] R. Aaij *et al.* [LHCb Collaboration]. "Observation of Two New Excited Ξ_b^0 States Decaying to $\Lambda_b^0 K^- \pi^+$". In: *Phys. Rev. Lett.* 128 (16 2022), p. 162001. DOI: 10.1103/PhysRevLett.128.162001. URL: https://link.aps.org/doi/10.1103/PhysRevLett.128.162001.

[30] R. Aaij *et al.* [LHCb Collaboration]. "Observation of New Baryons in the $\Xi_b^- \pi^+ \pi^-$ and $\Xi_b^0 \pi^+ \pi^-$ Systems". In: *Phys. Rev. Lett.* 131.17 (2023), p. 171901. DOI: 10.1103/PhysRevLett.131.171901. arXiv: 2307.13399 [hep-ex].

[31] J. Yelton et al. "Observation of Excited Ω_c Charmed Baryons in e^+e^- Collisions". In: *Phys. Rev. D* 97.5 (2018), p. 051102. DOI: 10.1103/PhysRevD.97.051102. arXiv: 1711.07927 [hep-ex].

[32] Y. B. Li et al. "Observation of $\Xi_c(2930)^0$ and updated measurement of $B^- \to K^- \Lambda_c^+ \bar{\Lambda}_c^-$ at Belle". In: *Eur. Phys. J. C* 78.3 (2018), p. 252. DOI: 10.1140/epjc/s10052-018-5720-5. arXiv: 1712.03612 [hep-ex].

[33] H. Garcia-Tecocoatzi et al. "Strong decay widths and mass spectra of charmed baryons". In: *Phys. Rev. D* 107.3 (2023), p. 034031. DOI: 10.1103/PhysRevD.107.034031. arXiv: 2205.07049 [hep-ph].

[34] Simon Capstick and Nathan Isgur. "Baryons in a Relativized Quark Model with Chromodynamics". In: *AIP Conf. Proc.* 132 (1985). Ed. by S. Oneda, pp. 267–271. DOI: 10.1063/1.35361.

[35] Simon Capstick and Nathan Isgur. "Baryons in a relativized quark model with chromodynamics". In: *Phys. Rev. D* 34 (9 1986), pp. 2809–2835. DOI: 10.1103/PhysRevD.34.2809. URL: https://link.aps.org/doi/10.1103/PhysRevD.34.2809.

[36] E. Bagan et al. "Spectra of heavy baryons from QCD spectral sum rules". In: *Phys. Lett. B* 287 (1992), pp. 176–178. DOI: 10.1016/0370-2693(92)91896-H.

[37] R. Roncaglia, D. B. Lichtenberg, and E. Predazzi. "Predicting the masses of baryons containing one or two heavy quarks". In: *Phys. Rev. D* 52 (1995), pp. 1722–1725. DOI: 10.1103/PhysRevD.52.1722. arXiv: hep-ph/9502251.

[38] B. Silvestre-Brac. "Spectrum and static properties of heavy baryons". In: *Few Body Syst.* 20 (1996), pp. 1–25. DOI: 10.1007/s006010050028.

[39] K. C. Bowler et al. "Heavy baryon spectroscopy from the lattice". In: *Phys. Rev. D* 54 (1996), pp. 3619–3633. DOI: 10.1103/PhysRevD.54.3619. arXiv: hep-lat/9601022.

[40] Elizabeth Ellen Jenkins. "Heavy baryon masses in the 1/m(Q) and 1/N(c) expansions". In: *Phys. Rev. D* 54 (1996), pp. 4515–4531. DOI: 10.1103/PhysRevD.54.4515. arXiv: hep-ph/9603449.

[41] Nilmani Mathur, Randy Lewis, and R. M. Woloshyn. "Charmed and bottom baryons from lattice NRQCD". In: *Phys. Rev. D* 66 (2002), p. 014502. DOI: 10.1103/PhysRevD.66.014502. arXiv: hep-ph/0203253.

[42] C. Albertus et al. "Charmed and bottom baryons: A Variational approach based on heavy quark symmetry". In: *Nucl. Phys. A* 740 (2004), pp. 333–361. DOI: 10.1016/j.nuclphysa.2004.04.114. arXiv: nucl-th/0311100.

[43] H. Garcilazo, J. Vijande, and A. Valcarce. "Faddeev study of heavy baryon spectroscopy". In: *J. Phys. G* 34 (2007), pp. 961–976. DOI: 10.1088/0954-3899/34/5/014. arXiv: hep-ph/0703257.

[44] A. Valcarce, H. Garcilazo, and J. Vijande. "Towards an understanding of heavy baryon spectroscopy". In: *Eur. Phys. J. A* 37 (2008), pp. 217–225. DOI: 10.1140/epja/i2008-10616-4. arXiv: 0807.2973 [hep-ph].

[45] Gang Yang, Jialun Ping, and Jorge Segovia. "The S- and P-Wave Low-Lying Baryons in the Chiral Quark Model". In: *Few Body Syst.* 59.6 (2018), p. 113. DOI: 10.1007/s00601-018-1433-4. arXiv: 1709.09315 [hep-ph].

[46] D. Ebert, R. N. Faustov, and V. O. Galkin. "Masses of excited heavy baryons in the relativistic quark model". In: *Phys. Lett. B* 659 (2008), pp. 612–620. DOI: 10.1016/j.physletb.2007.11.037. arXiv: 0705.2957 [hep-ph].

[47] D. Ebert, R. N. Faustov, and V. O. Galkin. "Spectroscopy and Regge trajectories of heavy baryons in the relativistic quark-diquark picture". In: *Phys. Rev. D* 84 (2011), p. 014025. DOI: 10.1103/PhysRevD.84.014025. arXiv: 1105.0583 [hep-ph].

[48] W. Roberts and Muslema Pervin. "Heavy baryons in a quark model". In: *Int. J. Mod. Phys. A* 23 (2008), pp. 2817–2860. DOI: 10.1142/S0217751X08041219. arXiv: 0711.2492 [nucl-th].

[49] Marek Karliner et al. "The Quark Model and *b* Baryons". In: *Annals Phys.* 324 (2009), pp. 2–15. DOI: 10.1016/j.aop.2008.05.003. arXiv: 0804.1575 [hep-ph].

[50] Tetsuya Yoshida et al. "Spectrum of heavy baryons in the quark model". In: *Phys. Rev. D* 92.11 (2015), p. 114029. DOI: 10.1103/PhysRevD.92.114029. arXiv: 1510.01067 [hep-ph].

[51] Ke-Wei Wei et al. "Spectroscopy of singly, doubly, and triply bottom baryons". In: *Phys. Rev. D* 95.11 (2017), p. 116005. DOI: 10.1103/PhysRevD.95.116005. arXiv: 1609.02512 [hep-ph].

[52] M. Ferraris et al. "A Three body force model for the baryon spectrum". In: *Phys. Lett. B* 364 (1995), pp. 231–238. DOI: 10.1016/0370-2693(95)01091-2.

[53] E. Santopinto, F. Iachello, and M. M. Giannini. "Exactly solvable models of baryon spectroscopy". In: *Nucl. Phys. A* 623 (1997). Ed. by R. Baldini et al., pp. 100C–109C. DOI: 10.1016/S0375-9474(97)00427-2.

[54] E. Santopinto, F. Iachello, and M. M. Giannini. "Nucleon form-factors in a simple three-body quark model". In: *Eur. Phys. J. A* 1 (1998), pp. 307–315. DOI: 10.1007/s100500050065.

[55] M. M. Giannini and E. Santopinto. "The hypercentral Constituent Quark Model and its application to baryon properties". In: *Chin. J. Phys.* 53 (2015), p. 020301. DOI: 10.6122/CJP.20150120. arXiv: 1501.03722 [nucl-th].

[56] Halil Mutuk. "A study of excited Ω_b^- states in hypercentral constituent quark model via artificial neural network". In: *Eur. Phys. J. A* 56.5 (2020), p. 146. DOI: 10.1140/epja/s10050-020-00161-5. arXiv: 2002.03695 [hep-ph].

[57] Hua-Xing Chen et al. "D-wave charmed and bottomed baryons from QCD sum rules". In: *Phys. Rev. D* 94.11 (2016), p. 114016. DOI: 10.1103/PhysRevD.94.114016. arXiv: 1611.02677 [hep-ph].

[58] Zhi-Gang Wang. "Analysis of the $1/2^-$ and $3/2^-$ heavy and doubly heavy baryon states with QCD sum rules". In: *Eur. Phys. J. A* 47 (2011), p. 81. DOI: 10.1140/epja/i2011-11081-8. arXiv: 1003.2838 [hep-ph].

[59] Xiang Liu et al. "Bottom baryons". In: *Phys. Rev. D* 77 (1 2008), p. 014031. DOI: 10.1103/PhysRevD.77.014031. URL: https://link.aps.org/doi/10.1103/PhysRevD.77.014031.

[60] Qiang Mao et al. "QCD sum rule calculation for P-wave bottom baryons". In: *Phys. Rev. D* 92 (11 2015), p. 114007. DOI: 10.1103/PhysRevD.92.114007. URL: https://link.aps.org/doi/10.1103/PhysRevD.92.114007.

[61] Guo-Liang Yu, Zhi-Gang Wang, and Xiu-Wu Wang. "1Dand 2D Ξ_b and Λ_b baryons *". In: *Chin. Phys. C* 46.9 (2022), p. 093102. DOI: 10.1088/1674-1137/ac6dc6. arXiv: 2109.02217 [hep-ph].

[62] L. X. Gutiérrez-Guerrero et al. "Masses of Light and Heavy Mesons and Baryons: A Unified Picture". In: *Phys. Rev. D* 100.11 (2019), p. 114032. DOI: 10.1103/PhysRevD.100.114032. arXiv: 1911.09213 [nucl-th].

[63] P. Hasenfratz et al. "Heavy Baryon Spectroscopy in the QCD Bag Model". In: *Phys. Lett. B* 94 (1980), pp. 401–404. DOI: 10.1016/0370-2693(80)90906-5.

[64] Yonghee Kim et al. "Spectrum of singly heavy baryons from a chiral effective theory of diquarks". In: *Phys. Rev. D* 102.1 (2020), p. 014004. DOI: 10.1103/PhysRevD.102.014004. arXiv: 2003.03525 [hep-ph].

[65] Yonghee Kim et al. "Heavy baryon spectrum with chiral multiplets of scalar and vector diquarks". In: *Phys. Rev. D* 104.5 (2021), p. 054012. DOI: 10.1103/PhysRevD.104.054012. arXiv: 2105.09087 [hep-ph].

[66] Yao Ma et al. "Ground state baryons in the flux-tube three-body confinement model using diffusion Monte Carlo". In: *Phys. Rev. D* 107.5 (2023), p. 054035. DOI: 10.1103/PhysRevD.107.054035. arXiv: 2211.09021 [hep-ph].

[67] J. Vijande, A. Valcarce, and H. Garcilazo. "Heavy-baryon quark model picture from lattice QCD". In: *Phys. Rev. D* 90.9 (2014), p. 094004. DOI: 10.1103/PhysRevD.90.094004. arXiv: 1507.03736 [hep-ph].

[68] Protick Mohanta and Subhasish Basak. "Heavy baryon spectrum on the lattice with NRQCD bottom and HISQ lighter quarks". In: *Phys. Rev. D* 101 (9 2020), p. 094503. DOI: 10.1103/PhysRevD.101.094503. URL: https://link.aps.org/doi/10.1103/PhysRevD.101.094503.

[69] Ayut Limphirat et al. "Decay widths of ground-state and excited Ξ_b baryons in a nonrelativistic quark model". In: *Phys. Rev. C* 82 (2010), p. 055201. DOI: 10.1103/PhysRevC.82.055201.

[70] Kai-Lei Wang et al. "Strong and radiative decays of the low-lying S- and P-wave singly heavy baryons". In: *Phys. Rev. D* 96.11 (2017), p. 116016. DOI: 10.1103/PhysRevD.96.116016. arXiv: 1709.04268 [hep-ph].

[71] Ya-Xiong Yao, Kai-Lei Wang, and Xian-Hui Zhong. "Strong and radiative decays of the low-lying D-wave singly heavy baryons". In: *Phys. Rev. D* 98.7 (2018), p. 076015. DOI: 10.1103/PhysRevD.98.076015. arXiv: 1803.00364 [hep-ph].

[72] Wen-Jia Wang, Li-Ye Xiao, and Xian-Hui Zhong. "Strong decays of the low-lying ρ-mode 1P-wave singly heavy baryons". In: *Phys. Rev. D* 106.7 (2022), p. 074020. DOI: 10.1103/PhysRevD.106.074020. arXiv: 2208.10116 [hep-ph].

[73] Wen-Jia Wang et al. "1D-wave bottom-strange baryons and possible interpretation of $\Xi_b(6327)^0$ and $\Xi_b(6333)^0$". In: *Phys. Rev. D* 105.7 (2022), p. 074008. DOI: 10.1103/PhysRevD.105.074008. arXiv: 2202.05426 [hep-ph].

[74] Li-Ye Xiao and Xian-Hui Zhong. "Toward establishing the low-lying P-wave Σ_b states". In: *Phys. Rev. D* 102.1 (2020), p. 014009. DOI: 10.1103/PhysRevD.102.014009. arXiv: 2004.11106 [hep-ph].

[75] Wei Liang and Qi-Fang Lü. "Strong decays of the newly observed narrow Ω_b structures". In: *The European Physical Journal C* 80.3 (2020), p. 198. ISSN: 1434-6052. DOI: 10.1140/epjc/s10052-020-7759-3. URL: https://doi.org/10.1140/epjc/s10052-020-7759-3.

[76] Wei Liang and Qi-Fang Lü. "The newly observed $\Lambda_b(6072)^0$ structure and its $\rho-$mode nonstrange partners". In: *Eur. Phys. J. C* 80.8 (2020), p. 690. DOI: 10.1140/epjc/s10052-020-8274-2. arXiv: 2004.13568 [hep-ph].

[77] He, Hui-Zhen and Liang, Wei and Lü, Qi-Fang and Dong, Yu-Bing. "Strong decays of the low-lying bottom strange baryons". In: *Science China Physics, Mechanics and Astronomy* 64.6 (2021), p. 261012. ISSN: 1869-1927. DOI: 10.1007/s11433-021-1704-x. URL: https://doi.org/10.1007/s11433-021-1704-x.

[78] Qi-Fang Lü and Xian-Hui Zhong. "Strong decays of the higher excited Λ_Q and Σ_Q baryons". In: *Phys. Rev. D* 101.1 (2020), p. 014017. DOI: 10.1103/PhysRevD.101.014017. arXiv: 1910.06126 [hep-ph].

[79] Bing Chen et al. "Role of newly discovered $\Xi_b(6227)^-$ for constructing excited bottom baryon family". In: *Phys. Rev. D* 98.3 (2018), p. 031502. DOI: 10.1103/PhysRevD.98.031502. arXiv: 1805.10826 [hep-ph].

[80] Bing Chen and Xiang Liu. "Assigning the newly reported $\Sigma_b(6097)$ as a P-wave excited state and predicting its partners". In: *Phys. Rev. D* 98.7 (2018), p. 074032. DOI: 10.1103/PhysRevD.98.074032. arXiv: 1810.00389 [hep-ph].

[81] Yu-Hui Zhou et al. "Strong decays of low-lying D-wave Ξ_b and Ξ_b' baryons with quark-pair creation model". In: *Phys. Rev. D* 108.9 (2023), p. 094032. DOI: 10.1103/PhysRevD.108.094032. arXiv: 2309.13906 [hep-ph].

[82] Yu-Xin Peng, Si-Qiang Luo, and Xiang Liu. "Refining radiative decay studies in singly heavy baryons". In: *Phys. Rev. D* 110.7 (2024), p. 074034. DOI: 10.1103/PhysRevD.110.074034. arXiv: 2405.12812 [hep-ph].

[83] E. Santopinto et al. "The Ω_c-puzzle solved by means of quark model predictions". In: *Eur. Phys. J. C* 79.12 (2019), p. 1012. DOI: 10.1140/epjc/s10052-019-7527-4. arXiv: 1811.01799 [hep-ph].

[84] L. Micu. "Decay rates of meson resonances in a quark model". In: *Nucl. Phys. B* 10 (1969), pp. 521–526. DOI: 10.1016/0550-3213(69)90039-X.

[85] A. Le Yaouanc et al. "Naive quark pair creation model of strong interaction vertices". In: *Phys. Rev. D* 8 (1973), pp. 2223–2234. DOI: 10.1103/PhysRevD.8.2223.

[86] A. Le Yaouanc et al. *Hadron Transitions in the Quark Model*. Gordon and Breach Science Publishers, 1988. ISBN: 9782881242144. URL: https://books.google.it/books?id=lSTbwAEACAAJ.

[87] W. Roberts and B. Silvestre-Brac. "General method of calculation of any hadronic decay in the $^3P_0$ model". In: *Few-Body Systems* 11.4 (1992), pp. 171–193. ISSN: 1432-5411. DOI: 10.1007/BF01641821. URL: https://doi.org/10.1007/BF01641821.

[88] J. Ferretti and E. Santopinto. "Open-flavor strong decays of open-charm and open-bottom mesons in the $^3P_0$ model". In: *Phys. Rev. D* 97 (11 2018), p. 114020. DOI: 10.1103/PhysRevD.97.114020. URL: https://link.aps.org/doi/10.1103/PhysRevD.97.114020.

[89] S. Navas et al. "Review of particle physics". In: *Phys. Rev. D* 110.3 (2024), p. 030001. DOI: 10.1103/PhysRevD.110.030001.

[90] H. García-Tecocoatzi et al. "Strong decay widths and mass spectra of the 1D, 2P and 2S singly bottom baryons". In: *Phys. Rev. D* 110.11 (2024), p. 114005. DOI: 10.1103/PhysRevD.110.114005. arXiv: 2307.00505 [hep-ph].

[91] Ailier Rivero-Acosta et al. "Radiative decays of the second shell Λ_b and Ξ_b bottom baryons". In: *In preparation* (2025).

[92] Ailier Rivero-Acosta et al. "Radiative decays of the second shell Σ_b, Ξ_b' and Ω_b bottom baryons". In: *In preparation* (2025).

[93] J. Yelton et al. "Study of electromagnetic decays of orbitally excited Ξ_c baryons". In: *Phys. Rev. D* 102.7 (2020), p. 071103. DOI: 10.1103/PhysRevD.102.071103. arXiv: 2009.03951 [hep-ex].

[94] H. García-Tecocoatzi et al. "$\Xi_c(2790)^{+/0}$ and $\Xi_c(2815)^{+/0}$ radiative decays". In: (Jan. 2025). arXiv: 2501.08798 [hep-ph].

[95] G. Bari *et al.* "The Λ_b^0 Beauty Baryon Production in Proton-Proton Interactions at $\sqrt{s} =$ 62 GeV: a Second Observation". In: *Il Nuovo Cimento* 104 A (1991).

[96] C. Albajar *et al.* (UA1 Collaboration). "First observation of the beauty baryon Λ_b in the decay channel $\Lambda_b \to J/\Psi\Lambda$ at the CERN proton-antiproton collider". In: *Physics Letters B.* 273 (1991).

[97] C. Albajar *et al.* (ALEPH Collaboration). "Measurement of the mass of the Λ_b baryon". In: *Physics Letters B.* 380 (1996).

[98] P. Abreu *et al.* (DELPHI Collaboration). "Search for exclusive decays of the Λ_b baryon and measurement of its mass". In: *Physics Letters B.* 374 (1996).

[99] T. Aaltonen *et al.* [CDF Collaboration]. "Observation of the Ω_b^- and Measurement of the Properties of the Ξ_b^- and Ω_b^-". In: *Phys. Rev. D* 80 (2009), p. 072003. DOI: 10.1103/PhysRevD.80.072003. arXiv: 0905.3123 [hep-ex].

[100] T. Aaltonen *et al.* [CDF Collaboration]. "Evidence for a bottom baryon resonance Λ_b^{*0} in CDF data". In: *Phys. Rev. D* 88 (7 2013), p. 071101. DOI: 10.1103/PhysRevD.88.071101. URL: https://link.aps.org/doi/10.1103/PhysRevD.88.071101.

[101] R. Aaij *et al.* [LHCb Collaboration]. "Observation of New Resonances in the $\Lambda_b^0\pi^+\pi^-$ System". In: *Phys. Rev. Lett.* 123 (15 2019), p. 152001. DOI: 10.1103/PhysRevLett.123.152001. URL: https://link.aps.org/doi/10.1103/PhysRevLett.123.152001.

[102] Albert M Sirunyan et al. "Observation of a New Excited Beauty Strange Baryon Decaying to $\Xi_b^-\pi^+\pi^-$". In: *Phys. Rev. Lett.* 126.25 (2021), p. 252003. DOI: 10.1103/PhysRevLett.126.252003. arXiv: 2102.04524 [hep-ex].

[103] Eberhard Klempt and Jean-Marc Richard. "Baryon spectroscopy". In: *Rev. Mod. Phys.* 82 (2010), pp. 1095–1153. DOI: 10.1103/RevModPhys.82.1095. arXiv: 0901.2055 [hep-ph].

[104] J. G. Korner, M. Kramer, and D. Pirjol. "Heavy baryons". In: *Prog. Part. Nucl. Phys.* 33 (1994), pp. 787–868. DOI: 10.1016/0146-6410(94)90053-1. arXiv: hep-ph/9406359.

[105] Hua-Xing Chen et al. "A review of the open charm and open bottom systems". In: *Rept. Prog. Phys.* 80.7 (2017), p. 076201. DOI: 10.1088/1361-6633/aa6420. arXiv: 1609.08928 [hep-ph].

[106] V. Crede and W. Roberts. "Progress towards understanding baryon resonances". In: *Rept. Prog. Phys.* 76 (2013), p. 076301. DOI: 10.1088/0034-4885/76/7/076301. arXiv: 1302.7299 [nucl-ex].

[107] Yasmine Sara Amhis et al. "Averages of b-hadron, c-hadron, and τ-lepton properties as of 2018". In: *Eur. Phys. J. C* 81.3 (2021), p. 226. DOI: 10.1140/epjc/s10052-020-8156-7. arXiv: 1909.12524 [hep-ex].

[108] Hua-Xing Chen et al. "An updated review of the new hadron states". In: *Rept. Prog. Phys.* 86.2 (2023), p. 026201. DOI: 10.1088/1361-6633/aca3b6. arXiv: 2204.02649 [hep-ph].

[109] Chien-Wen Hwang. "Combined Chiral Dynamics and MIT Bag Model Study of Strong $\Sigma_Q^{(*)} \to \Lambda_Q\pi$ Decays". In: *Eur. Phys. J. C* 50 (2007), pp. 793–799. DOI: 10.1140/epjc/s10052-007-0267-x. arXiv: hep-ph/0611221.

[110] E. Hernandez and J. Nieves. "Study of the strong $\Sigma_b \to \Lambda_b \pi$ and $\Sigma_b^* \to \Lambda_b \pi$ in a non-relativistic quark model". In: *Phys. Rev. D* 84 (2011), p. 057902. DOI: 10.1103/PhysRevD.84.057902. arXiv: 1108.0259 [hep-ph].

[111] Hua-Xing Chen et al. "Excited Ω_b baryons and fine structure of strong interaction". In: *Eur. Phys. J. C* 80.3 (2020), p. 256. DOI: 10.1140/epjc/s10052-020-7824-y. arXiv: 2001.02147 [hep-ph].

[112] Yonghee Kim et al. "Strong decays of singly heavy baryons from a chiral effective theory of diquarks". In: *Phys. Rev. D* 107.7 (2023), p. 074015. DOI: 10.1103/PhysRevD.107.074015. arXiv: 2212.08338 [hep-ph].

[113] B. Grinstein. *Introductory lectures on QCD*. Tech. rep. University of California at San Diego, 2003. DOI: 10.5170/CERN-2006-001.27.

[114] Paul Langacker. *The standard model and beyond*. 2010. ISBN: 978-1-4200-7906-7.

[115] Emmanuel Ortiz-Pacheco and Roelof Bijker. "Masses and radiative decay widths of *S*- and *P*-wave singly, doubly, and triply heavy charm and bottom baryons". In: *Phys. Rev. D* 108 (5 2023), p. 054014. DOI: 10.1103/PhysRevD.108.054014. URL: https://link.aps.org/doi/10.1103/PhysRevD.108.054014.

[116] Jean-Marc Richard. "An introduction to the quark model". In: *Ferrara International School Niccolò Cabeo 2012: Hadronic spectroscopy*. May 2012. arXiv: 1205.4326 [hep-ph].

[117] R. Aaij *et al.* [LHCb Collaboration]. "Observation of New Ξ_c^0 Baryons Decaying to $\Lambda_c^+ K^-$". In: *Phys. Rev. Lett.* 124.22 (2020), p. 222001. DOI: 10.1103/PhysRevLett.124.222001. arXiv: 2003.13649 [hep-ex].

[118] E. Santopinto. "Interacting quark-diquark model of baryons". In: *Phys. Rev. C* 72 (2 2005), p. 022201. DOI: 10.1103/PhysRevC.72.022201. URL: https://link.aps.org/doi/10.1103/PhysRevC.72.022201.

[119] B. Efron and R.J. Tibshirani. *An Introduction to the Bootstrap*. Monographs on statistics and applied probability. Chapman & Hall, 1993. URL: https://books.google.com.mx/books?id=qLHBSAAACAAJ.

[120] David Molina et al. "Bottomonium spectrum with a Dirac potential model in the momentum space". In: *Eur. Phys. J. C* 80.6 (2020), p. 526. DOI: 10.1140/epjc/s10052-020-8099-z. arXiv: 2001.05408 [hep-ph].

[121] F. James and M. Roos. "Minuit: A System for Function Minimization and Analysis of the Parameter Errors and Correlations". In: *Comput. Phys. Commun.* 10 (1975), pp. 343–367. DOI: 10.1016/0010-4655(75)90039-9.

[122] Charles R. Harris et al. "Array programming with NumPy". In: *Nature* 585.7825 (2020), pp. 357–362. ISSN: 1476-4687. DOI: 10.1038/s41586-020-2649-2. URL: https://doi.org/10.1038/s41586-020-2649-2.

[123] R. Bijker et al. "Strong decays of baryons and missing resonances". In: *Phys. Rev. D* 94.7 (2016), p. 074040. DOI: 10.1103/PhysRevD.94.074040. arXiv: 1506.07469 [hep-ph].

[124] Chong Chen et al. "Strong decays of charmed baryons". In: *Phys. Rev. D* 75 (2007), p. 094017. DOI: 10.1103/PhysRevD.75.094017. arXiv: 0704.0075 [hep-ph].

[125] Harry G. Blundell and Stephen Godfrey. "The $\xi(2220)$ revisited: Strong decays of the 1^3F_2 1^3F_4 $s\bar{s}$ mesons". In: *Phys. Rev. D* 53 (1996), pp. 3700–3711. DOI: 10.1103/PhysRevD.53.3700. arXiv: hep-ph/9508264.

[126] Roelof Bijker et al. "Masses and decay widths of $\Xi_{c/b}$ and $\Xi'_{c/b}$ baryons". In: *Phys. Rev. D* 105.7 (2022), p. 074029. DOI: 10.1103/PhysRevD.105.074029. arXiv: 2010.12437 [hep-ph].

[127] M. Artuso et al. "Observation of new states decaying into $\Lambda_c^+\pi^-\pi^+$". In: *Phys. Rev. Lett.* 86 (2001), pp. 4479–4482. DOI: 10.1103/PhysRevLett.86.4479. arXiv: hep-ex/0010080.

[128] K. W. Edwards et al. "Observation of excited baryon states decaying to $\Lambda_c^+\pi^+\pi^-$ ". In: *Phys. Rev. Lett.* 74 (1995), pp. 3331–3335. DOI: 10.1103/PhysRevLett.74.3331.

[129] Shi-Lin Zhu and Yuan-Ben Dai. "Radiative decays of heavy hadrons from light-cone QCD sum rules in the leading order of HQET". In: *Phys. Rev. D* 59 (11 1999), p. 114015. DOI: 10.1103/PhysRevD.59.114015. URL: https://link.aps.org/doi/10.1103/PhysRevD.59.114015.

[130] Zhi-Gang Wang. "Analysis of the vertexes $\Xi_Q^*\Xi_Q'$V , Σ_Q^* Σ_Q'V and radiative decays Ξ_Q^* $\to \Xi_Q'\gamma$, $\Sigma_Q^* \to \Sigma_Q$ γ". In: *The European Physical Journal A* 44.1 (2010), pp. 105–117. ISSN: 1434-601X. DOI: 10.1140/epja/i2010-10952-8. URL: https://doi.org/10.1140/epja/i2010-10952-8.

[131] Zhi-Gang Wang. "Analysis of the vertices $\Omega_Q * \Omega_Q\phi$ and radiative decays $\Omega_Q* \to \Omega_Q\gamma$". In: *Phys. Rev. D* 81 (3 2010), p. 036002. DOI: 10.1103/PhysRevD.81.036002. URL: https://link.aps.org/doi/10.1103/PhysRevD.81.036002.

[132] T. M. Aliev, K. Azizi, and H. Sundu. "Radiative $\Omega_Q^* \to \Omega_Q\gamma$ and $\Xi_Q^* \to \Xi_Q'\gamma$ transitions in light cone QCD". In: *Eur. Phys. J. C* 75.1 (2015), p. 14. DOI: 10.1140/epjc/s10052-014-3229-0. arXiv: 1409.7577 [hep-ph].

[133] T. M. Aliev, K. Azizi, and A. Ozpineci. "Radiative decays of the heavy flavored baryons in light cone QCD sum rules". In: *Phys. Rev. D* 79 (5 2009), p. 056005. DOI: 10.1103/PhysRevD.79.056005. URL: https://link.aps.org/doi/10.1103/PhysRevD.79.056005.

[134] T. M. Aliev, T. Barakat, and M. Savci. "Analysis of the radiative decays $\Sigma_Q \to \Lambda_Q\gamma$ and $\Xi_Q' \to \Xi_Q\gamma$ in light cone sum rules". In: *Phys. Rev. D* 93 (5 2016), p. 056007. DOI: 10.1103/PhysRevD.93.056007. URL: https://link.aps.org/doi/10.1103/PhysRevD.93.056007.

[135] T. M. Aliev, M. Savcı and V. S. Zamiralov. "Vector meson dominance and radiative decays of heavy spin-3/2 baryons to heavy spin-1/2 baryons". In: *Modern Physics Letters A* 27.11 (2012), p. 1250054. DOI: 10.1142/S021773231250054X. eprint: https://doi.org/10.1142/S021773231250054X. URL: https://doi.org/10.1142/S021773231250054X.

[136] Hai-Yang Cheng et al. "Chiral Lagrangians for radiative decays of heavy hadrons". In: *Phys. Rev. D* 47 (3 1993), pp. 1030–1042. DOI: 10.1103/PhysRevD.47.1030. URL: https://link.aps.org/doi/10.1103/PhysRevD.47.1030.

[137] Bañuls, M. C. and Pich, A. and Scimemi, I. "Electromagnetic decays of heavy baryons". In: *Phys. Rev. D* 61 (9 2000), p. 094009. DOI: 10.1103/PhysRevD.61.094009. URL: https://link.aps.org/doi/10.1103/PhysRevD.61.094009.

[138] Nan Jiang, Xiao-Lin Chen, and Shi-Lin Zhu. "Electromagnetic decays of the charmed and bottom baryons in chiral perturbation theory". In: *Phys. Rev. D* 92 (5 2015), p. 054017. DOI: 10.1103/PhysRevD.92.054017. URL: https://link.aps.org/doi/10.1103/PhysRevD.92.054017.

[139] A. Bernotas. "Radiative M1 transitions of heavy baryons in the bag model". In: *Phys. Rev. D* 87 (7 2013), p. 074016. DOI: 10.1103/PhysRevD.87.074016. URL: https://link.aps.org/doi/10.1103/PhysRevD.87.074016.

[140] Chi-Keung Chow. "Radiative decays of excited Λ_Q baryons in the bound state picture". In: *Phys. Rev. D* 54 (5 1996), pp. 3374–3376. DOI: 10.1103/PhysRevD.54.3374. URL: https://link.aps.org/doi/10.1103/PhysRevD.54.3374.

[141] M.A. Ivanov, J.G. Körner, and V.E. Lyubovitskij. "One-photon transitions between heavy baryons in a relativistic three-quark model". In: *Physics Letters B* 448.1 (7 1999), pp. 143–151. ISSN: 0370-2693. DOI: https://doi.org/10.1016/S0370-2693(99)00029-5. URL: https://link.aps.org/doi/10.1103/PhysRevD.87.074016.

[142] Salam Tawfiq, J. G. Körner, and Patrick J. O'Donnell. "Electromagnetic transitions of heavy baryons in the $SU(2N_f) \otimes O(3)$ symmetry". In: *Phys. Rev. D* 63 (3 2001), p. 034005. DOI: 10.1103/PhysRevD.63.034005. URL: https://link.aps.org/doi/10.1103/PhysRevD.63.034005.

[143] F. E. Close and L. A. Copley. "Electromagnetic interactions of weakly bound composite systems". In: *Nucl. Phys. B* 19 (7 1970), pp. 477–500. DOI: 10.1016/0550-3213(70)90362-7. URL: https://link.aps.org/doi/10.1103/PhysRevD.87.074016.

[144] F. Iachello and D. Kusnezov. "Radiative decays of $(Q\bar{Q})$ mesons". In: *Phys. Rev. D* 45 (7 1992), pp. 4156–4177. DOI: 10.1103/PhysRevD.45.4156. URL: https://link.aps.org/doi/10.1103/PhysRevD.87.074016.

[145] Zhen-ping Li, Hong-xing Ye, and Ming-hui Lu. "An Unified approach to pseudoscalar meson photoproductions off nucleons in the quark model". In: *Phys. Rev. C* 56 (7 1997), pp. 1099–1113. DOI: 10.1103/PhysRevC.56.1099. arXiv: nucl-th/9706010. URL: https://link.aps.org/doi/10.1103/PhysRevD.87.074016.

[146] Qiang Zhao et al. "Pion photoproduction on the nucleon in the quark model". In: *Phys. Rev. C* 65 (7 2002), p. 065204. DOI: 10.1103/PhysRevC.65.065204. arXiv: nucl-th/0202067. URL: https://link.aps.org/doi/10.1103/PhysRevD.87.074016.

[147] Wei-Jun Deng et al. "Spectrum and electromagnetic transitions of bottomonium". In: *Phys. Rev. D* 95.7 (7 2017), p. 074002. DOI: 10.1103/PhysRevD.95.074002. arXiv: 1607.04696 [hep-ph]. URL: https://link.aps.org/doi/10.1103/PhysRevD.87.074016.

[148] Wei-Jun Deng et al. "Charmonium spectrum and their electromagnetic transitions with higher multipole contributions". In: *Phys. Rev. D* 95.3 (7 2017), p. 034026. DOI: 10.1103/PhysRevD.95.034026. arXiv: 1608.00287 [hep-ph]. URL: https://link.aps.org/doi/10.1103/PhysRevD.87.074016.

[149] Bernard Aubert et al. "Observation of an excited charm baryon Ω_c^* decaying to $\Omega_c^0\gamma$". In: *Phys. Rev. Lett.* 97 (7 2006). Ed. by Alexey Sissakian, Gennady Kozlov, and Elena Kolganova, p. 232001. DOI: 10.1103/PhysRevLett.97.232001. arXiv: hep-ex/0608055. URL: https://link.aps.org/doi/10.1103/PhysRevD.87.074016.

[150] E. Solovieva et al. "Study of Ω_c^0 and Ω_c^{*0} Baryons at Belle". In: *Phys. Lett. B* 672 (7 2009), pp. 1–5. DOI: 10.1016/j.physletb.2008.12.062. arXiv: 0808.3677 [hep-ex]. URL: https://link.aps.org/doi/10.1103/PhysRevD.87.074016.

[151] C. P. Jessop et al. "Observation of two narrow states decaying into $\Xi_c^+\gamma$ and $\Xi_c^0\gamma$ ". In: *Phys. Rev. Lett.* 82 (7 1999), pp. 492–496. DOI: 10.1103/PhysRevLett.82.492. arXiv: hep-ex/9810036. URL: https://link.aps.org/doi/10.1103/PhysRevD.87.074016.

[152] J. Yelton et al. "Study of Excited Ξ_c States Decaying into Ξ_c^0 and Ξ_c^+ Baryons". In: *Phys. Rev. D* 94.5 (7 2016), p. 052011. DOI: 10.1103/PhysRevD.94.052011. arXiv: 1607.07123 [hep-ex]. URL: https://link.aps.org/doi/10.1103/PhysRevD.87.074016.

[153] J. Dey et al. "Radiative decays of S-wave charmed baryons". In: *Physics Letters B* 337.1 (7 1994), pp. 185–188. ISSN: 0370-2693. DOI: https://doi.org/10.1016/0370-2693(94)91466-4. URL: https://www.sciencedirect.com/science/article/pii/0370269394914664.

[154] H. Bahtiyar et al. "$\Xi_c\gamma \to \Xi_c'$ transition in lattice QCD". In: *Phys. Lett. B* 772 (7 2017), pp. 121–126. DOI: 10.1016/j.physletb.2017.06.022. arXiv: 1612.05722 [hep-lat]. URL: https://link.aps.org/doi/10.1103/PhysRevD.87.074016.

[155] H. Bahtiyar et al. "$\Omega_c\gamma \to \Omega_c^*$ transition in lattice QCD". In: *Phys. Lett. B* 747 (7 2015), pp. 281–286. DOI: 10.1016/j.physletb.2015.06.006. arXiv: 1503.07361 [hep-lat]. URL: https://link.aps.org/doi/10.1103/PhysRevD.87.074016.

[156] Martin J. Savage. "E2 strength in the radiative charmed baryon decay $\Sigma_c^* \to \Lambda_c\gamma$ ". In: *Phys. Lett. B* 345 (7 1995), pp. 61–66. DOI: 10.1016/0370-2693(94)01597-6. arXiv: hep-ph/9408294. URL: https://link.aps.org/doi/10.1103/PhysRevD.87.074016.

[157] Peter L. Cho. "Strong and electromagnetic decays of two new Λ_c^* baryons". In: *Phys. Rev. D* 50 (7 1994), pp. 3295–3302. DOI: 10.1103/PhysRevD.50.3295. arXiv: hep-ph/9401276. URL: https://link.aps.org/doi/10.1103/PhysRevD.87.074016.

[158] Guang-Juan Wang, Lu Meng, and Shi-Lin Zhu. "Radiative decays of the singly heavy baryons in chiral perturbation theory". In: *Phys. Rev. D* 99.3 (7 2019), p. 034021. DOI: 10.1103/PhysRevD.99.034021. arXiv: 1811.06208 [hep-ph]. URL: https://link.aps.org/doi/10.1103/PhysRevD.87.074016.

[159] Hai-Yang Cheng. "Remarks on the strong coupling constants in heavy hadron chiral Lagrangians". In: *Phys. Lett. B* 399 (7 1997), pp. 281–286. DOI: 10.1016/S0370-2693(97)00305-5. arXiv: hep-ph/9701234. URL: https://link.aps.org/doi/10.1103/PhysRevD.87.074016.

[160] Vytautas Simonis. "Improved predictions for magnetic moments and M1 decay widths of heavy hadrons". In: *Phys. Rev. D* 87 (7 Mar. 2018), p. 074016. DOI: 10.1103/PhysRevD.87.074016. arXiv: 1803.01809 [hep-ph]. URL: https://link.aps.org/doi/10.1103/PhysRevD.87.074016.

[161] Ajay Majethiya, Bhavin Patel, and P C Vinodkumar. "Radiative decays of single heavy flavour baryons". In: *Eur. Phys. J. A* 42 (7 2009), pp. 213–218. DOI: 10.1140/epja/i2009-10880-8. arXiv: 0902.2536 [hep-ph]. URL: https://link.aps.org/doi/10.1103/PhysRevD.87.074016.

[162] Avijit Hazra, Saheli Rakshit, and Rohit Dhir. "Radiative M1 transitions of heavy baryons: Effective quark mass scheme". In: *Phys. Rev. D* 104.5 (7 2021), p. 053002. DOI: 10.1103/PhysRevD.104.053002. arXiv: 2108.01840 [hep-ph]. URL: https://link.aps.org/doi/10.1103/PhysRevD.87.074016.

[163] M. A. Ivanov et al. "Strong and radiative decays of heavy flavored baryons". In: *Phys. Rev. D* 60 (9 1999), p. 094002. DOI: 10.1103/PhysRevD.60.094002. URL: https://link.aps.org/doi/10.1103/PhysRevD.60.094002.

[164] D. Gamermann, C. E. Jiménez-Tejero, and A. Ramos. "Radiative decays of dynamically generated charmed baryons". In: *Phys. Rev. D* 83 (7 2011), p. 074018. DOI: 10.1103/PhysRevD.83.074018. URL: https://link.aps.org/doi/10.1103/PhysRevD.83.074018.

[165] T. M. Aliev, T. Barakat, and M. Savcı. "Radiative decays of the p-wave charmed heavy baryons". In: *Eur. Phys. J. C* 79.5 (7 2019), p. 437. DOI: 10.1140/epjc/s10052-019-6947-5. arXiv: 1904.11305 [hep-ph]. URL: https://link.aps.org/doi/10.1103/PhysRevD.87.074016.

[166] Hai-Yang Cheng. "Charm baryon production and decays". In: *Int. J. Mod. Phys. A* 24S1 (7 2009), pp. 593–626. DOI: 10.1142/S0217751X09046680. URL: https://link.aps.org/doi/10.1103/PhysRevD.87.074016.

[167] Hai-Yang Cheng. "Charmed baryons circa 2015". In: *Front. Phys. (Beijing)* 10.6 (7 2015), p. 101406. DOI: 10.1007/s11467-015-0483-z. URL: https://link.aps.org/doi/10.1103/PhysRevD.87.074016.

[168] Hai-Yang Cheng. "Charmed baryon physics circa 2021". In: *Chin. J. Phys.* 78 (7 2022), pp. 324–362. DOI: 10.1016/j.cjph.2022.06.021. arXiv: 2109.01216 [hep-ph]. URL: https://link.aps.org/doi/10.1103/PhysRevD.87.074016.

Report of Activities

During the Doctoral Program, I began in the first year by studying theoretical aspects of Quantum Field Theory, Particle Physics, and Hadron Physics. Concurrently, I reviewed articles related to the thesis topic, which is the phenomenology of heavy baryons, and initiated the necessary calculations.

Throughout the Ph.D., my work has focused on calculating the mass spectra, as well as the strong and electromagnetic decay widths of singly bottom baryons, and the electromagnetic decay widths of singly charmed baryons. My primary contributions have been centered on the calculations of the electromagnetic decays of singly heavy baryons.

In addition to my research, I completed several subjects, participated in academic schools and conferences, and contributed to the production of several research articles. A detailed list of the subjects taken, articles published or in progress, and activities conducted during the Ph.D. is provided below.

Ph.D. courses:

- Selected Topics of Physics I (64 hours): Study of theoretical aspects of Quantum Field Theory.
- Research Seminar I (64 hours): Conducted a study of theoretical aspects of hadron physics. Reviewed relevant articles on the topic and developed calculations for heavy baryons within the framework of the Quark Model. Wrote on the Thesis the results obtained.
- Gauge Theories (64 hours): Study of the Standard Model and some aspects about the Quark Model.
- Research Seminar II (64 hours): Conducted a study of theoretical aspects of hadron physics. Reviewed relevant articles on the topic and developed calculations for heavy baryons within the framework of the Quark Model. Wrote on the Thesis the results obtained.
- Research Seminar III (64 hours): Conducted a study of theoretical aspects of hadron physics. Reviewed relevant articles on the topic and developed calculations for heavy baryons within the framework of the Quark Model. Wrote on the Thesis the results obtained.
- Research Seminar IV (64 hours): Conducted a study of theoretical aspects of hadron physics. Reviewed relevant articles on the topic and developed calculations for heavy baryons within the framework of the Quark Model. Wrote on the Thesis the results obtained.
- Group Theory (64 hours): Study of some aspects of Group Theory related to Hadron Physics.

- Research Seminar V (64 hours): Conducted a study of theoretical aspects of hadron physics. Reviewed relevant articles on the topic and developed calculations for heavy baryons within the framework of the Quark Model. Wrote on the Thesis the results obtained.
- Research Seminar VI (64 hours): Conducted a study of theoretical aspects of hadron physics. Reviewed relevant articles on the topic and developed calculations for heavy baryons within the framework of the Quark Model. Wrote on the Thesis the results obtained.
- Selected Topics of Physics II (64 hours): Conducted a study of theoretical aspects of hadron physics. Reviewed relevant articles on the topic and developed calculations for heavy baryons within the framework of the Quark Model. Wrote on the Thesis the results obtained.

Schools

I attended the following Ph.D. schools:

- 06/2023: Tri-Institute Summer School on Elementary Particles (TRISEP), School held by the Perimeter Institute for Theoretical Physics, Waterloo, Canada (Online participation)
- 01/2023: Graduate Winter School on Symmetries, School organized by the Perimeter Institute for Theoretical Physics, Waterloo, Canada (Online participation)
- 02/2022: Frontiers in Nuclear and Hadronic Physics, Online School organized by the Galileo Galilei Institute for Theoretical Physics, Firenze, Italy

Publications:

- 01/ 2025: "$\Xi_c(2790)^{+/0}$ and $\Xi_c(2815)^{+/0}$ radiative decays",
  H. García-Tecocoatzi, A. Ramirez-Morales, A. Rivero-Acosta, E. Santopinto and C. A. Vaquera-Araujo, *Submitted to Physics Letters B* arXiv:2501.08798
- 12/ 2024: "Strong decay widths and mass spectra of the $1D$, $2P$ and $2S$ singly bottom baryons",
  H. García-Tecocoatzi, A. Giachino, A. Ramirez-Morales, A. Rivero-Acosta, E. Santopinto and C. A. Vaquera-Araujo, *Physical Review D* 110, no.11, 114005 (2024)

Works in progress:

- "Radiative decays of the second shell Λ_b and Ξ_b bottom baryons",
  Ailier Rivero-Acosta, H. García-Tecocoatzi, A. Ramirez-Morales, E. Santopinto and Carlos Alberto Vaquera-Araujo
- "Radiative decays of the second shell Σ_b, Ξ_b', and Ω_b bottom baryons",
  Ailier Rivero-Acosta, H. García-Tecocoatzi, A. Ramirez-Morales, E. Santopinto and Carlos Alberto Vaquera-Araujo

Talks

I attended the following Conferences:

- 02/2024: Sesto Incontro Nazionale di Fisica Nucleare, Trento, Italy
  "Mass spectra and electromagnetic decays of single bottom baryons",
- 08/2022: Canadian-Cuban-American-Mexican Graduate Student Physics Conference (Online)
  "Renormalization of a model for spin-1 matter fields".

TOR VERGATA
UNIVERSITÀ DEGLI STUDI DI ROMA

Dipartimento di Fisica

Prof. Annalisa D'Angelo
Tel + 39 06 72594562

March 31st, 2025

Report PhD thesis Dr. Ailier Rivero Acosta
with the title "Study of Heavy Baryons Phenomenology"

The thesis is concerned with the theoretical study of the singly heavy baryons within the constituent quark model. Comparison of Lattice QCD (LQCD) calculations on light baryons spectrum with non-relativistic constituent quark models (CQM) results have already shown striking similarities such as the same SU(6)×O(3) symmetry features and level counting, proving CQM to be effective in predicting the spectrum and the decay of hadrons. LQCD calculations on heavy baryons spectra, however, are still in an early stage, making CQM approaches an essential tool for the interpretation of the observed heavy baryons and the assignment of their quantum numbers.
In his PhD thesis, Dr. Ailier Rivero Acosta has studied the phenomenology of baryons made of two light quarks (u,p,s) and one heavy quark (c,b), by evaluating the wave functions, the mass spectrum, the J^P quantum numbers and the decay modes using both a three quark and a quark di-quark scheme, within a non-relativistic constituent quark model.
He has nicely summarized the experimental evidence of observed heavy baryons with one bottom quark, from the ALEPH, D0, CDF, LHCb and CMS collaborations and the status of predictions from quark models. Chapter 2 is dedicated to the explicit determination of the three-particle wave functions, in the flavor, spin, orbital and radial coordinates using the harmonic oscillator potential in Jacobi coordinates and including spin, spin-orbit, isospin, and flavor dependent contributions to evaluate the mass spectrum. The wave functions and the mass spectrum have also been evaluated in the hypothesis that the light two quarks are bonded in a di-quark state interacting with the heavy bottom quark.
The model has a total of eight parameters in the case of the three-quark scheme and nine in the case of the quark-diquark scheme, which have been determined by fitting the values of the masses of the thirteen best experimentally know heavy baryons with one bottom quark. The associated error has been determined via a Monte Carlo bootstrap procedure.
The mass values and the quantum numbers of the states not used in the fit may be compared with the less known experimentally observed states and used to predict their quantum numbers, when not yet measured. The last part of chapter 2 is dedicated to the evaluation of the hadronic decay modes using the so-called $^3P_0$ model. Results of the mass spectrum and strong decay widths are compared with the experimental values of the observed baryons and with predictions from other theoretical approaches. Assignment of quantum numbers to the observed states from the CQM is then attempted, by comparing the predicted and the measured masses of the heavy baryons. Results from this chapter have been published in Physical Review D.
Chapters 3 and 4 are then dedicated to the evaluation of the electromagnetic decay widths of singly bottom baryons to another singly bottom baryon, and from the second shell to the ground states and P-wave states, respectively.
The results of these electromagnetic decay widths may be useful in the assignments of resonances when the states have the same mass and total decay widths and are the subject of two different journal articles in preparation.

Via Della Ricerca Scientifica, 1 – 00133 Roma
www.fisica.uniroma2.it
annalisa.dangelo@roma2.infn.it

TOR VERGATA
UNIVERSITÀ DEGLI STUDI DI ROMA

Dipartimento di Fisica

Dr. Ailier Rivero Acosta has dedicated the last chapter of his thesis to the calculation of electromagnetic decay widths of singly charmed baryons, to complement the available mass spectrum and hadron decay widths results, previously calculated within the same model by the research group. Comparison with experimental data and different theoretical approaches shows the higher accuracy of the results obtained by the candidate. The results have been summarized in a pre-print, submitted for publication to Physics Letters B.

The thesis is written in high quality English language. The writing style of the thesis is easy to read, and all the steps are clearly explained, as it is also proved by the rich bibliography. The topics addressed by the thesis cover several complementary calculations and are presented in a clear and exhaustive manner, proving that the candidate has reached an excellent scientific maturity.

To summarize, Dr. Ailier Rivero Acosta presents a thesis in which extensive work on mass spectrum, hadron and electromagnetic decays of singly heavy baryons has been reported. His work may play a crucial role in the assignment of unmeasured quantum number the poorly known heavy resonances and its results may produce up to four publications in high-impact journals.
In my evaluation, I consider the thesis to be is of excellent quality and the candidate mature for its public defense.

Sincerely,

Professor Annalisa D'Angelo

Via Della Ricerca Scientifica, 1 – 00133 Roma
www.fisica.uniroma2.it
annalisa.dangelo@roma2.infn.it

Genova, April 9th, 2025

Dr. Modesto Antonio Sosa Aquino
Director
Division de Sciences and Engineering

I hereby inform you that I have read and reviewed the thesis entitled **"Study of heavy baryons phenomenology"**, which was prepared by the student Ailier Rivero Acosta for the degree of Doctor in Physics. In my opinion, the thesis meets the quality requirements corresponding to the academic degree to which the thesis is aspired. Therefore, I recommend that the thesis be defended.

Sincerely

Dr. Silvano Tosi
Professor
Department of Physics
University of Genoa

Via Dodecaneso 33
16146 Genova, Italy
https://www.difi.unige.it

Tecnológico de Monterrey

Guadalajara, Jalisco, 10 de abril de 2025

Dr. Modesto Antonio Sosa Aquino
Director
División de Ciencias e Ingenierías
PRESENTE

Por medio de la presente me permito informar que he leído la tesis titulada **"Study of heavy baryons phenomenology"**, que para obtener el grado de **Doctor en Física** ha sido elaborada por el estudiante **Ailier Rivero Acosta**. En mi opinión, la tesis cumple con los requisitos de calidad correspondientes al grado académico al que se aspira. Las correcciones sugeridas por mi parte han sido atendidas, por lo cual recomiendo se proceda a la defensa de la tesis.

Atentamente

Dr. Hugo Garcia Tecocoatzi
Profesor | Departamento de Ciencias
Escuela de Ingeniería y Ciencias
Región Occidente | Campus Guadalajara
Tecnológico de Monterrey
Email: hugo.garcia.t@tec.mx

León, Guanajuato, 7 de mayo de 2025

Dr. MODESTO ANTONIO SOSA AQUINO
DIRECTOR DE LA DIVISIÓN DE CIENCIAS E INGENIERÍAS
P R E S E N T E

Estimado Doctor Modesto Antonio Sosa Aquino,

Por este medio le informo que he leído y revisado la tesis de doctorado del estudiante M.F.Ailier Rivero Acosta. El trabajo se titula: **"Study of Heavy Baryons Phenomenology"**, y el asesor es el Dr. Carlos Vaquera Araujo(UG-CONAHCyT) y la asesora la Dra. Elena Santopinto (INFN, Sezione di Genova).

He hecho al estudiante recomendaciones para el documento final, hemos discutido sobre el trabajo y he constatado que posee un excelente dominio del tema de su tesis. Además de que los resultados por él obtenidos, son de relevancia y originalidad científica, lo cual es avalado por un artículo publicado, otro artículo en proceso de arbitraje y otros dos proyectos terminados. Me complace informarle que estoy de acuerdo con que se realice la presentación del trabajo de tesis, puesto que el mismo cuenta con sobrados requisitos para la obtención del grado de Doctorado en Física.

ATENTAMENTE
"LA VERDAD OS HARÁ LIBRES"

Dra. Nana Geraldine Cabo Bizet
Departamento de Física
División de Ciencias e Ingenierías
Universidad de Guanajuato

León, Guanajuato, 09 de Abril de 2025

Dr. Modesto Sosa Aquino

Director DCI

Presente

Por este conducto le informo que he leído la tesis titulada *"Study of heavy baryons phenomenology"* que para obtener el grado de Doctor en Física ha formulado el M.F. **Ailier Rivero Acosta** bajo la dirección del Dr. Carlos Alberto Vaquera Araujo y la Dra. Elena Santopinto.

En mi opinión, este trabajo reúne las características de calidad y forma para el grado al que se aspira, por lo cual no tengo inconveniente en que se realice la defensa correspondiente.

Sin otro particular, reciba un cordial saludo.

Atentamente

Dr. Mauro Napsuciale Mendivil

Profesor Titular "C"

c.c.p. archivo

DEPARTAMENTO DE FISICA, DIVISION DE CIENCIAS E INGENIERÍAS, CAMPUS LEÓN
Loma del Bosque 103, Fracc. Lomas del Campestre C.P. 37150 León, Gto., Ap. Postal E-143 C.P. 37000 Tel. (477) 788-5100, Fax: (477) 788-5100 ext. 8410, http://www.fisica.ugto.mx

Genova, April 4th, 2025

Dr. Modesto Antonio Sosa Aquino
Director
Division de Sciences and Engineering

I hereby inform you that I have read and reviewed the thesis entitled **"Study of heavy baryons phenomenology"**, which was prepared by the student Ailier Rivero Acosta for the degree of Doctor in Physics. In my opinion, the thesis meets the quality requirements corresponding to the academic degree to which the thesis is aspired. Therefore, I recommend that the thesis be defended.

Sincerely

Dr. Elena Santopinto
Director of Research
INFN, Sezione di Genova

Via Dodecaneso 33
16146 Genova, Italy

UNIVERSIDAD DE GUANAJUATO

León, Guanajuato, 4 de abril de 2025

Dr. Modesto Antonio Sosa Aquino
Director
División de Ciencias e Ingenierías
PRESENTE

Por medio de la presente me permito informar que he leído la tesis titulada **"Study of Heavy Baryons Phenomenology"**, que para obtener el grado de Doctor en Física ha sido elaborada por el **M. F. Ailier Rivero Acosta** bajo mi dirección, en co-asesoría con la **Dra. Elena Santopinto** Del Instituto Nazionale di Fisica Nucleare, Sezione di Genova. En mi opinión, la tesis cumple con los requisitos de calidad correspondientes al grado académico al que se aspira. Las correcciones sugeridas por mi parte han sido atendidas, por lo cual recomiendo se proceda a la defensa de la tesis.

Sin más por el momento quedo a sus órdenes para cualquier aclaración.

Atentamente

Dr. Carlos Alberto Vaquera Araujo
Investigador por México, Secihti
Departamento de Física
DCI, Campus León
vaquera@fisica.ugto.mx